The pervaporative dewatering of alcohol using caesium polyacrylate membranes

Burslem, Rosemary Helen

Award date:
1996

Awarding institution:
University of Bath

THE PERVAPORATIVE DEWATERING OF ALCOHOL USING CAESIUM POLYACRYLATE MEMBRANES

submitted by

Rosemary Helen Burslem

for the degree of PhD

of the University of Bath

1996

ProQuest LLC
789 East Eisenhower Parkway
P.O. Box 1346
Ann Arbor, MI 48106-1346

ACKNOWLEDGEMENTS

First and foremost, thanks must go to both my supervisors, Dr Robert Field and Dr Tim deV Naylor, for their unfailing support and encouragement throughout the course of this work. I couldn't have done it without either of you!

Gratitude also to the SERC and BP Research, UK, for supporting the work financially.

Thanks to staff at Bath University who contributed in any way: Geoff, Les and Mike in the workshop; technicians: Ann, Fernando, Richard, Tom and Mac; other support staff: Paula, Elaine, Liz and Crocetta, without whom orders wouldn't be forthcoming and I wouldn't always have been able to find Robert when I needed to!

A mention must be given to friends I have made in Bath who have contributed to the good times: Susan, Phil, John, Ann, Wai Ng, Fang Ming, Maria, Claire, Paul, Meloney, Dave, Sanjay, Ben, Ping, Torsten, Alex, Olga, Kathy, Becca, Peter and especially Mary and Rob, who have been wonderful friends, around from Day 1 until the bitter end.

Much appreciation and respect is due to those who have had to put up with sharing a house with me over the last few years: Andrew, Richard, Clare, Torsten, Pete, Anthony and Nick. Most of you were very sympathetic to my moans!

Last, but not least, this thesis is dedicated to my family: Mum, Dad, Anne (and Phil), Grandma and Granddad. You have always been supportive and proud of whatever I do. Thank you for everything you've done for me.

Close to the Western summit there is the dried and frozen carcass of a leopard. No one has explained what the leopard was seeking at that altitude.

Ernest Hemmingway, The Snows of Kilimanjaro

TABLE OF CONTENTS

LIST OF FIGURES

LIST OF TABLES

ABSTRACT

The aim of the research was to investigate the performance of a caesium polyacrylate (CsPA) pervaporation membrane for the dewatering of 2-propanol. Simple modelling to decouple the properties and performance of the membrane from those of the system in which it was used. The approach developed will be useful in the analysis of other pervaporation systems.

Composite membranes were fabricated and tested within a small-scale batch dehydration rig. The feed and permeate side compositions were measured, along with the permeation flux. Performance is presented as plots of separation factor and flux against feed-side activity and modelled by a semi-empirical relation. Factors investigated were the temperature, conditions of formation and thickness of the dense membrane layer, turbulence of the feedstock, type of support layer used, permeate pressure and feed temperature.

Both dry and swollen thicknesses of the CsPA layer were estimated using scanning electron microscopy. Water and 2-propanol fluxes both increased with decreasing membrane thickness and significant loss of selectivity was found at the lowest thickness tested (7μm). The predictions of Fick's law were not obeyed for the overall system. The effects of concentration polarisation within the system account for this. Increasing the turbulence of the feed liquid increased the flux but this was accompanied by a slight decrease in selectivity.

Several porous materials were tested as support layers to the pervaporation membrane. Microporous materials generally resulted in a loss of selectivity at relatively low feed water concentrations ($>$5wt%) as the swollen polymer sank into the pores. Gortex and Polyvinyldifluoride support layers achieved higher fluxes than Polysulfone (PSf) or Rigidmesh supports, across a range of feed compositions. The Permeate pressures were varied between 0.4 and 9.1mbar and were not found to influence water flux within this region, although a decrease in separation factor was found at the highest permeate pressure tested.

Both flux and selectivity increased with feed temperature between the range of 23°C and 70°C. An average apparent activation energy of 40kJmol$_{-1}$ was calculated by constructing an Arrhenius plot using data from experiments where temperature was varied between 23 and 59°C.

A simple resistances-in-series model has been used to decouple the resistances to mass transport within the system. The boundary layer resistance was a major resistance for this system, accounting for between 5% and 83% of the overall resistance, depending upon conditions used. Its relative importance varied only slightly with feed composition but increased as the membrane decreased in thickness or when the overall resistance of the composite membrane is lower. The membrane resistance increased in proportion to the thickness and varied slightly with the feed concentration. The resistance of the porous support layer was found to be significant.

Predicted boundary layer resistances were calculated for experiments conducted at different temperatures. Boundary layer effects were found to be more significant at higher temperatures. Intrinsic activation energies were calculated utilising the flux and the concentration driving force across the composite membrane only. These values were found to be higher than the apparent activation energies by around 25%, indicating that boundary layer effects influence the value of the parameter.

NOMENCLATURE

		Typical units
a	Activity	-
A	Semi-empirical coefficient	$kgm^{-2}h^{-1}$
A_{12}	Adjustable parameter in Van Laar equation	-
A_{21}	Adjustable parameter in Van Laar equation	-
b	Cell radius	m
B	Semi-empirical coefficient	-
c	Concentration	kgm^{-3}
d_h	Hydraulic diameter	m
D	Diffusion coefficient	m^2s^{-1}
D_0	Concentration-independent, activity-based diffusion coefficient	m^2s^{-1}
D^0	Diffusion coefficient for zero penetrant concentration in the membrane	m^2s^{-1}
E	Activation energy	kJ/mol
f	Fugacity	Pa
F	Correction factor for mass transfer equations	-
g^E	Excess Gibb's energy	$Jmol^{-1}$
G^E	Excess Gibb's energy	J
J	Flux	$kgm^{-2}s^{-1}$
k	Plasticizing parameter (Equation 1.12, 4.7 and 4.8)	-
k_{BL}	Boundary layer mass transfer coefficient	ms^{-1}
l	Membrane (active layer) thickness	m
L	Phenomenological coefficient (Chapters 1 and 2)	Variable
L	Length of module or flow channel (Chapter 5)	m
M	Factor to convert weight fractions to activities	kgm^{-3}
N	Empirical parameter	-
p	Partial vapour pressure	Pa
p^0	Saturation vapour pressure	Pa
P	Permeability	m^2s^{-1}
P_0	Concentration-independent, activity-based permeability	m^2s^{-1}
P	Pressure (Equation 2.4 and Appendix D)	Pa
Q	Empirical parameter	kgm^{-3}

R	Gas constant	$JK^{-1}mol^{-1}$
R	Resistance to mass transport	sm^{-1}
Re	Reynold's number	-
S	Selectivity (Equation 1.3)	-
S	Solubility coefficient	-
Sc	Schmidt number	-
Sh	Sherwood number	-
T	Temperature	K
T_g	Glass transition temperature	K
V	Volume	m^3
w	Weight fraction	kg/kg
x	Mole fraction	mol/mol
X	Driving force (Equation 1.1)	-
y	Mole fraction of vaporous component	mol/mol
α_D	Diffusion selectivity (Equation 1.11)	-
α_{ij}	Separation factor	-
α_{PV}	Pervaporation selectivity (Equation 1.11)	-
α_S	Sorption selectivity (Equation 1.11)	-
β_i	Enrichment factor	-
γ	Activity coefficient	-
γ	Shear rate	s^{-1}
δ	Laminar boundary layer thickness	m
ΔH_S	Gas-polymer heat of solution	$Jmol^{-1}$
η	Solution viscosity	Pas
μ	Chemical potential	
ν	Kinematic viscosity	m^2s^{-1}
ρ	Liquid density	kgm^3
σ	Applied shear stress	Pa
ω	Radial velocity	$rads^{-1}$

Superscripts

'	Feed side
''	Permeate side
L	Liquid

Subscripts

b	Bulk feed liquid
BL	Liquid boundary layer
f	Feed-side
i	Component i (More permeable component)
j	Component j (Less permeable component)
k	Component k
m	Membrane
1	Component 1 (more permeable component)
2	Component 2 (less permeable component)
p	Permeate-side

LIST OF ABBREVIATIONS USED

CsPA	Caesium polyacrylate
EPDM	Ethylene propylene rubber
GS	Gas separation
IPA	Iso-propyl alcohol (Propan-2-ol)
MF	Microfiltration
MW	Molecular weight
PAA	Polyacrylic acid
PAN	Polyacrylonitrile
PDMS	Polydimethylsiloxane
PES	Polyethersulfone
PSf	Polysulfone
PV	Pervaporation
PVA	Polyvinylalcohol
PVC	Polyvinyl chloride
PVDF	Polyvinylidenefluoride
RO	Reverse osmosis
SEM	Scanning electron micrograph
TCE	Trichloroethylene
UF	Ultrafiltration
VP	Vapour permeation

CHAPTER 1

LITERATURE SURVEY

1.1 MEMBRANE PROCESSES

Natural membranes have many functions in living organisms, surrounding cells as well as organs such as the liver. Biological membranes are rarely used in industrial processing, but the study of these membranes today may aid the path to further developments in the use of synthetic membranes. A synthetic membrane acts as a thin interface, separating two homogeneous phases and restricting the transport of components across it in some sort of specific manner. Membranes can be used for the separation, purification and concentration of molecular mixtures to generate high grade products for the chemical, food and pharmaceutical industries. Membrane processes compete with "traditional" separation methods including distillation, crystallisation, precipitation, adsorption, extraction and ion-exchange. Hybrid processes, combining a membrane separation and a traditional process are now being developed. Membranes are made from a wide variety of materials, such as polymers, metals and ceramics and a variety of separation principles are utilised.

Reviews of the history of membrane experimentation and the progress of membrane technology have been published (Lonsdale, 1982, 1987; Mason, 1991). The phenomenon of osmosis was first observed by the Abbé Jean Antoine Nollet in the eighteenth century, using a pig's bladder. The first examination of a synthetic membrane was by Graham in 1833. He used a tube plugged with plaster of Paris to simulate a cracked jar through which gases may diffuse. Synthetic membranes were first prepared by the precipitation of films by Moritz Traube in 1867 but synthetic membrane technology has only really developed from a small scale laboratory

technique to an industrial process in the last thirty years. Before the 1960s, membranes were too thick to yield high fluxes but the development of an asymmetric membrane for reverse osmosis (Loeb and Sourirajan, 1962) and the production of many new polymers since then has expanded the potential of membrane separations. The first commercially used membrane separation process was dialysis. Haemodialysis is still the largest single application of a membrane separation process with over 50 million dialysers produced every year. Ultrafiltration (UF), microfiltration (MF) and reverse osmosis (RO) are also commercially very well established processes, with a large variety of membrane materials and structures being available. MF and UF utilise porous membranes whilst Mulder (1991) states that RO membranes "can be considered as being intermediate between open porous types of membrane and dense, non-porous membranes."

Pervaporation (PV), gas separation (GS) and vapour permeation (VP) all utilise non-porous (dense) membranes. Some applications of these processes are well established, such as hydrogen recovery (GS) and dewatering of alcohols (PV) whilst further applications are the subject of much research.

The development of liquid membranes is still at an early stage, the major factor discouraging their use being their lack of stability. The membrane is either immobilised in the pores of a support material or is part of a double emulsion. The liquid can contain a dissolved carrier which facilitates the transport of one or more components across the barrier. Facilitated transport enables components to move against a transport gradient.

Ceramic membranes were developed at the end of the 1950s for the enrichment of uranium. They have a very high chemical and thermal resistance and

have been developed for UF and MF applications where the resistance of polymeric membranes is insufficient. Stainless steel microfiltration membranes are also now being produced.

Other membrane processes include membrane distillation, osmotic distillation, electrodialysis and the exciting area of membrane reactors, where transport through the membrane unit includes a chemical change as well as a separation process.

Compared to conventional separation processes, membrane separations generally possess a low energy consumption, particularly since they can be operated at ambient temperature. Continuous separation, modular design enabling easier scale-up and a wide variety of membrane materials and processes are other advantages. Membranes are especially good for rough separations. A disadvantage of using membranes is that they need to be replaced at intervals and fouling is a particular problem with UF and MF. The thermal and chemical stability of some polymers is also inadequate.

1.1.1 MASS TRANSPORT IN MEMBRANES

The transport rate of a component across a membrane is determined by the driving force acting on that component, its mobility and concentration within the membrane. Mobility within the membrane is determined by the molecular size of the component and the physical structure of the membrane. Concentration is determined by chemical compatibility of the permeating molecule and the membrane material.

Most synthetic membrane processes exhibit passive transport, i.e. transport is effected by the driving force of a gradient in electrochemical potential caused by hydrostatic pressure, concentration, temperature or electrical potential differences between the two sides of the membrane. Other forms of transport are facilitated

(employed by liquid membranes) and active transport (exhibited by biological membranes).

Transport processes may be described by phenomenological equations which relate flux to driving force. These include Fick's (flux $\propto$ concentration difference), Ohm's (electrical potential), Fourier's (heat) and Poiseulle's (pressure) equations. In such phenomenological equations, the transport process is considered as a macroscopic process and the membrane as a black box. The factor "membrane structure" is represented by the phenomenological coefficient.

The most comprehensive mathematical description of mass transport through membranes is given by a general phenomenological equation:

$$J_i = \sum L_{ik} X_k \quad (i,k = 1,2,3...m) \tag{1.1}$$

where J_i is the flux of each component, X_k is each driving force and L_{ik} is the phenomenological coefficient relating J to X.

For multi-component systems with fluxes of heat, volume and electrical potential, equation 1.1 can be written as a matrix. However, the practical value of this equation is limited because it assumes a linear relationship between flux and driving force which is applicable only close to equilibrium and also it includes many coefficients which are functions of state variables, such as temperature, pressure or composition, and are hard to determine by independent measurements. Practically, the only fluxes of concern are those of matter and the kinetic coupling of individual components can be ignored.

1.2 PERVAPORATION

Pervaporation (PV) is the transfer of matter from the liquid phase to the vapour phase through a non-porous polymeric membrane. The driving force for mass

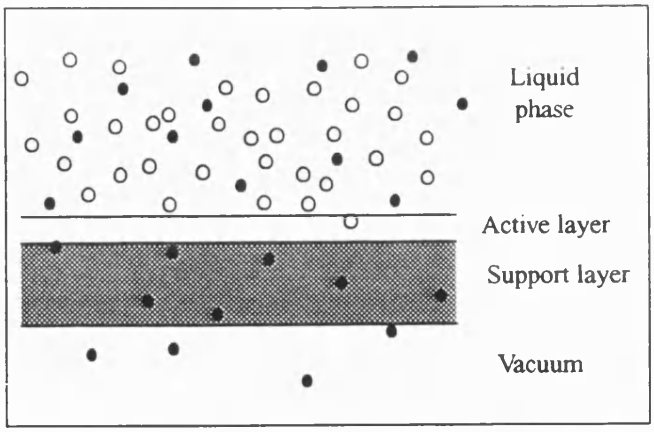

Figure 1.1 Principle of pervaporative separation

transport is a chemical potential difference between the two phases separated by the membrane, resulting in an induced concentration gradient within the membrane interphase. The chemical potential gradient is effected by either applying a vacuum on the permeate side, using a sweep gas to remove permeate or by use of a temperature gradient. Heat of evaporation is required by the permeating component(s) and hence, a temperature drop both of the retentate and across the membrane to the permeate occurs. A unique feature of pervaporation is the anisotropic swelling of the membrane as a result of the concentration gradient, from the highly swollen feed side to the virtually dry permeate side.

Separation of feed components is determined by differences in partial vapour pressures and permeation rate through the membrane. If significant differences in membrane permeability of each component of the mixture are found under the process conditions used, PV may be used as a separation process for the fractionation of liquid mixtures. Factors which affect the efficiency of the process include membrane type and structure, operational temperature, downstream (permeate) pressure, feed composition, module and system design. Tailor-made membranes are required for effective separations.

1.2.1 MODES OF OPERATION

Three modes of operation are in use:

Vacuum Pervaporation

This is the most common mode of operation. Partial pressures of permeants are reduced by decreasing the total downstream pressure. Ideal fluxes and intrinsic membrane selectivity can usually be obtained when the fugacity, or in other terms the chemical potential, is held close to zero.

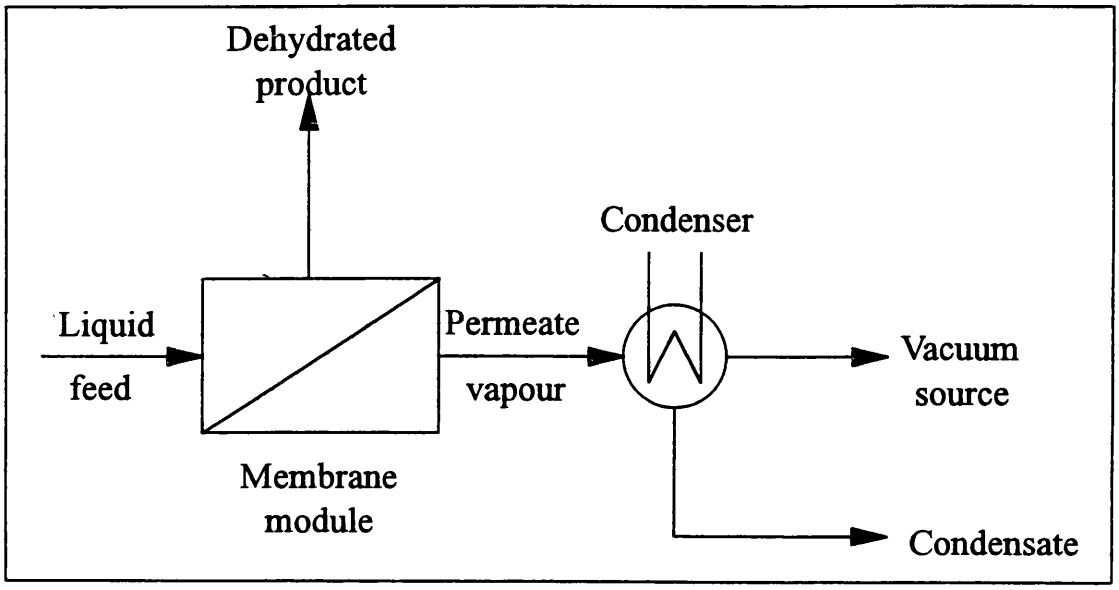

Figure 1.2 Basic module diagram (Strathmann, 1990a)

Sweep gas pervaporation

Partial pressures of permeants are reduced by gaseous dilution. Molecules desorbed by the membrane are removed by the flow of a permanent gas through the permeate compartment of the module. Vapour-loaded sweep gas can be cooled in liquid nitrogen where permeate vapours are frozen out. The cooled gas can be reheated and recycled.

A disadvantage of this mode of operation is that lower fluxes are obtained than for vacuum pervaporation: the porous support has a higher hydrodynamic resistance as the pores are filled with gas molecules leading to an additional diffusional transport resistance. Also, a large gas stream has to be cooled to low temperature and there

is decreased condensation efficiency due to the high concentration of inert gas and low pressures of the vapours. Therefore, sweep gas pervaporation is only really useful when the permeate and carrier gas can be discharged to the atmosphere.

Thermopervaporation

A chemical potential difference is created by maintenance of a temperature gradient across the membrane. Flux increases with the temperature difference until comparable fluxes with vacuum pervaporation are achieved (Strathmann, 1990b). Selectivity also increases with increasing temperature difference until the maximum for vacuum pervaporation is achieved.

The drawbacks to the use of thermopervaporation are that a temperature difference of at least 50°C must be used for high flux and selectivity. Use of very low temperature on the permeate side is expensive, therefore the use of a temperature of 0-15°C on the permeate side and a high feed temperature (e.g. 80°C) is recommended. This could be a problem for some applications and module design is also expensive.

Böddeker (1990) discourages the use of the term thermopervaporation, however, and states that "the permeate is liquified on a condenser surface...since non-condensable gases are excluded this variant is adequately addressed as vacuum pervaporation."

1.2.2 ASSESSMENT OF PERFORMANCE

Performance is assessed in terms of flux, selectivity and energy consumption. An economical evaluation would account for energy costs, membrane costs and the value of the product.

Flux

Permeation fluxes are calculated from the mass and composition of the permeate. Using flux as a performance indicator infers that performance assessment is based upon mass transfer of the permeated species irrespective of whether this or the retentate are the desired product.

$$\textit{Flux} = \textit{Permeability} \times \textit{Driving Force} \tag{1.2}$$

Permeabilities of individual permeants in a mixture differ from the corresponding single component permeabilities because of interactions between components.

Selectivity

Three dimensionless terms are in use: S (selectivity), α (separation factor) and β (enrichment factor). For binary mixtures:

$$S_{i,j} = P_i/P_j \tag{1.3}$$

The selectivity is the ratio of permeabilities and is useful for characterising a membrane. It is determined only by the membrane and the permeating components, not the feed composition, provided permeabilities are independent of concentration.

The separation factor is defined as:

$$\alpha_{ij} = \frac{(w_i/w_j)''}{(w_i/w_j)'} = \frac{(p_i/p_j)''}{(p_i/p_j)'} = \frac{(x_i/x_j)''}{(x_i/x_j)'} \tag{1.4}$$

α has the same numerical value whether weight fraction, partial pressure or molar fraction terms are used. α is usually fixed to be greater than 1. It relates directly to the inlet feed composition and is therefore problem orientated, but it is not an "effective separation factor" which would compare compositions of the products,

i.e., the retentate and permeate. If $\alpha=1$ at any point during the pervaporation process, the feed is known as a quasi-azeotrope.

The enrichment factor, β_i, is defined as:

$$\begin{aligned} \beta_i^w &= w_i''/w_i' \\ \beta_i^x &= x_i''/x_i' \\ \beta_i^w &\neq \beta_i^x \end{aligned} \qquad (1.5)$$

If the units used for α and β are the same, α is always greater than β.

Selectivity can also be visualised by a McCabe-Thiele diagram (Figure 1.3). This can indicate membrane selectivity across a range of feed compositions, which is more useful than a single value of α or β.

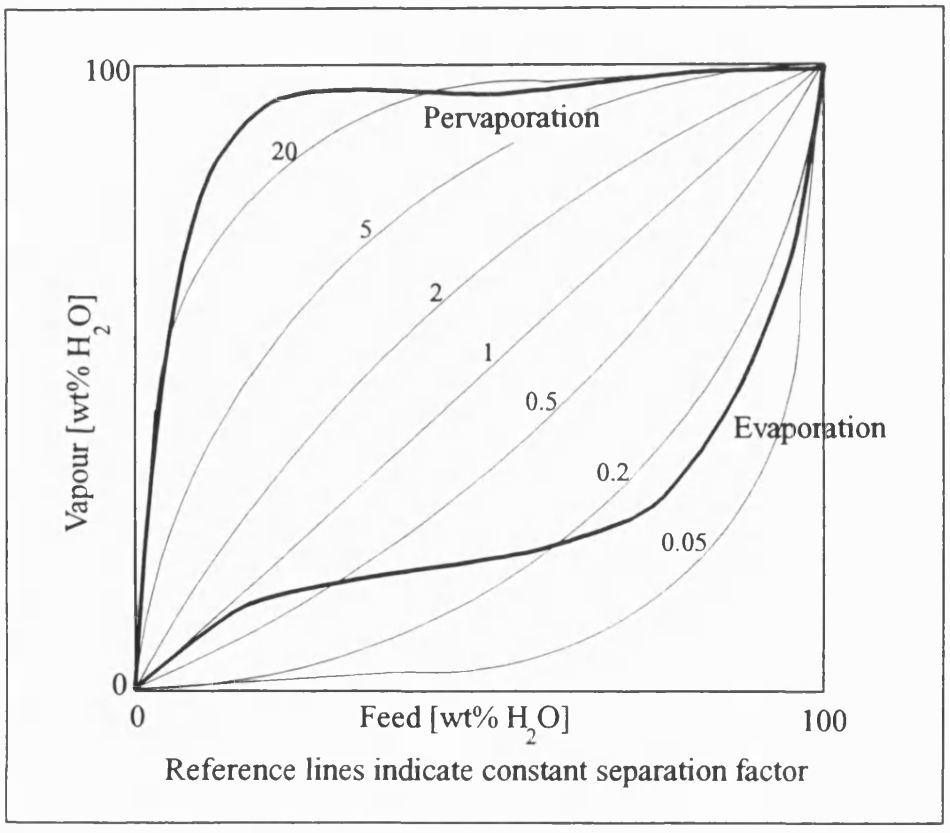

Figure 1.3 McCabe -Thiele diagram (Böddeker, 1990)

1.2.3 APPROACHES TO MODELLING THE MASS TRANSPORT

Three approaches to modelling the mass transport in pervaporation are found: an adapted solution-diffusion model, a thermodynamic accounting approach and the novel pore-flow model. The solution-diffusion model is the most widely used and is considered below in detail. Thermodynamic accounting is envisaged to be a two-step process: an equilibrium evaporation followed by membrane permeation by the hypothetical vapour. The approach may be visualised by a Thompson diagram (Figure 1.4). A more recent use of this approach is contained in a paper by Wijmans and Baker (1993). The development of the pore flow model is given by Okada and Matsuura (1991, 1992).

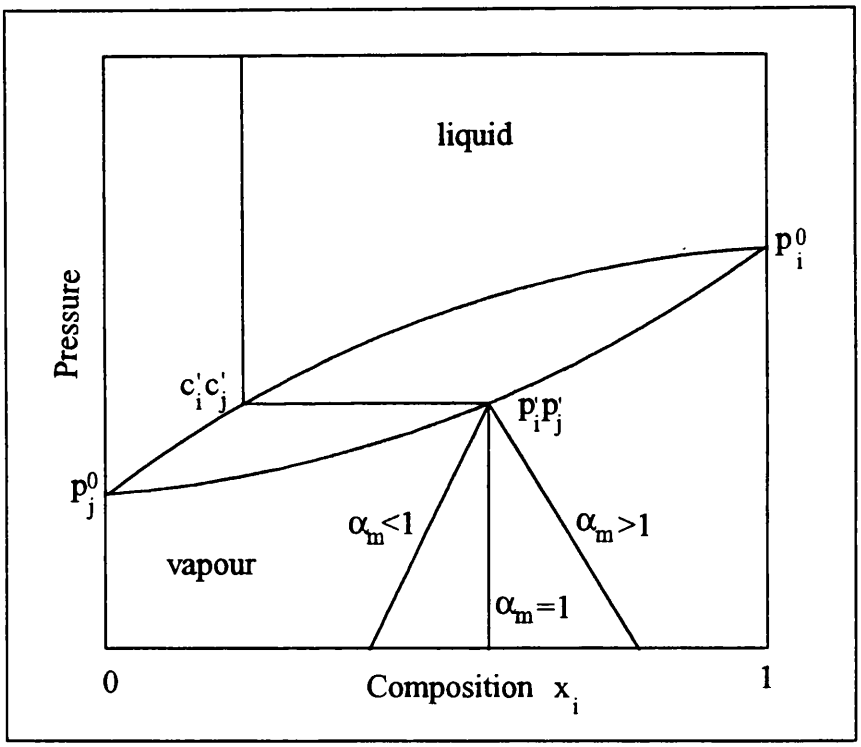

Figure 1.4 Thompson diagram (Shelden and Thompson, 1978)

Solution-Diffusion Model

The solution-diffusion transport model was first suggested by Lonsdale,

Merten and Riley in 1965. A series of papers by Shelden, Thompson and co-workers (Duggel and Thompson, 1986; Greenlaw *et al.*, 1977, 1978; Knight *et al.*, 1986, Shelden and Thompson, 1978, 1984) further developed and applied the model to differing systems. Several assumptions are made:

(i) Fick's law is applicable:

$$J_i = -D_i \frac{dc_i}{dz} \tag{1.6}$$

and the diffusion coefficient, D, is concentration independent.

(ii) At each membrane interface, the solution in contact with the membrane is in equilibrium with the permeant dissolved in the polymer at the membrane face and the concentration of each component is proportional to the activity in the outer phase adjacent to the membrane interface. Molecular diffusion at interfaces is much faster than the diffusion in the membrane.

(iii) The pressure throughout the membrane is constant and is equal to the upstream pressure.

Integrating equation (1.6) across the membrane thickness, l, gives:

$$J_i = \frac{D_i(c_i' - c_i'')}{l} \tag{1.7}$$

For an ideal gas, Henry's law states:

$$c_i = S_i p_i \tag{1.8}$$

where S_i is the solubility coefficient of component i, which depends upon the temperature and nature of the system. If assumption (ii) holds:

$$J_i = \frac{D_i S_i (p_i' - p_i'')}{l} \qquad (1.9)$$

However, in general, both D and S vary with feed composition and Henry's law is not obeyed.

It is readily seen that:

$$P_i = S_i D_i \qquad (1.10)$$

The permeability varies with the sorption (solubility) and diffusion coefficients and therefore, increases with increasing tendency of the permeating component to dissolve in the membrane material and decreasing resistance to its motion through the membrane. For feed mixtures, interactions between components must also be considered. Modelling efforts which relate pervaporation selectivity to the ratio of pure component permeabilities are usually non-predictive.

Sorption

Sorption of a component occurs at the feed-membrane interface and can be approximated by liquid-phase or saturated vapour equilibrium sorption measurements. Sorption selectivity occurs when one or more permeants is preferentially sorbed. Selectivity and the extent of sorption is dependent upon interactions between solvent molecules and the membrane. The stronger the chemical interaction between solvent and polymer, the better the sorption. Affinity between species comes from van der Waals forces, hydrogen bonding and sometimes complexation. If interactions are particularly strong, the polymer may dissolve in the solvent but this is inexpedient in a membrane process and must be prevented by either chemical cross-linking, grafting or blending with a more inert polymer. The extent of swelling is dependent upon the chemical nature of mixing and the elasticity of the polymer network. Cross-linking

the polymer restricts swelling and a membrane with many cross-links is less sensitive to changes in feed composition as volume expansion is more limited.

In the solution-diffusion model, selectivity may be due to a difference in the sorption coefficient, the diffusion coefficient, or both. If the permeant molecules are a similar size and shape, sorption selectivity is likely to be more important, whereas if they are very different in size, there may be a pronounced difference in the diffusion coefficients. Therefore, sorption selectivity is not necessarily the same as pervaporation selectivity.

$$\alpha_{PV} = \alpha_S \alpha_D \tag{1.11}$$

The effect of concentration on sorption selectivity depends upon the concentration dependence of the activity coefficient of the preferentially sorbed permeant. If, at high concentration, the preferentially-sorbed species causes significant swelling of the polymer network, molecules of the non-preferentially sorbed species may enter the membrane.

Hence, where an increase in flux occurs due to improved sorption, a loss in selectivity may also be noted (Nguyen, 1986; Ping *et al.*, 1990; Rautenbach *et al.*, 1988b). The concentration dependence of polymer sorption is shown by sorption isotherms (Figure 1.5).

Diffusion

Diffusion is concentration dependent and therefore varies across the thickness of the membrane. For pervaporation of a pure liquid through a given membrane, the

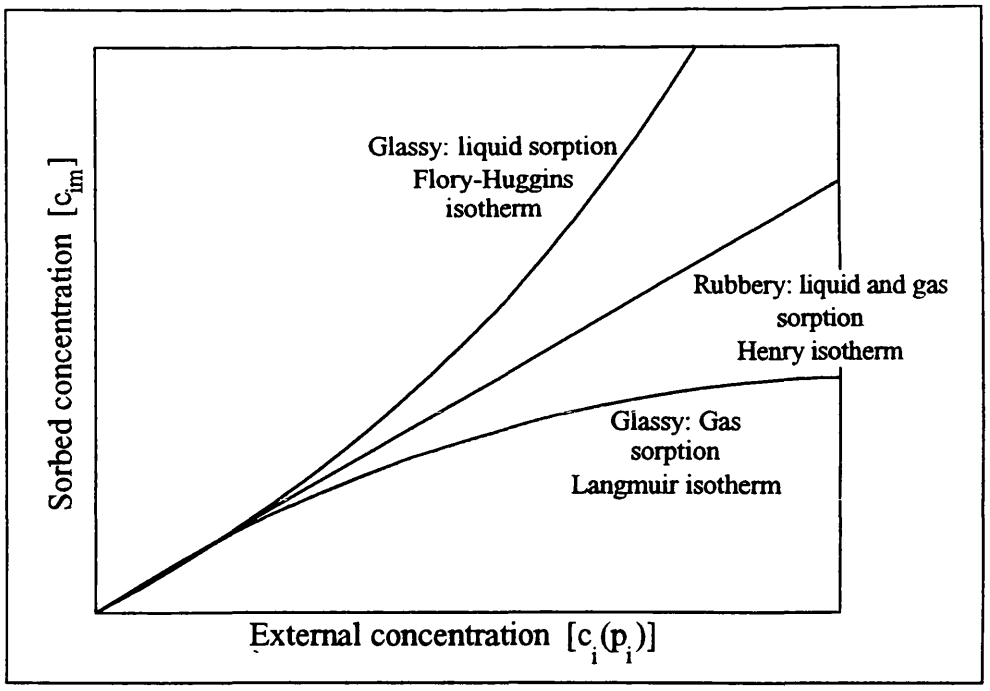

Figure 1.5 Sorption isotherms (Böddeker, 1990)

most common functional relationship for the effect of concentration on diffusivity is (Nguyen, 1986):

$$D_i = D_i^0 \exp(k_i c_{im}) \tag{1.12}$$

where c_{im} is the local concentration and D_i^0 is the diffusion coefficient for zero permeant concentration in the membrane. The latter is a function of the structures of both the solvent molecule and the polymer. More bulky solvent molecules manifest lower values of the diffusion coefficient. k_i is the plasticizing parameter which characterises the membrane-permeant interaction. Liquid can act as a plasticizer, allowing stiff polymer chains to move more easily amongst very mobile solvent molecules. k_i is related to the interaction parameter of Flory-Huggins theory of solvent solubility in polymers.

In some cases, the diffusion coefficient decreases with increasing concentration. This is ascribed to the tendency of some molecules to mutually associate, forming "clusters," e.g. water. Molecules in a cluster are much more

immobile (Nguyen, 1986).

In multi-component systems, diffusion for an individual permeant is dependent upon the concentration of all species at the membrane surface (not necessarily the bulk concentrations) and additional coupling and interaction parameters are required to define its relationship with concentration. For a binary mixture, Nguyen (1986) suggests the relationship:

$$D_i = D_i^0 \exp(k_{ii}c_i + k_{ij}c_j)$$
$$D_j = D_j^0 \exp(k_{ji}c_i + k_{jj}c_j) \qquad (1.13)$$

where k_{ij} represents the plasticizing effect of the j component on the diffusion of the i component. The term "negative coupling" is used to describe the inhibition of one component towards the diffusion of another. "Positive coupling" can also occur. Empirical constants such as k_{ii} and k_{ij} are required for many simulation models.

1.2.4 MEMBRANE POLYMERS

The correct type of polymer must be chosen for the application under consideration. It must give the required flux and selectivity plus resistance to the feed components at the temperatures used. For the separation of aqueous-organic mixtures, polymer materials fall into three structural groups:

Glassy (amorphous) Polymers : These preferentially permeate water molecules, although those incorporating fluorinated surface groups can permeate organics (Brüschke, 1991).

Elastomeric Polymers : These preferentially interact with the organic component. The polymers may be rubbery or segment-elastomeric.

Ion-Exchange Polymers : These may be viewed as cross-linked electrolytes. They interact with water but also some organic substances such as carboxylic acids and

phenols by specific reactions. For example, Ping *et al.* (1990) loaded a grafted poly(acrylic acid) membrane with different counter ions and looked at the effect on swelling and permeation characteristics. Permeation of water from an ethanol-water mixture was increased by the addition of K^+ or Na^+ ions to the membrane.

Selection of the polymer for an application may be aided by sorption and diffusion studies (Naylor, 1993). Saturated vapour studies can measure the ratios of feed components sorption in polymers. The diffusion of water in a membrane may be measured by pulsed field gradient spin echo nuclear magnetic resonance.

Materials may also be classed simply as hydrophilic or hydrophobic. There are four main types of hydrophilic membranes, given in Table 1.1.

POLYMER	WATER FLUX	SELECTIVITY	SOLVENT RANGE
PVA	Medium	Medium	Wide
Plasma	High	High	Wide
Polyacrylate	Very high	Very high	Not acidic feeds
Polyimide	Medium	High	Not chlorinated solvents

Table 1.1 Properties of Hydrophilic Membranes (Naylor, 1993)

Hydrophobic membranes are used for the removal of organics from waste water. They include polydimethyl siloxane, propriety silicone, polyetherblockamide and polybutadiene. The selectivity of hydrophobic membranes is currently not as high as for hydrophilic membranes.

An effective pervaporation membrane must exhibit strong interactions with one component of the feed mixture and swelling of the membrane may occur. The extent of sorption is dependent upon the equilibrium between the chemical tendency towards mixing and the allowed elasticity of the polymer network.

1.2.5 MEMBRANE STRUCTURE

Pervaporation membranes are dense, homogeneous films. The membrane should have a thickness that is commensurate with performance. Although pervaporation membranes are thicker than those used for reverse osmosis (greater than 1μm compared to a reverse osmosis skin layer of, typically, 0.1-0.5μm), a composite structure is nevertheless recommended for handling reasons. The GFT membrane emphasises this (Brüschke, 1988): the poly(vinyl alcohol) (PVA) separating layer is supported not only by a layer of porous poly(acrylonitrile) but also a layer of textile fabric for extra support and mechanical strength.

One interesting feature of asymmetric membranes was demonstrated by Rautenbach and Albrecht (1982, 1987). Permeation varied with the alignment of the membrane. If the thin, active layer faced the feed ("skin up"), a lower flux, but higher selectivity occurred than if used in the opposite direction ("skin down") In the skin down position, evaporation on the permeate side was unhindered, so a high flux resulted. However, concentration polarisation occurred in the pores of the support layer, adjacent to the feed solution, a problem which cannot be resolved by the alteration of flow conditions. In the skin up mode, high selectivity occurred, but transport away from the membrane was hindered on the permeate side by the convective transport of permeate in vapour in the pores. Hence, a lower flux resulted. These results may seem odd since it could be inferred that concentration polarisation occurring in the skin down mode of operation would lower the flux. However, in this case, it appear that "transport resistances in the porous supporting layer are so large that the flux scarcely differs from that of a symmetrical membrane of the same total thickness" (Rautenbach and Albrecht, 1987, p.15).

The microporous sublayer is a solid matrix with well defined holes which can range in diameter from less than 1μm to above 20μm. The sublayer can be symmetric or asymmetric and be made from a variety of materials, e.g. ceramics, metals or polymers. However, pressure loss of the permeate vapour in the porous substructure must be negligible to prevent a loss of driving force. As well as the Rautenbach and Albrecht paper, recent studies (Burslem, Naylor and Field, 1992) have shown that this may not always be the case as flux was found to vary with a change in support layer material and is further discussed in Chapter 6 of this thesis. The membrane should also have dimensional stability under swelling conditions.

1.2.6 MEMBRANE THICKNESS

Anisotropic swelling is a unique feature of pervaporation. The actual thickness of a membrane is dependent upon its swelling and therefore the feed to which it is exposed. However, in modelling, the membrane thickness is usually taken to be the dry thickness. From equation (1.9), flux is inversely proportional to thickness, therefore it may be presumed that an ultra-thin membrane is optimum. However, in multi-component pervaporation flux enhancement for all components to different degrees may adversely effect selectivity. The lower limit of practical membrane thickness depends upon the extent of interaction between system components and also the physical stability of the membrane. As a rule, highly swelling elastomeric membranes need to be thicker than low-swelling glassy membranes to maintain selectivity. Very thin membranes yield an enhanced flux which may also lead to difficulties in maintaining the downstream pressure and the avoidance of concentration polarisation. The influence of membrane thickness is further discussed in Chapter 4.

1.2.7 PERMEATE PRESSURE

The permeate pressure, practically taken to be the gauged downstream pressure, is the total pressure of vaporised permeant(s) in contact with the membrane, ideally devoid of non-condensible gases. It governs the chemical potential of the pervaporant at the membrane-vapour interface and therefore the driving force for mass transport. Many workers have looked at the consequences of varying this parameter (Blume *et al.*, 1990; Greenlaw *et al.*, 1977; Knight *et al.*, 1986; Néel *et al.*, 1986; Nguyen, 1986, 1987; Shelden and Thompson, 1978, 1984). In all cases, as the downstream pressure increases, the driving force, and therefore the flux, decreases, although there is a region of very low downstream pressure where flux remains constant. A Thompson diagram (Figure 1.4) may be used to visualise the effect of permeate pressure on permeate composition. Usually, the selectivity decreases as the pressure increases because the membrane becomes more swollen and penetration of the polymer network by the non-preferential component is more easily achieved. An exception to this occurs when the more volatile component is preferentially permeated (see Section 1.2.8).

The highest conceivable component partial pressure is the saturation vapour pressure, p^0. When the downstream pressure exceeds that of saturation, virtually no separation is achieved. Conditions of high vacuum are preferable but economic feasibility must be considered. A technical operation will compensate optimal driving force with feasible permeate pressure. A typical industrial operating pressure is 10mbara.

1.2.8 FEED COMPOSITION

Knight *et al.* (1986) identified three categories of feed mixture practically by observing changes in selectivity with alteration of downstream pressure:

(i) The preferentially permeating solvent has lower volatility. Although at high vacuum on the downstream side there is little diffusivity of the more volatile component, as the downstream pressure increases the membrane becomes more swollen and the diffusion of this component increases. As it has higher volatility, the movement across the membrane is less restricted than that of other components as the pressure increases. Selectivity reversal may even occur. However, both maximum flux and selectivity occur at vacuum downstream. Pervaporation of this mixture is superior to partial vaporisation.

(ii) The more volatile component is preferentially permeated and selectivity increases with increasing downstream pressure. These mixtures tend to be non-ideal solutions where the less volatile component is highly branched or polar.

(iii) The more volatile component is preferentially permeated but flux and selectivity decrease with increasing downstream pressure. Only a modest separation is achieved and at best, the richest product obtainable by equilibrium vaporisation is achieved.

Solvent interaction is further important in selectivity with regard to the breakage of azeotropes. A positive azeotrope is one in which interaction between identical solvent molecules is stronger than that between different molecules. This type of mixture can be efficiently separated by pervaporation. Negative azeotropes are not separated by pervaporation.

1.2.9 FEED CONCENTRATION

The concentration of feed at the feed-membrane interface is a product of the activity of the component and its solubility in the polymer. Viewing sorption only as an equilibrium distribution ignores the importance of activity of the solution components at the feed-membrane interface. The thermodynamic activity of a liquid solution component is manifested by its partial vapour pressure:

$$p_i' = x_i \gamma_i p_i^0 = a_i p_i^0 \qquad (1.14)$$

Notes about the calculation of activity coefficients and activities are found in Appendix D. Ideal solution behaviour occurs when $\gamma_i = 1$ ($a_i = x_i$) and $\gamma_i \to 1$ for $x_i \to 1$. If $\gamma_i > 1$ (positive deviation), the thermodynamic activity is higher than the concentration and this effect increases with dilution. As a result, the pervaporation separation effect, in terms of selectivity, tends to increase as depletion progresses. If $\gamma_i < 1$ (negative deviation), the thermodynamic activity is less than the concentration and polymer sorption of the component is decreased, adversely affecting separation. Positive deviations from Raoult's Law are associated with positive azeotropes, which, as stated in Section 1.2.8, are readily separated by pervaporation. Negative azeotropes are not separated by pervaporation.

In membranes made from polymer blends, a higher concentration of strongly interacting polymer component in the membrane will lead to increased swelling with the resultant increased fractional free volume in the polymer network. The result of this is that molecules of the less well interacting feed component can penetrate the membrane interphase and selectivity will drop. However, if the polymer network is linked, either physically, by crystals or inert portions of polymer, or chemically, by cross-links, polymer volume expansion is limited and therefore there is less variation

in the extent of sorption. A cross-linked membrane should be less sensitive to composition changes. Figure 1.6 illustrates this.

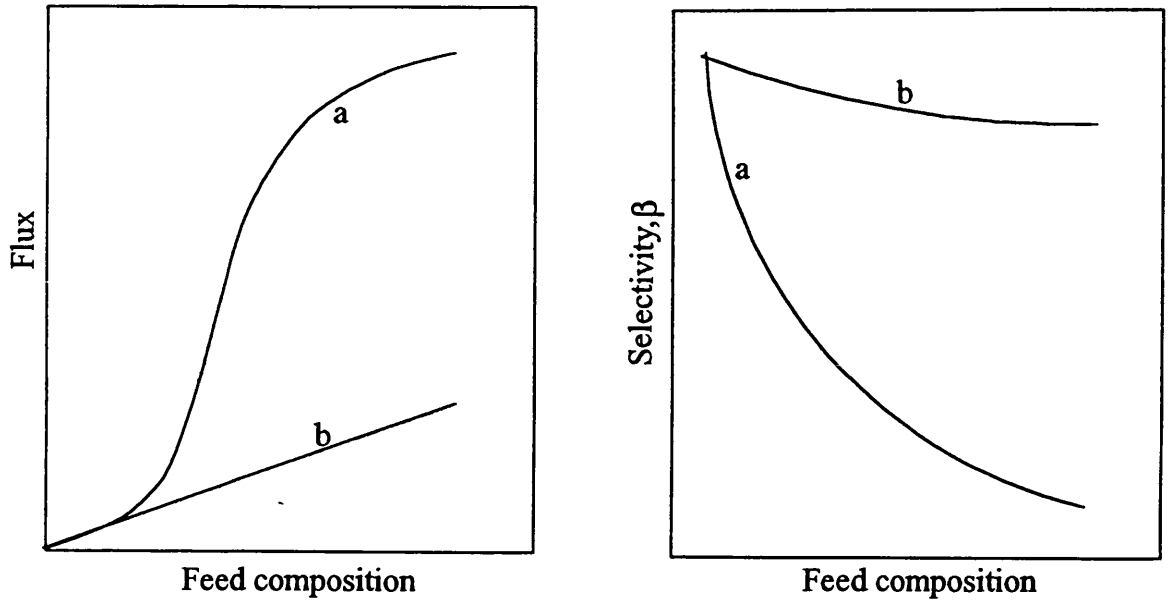

Figure 1.6 Flux and selectivity vs concentration (adapted from Nguyen, 1986)

It can be seen that the cross-linked membrane suffers less of a decrease in selectivity with increasing concentrations of the preferentially permeating component. The flux curve for the non-cross-linked membrane is S-shaped. The initial increase in flux is due to the exponential dependence of the diffusion coefficient on the concentration of sorbed permeants and the increase in sorbed amounts due to the increase of preferential solvent in the feed. The increase in flux then slows down markedly at high concentrations of preferential solvent due to the fact that the polymer network cannot swell beyond the limit of elasticity of the material.

1.2.10 TEMPERATURE

The process temperature is taken to be that of the inlet or an average of the module inlet and outlet temperatures. The dependence of flux upon temperature generally follows an Arrhenius-type relationship (Cabasso *et al.*, 1974; Huang and

Jarvis, 1970):

$$J = J_0 \exp(E_p/RT) \qquad (1.15)$$

where E_P is the apparent activation energy for permeation, usually between 4 and 15kcal/mol (16-63kJmol^{-1}) (Nguyen, 1986). An increase in flux should be catered for by an efficient vapour removal system otherwise an increase in downstream pressure may lead to a loss of selectivity. The effect of the temperature rise itself on selectivity depends upon the major factor which governs it. If selectivity is due to sorption, it should decrease with increasing temperature as solubility differences decrease. If selectivity is due to differences in diffusion rates, variation in selectivity depends upon the activation energies of each component (Nguyen, 1986; Rautenbach and Albrecht, 1987).

The apparent activation energy for permeation is a product of the heat of sorption and the apparent activation energy for diffusion of each component. Since heat of sorption is usually much smaller than the apparent activation energy for diffusion, the latter could be held to be the main contributor to the apparent activation energy for permeation. As revealed in Chapter 7, concentration polarisation influences the apparent value. A distinction will be made between the apparent and the actual (intrinsic) activation energy.

At higher temperatures, Nguyen (1987) claims that the pressure threshold at which the injurious effect of higher downstream pressure on selectivity start, increases rapidly. As the permeation flux simultaneously increases, necessitating increased pumping to maintain vacuum, this effect is not a great advantage.

Overall, an increase in temperature will lead to an increase in productivity, any loss in selectivity being compensated for by an increase in permeation rate.

However, to maintain performance, higher energy costs inflicted by the extra heat requirement and pumping power are required.

1.2.11 FEED FLOW

Flow regimes on both sides of the membrane can promote or inhibit mass transfer. Vapour transport through the pores of a support layer and away from the membrane can, as discussed in Sections 1.2.5, 1.2.7 and 1.2.12, affect process efficiency. Concentration polarisation on the feed side results in mass transfer inhibition. The liquid boundary layer can be seen as a homogeneous stagnant film which provides an additional resistance to permeation (Strathmann, 1990a). If the boundary layer and the membrane are seen as two resistances to mass transport in series, a transport equation may be constructed:

$$J_i = \frac{a_i' - a_i''}{(l_m/P_{i,m}) + (l_{BL}/P_{i,BL})} \qquad (1.16)$$

where a'_i and a''_i are feed and permeate side activities, respectively, and l_m and l_{BL} are the thicknesses of the membrane and the boundary layer. $P_{i,m}$ and $P_{i,BL}$ are the permeabilities of component i through the membrane and boundary layers.

The driving force in this equation is the activity difference across the two layers. A similar model will be used to decouple the resistances to mass transport existing for the work of this thesis (Chapters 4, 5 and 6).

If permeating components have low solubilities in the solvent and the membrane permeability is high, the liquid boundary layer will be very significant and could effect selectivity, as well as flux. Strathmann (1990a) found that for a feed mixture of acetone, butanol and ethanol in water, for the permeation of organics through a PDMS composite membrane with a hollow fibre module, the enrichment

factor, β, increased with increasing Reynold's number for the permeation of acetone and butanol. This suggests that the boundary layer partly controls selectivity, as well as individual component fluxes.

If the membrane has a low transport resistance (high flux) as compared to that of the liquid boundary layer, it determines the solvent flux but not that of the solute. Only if the membrane is the major transport resistance can its intrinsic selectivity be known. This relates to the concept of a limiting membrane thickness, i.e. the minimum thickness before selectivity declines.

Permeation through the boundary layer is affected by the fluids physical properties which are temperature dependent. Consequently, the resistance of this layer can only be influenced by temperature and hydrodynamics (Bengtson and Böddeker, 1988). Concentration polarisation may be avoided by increasing the turbulence. The effects of turbulent flow on mass transfer may be calculated from Sherwood correlations. These correlations are reviewed for membrane applications by Gekas and Hallström (1987).

Turbulence promoters and the potential of pulsatile flow has recently received attention (Colman and Mitchell, 1990; Kennedy *et al.*, 1974; Mackley, 1987; Nguyen, 1986; Poyen *et al.*, 1987). Despite increasing the mass transfer coefficient above that of laminar flow, turbulent flow still achieves low separation per unit length, necessitating the use of batch or recycle systems or much larger membrane area as well as high pumping costs. Even in the turbulent flow regime, radial velocity for tubular systems is still only 10% of the axial component and so radial velocity profiles develop across a tube. Mixing in this direction is less than satisfactory and hence poor mass transfer may result. Mackley (1987) outlined the

potential for oscillatory flow eddy mixing where fluid can be fully mixed by flow reversal around sharp edges, e.g. baffles. Even at low mean flow velocity the ejection and destruction of vortices create mixing. Low power consumption compared to turbulent cross-flow operation is a major advantage and separation per unit length is high. The use of baffles, whilst gaining momentum in MF and UF processes, has not yet received attention for use in pervaporation systems.

1.2.12 MODULES AND PROCESS DESIGN

If mass transport through the membrane only is considered, performance is over-estimated. Predictive calculations should also take concentration boundary layers, pressure drops, flow patterns and heat fluxes into account.

At present, module designs are based upon those of other membrane separation systems, e.g. plate and frame, spiral wound, hollow fibre, tubular. Plate and frame modules contain many "o" ring seals with the potential for leaks but a wide range of seal materials are available and comparability with the feed is not a problem. Spiral wound and hollow fibre modules both use glues for sealing and some doubt may exist about their long term stability but work carried out by a Texaco research team would seek to discredit this notion (Bartels *et al.*, 1992).

A low cost module per installed membrane area is preferable as is high packing density (m^2m^{-3} of permeate vessel). Gains in packing density for spiral wound and hollow fibre modules in gas separations are not replicated in pervaporation usage without an increase in downstream pressure attainable. Modules should be designed to minimise downstream pressure losses. Pressure build-up can occur in a part of a module if the amount of preferentially permeating component is high and the volume available for vapour transmission is small. For example, in plate and

frame modules, pressure build-up may occur near the feed inlet if the vapour pumping port is far away. A multi-port system is preferable. Hollow fibre modules are particularly prone to vapour build-up and condensation may even occur at the contact point between two fibres (Nguyen, 1986). A gain in compactness is accompanied by a decrease in performance. It is better to over-design the vacuum pumping system to account for variations in flux than to under-design it. Detailed investigations may bring further design improvements. For example, Rautenbach and Albrecht (1987) have suggested that for hollow fibre designs, each fibre length has an optimum diameter for efficient performance.

Heat of evaporation is consumed from the feed solution, resulting in cooling along the module. Feed solution temperature must be maintained, which may require heating stages between modules. Individual plants can be tailored to needs by using larger membrane areas between heating stages as the concentration of preferentially permeating component, and therefore flux and temperature drop, decrease.

Single stage and permeation cascades are the simplest designs. In the cascade system, groups of modules, in parallel or series, are interspersed with heat exchangers to maintain the feed temperature. Partial permeate or product recycle may be used to keep the feed composition constant.

A pervaporation cascade may utilise the permeate of one stage as the feed of the second stage. For example, the recovery of fermentation alcohol can be achieved by pre-enrichment using an elastomeric membrane and subsequent dehydration making use of a glassy membrane.

1.2.13 ENERGY REQUIREMENTS

Parts of the pervaporation process that require energy input are feed input

(pumping), feed heating, permeate removal and permeate condensation. Feed side pumping requirements are low as the feed is only pressurised such that it remains liquid at elevated temperatures and to overcome any pressure loss due to the flow path. Whilst operating temperatures are lower than distillation, for dewatering processes, feed heat requirements are significant as the latent heat for evaporation of the permeate is gained from the sensible heat of the feed. The temperature used is the maximum that the feed or membrane can withstand. Processes which involve the removal of organics or heat sensitive compounds usually operate at low temperatures and therefore the heat requirement is less significant.

Vacuum pump power requirements are very low. In most industrial systems the pump is used for start-up and the removal of non-condensibles (from system leakages) only. The condenser maintains the low permeate pressure, which is determined by the condenser temperature. Permeate vapour is normally condensed for recovery, recycle or disposal. The energy requirement for this is equivalent to the latent heat required for evaporation of the permeate. A refrigeration energy input is normally required as condensation is usually carried out at 0-10°C.

1.2.14 APPLICATIONS

The term "pervaporation" was first used by Kober in 1917 but the first reported separation of a liquid mixture by the technique was in 1906 (Kahlenburg, 1906). The first study of alcohol dehydration by pervaporation was a thesis produced in France (Schwob, 1949).

The first commercial venture involving pervaporation was implemented by Binning and co-workers (Binning *et al.*, 1960, 1961) but there was little success at that time. The more recent increase in the number of polymer materials available and

the ability to produce ultra-thin membranes has yielded more applicable flux and selectivity values. The company GFT introduced the first successful pervaporation plant for alcohol dehydration in 1982 and where other plants are now in use it is mainly for this application. The water-selective membrane currently in use in industrial plants worldwide is the GFT composite membrane made from cross-linked poly(vinyl alcohol) (PVA) with a microporous poly(acrylonitrile) (PAN) support. In the UK, British Petroleum developed an alkaline metal polyacrylate membrane, upon the use of which this thesis is based, but its commercial success has been limited. Alternatives, which have been used on a laboratory scale but not installed industrially, are sulfonated poly(ethylene), poly(ethersulfone) and chitosan.

Alcohol dehydration by pervaporation is used as an alternative to, or in combination with, distillation, successfully utilising the former's ability to break azeotropes. The pervaporation selectivity can be very different from the distillation selectivity for a given mixture and may even be inverted. The advocates of one distillation/pervaporation hybrid process (Brüschke, 1988) claim that great savings can be made using this as an alternative to conventional distillation. Other hybrid processes, such as a combination of pervaporation and reverse osmosis, have been proposed (Rautenbach, Herion and Franke, 1988a).

The use of pervaporation is limited to the removal of volatile components only. Since the permeate must be provided with the energy of vaporisation and minimum energy expenditure is a primary aim of any separation process, most applications for pervaporation aim at depleting the feed of minor components. The potential of pervaporation in the commercial sector is likely to remain limited to processes where conventional technologies fail or are difficult to operate. These

include the breakage of azeotropes, separation of close boiling compounds, enrichment of heat sensitive products and elimination of trace impurities. Blume *et al.* (1990) found that water treatment to remove trace organic solvents from a level of 0.1wt% to 0.01wt% by pervaporation was economically competitive with other conventional processes, although the current feasibility of scale-up of this application is doubted by others (Rautenbach, Klatt and Vier, 1992). The enrichment required can be a determining factor as, along with most other membrane separation processes, it can cost as much to remove the last 9% of permeating solvent as the first 90%.

Pervaporation is useful in applications of biotechnology (Strathmann, 1990b) because the separation is a physical process which can often be carried out at ambient temperatures. It does not require high pressures, or additional chemicals. The structure of micro-organisms, enzymes and proteins will not be damaged and the process can be integrated directly into a fermentation process to continuously remove biosolvents with inhibitory effects on the rate of production in fermentation broths, resulting in higher production rates and decreased downstream processing costs. The removed component may be a product or a by-product and high selectivity, high flux membranes are not always necessary.

1.2.15 RELATED PROCESSES

Pervaporation can be distinguished from a number of similar processes.

Membrane Distillation

A non-wetted, microporous membrane separates two liquid phases which are at different temperatures (Burslem, 1993; Drioli, Yonglie and Calabro, 1987). The temperature difference results in a vapour pressure gradient across the two membrane faces and hence, a driving force for mass transfer. Molecules of the more volatile

component of the feed (hot) side evaporate and are transported, as a vapour, through the pores of the membrane to the cool opposite faces where they are condensed. The membrane only acts as a barrier between the two liquid phases and is not directly involved in the separation. Membrane distillation is most useful for the purification of water containing inorganic solutes, e.g. seawater. The permeate produced is high quality water suitable for use in the semiconductor industry or as boiler feed water for power plants.

Membrane Evaporation

In some respects similar to membrane distillation, this is the transfer of matter from the liquid phase to the vapour phase through the pores of a non-wetted porous membrane (Böddeker, 1990). Rather than low temperature liquid on the permeate side, a vacuum is applied to effect a mass transfer driving force. Membrane evaporation may be used for the purification of water containing trace amounts of volatile organics, such as ethanol or trichloroethylene. The volatile component has a partial pressure much higher than that of water and the permeate is enriched in this component. The separation is not dependent upon the chemistry of the membrane, as in pervaporation, but simply on the liquid-vapour equilibria.

Osmotic Distillation

Again, similar to membrane distillation, osmotic distillation involves the separation of two aqueous streams by a non-wetted, porous membrane. In this case, a concentrated brine solution (seawater and highly concentrated Magnesium sulphate have both been used) passes along one face of the membrane and the aqueous feed solution along the other. An osmotic pressure difference is set up and a water vapour flux occurs from the feed solution to the brine. Although flux increases with

temperature, the process can be run at or even below, ambient temperature, making osmotic distillation an attractive proposition for the food and pharmaceutical industries. It has successfully been applied to the concentration of fruit and vegetable juices by Lefebvre *et al.* (1987).

Pertraction

The permeate is dissolved in a circulating carrier fluid rather than being vaporised. The carrier fluid does not interact with the membrane and is subsequently separated from the permeate by distillation (Böddeker, 1990). This process has attracted little interest.

Vapour Permeation

The feed is vaporised before contact with the membrane. If the permeants are at saturation vapour pressure on the feed side, vapour permeation is thermodynamically equivalent to pervaporation but no phase change is involved. In energy terms, vapour permeation is disadvantageous unless the feed is already in the vapour state, *e.g.* a distillation column top product. Typical application proposed are solvent dehydration, azeotrope breakage (Sander and Janssen, 1991) and gasoline vapour recovery (Peinemann *et al.*, 1994).

1.3 SOLVENT RECOVERY

In 1990 the contribution of used solvents (both industrial and domestic) to the level of Western European volatile organic compounds (VOCs) was around 40% of the ten million ton total (Smallwood, 1993). This is the same contribution as was made by petrol distribution and use. VOCs are the precursors of photochemical oxidants such as ozone and therefore, solvent discharge into the atmosphere contributes to dangerous low level ozone generation.

Solvents are used in surface and metal coating, pharmaceutical production, household products, adhesives, dry cleaning and many other areas. Some solvents are incinerated in such a way that VOCs are not formed (although "greenhouse gases" are) but unless recovered, the rest is eventually discharged into the environment. Products may be reformulated to use less harmful solvents or water based emulsions and processes may be redesigned to use lesser volumes of more effective solvents. However, the use of solvents will never be eliminated and their recovery and recycling is a vital way of reducing atmospheric pollution from this source.

Ozone destruction at high atmospheric level is mainly due to two solvents: 1,1,1-trichloroethane and 1,1,2-trichlorotrifluoroethane. The former is used in metal cleaning whilst the latter is used more frequently in the electronics industry. Whilst ozone destruction is a worldwide problem, ozone generation is problematic on a more local scale.

The dumping of solvents was once commonplace but modern discharge standards are high and retrofitting equipment can be expensive and cause problems with plant layout. Legislation for a high percentage of solvent recovery is evolving in industrialised countries and the costs of recovery and destruction often parallel each

other. A third option is to utilise the solvent as a fuel but only hydrocarbons and methanol are economically comparable with the use of standard fuels. Chlorinated solvents are particularly attractive for recovery as they cannot be used as fuels and incineration costs can be three times the price of the virgin solvent.

Solvents to be recovered can be part of a mixture with air, water, solute or other solvents. The most desirable product of recovery is one that can be used in place of virgin solvent in the process in which it was generated, although its specification may not be as tight. In any recycle system, regard must be paid to the concentration build-up of harmful contaminants.

1.3.1 DRYING SOLVENTS

In organic solvent recovery, the most common separation is the removal of water. The specification for water content of the recovered solvent depends upon the negative effect water has on the process. Water can spoil solvent power, can slow down a reaction, e.g. esterification, and can even destroy some reagents, e.g. Grignard reagent. In the first instance, a solvent water content of 1wt% may be economically acceptable whereas in the last a water content of 100ppm or under may be required.

There are many drying methods to chose from, applicable for various situations. As well as examining the separation method from a recovery efficiency angle, the safe disposal of water removed must also be considered. This may contribute a significant cost to the process.

In the first instance, fractional distillation methods are usually considered. These exploit differences in relative volatility between components of a mixture and include atmospheric, vacuum, steam, azeotropic, extractive and pressure distillation.

Distilling under low, rather than atmospheric, pressure usually increases the relative volatility of components and also has the advantage that temperatures can be kept low, although condenser size must be increased.

Medium volatility solvents usually form azeotropes and distillation is affected by this. It is overcome in azeotropic and extractive distillation by the use of an entrainer and the choice of such is vital. In azeotropic distillation the entrainer forms an azeotrope with one component but not the other(s). The entrainer azeotrope should be easily fractionated by e.g. phase separation or fractionation. Energy expenditure in reaching and breaking the azeotrope, and recovering the entrainer, are high. A flowsheet for the azeotropic distillation of a water/2-propanol (IPA) mixture is given in Figure 1.7. Extractive distillation is based on using an entrainer that modifies the relative values of the activity coefficients to increase relative volatility. High volumes of entrainer and specialised equipment are required.

In pressure distillation, the composition of the azeotrope is altered by varying the pressure but this is a treatment only suitable for certain mixtures and also requires specialised equipment. The hazards of handling solvents at high pressures must also be considered.

Preferential adsorption of water onto molecular sieve, silica gel, alumina or organic adsorbents of an ion-exchange resin-type is a good method for drying solvents containing small amounts of water e.g. from 1% to 100ppm but the process cannot be made continuous easily.

Pervaporation is a continuous process and unlike distillation is not affected by azeotropes. Process cost will depend upon the product specification; to achieve low water levels it is necessary to accept a low driving force caused by the low partial

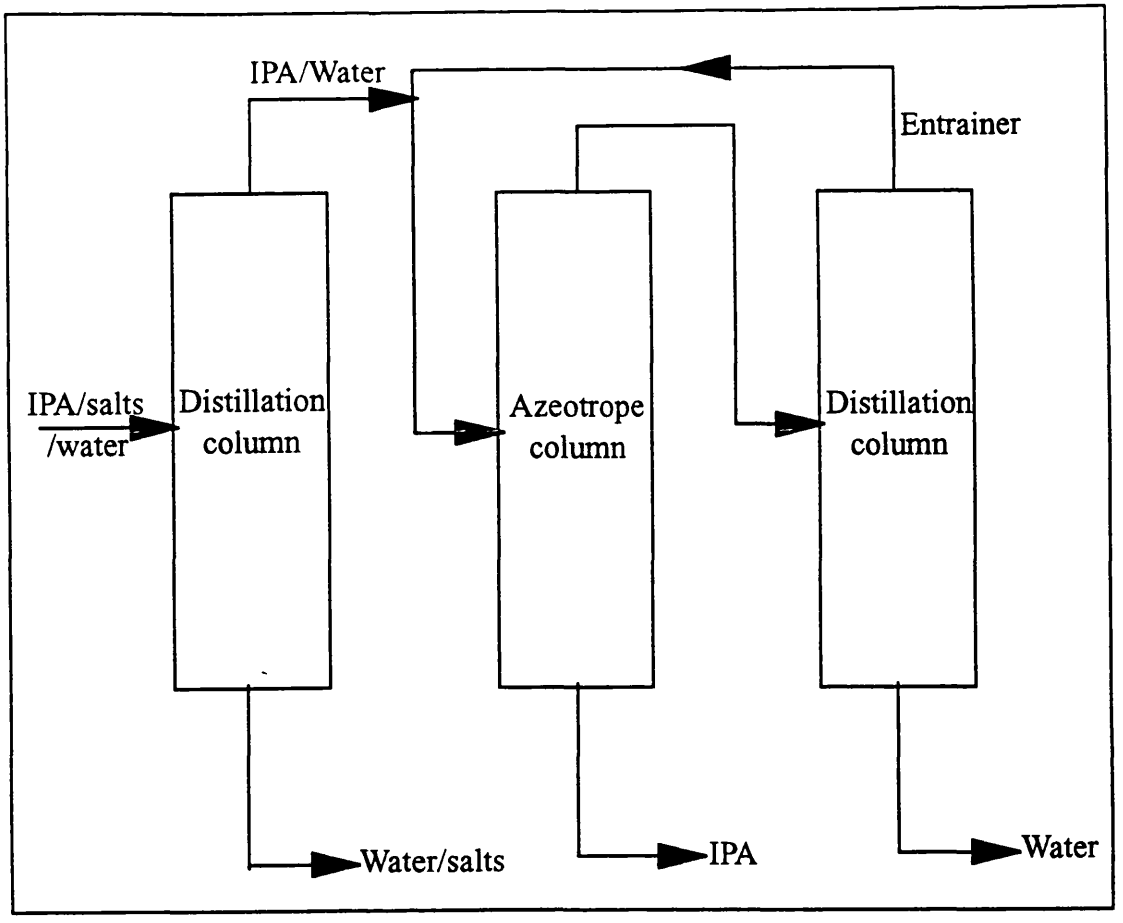

Figure 1.7 Process flowsheet for the azeotropic distillation of a water/2-propanol mixture

pressure of water in the solvent, although this is offset in most instances by the high activity coefficient of water in many solvents. Another restriction may be the poor resistance of the membrane material to the solvent. Membrane flux and lifetime will obviously also effect costs. The advantage of pervaporation is greatest on a small scale as its modular nature means that economics of scale do not apply. Unlike distillation, pervaporation is not affected by impurities in the feed and its optimum range is 1-15% water in the feed.

Some solvents may be suitable for liquid-liquid extraction if a suitable hydrophobic solvent can be found. The wet mixture is contacted with a very hydrophobic solvent into which the organic component preferentially moves. The

resultant two phases can be separated easily but the water will contain some solvent and may be unfit for disposal into effluent. Fractional liquid extraction uses two solvents and several extraction stages.

Chemicals can be used to dry solvents by hydration, reaction and chemisorption but this is more common on a small scale or for a final purification step. Salting-out contacts the wet solvent with a solid or an aqueous solution which has the power to remove some water. This technique is used in the drying of pyridine and MEK. In coalescing, the temperature of the mixture is reduced which usually causes some water to leave the solvent phase. A coalescing pad or electrostatic field is required to remove them quickly. Similarly, fractional freezing can be used on a laboratory scale for solvents with freezing points above 0°C.

There is almost always more than one possible separation method for a given system and the choice will depend upon the equipment available and the process economics. The effect of small concentrations of impurities such as inhibitors (e.g. ethanol in chloroform), denaturants (e.g. methylated spirits in ethanol) and plant rinsing chemicals must be considered as they can effect such properties as solubility coefficients. A combination of two methods is often economical, for example distillation to remove water to 1wt% followed by adsorption to 100ppm or the debottlenecking of a distillation process using pervaporation to break the azeotrope. A flowsheet for the latter is given in Figure 1.8.

1.4 PROPAN-2-OL

Alcohols account for approximately 14% of solvent consumption in Western Europe (Smallwood, 1993) and propan-2-ol (IPA) has been chosen as an example with which to investigate pervaporative drying. It has a low toxicity and contains

neither denaturants or inhibitors. It is totally miscible with water.

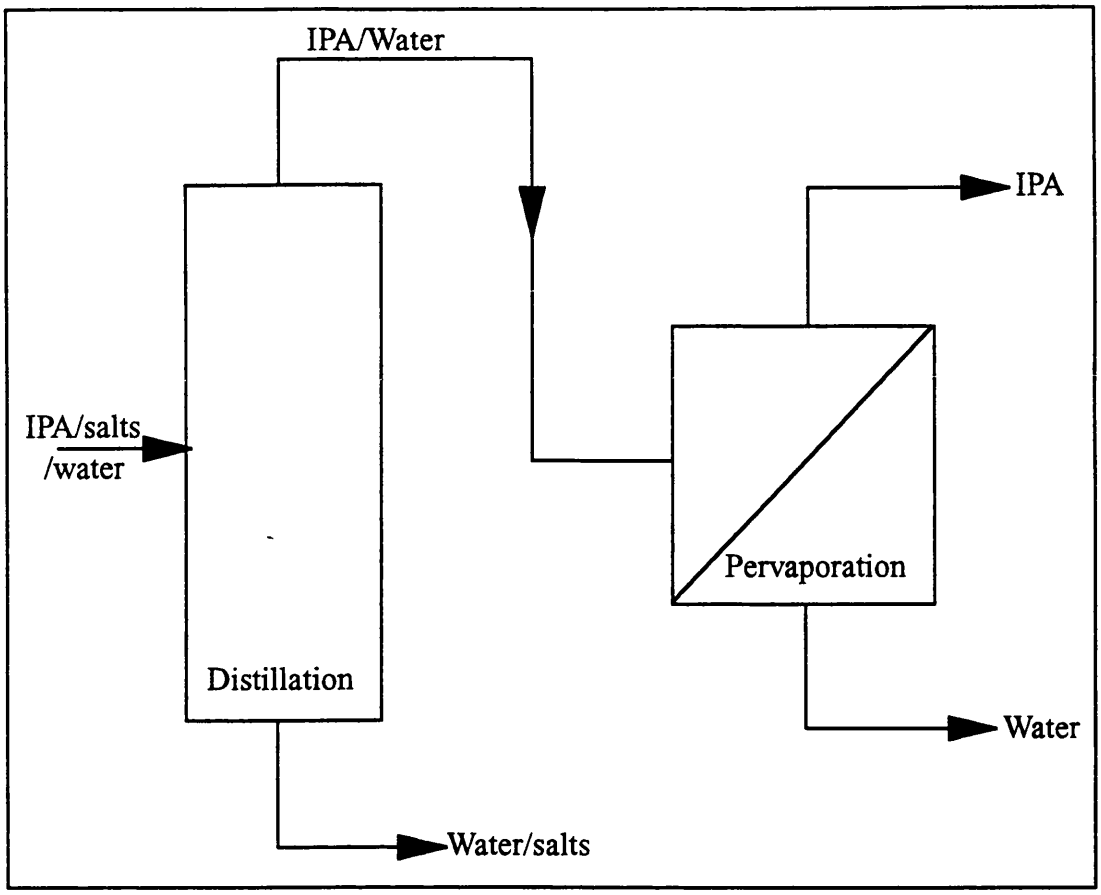

Figure 1.8 Process flowsheet for a distillation-pervaporation hybrid fractionation process (Naylor, 1993)

IPA forms an azeotrope with water at 88wt% IPA at 80°C therefore, if fractionation is chosen as the recovery method, it must be azeotropic distillation. Possible entrainers include diisopropyl ether (DIPE), toluene, benzene, diisobutylene (DIB), isopropyl acetate, cyclohexane and 1,2-Dichloroethane. Unfortunately, all of them form ternary, rather than binary azeotropes with the solvent mixture but once the azeotrope is overcome very dry IPA can be made as the relative volatility of the azeotrope from dry IPA is high.

Other suitable separation methods are adsorption and hydration.

Three examples of the requirement for IPA dewatering in industry and the effectiveness of pervaporation for such a purpose have been given by Naylor (1993). In the first, IPA was used as a carrier solvent and the dewatering of an IPA/reaction intermediate mixture was required. Initially, water created in the reaction stage was removed as the IPA azeotrope and the IPA then recovered by azeotropic distillation. In place of this, a single stage pervaporation step was used to reduce the water content of the batch from 7wt% to 2wt%. The water removed was clean enough to be disposed of direct to the effluent plant. Improved automation was introduced and with batch times being significantly lower than those for distillation, less than 18 months payback time for the pervaporation plant was achieved.

The second example was of the debottlenecking of an IPA/water distillation process. Plant production was bottlenecked by the azeotrope column. Pervaporation was used to enrich the feed to the azeotrope column resulting in an increase in production of pure IPA at the azeotrope column base.

The final example was of production improvement in the pharmaceutical industry. IPA was used as a reactant in an esterification reaction and could be recycled to the process provided that its water content was less than 1-2%. The use of pervaporation to achieve this dewatering was more economic than azeotropic distillation and batch times were less. Consequently, plant capacity was increased and for the pervaporation plant a payback time of under two years was achieved.

1.5 CONCLUSIONS

Pervaporation is still a relatively "young" membrane process in terms of commercial development. Within this chapter, its place within the range of membrane processes has been indicated and the parameters which affect performance discussed. Current applications have been reviewed and the requirement for solvent dewatering and recycling expounded. The experimental work undertaken to produce this thesis has applied a caesium polyacrylate membrane for the dewatering of 2-propanol. This membrane was developed by British Petroleum (BP) and has already been the subject of several published papers (Colman and Mitchell, 1990; Colman and Naylor, 1991; Colman, Naylor and Pearce, 1989, 1990; Colman *et al.*, 1989; Naylor *et al.* 1989). A more wide-ranging study of its properties is contained in the proceeding chapters, including some simple modelling to decouple the properties and performance of the membrane from those of the system in which it was used. The approach developed will be useful in the analysis of other pervaporation systems.

CHAPTER 2

PREPARATION OF MEMBRANES AND TEST RIG

2.1 INTRODUCTION

Polyacrylate membranes have been successfully developed by BP Research for the dehydration of alcohols (Colman *et al.*, 1989, 1990). The purpose of this work was to assess the properties of such membranes and the effect of process conditions on the efficiency of operation. For this purpose, membranes were fabricated and a test rig was constructed. The operation of the rig is detailed within this chapter along with an outline of the analytical methods used and details of the form of graphical presentation used for the results.

2.2 MEMBRANE FABRICATION

2.2.1 MATERIALS

General purpose polyacrylic acid with average molecular weights of 2000, 250000 and 4 million were supplied by Aldrich Chemicals. Caesium hydroxide was used in the form of a 50wt% solution, also supplied by Aldrich Chemicals.

2-propanol (GPR grade) was supplied by BDH and de-ionised water was produced within the department.

Porous support materials used included a polysulfone ultrafiltration membrane, GR40PP, with a 100 000 nominal molecular weight cut-off, supplied by Der Danske Suker Fabricker of Denmark. This company also supplied a poly(vinylidene fluoride) ultrafiltration membrane with a 30 000 nominal molecular weight cut-off. WL Gore supplied a Gortex membrane, with pore size 0.25-0.4μm and Bekaert Fibre Technologies supplied a stainless steel microporous membrane, Bekipor 5BL3, which had an average pore size of 5.3μm. Rigidmesh sintered stainless steel support

material was supplied by Pall International and had an average pore size of up to 15μm and a porosity of 31%.

2.2.2 METHOD

Polyacrylic acid powder, MW 250 000, was dissolved with stirring in deionised water to produce a solution of concentration 0.5wt%. For polymer of molecular weights 5000 and 4 million, a 5wt% solution and an 0.1wt% solution were produced, respectively. The variation in concentration was necessary to produce a solution within the viscosity range desirable for casting (Appendix A). The acidity of the polymer solution was pH 2. This pH was then adjusted to the desired membrane pH value by the slow addition of caesium hydroxide solution to form caesium polyacrylate (CsPA) casting solution, stirring well between each addition. When producing 500ml of solution, the neutralisation took up to 6 hours.

Two methods of casting the membranes were used.

Method 1 : The support material was first prepared. Polysulfone (PSf) and poly(vinylidene fluoride) (PVDF) membranes were soaked in two changes of deionised water for a total of two hours to remove the propionic acid, caustic soda and glycerine solution used to preserve their porous structure. They were then dried at room temperature. Bekipor, Rigidmesh and Gortex membranes required no preparation.

The support material was placed onto a glass plate. A known weight of polyacrylate solution was pipetted onto the support material into an area enclosed by a stainless steel ring. The glass plate was placed on a stand inside a fan oven, the feet of the stand having previously been adjusted such that the plate was horizontal. The water from the casting solution was allowed to evaporate at the required

temperature overnight, to leave a colourless film. The film and support material were cut around the inner circumference of the ring to yield a pervaporation membrane.

Method 2 : The polyacrylate solution was cast into a ring and dried as above, but the support material used for this process was Parafilm. Meanwhile, the porous support material to be used was prepared as outlined above. Immediately after drying, the pre-cut support layer was positioned on top of the polyacrylate layer, still attatched to the ring. The Parafilm was then carefully cut away from the ring and the polyacrylate layer. This layer was then gently cut out of the ring, taking care not to damage it.

Initially, for both methods, a check of final membrane weight was used to ensure that each membrane was dried to the same degree. Quality control for the membranes prepared was visual only. The absence of defects could only be ascertained once the membrane was in use in a pervaporation cell.

2.3 PERVAPORATION CELL

A cross-section of the test cell is shown in Figure 2.1. The cell was fabricated from stainless steel and comprised of two parts clamped together during operation by six bolts. The membrane was contained between the two parts. The area of the membrane enclosed by the upper portion of the cell was $1.810 \times 10^{-3} m^2$. The upper part of the cell included a magnetic stirrer bar which was suspended by a metal rod. There were three ports at the top of the cell which acted as a feed inlet and sampling port, an inlet for water metering (for constant feed composition experiments) and an inlet for thermocouples. The capacity of the cell was 500ml.

The lower part of the cell contained the permeate line and a porous metal disc which supported the membrane. The inner O ring provided a leak-free seal for the feed whilst the larger O ring sealed the vacuum system. Both O rings were made of Viton.

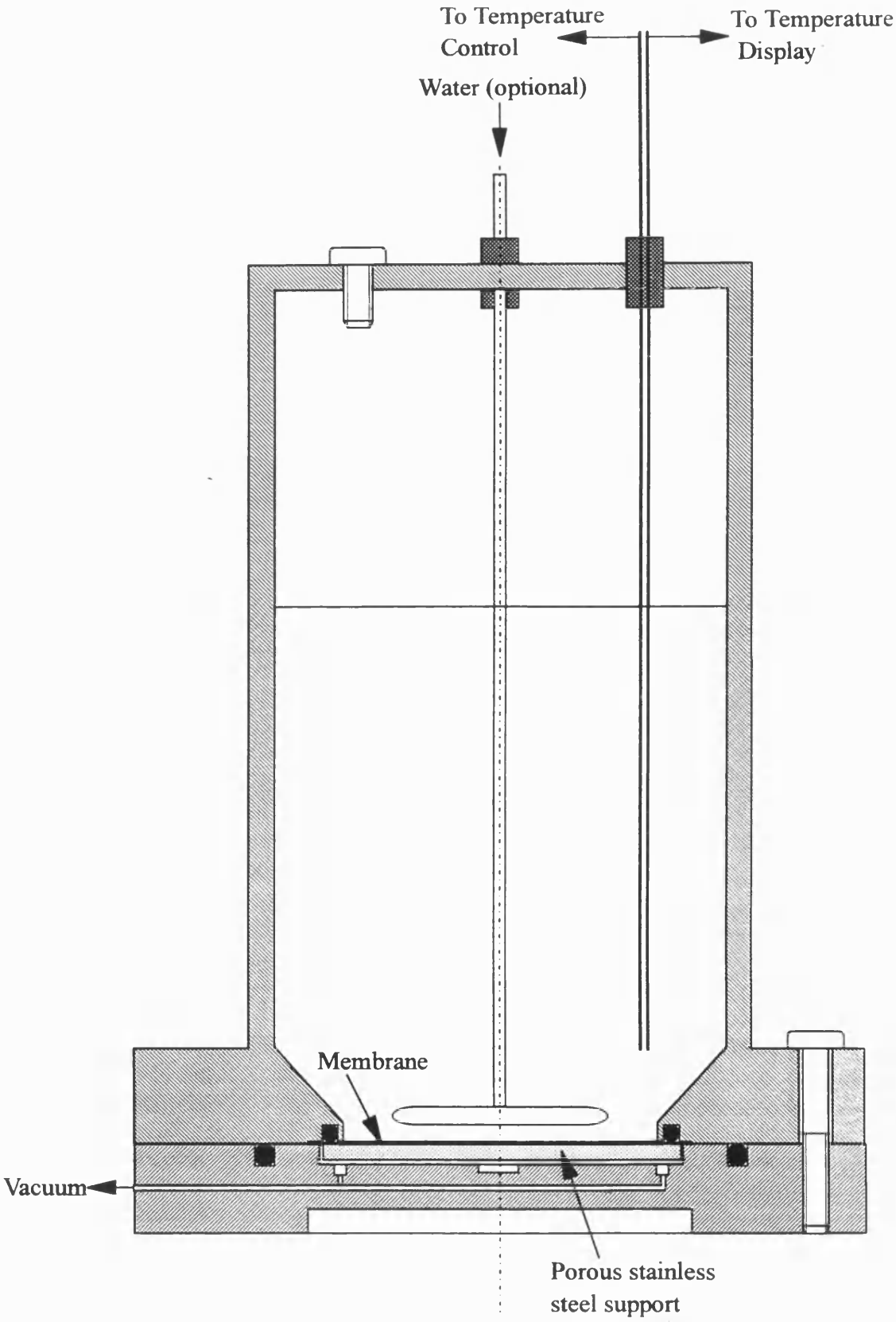

Figure 2.1 The pervaporation cell

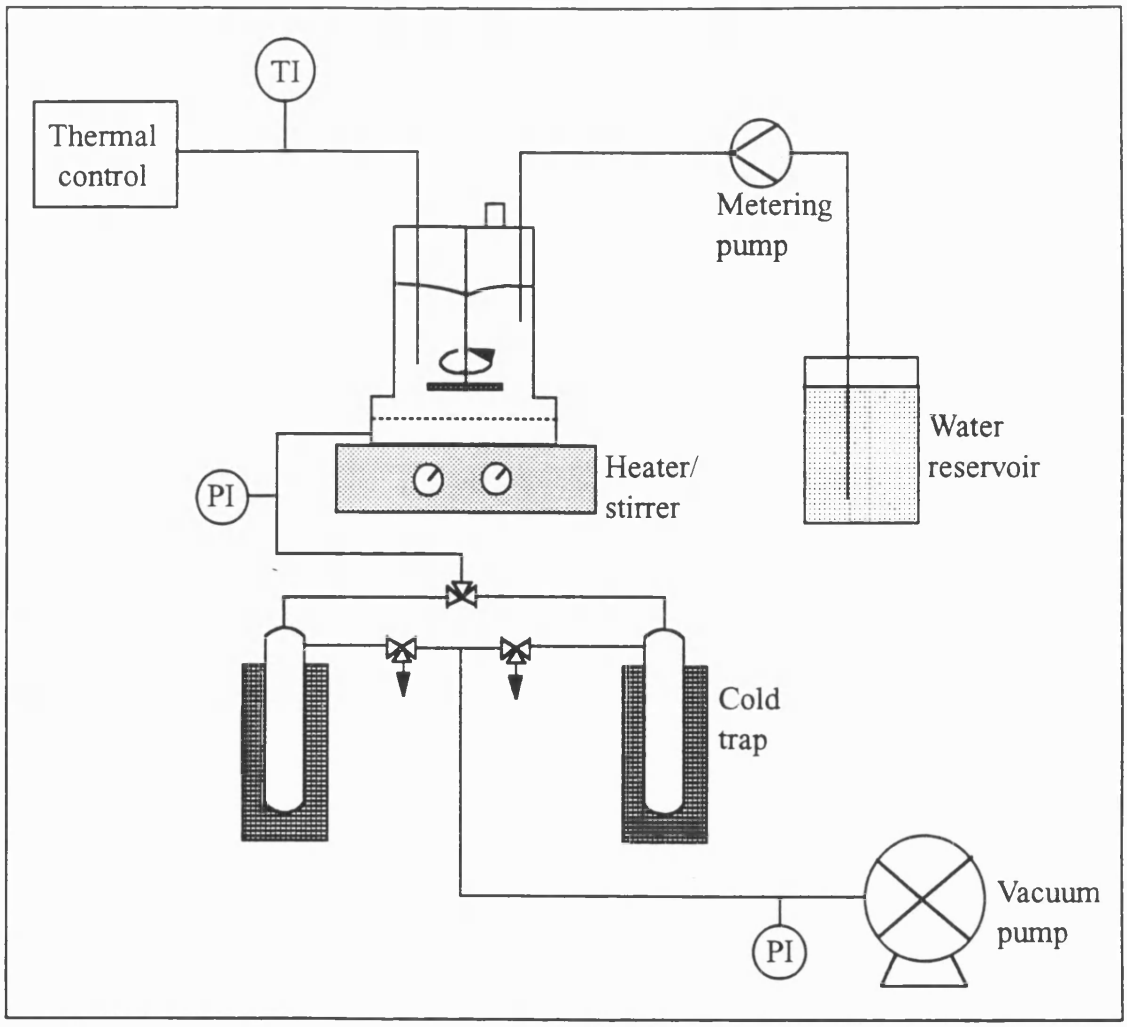

Figure 2.2 The pervaporation rig

2.4 PERVAPORATION RIG

A schematic diagram of the test apparatus is shown in Figure 2.2. A hotplate/stirrer (Heidolph MR20002) provided the heat and controlled the rate of stirring. Temperature was controlled by an integral control system, made within the department. An external water reservoir and metering pump (Milton Roy miniPump) enabled constant composition experiments to be performed. The vacuum line (inner diameter 8mm) and permeate traps were made of glass, being connected to the cell and vacuum pump with rubber vacuum tubing. Glass three-way taps enabled the

permeate to be channelled to either of the permeate traps and vacuum be released as required. Glass ball and socket joints on either side of each permeate trap facilitated easy removal of the traps from the system. Permeate was condensed by liquid nitrogen in cold traps of 2l capacity each. Downstream pressure could be measured both next to the cell and next to the vacuum pump by Edwards Vacustats (0.1-10mbar). The vacuum pump was supplied by Edwards.

2.5 EXPERIMENTATION

2.5.1 BATCH DEWATERING

A mixture of 2-propanol and water was made up to the required concentration. The membrane to be tested was sealed into the cell and the cell was positioned in the rig. The vacuum pump was turned on, the permeate line evacuated and the cold traps were filled with liquid nitrogen. The hotplate was turned on. The feed liquid mixture was poured through a funnel into the upper portion of the cell. The stirrer speed was set. The system was left, with permeate collecting in one cold trap, until it reached the required temperature. Thereafter, simultaneous feed and permeate samples were then taken at intervals, also noting down the time, feed temperature and downstream pressure. A feed sample was taken for analysis using a pasteur pipette. Permeate samples were taken by switching permeate collection to the other trap, then removing the permeate-containing trap, sealing it from the atmosphere, allowing the frozen permeate to thaw, then weighing and analyzing it. Sampling was carried out less frequently as the concentration of water in the feed fell. The experiment was stopped either when the target concentration had been reached, or when the membrane had been irreconcilably damaged.

2.5.2 CONSTANT COMPOSITION EXPERIMENTS

The experiment was carried out in the same way as a dehydration experiment except that the metering pump was used to keep the feed concentration constant. Assuming the permeate composition is better than 99wt% water and knowing the expected water flux, the pump was set to an appropriate speed such that water was added to the feed liquid by the pump at the same rate as it was being removed by the membrane. Feed and permeate samples were taken at regular intervals and the experiment was continued for a specified amount of time.

2.6 SAMPLE ANALYSIS

Feed samples were analysed for water content using a Mettler Karl Fischer Auto-titrator (Appendix B). The composition of permeate samples was found by using a gas chromatograph (Hewlett Packard, Series II, Model 5890) with a flame ionisation detector and an HP1 capillary column (Appendix C).

The permeation flux was calculated from the mass of permeate, knowing the sampling time and membrane area:

$$Flux = \frac{Sample\ mass}{Membrane\ area \times Sample\ time} \tag{2.1}$$

$$Flux = \frac{Sample\ mass\ (g)}{Sample\ time\ (mins)} \times 33.15 \tag{2.2}$$

The units of flux were $kgm^{-2}hr^{-1}$. For a batch dewatering experiment, the flux calculated was taken to be that for the arithmetic mean of the compositions at the start and end of the sampling time. Individual permeant fluxes could also be calculated knowing the permeate composition and selectivity, in terms of separation factor, could be calculated (see Section 2.8).

2.7 ERRORS

Errors in sample composition analysis are given in the relevant appendices. Errors in flux measurement during an experiment are derived from the measurement of permeate mass, sample time and membrane area. Permeate mass is calculated from the difference between the permeate trap containing the sample and the clean, dry trap. The error is estimated to be ± 0.1g. Error in sampling time is judged to be ± 2 seconds. Any error in area measurement is systematic and is disregarded. The combination of errors results in an overall error of $\pm 2\%$, on average, in the flux measurement although this increases when the weight of permeate collected is very small (e.g. < 2g) and the flux is low (e.g. $< 1 kgm^{-2}h^{-1}$). For example, for a standard membrane used (10g CsPA solution cast onto PVDF), the error in flux measurement at a feed composition of 19wt% water was less than 1% compared with a possible error of 9.5% at a feed composition of 1.5wt% water.

At low feed water contents in batch dewatering, a compromise between change in feed composition and permeate mass collected must be made to limit errors. If the variation in feed composition at the start and end of sampling was large, using an arithmetic mean of the compositions may introduce error into the flux-composition curve. To assess the extent of this error, different calculations were made using experimental data. Firstly, a flux-composition curve was constructed in the normal way. The experimental data was then manipulated such that two consecutive permeate samples were treated as one, creating an increase in the feed composition range associated with one flux point. A second series of "experimental" flux points was plotted. This procedure was repeated using three consecutive permeate samples. The result is shown in Figure 2.3.

The figure shows that sampling time has little effect on the resultant flux curve unless the feed composition is less than 8wt% water. From this result, a feed composition change of ≤3wt% water was set as the maximum for sampling at compositions of less than 10wt% water.

A suggested problem with the use of ionic membranes is the leaching of ions from the membrane into the feed, resulting in a change in membrane performance. The influence of any leaching of caesium ions on membrane performance was assessed by executing an experiment at a high water concentration for over 4 hours,

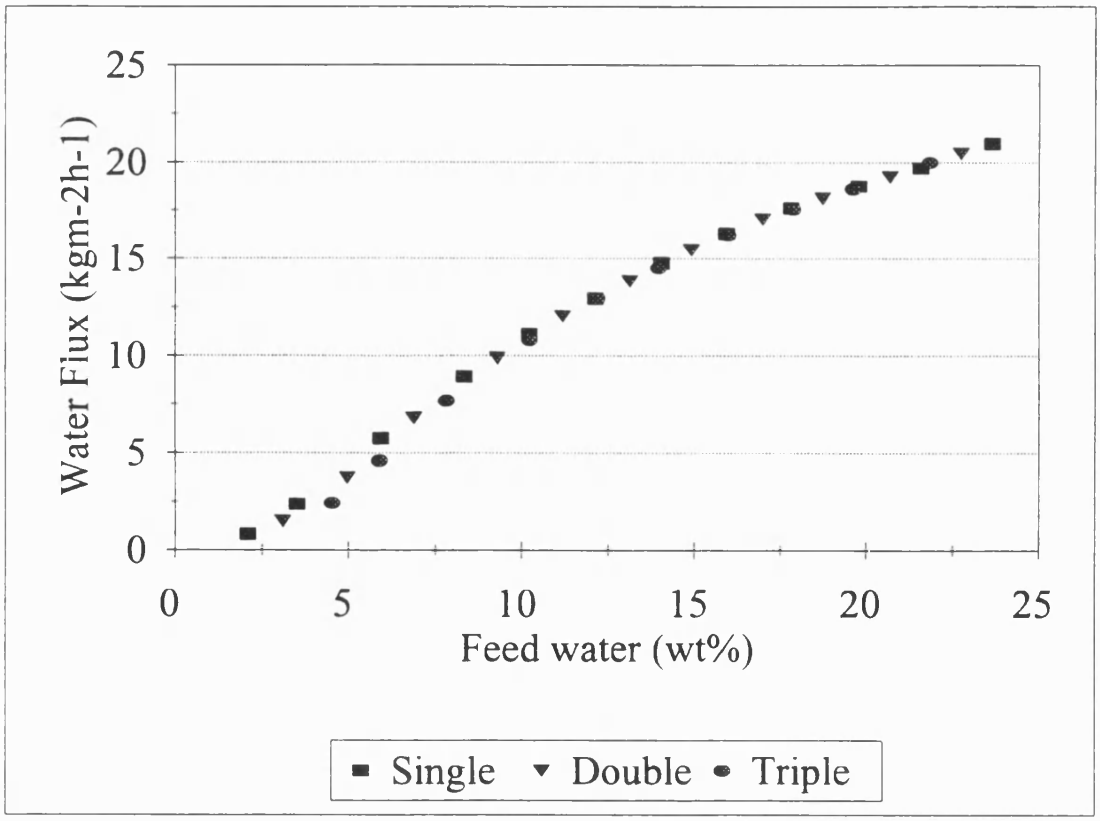

Figure 2.3 Batch dehydration results with varying sampling time. 60°C.

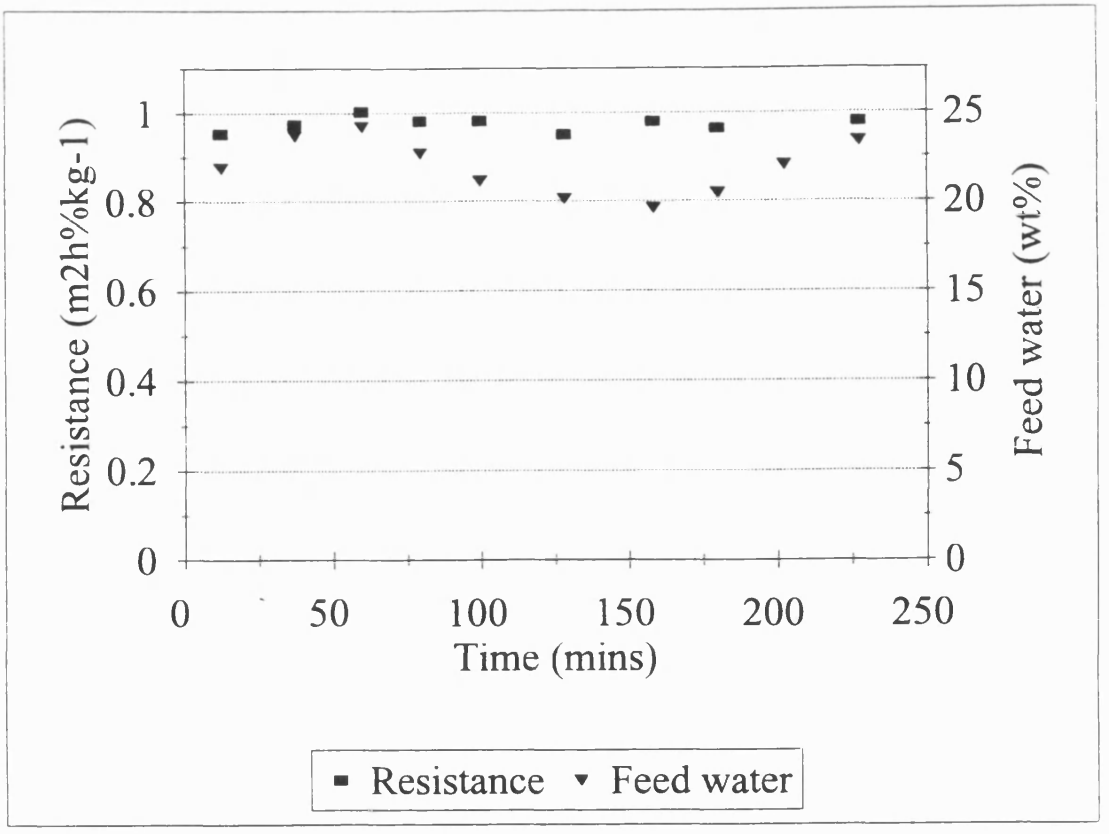

Figure 2.4 Variation in feed concentration (maintained in the range 19-25wt% water) and permeation resistance with time. 70°C.

which was the normal length of time of an experiment. The resistance to permeation (flux/feed water concentration) was measured over this period and is shown graphically in Figure 2.4.

Any variation in permeation resistance over this timescale is insignificant and can be ignored.

Errors in consistency between experiment sets may occur from differences in polymer batch, preparation conditions or from the measurement of parameters which affect the flux attained e.g. vacuum and temperature. These will be discussed as necessary in later chapters.

2.8 PRESENTATION OF RESULTS

Flux results may be presented graphically against feed composition, in wt% or mole fraction, or against feed water activity. As a reference, a plot of feed water (wt%) against feed water (mole fraction) and feed water activity is given in Figure 2.5.

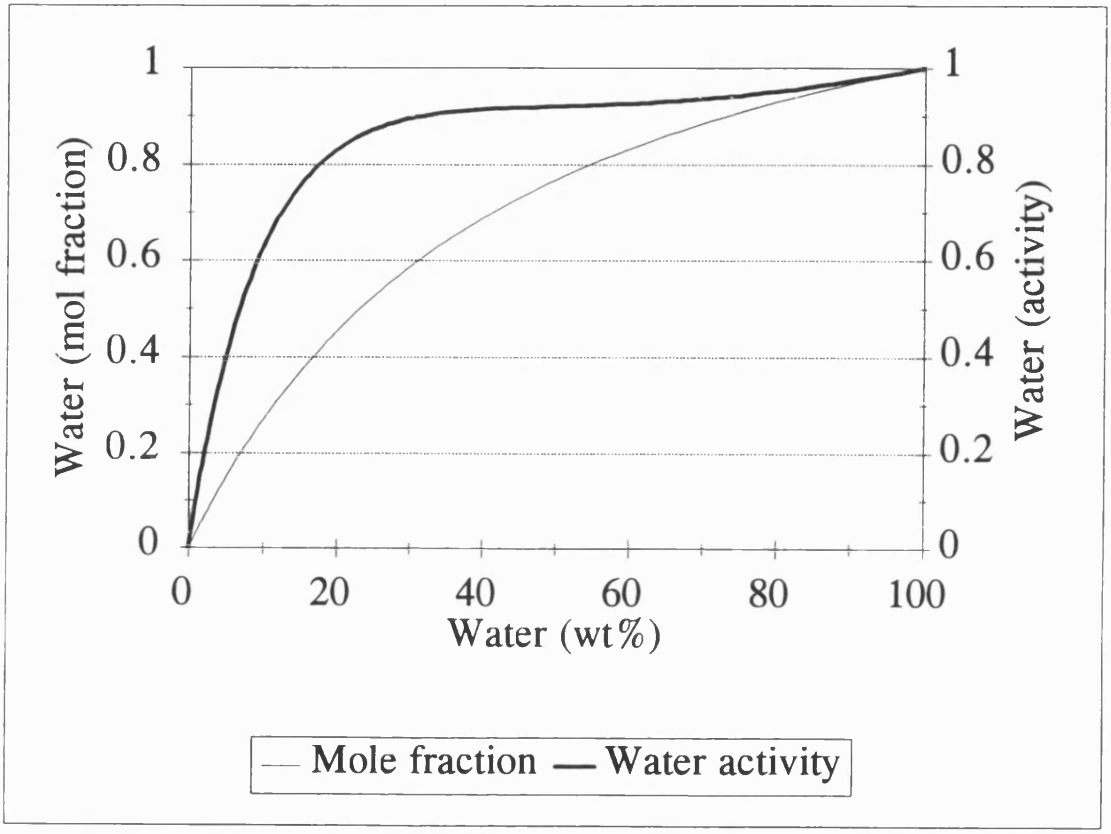

Figure 2.5 Comparison of units for the measurement of feed composition

The fundamental way of expressing the driving force in a membrane process is in terms of the gradient of chemical potential, $d\mu_i$. A simple transport equation can be derived:

$$J_i = -L_i \frac{d\mu_i}{dx} \qquad (2.3)$$

where L_i is a phenomenological coefficient.

For isothermal processes, the chemical potential is a function of activity and pressure:

$$\mu_i = \mu_i^0 + RT\ln a_i + V_i(P_i - P_{ref}) \tag{2.4}$$

where P is the total pressure.

Therefore

$$\frac{d\mu_i}{dx} = RT\frac{d(\ln a_i)}{dx} + V_i\frac{dP_i}{dx} \tag{2.5}$$

It can be shown (Koops, 1992) that the pressure term can be neglected because the pressure difference between the feed and permeate sides is only 1 bar.

Hence, combining equations (2.3) and (2.5):

$$J_i = -L_iRT\frac{d\ln a_i}{dx} \tag{2.6}$$

which can be rearranged to:

$$J_i = \frac{-L_iRT}{a_i}\frac{da_i}{dx} \tag{2.7}$$

A diffusion coefficient for component i <u>in the membrane phase</u> can be defined:

$$D_i(a_i) = \frac{L_iRT}{a_i} \tag{2.8}$$

such that

$$J_i = -D_i(a_i)\frac{da_i}{dx} \tag{2.9}$$

The diffusion coefficient, $D_i(a_i)$, is a function of the activity:

$$a_i = p_i / p_i^0 \qquad (2.10)$$

where p_i is the vapour pressure of component i and p_i^0 is its saturation pressure. The permeate side activity is negligible whilst the feed side activity can be calculated from van Laar equations knowing the feed liquid composition, as described in Appendix D.

The advantage of using an activity rather than a concentration based expression is that thermodynamic equilibrium is assumed at the membrane interfaces. This means that the activities of the feed-side solution at the membrane surface and of the permeate at the permeate side of the membrane can be used as boundary conditions for the diffusion equation without having to introduce an additional model for the sorption at phase boundaries.

A semi-empirical relation between flux and activity has been assumed for water permeation. The activity-dependent permeability has been written as Ae^{Ba}. Hence:

$$J_i = Ae^{Ba_i} . a_i \qquad (2.11)$$

In the absence of concentration polarisation, A is expected to be inversely proportional to the membrane thickness. The term B is a form of plasticization factor.

Selectivity is presented in terms of the separation factor, $\alpha_{H2O/IPA}$, plotted against feed composition.

$$\alpha_{H2O/IPA} = \frac{x''_{H2O}}{x'_{H2O}} \times \frac{x'_{IPA}}{x''_{IPA}} \qquad (2.12)$$

2.9 CONCLUSIONS

Composite membranes were fabricated and a pervaporation rig and analytical procedure were set up to test their performance. Errors in the reporting of results have been assessed. Permeation results will be presented as plots of flux and separation factor against feed-side water activity, which is a more fundamental measure of driving force than concentration, and modelled by a semi-empirical relation.

CHAPTER 3

INFLUENCE OF ACTIVE LAYER PREPARATION

3.1 INTRODUCTION

The membrane used for this work was a composite membrane formed by the simplest technique possible, precipitation by solvent evaporation. Caesium polyacrylate formed the non-porous top layer and its intrinsic properties were responsible for the membrane's selectivity characteristics, the porous sublayer merely providing mechanical support. It was possible that the preparation conditions, i.e. drying temperature and conditions, affected the morphology of the active membrane and the support layer and a report on the testing of this hypothesis is given here.

The role of the counter ion is assessed within this chapter. Variation in permeation characteristics with counter-ion loading has been observed by several workers (Li, Xue and Cabasso, 1988; Naylor *et al.*, 1989; Néel *et al.*, 1988; Ping *et al.*, 1990; Wenzlaff *et al.*, 1985; Yamada and Nakagawa, 1991). Various effects on flux and separation factor were found, depending upon the counter ions and polymers used. Naylor *et al.* (1989), Néel *et al.* (1988) and Yamada and Nakagawa (1991) found that for the alkaline metal group, increasing counter ion size parallels increasing effectiveness for use in a water selective pervaporation membrane.

Naylor, Zelaya and Bratton (1989) neutralised polyacrylic acid with sodium, lithium and caesium ions and measured sorption and diffusion characteristics, as well as permeation properties. Caesium was found to be the most effective neutralising ion for dewatering purposes, hence its use in this work. It sorbed more water per mole of polymer than the lithium salt and provided a water diffusion coefficient an order of magnitude higher than the sodium salt. The latter is believed to arise from

the relative tightness with which diffusing water molecules bind to the counter ion, with caesium binding fewer molecules less tightly than sodium due to its lower charge density. Therefore the water molecules diffuse through the polymer more easily, allowing further molecules to sorb.

An alternative theory is provided by Néel *et al.* (1988). They studied the transport of water through a membrane of polyethylene grafted with acrylic acid which was neutralised with a series of alkaline metals. The films were impregnated by water-ethanol mixtures of 0-20wt% water and infra-red spectroscopy was used to gain information about interactions between water, ethanol and the different macrosalts. When water exceeded a critical concentration a splitting of the band ascribed to the asymmetrical vibration of the carboxylate group was found. It is suggested that above this concentration, vibrations of the carboxylate groupings are perturbed by the insertion of water molecules, resulting in a loosening of the ion pairs and enhancing the mobility of water in the virtually dry material. The critical concentration decreased and selectivity increased as the size of counter ion increased. For potassium counter ion, the critical concentration was approximately 5wt% water. The authors suggest that water moves in clusters through the swollen part of the membrane.

Since the type of neutralising ion effects pervaporation performance, it may be hypothesised that the degree of neutralisation is also important. This is investigated within this chapter, along with the effect of adding counter ions to the feed.

Chain flexibility affects diffusion through a polymer and the molecular weight of the polymer may be a contributing factor to the degree of freedom available. A

study of the resultant effect of molecular weight on permeation properties of the membrane is the third matter considered in this chapter.

3.2 EXPERIMENTAL

The performance of all prepared membranes was tested by batch dewatering of an IPA solution with a feed temperature of 70°C and stirrer speed of 1000rpm. The vacuum was less than 4.5mbar, measured next to the vacuum pump.

3.2.1 DRYING CONDITIONS

For this investigation each membrane, 10g of 0.5wt% caesium polyacrylate solution, molecular weight (MW) 250 000, pH 8.5, was cast onto PVDF. Following the casting of polymer solution onto the support material, the solvent was evaporated to precipitate the dense, homogeneous membrane. Since the solvent involved was water, an inert atmosphere was not required. Membranes were dried at room temperature (20°C), 40°C, 75°C and 86°C. Also, two membranes were dried at 70°C but under different conditions. One was dried in an atmosphere saturated with water vapour whilst the other was dried in a "dry" atmosphere, the oven containing a large amount of molecular sieve.

3.2.2 DEGREE OF POLYMER NEUTRALISATION

Each membrane was constructed from 10g of 0.5wt% polyacrylic acid or caesium polyacrylate solution, MW 250 000, neutralised to the required pH, as outlined in Section 2.2.2, and cast onto PVDF. Membranes were dried at 35°C.

3.2.3 POLYMER MOLECULAR WEIGHT

For 250 000 MW polymer, 10g of 0.5wt% CsPA, pH 8.5, was cast onto the required substrate. For the 4M MW polymer, 50g of an 0.1wt% solution, pH 8.5, was cast onto the required substrate. The substrates used were PVDF and PSf. For

2000 MW polymer, 2.5g of a 5wt% solution of polymer, pH 8.5, was cast onto PVDF. Each membrane was dried at 35°C.

3.3 RESULTS AND DISCUSSION

3.3.1 DRYING CONDITIONS

At 20°C the membranes took up to 48 hours to dry. At other temperatures, the membranes were dried for 18 hours. The active layer looked and felt more dry and brittle after exposure to higher temperatures, although cracking was not observed at any temperature. Subsequent prolonged exposure to atmospheric conditions resulted in any active layer becoming as tacky as the membrane dried at room temperature. PVDF substrate dried at 75°C and 86°C turned dark pink in colour.

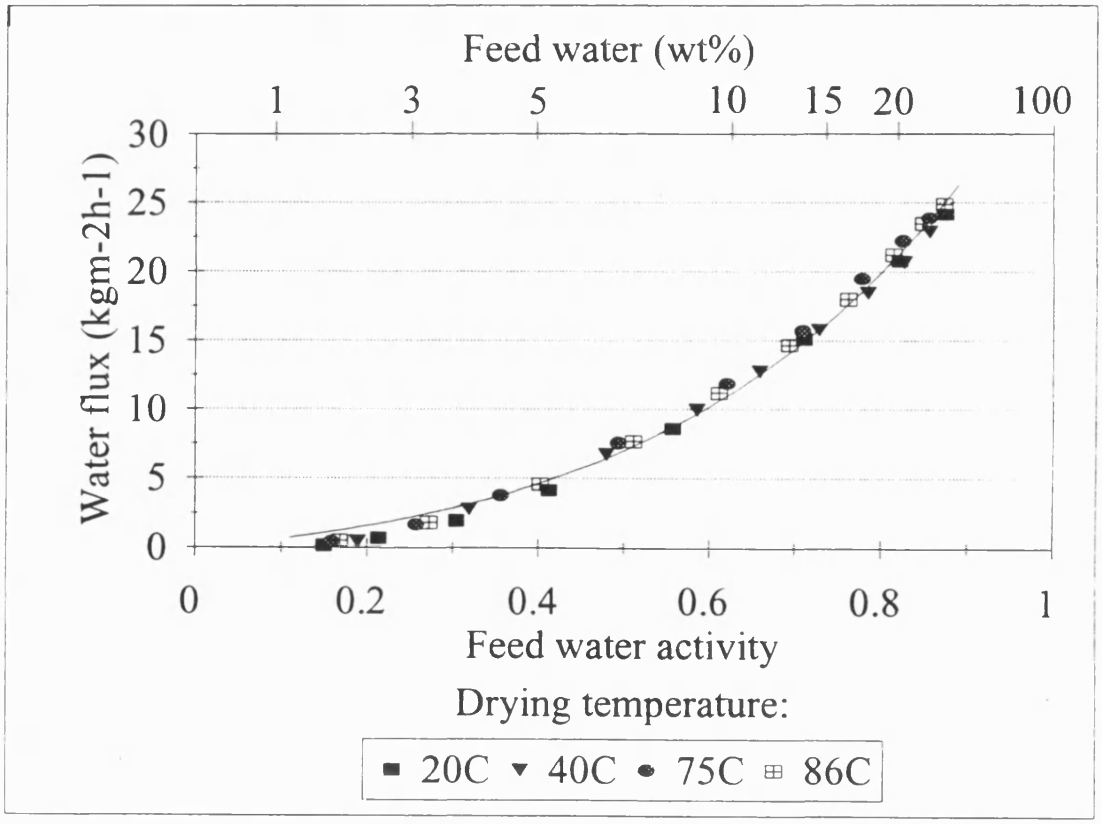

Figure 3.1 Effect of membrane drying temperature on flux

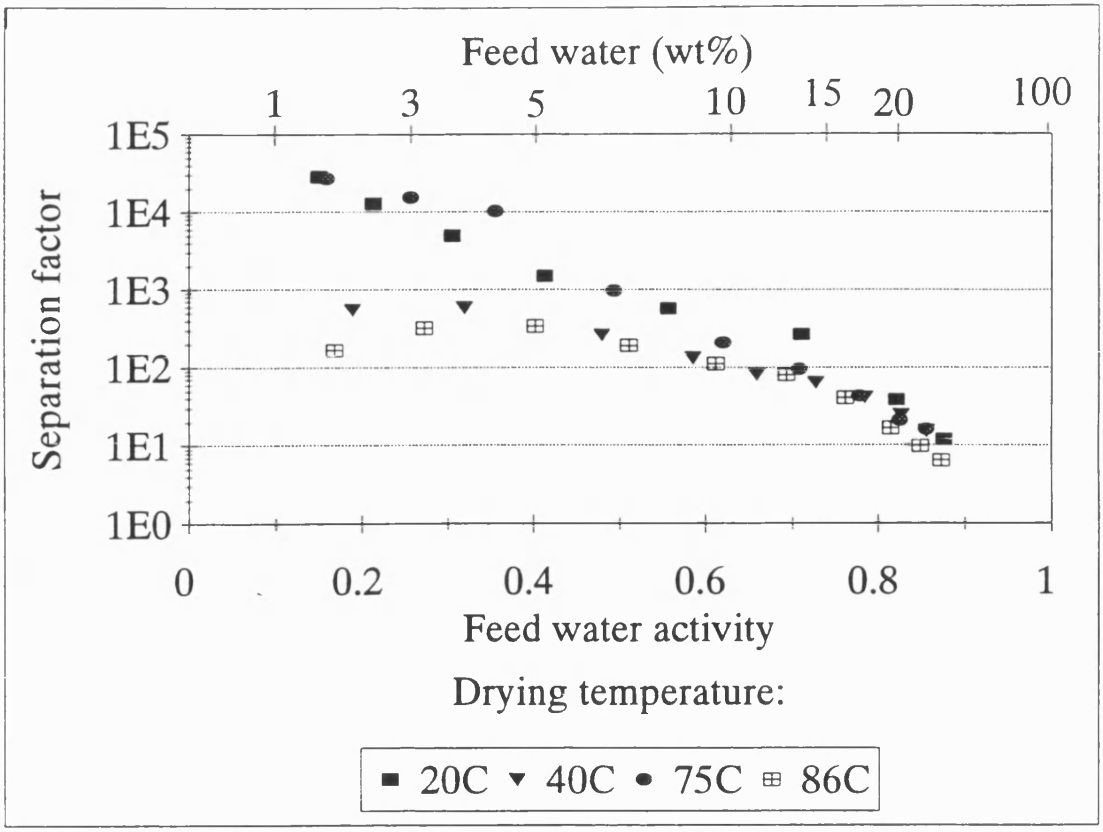

Figure 3.2 Effect of membrane drying temperature on separation factor

Figures 3.1 and 3.2 illustrate the effect drying temperature had upon performance. Drying temperature had no effect on water flux but did appear to have an effect on separation factor, α, due to an increase in the IPA flux. Separation factor is expected to decrease with an increasing concentration of preferentially permeating component if the membrane polymer is not cross-linked (Section 1.2.9). In this case, α is strongly influenced by feed composition, increasing by three orders of magnitude in most cases, when the water content of the feed drops from 25wt% to less than 2.5wt%. This result can be compared with a study by Choi *et al.* (1992). They studied the permeation properties of an aluminium polyacrylate-polysulfone composite membrane and found that the separation factor increased in the same manner. An increase is to be expected from the definition of separation factor, even

if the permeate composition is constant:

$$\alpha_{H2O/IPA} = \frac{x''_{H2O}}{x''_{IPA}} \times \frac{x'_{IPA}}{x'_{H2O}} \qquad (3.1)$$

In fact, permeate quality improved with decreasing feed water concentration, further accentuating the change in α. It must be remembered that a very small change in permeate quality can have a significant effect on the separation factor. For example, for feed containing 4wt% water, a change in permeate composition from 99.7wt% to 99.9wt% water results in an increase of 300% in the separation factor.

In all cases the permeate quality was better than 99wt% water for feed $<$11wt% water. The permeate composition for membranes dried at 20°C was greater than 99wt% water across the entire composition range tested but the membrane dried at 86°C had a permeate composition of 95wt% water for feed of 23.4wt% water. The overall trend is shown in Figure 3.2.

The effect of drying temperature upon flux and separation factor was also investigated by Spitzen *et al.* (1988). These workers studied the effect of the morphology of poly(acrylonitrile) (PAN) membranes on the permeation of an ethanol/water mixture by varying the evaporation rate of the solvent used for membrane preparation and by comparing multi-layered membranes with single layer membranes of the same thickness. They found that increasing the evaporation temperature ($20 \leq T \leq 150$°C) and therefore rate, led to a separation factor decrease but without a change in flux. Multi-layered membranes exhibited smaller separation factors but larger fluxes than single-layer ones. The selectivity decrease in both these cases was due to the shorter evaporation time, giving the polymer only a small chance to rearrange itself into a dense structure. The permeation of water is hardly affected

by the membrane density whilst the permeation of the larger molecule is.

It is doubtful whether the predictions of this theory fit the results obtained from the CsPA membranes, however, because the PAN membrane undergoes little swelling on exposure to feed solution whilst CsPA is not cross-linked and will therefore swell. Any difference in polymer density from a change in drying temperature will not be manifest in the swollen part of the membrane on exposure to the feed solution. This may explain why little difference exists in α at high feed water concentrations whilst a difference becomes more pronounced at low feed water concentrations where less swelling occurred although considering the error margin applicable, it is not surprising that a trend in separation factor with temperature is not clear in this case. Also, the temperature range used was not large. The membrane dried at 75°C exhibits exceptionally high selectivity at low feed water contents. For the membrane prepared at 86°C, a drop in α occurred at very low feed water content. A possible explanation for this has been suggested (Naylor, 1994). His explanation was that the reduced α value could be caused by "frozen in" stress. Rapid drying leads to the "freezing in" of structure due to hydrogen bonding between polymer chains. During pervaporation, stresses are set up in the membrane because of the process conditions. These are magnified in the "already stressed up" membrane and result in a loss of selectivity, although this probably only occurs adjacent to the support membrane since the rest will be *relatively* wet due to absorbed water.

The rate of solvent evaporation was reduced by drying the membranes in an atmosphere saturated with solvent vapour, a technique used by Spitzen *et al.* (1988). The performance results are shown in Figures 3.3 and 3.4. Again, this had no effect on flux whilst, in this case, the effect on separation factor became more pronounced

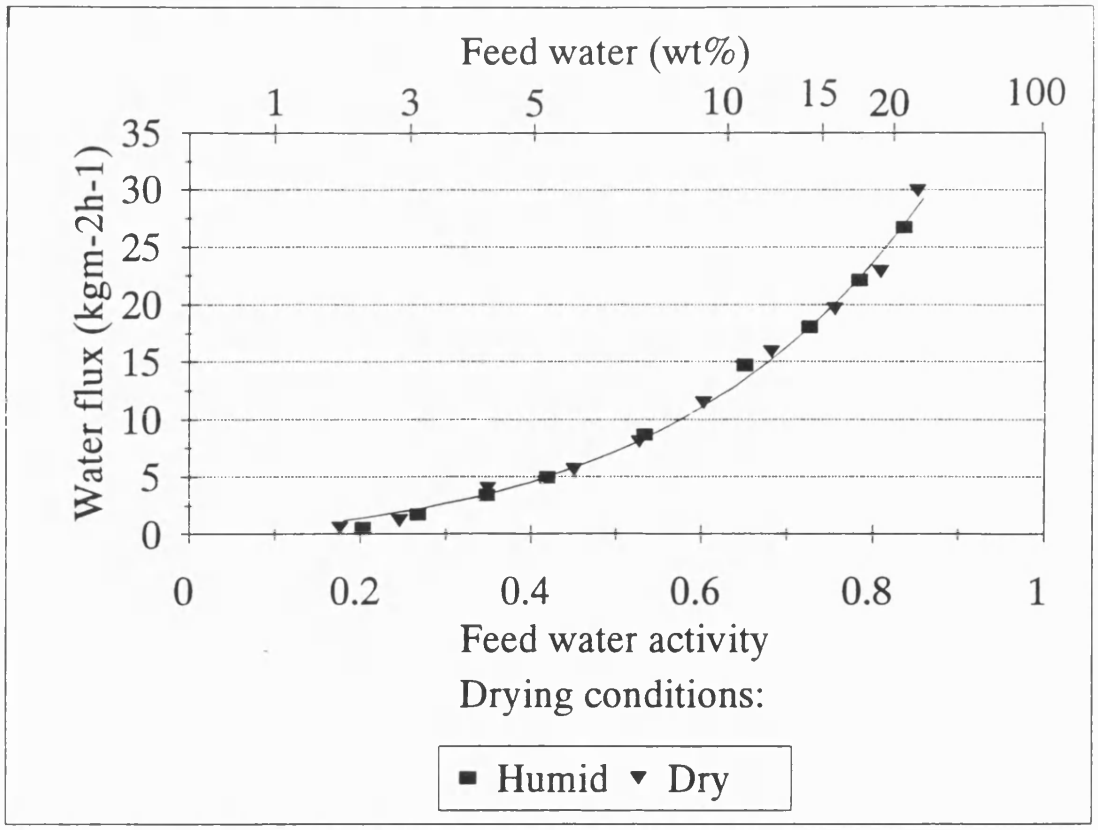

Figure 3.3 Effect of membrane drying conditions upon flux

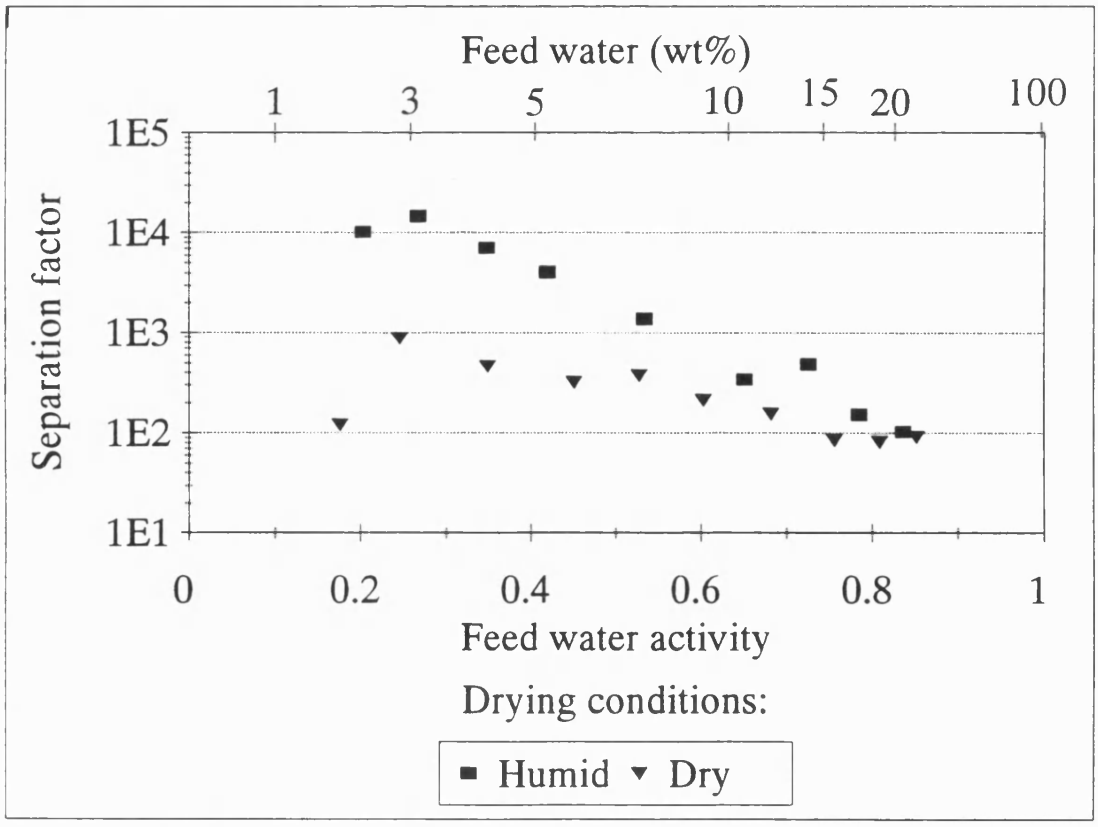

Figure 3.4 Effect of membrane drying conditions upon separation factor

as the concentration of water in the feed decreased. For example, a 16-fold increase in selectivity at 4wt% was evident from drying the membranes under humid conditions whilst at 10wt% a 3-fold increase was found. A possible explanation for this was the higher density of polymer in the membrane that had been dried more slowly. The performance of the membrane prepared at 70°C using a dry atmosphere was as bad as that of the membrane prepared at 86°C using "normal" conditions whilst the performance of the membrane prepared at 70°C using humid conditions was almost as good as that of the membrane prepared at 40°C using "normal" conditions (Figures 3.2 and 3.4). This suggests that the drying rate, which is dependant upon a difference in humidity, controls the outcome rather than the temperature per se.

The differences in membrane performance due to differences in membrane morphology could in principle be avoided if the membranes were heat treated after drying at a temperature above the glass transition temperature (106°C for polyacrylic acid (Choi *et al.*, 1992)). The optimal packing density could then be attained due to the rearrangement of the polymer chains, so-called relaxation. The stability of the porous support layer to heat treatment would have to be considered and Naylor (1994) has indicated that the glass transition temperature for caesium polyacrylate is around 250°C but us highly moisture sensitive. So maybe, the differences might be removed by conditioning in a humid atmosphere, not just by heating.

3.3.2 DEGREE OF POLYMER NEUTRALISATION

Little separation was achieved from the use of a polyacrylic acid membrane for alcohol dewatering but membrane selectivity was good for other membranes tested. Permeate quality was greater than 95wt% water for the membrane made from

pH 7.2 polymer and improved for all the higher pH membranes, being better than 99wt% water for all samples taken. Flux and separation factor results are shown in Figures 3.5 and 3.6.

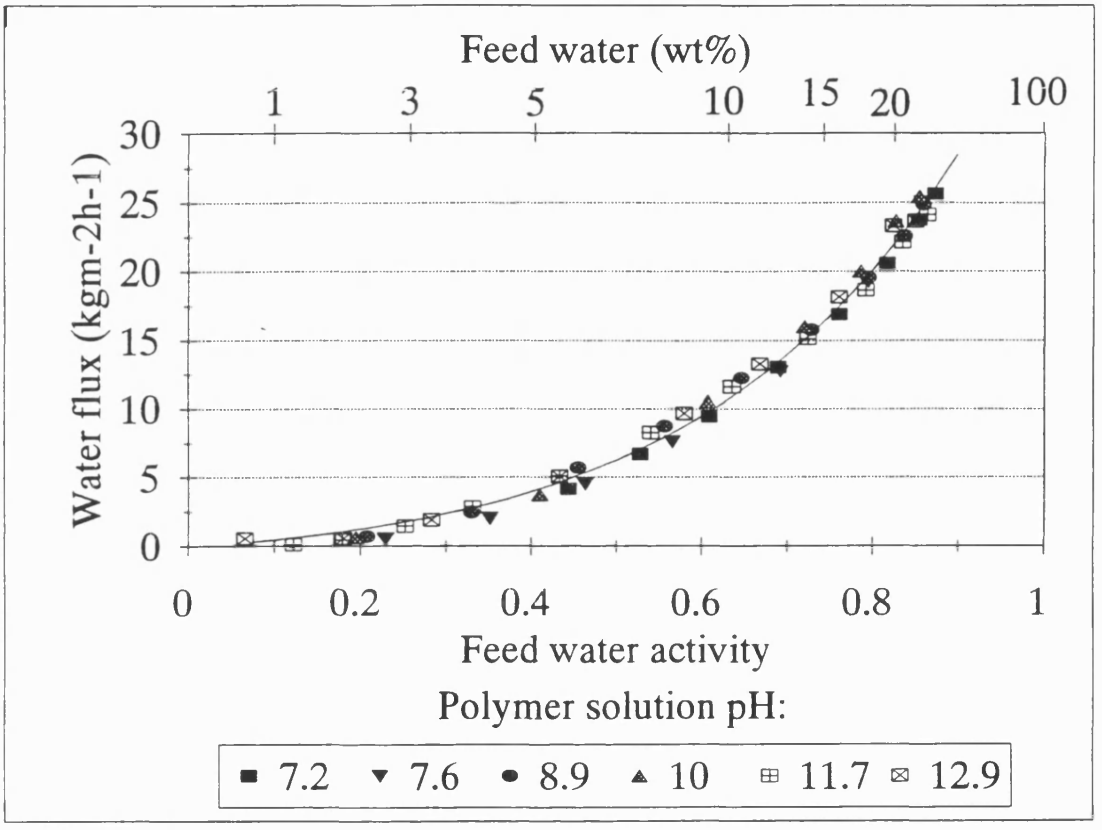

Figure 3.5 Effect of casting solution pH upon water permeation

Initial results indicated little difference in the performance of the set of membranes apart from the lower separation factor for the pH 7.2 membrane. A second set of experiments was carried out utilising three duplicate membranes to those used in the previous experiment but testing them with an IPA batch containing a lower initial water content. The flux results are shown in Figure 3.7.

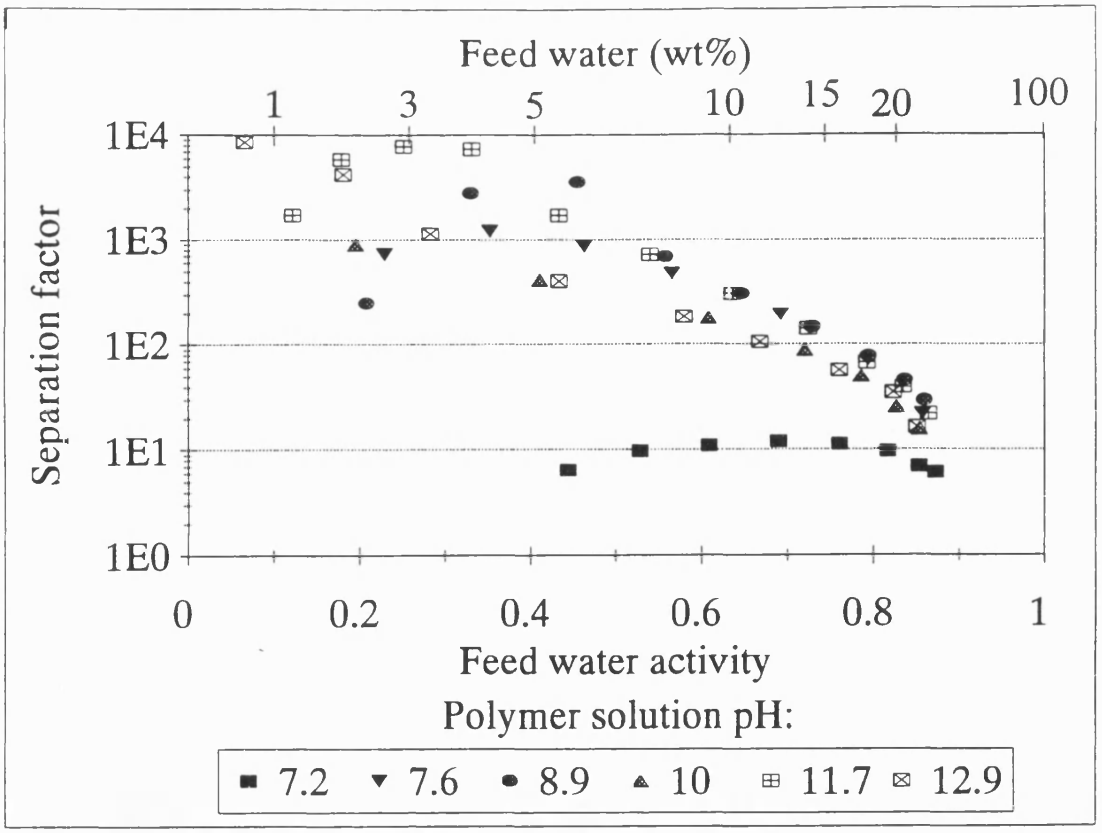

Figure 3.6 Effect of casting solution pH upon separation factor

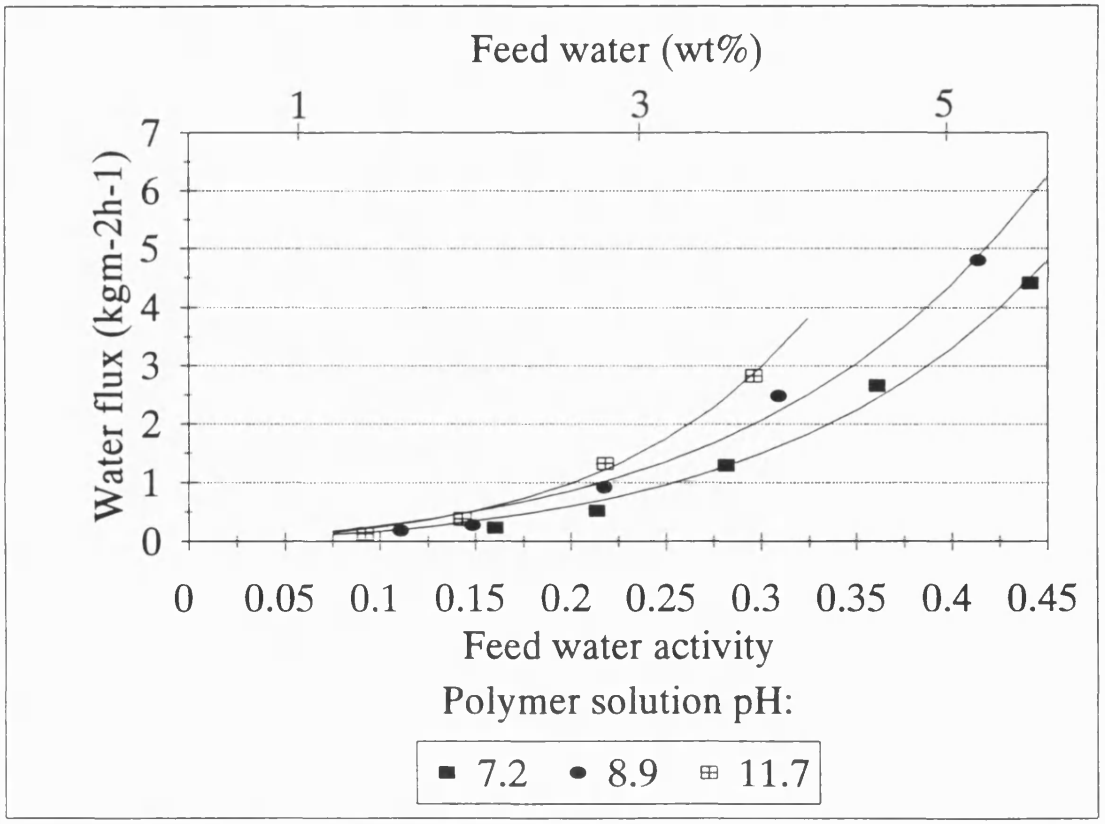

Figure 3.7 Effect of casting solution pH upon water permeation. Low initial feed water

The selectivity shown by all three membranes of this set was excellent, the permeate quality being greater than 99.9wt% water for all samples taken and no discernable effect on separation factor found. From these results there does appear to be a trend in performance with polymer pH. The membrane made from polymer of pH 7.2 gave the lowest flux and the highest pH polymer, the highest flux. At a feed water activity of 0.225 (2wt% water), the pH 8.9 membrane gives a 48% increase in water flux over the pH 7.2 membrane and the pH 11.7 membrane gives a further 42% increase.

Separation is a product of high sorption and diffusion coefficients for water compared to IPA. Neutralising the acid with caesium hydroxide causes the hydrogen ions in the carboxyl group to be replaced by metal ions resulting in a larger sorption coefficient (Thompson Hughes and Fordyce, 1956). It also leads to a reduction in both intra- and inter-chain hydrogen bonding with water molecules. This decreases the opportunity for permeating water molecules to bond to the polymer; also, greater chain mobility, resulting from a decrease in cohesive forces between the chains, decreases the activation energy for diffusion. The metal ion is larger than a hydrogen ion and greater space between polymer chains may also promote easier diffusion through the polymer.

Naylor, Zelaya and Bratton (1989) tested sodium polyacrylate membranes having different degrees of neutralisation ($7 \leq pH \leq 11$) for the dehydration of ethanol from a concentration of 11wt%. They concluded that the greater the degree of neutralisation, the higher the water flux and, to some extent, the better the selectivity. Naylor (1994) has also suggested that membranes of higher pH can also dehydrate to a lower level of water without loss of selectivity. This relates to the

lack of hydroxyl groups present which cause cracking of the selective layer at low feed water levels. Choi *et al.* (1992) tested cross-linked aluminium polyacrylate membranes and found that increasing the aluminium content increased flux, but this was accompanied by a decrease in the separation factor. No explanation for this was given.

The results here are slightly contradictory, the degree of neutralisation appearing to have little effect on flux except at low feed water contents, or separation factor, other than for the pH 7.2 membrane. It is suggested that at high feed water compositions, the membrane is very swollen and diffusion is unhindered. It is diffusion through the dry downstream layer which is rate limiting and this part of the membrane may increase in thickness at very low feed water contents. It is only then that the significance of increased chain spacing and decreased hydrogen bonding due to the metal ions are significant and a difference in permeation behaviour may be measured. No difference in separation factor is evident at this point because selectivity for each membrane is so high. Further, at pH 8.5, titration studies have shown that polyacrylic acid is 95% neutralised by the caesium ions. Increasing the pH above this value will result in only a small change in inter- and intra-hydrogen bonding and hence have little effect on permeation properties. However, for casting solutions of acidity less than pH 8.5, changing the pH should have more of an effect.

A third set of experiments was carried out. As well as varying the pH of the membrane polymer, the pH of the feed was also varied, by the addition of caesium hydroxide solution, to match that of the polymer. Three batch dehydrations were performed and the results are given in Figures 3.8 and 3.9.

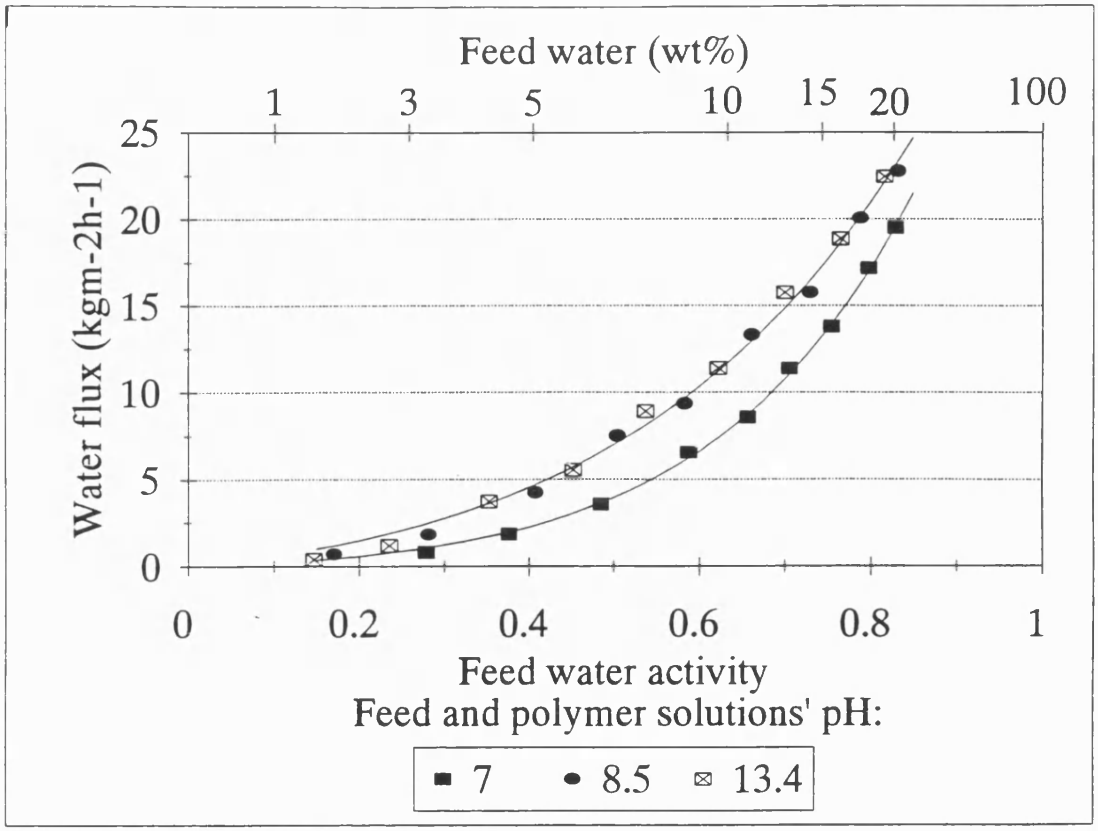

Figure 3.8 Comparison of the water fluxes of systems with varying polymer and feed solution pH. Polymer solution pH = Feed solution pH

Permeate quality was again good for all membranes (>99wt% water). The performances for the pH 8.5 and pH 13.4 mixtures were the same and do not differ from the performance of equivalent membranes when no caesium ions have been added to the feed liquid. The pH 7 membrane gave a lower water flux than the other two and worse than the pH 7.2 membrane of the first experimental set, even though the separation factor was larger.

Adding caesium ions to the feed may have been expected to reduce the water flux by holding water molecules in solution by its hydroscopic nature, lowering the feed water activity. The experimental results have shown that adding a certain level of caesium ions to the feed has no effect.

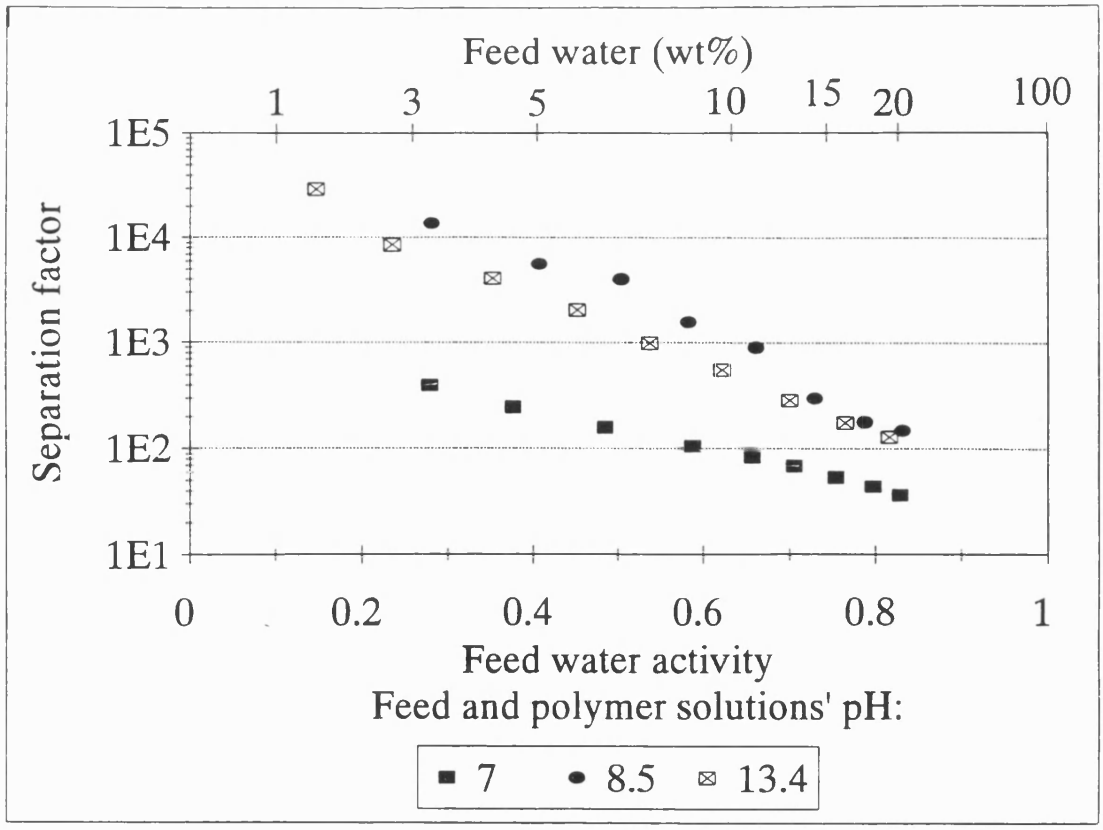

Figure 3.9 Comparison of selectivities of systems with varying polymer and feed solution pH. Polymer solution pH = Feed solution pH

3.3.3 POLYMER MOLECULAR WEIGHT

Although the concentrations of the three molecular weight polymer solutions were different, the same dry weight of polymer was cast by using appropriate weights of solution (see Appendix A).

The membrane produced from polymer of molecular weight 2000 was a total failure and dissolved in feed solution with a water content of 10wt%. This was due to excessive chain mobility. The polymer chains were not long enough for entanglements to prevent dissolution. Other membranes tested showed good selectivity (permeate > 98wt% water) and no effect on separation factor was found resulting from either a change in polymer molecular weight or support material. Fluxes for the 4M and 250K MW polymers were equivalent for both sets of

experiments, as can be seen in Figures 3.10 and 3.11. Fluxes attained for identical toplayers but different support layers were not the same. This will be further discussed in Chapter 6.

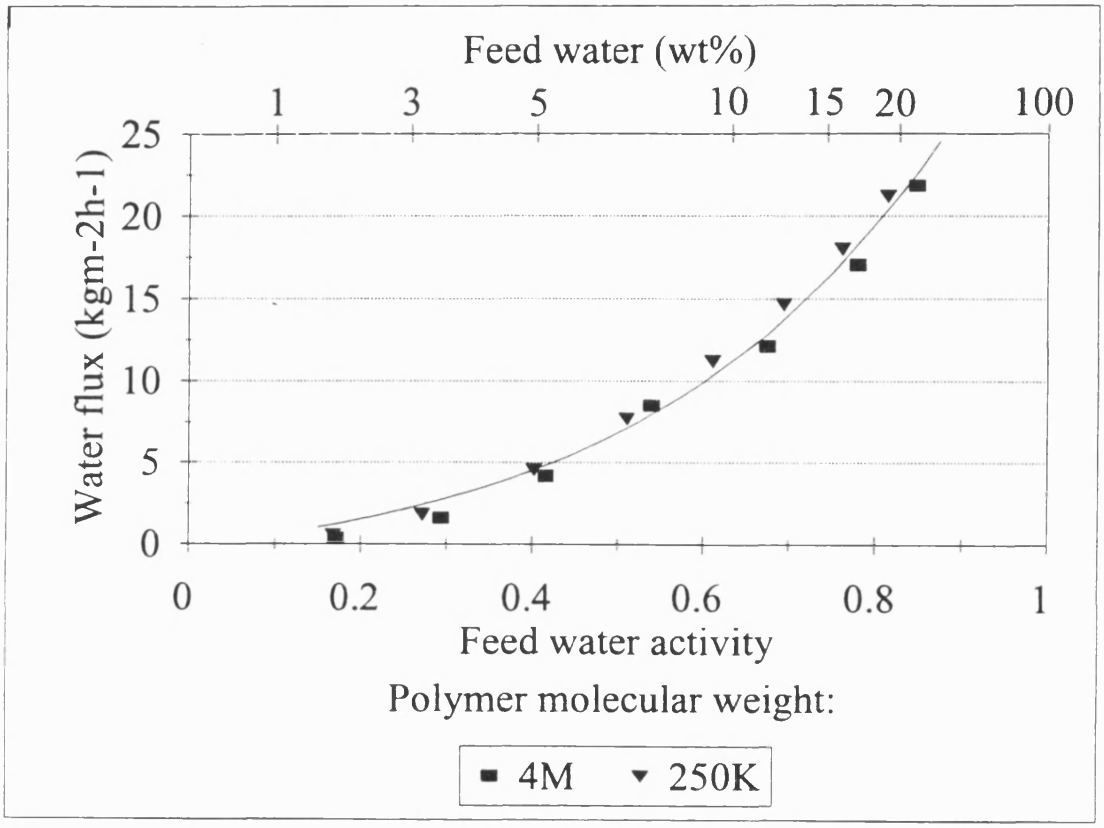

Figure 3.10 Effect of polymer molecular weight upon water flux. PVDF support

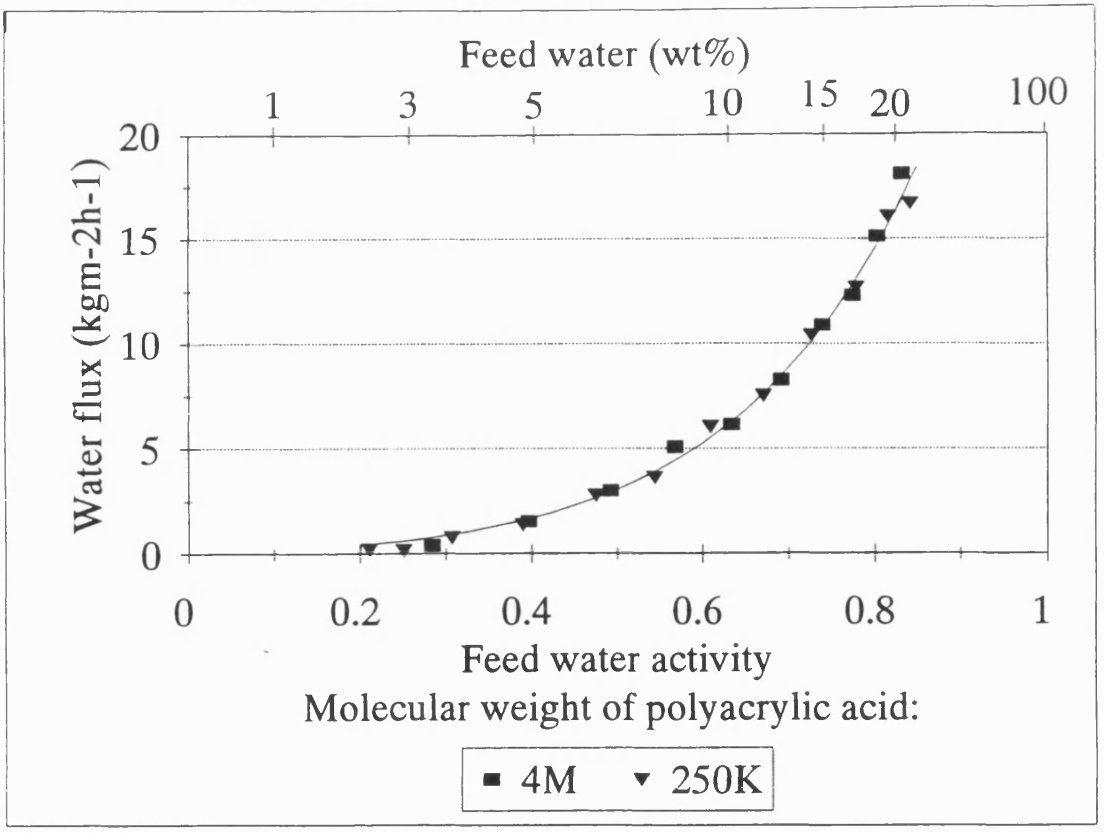

Figure 3.11 Effect of polymer molecular weight upon water flux. PSf support

The stability of the 2000 MW polymer was much lower than for the other two polymers tested making it unsuitable for use in an uncrosslinked membrane. The other two polymers tested performed equally successfully in the range of compositions tested, indicating that polymer flexibility was not affected by chain length. However, the instability of the 2000 MW polymer may imply that the highest molecular weight polymer would be the most stable for use across the widest composition range as an uncrosslinked membrane.

3.4 CONCLUSIONS

The temperature and conditions at which a cast membrane was dried had no effect on flux but, although not varied across a very wide range, some influence on the separation factor was found. This could be attributed to a change in the morphology of the resultant membrane. It is suggested that membranes dried slowly, either in a humid atmosphere or at low temperature, perform best.

The degree of neutralisation of the polyacrylic acid with caesium ions had little effect on flux or selectivity, except at very low feed water contents where the importance of interchain hydrogen bonding becomes evident. The addition of caesium ions to the feed was not influential.

Polyacrylic acid with a molecular weight of 2000 was unsuitable for use as an uncrosslinked membrane due to its lack of stability in solutions of IPA. Polymers of molecular weight 250 000 and 4 million performed with equal success implying that polymer molecular weight has no effect on membrane performance.

CHAPTER 4

INFLUENCE OF ACTIVE LAYER THICKNESS

4.1 INTRODUCTION

4.1.1 BACKGROUND LITERATURE

The thickness of the active layer of a composite membrane is a key factor in flux determination and can also affect permeation selectivity. Equation (2.9) demonstrated that the transport of components through the membrane occurs by diffusion resulting from a chemical activity gradient across the membrane. If the activity (concentration) dependence of the diffusion coefficient is ignored, integration of equation (2.9) provides a relationship where the flux of one component is inversely proportional to the membrane thickness.

$$J_i = \frac{-D_i(a_i)}{l}(a_f - a_p) \qquad (4.1)$$

For a binary mixture, this relationship is valid, in the absence of coupling, for both components. Therefore it is concluded that the membrane thickness has no effect on selectivity, provided that (a) a flaw-free membrane is formed and (b) the concentration dependence of the diffusion coefficient is negligible.

These assertions were confirmed by Binning *et al.* (1961) for the permeation of a 50-50 mixture of n-heptane and iso-octane through an unspecified polymer film. Thicknesses of 20μm to 47.5μm were tested. Indeed the authors state that film thicknesses as low as 7.5μm can be used without loss of selectivity.

Aptel *et al.* (1974) also investigated the influence of thickness, over a somewhat larger range, for films of PTFE grafted with either poly(N-vinylpyrrolidene) or poly(4-vinylpyridene). Flux was proportional to reciprocal

thickness for thicknesses of between 17μm and 250μm although grafting conditions affected the proportionality of this relationship.

Nevertheless, the literature contains evidence of deviations from this model. Kim and Kammermeyer (1970) studied the actual concentration profiles within membranes for several polymer-pure liquid systems using membrane stacks. They found that for some systems a critical membrane thickness existed. Above this thickness, flux was proportional to reciprocal thickness, but not below it. This was ascribed to the existence of an interface (sorption) resistance: at low thicknesses, the rate of diffusion through the membrane was less than expected because the permeant concentration at the membrane's upstream interface was lower than the equilibrium value. Concentration polarisation could now be considered to be responsible for this phenomenon.

Similarly, for the permeation of a butadiene-isobutene mixture through a butadiene-acrylonitrile copolymer, Brun *et al.* (1974) found an inverse proportionality between flux and thickness, except at the lower thicknesses ($\leq 12\mu$m), but in this case flux was higher than anticipated. A change in the membrane structure for these thin membranes was implicated since these had been produced by the biaxial stretching of thicker membranes. Selectivity was found to be constant for thicknesses above 100μm but below this it depended on experimental conditions: the selectivity decrease was stronger for higher downstream pressures and was virtually independent of thickness for vacuum conditions, although a definition of "vacuum" was not given. The authors explained this by considering the latex to be composed of very thin grains (0.5-5μm) which produce highly tortuous micropores in the membrane. Diffusion through these pores only becomes perceptible when thickness is comparable with the

size of the grain, and pressure exerts an influence because when the pressure gradient across the membrane is high, the micropores are crushed and disappear. Another explanation may be found by considering equation 4.1 and associated assumptions for each component. In this case:

$$\frac{(a_{fi} - a_{pi})}{(a_{fj} - a_{pj})} = Constant \qquad (4.2)$$

At vacuum conditions on the permeate side, both a_{pi} and a_{pj} approach zero and the selectivity will be constant with the change in membrane thickness. At higher permeate pressures, a_{pi} and a_{pj} must be considered. If the membrane is selective towards component i, then $a_{pi} > a_{pj}$ under most conditions and the driving force for the selective component will be reduced more than the dirving force for the other component. The overall effect is to reduce the selectivity.

Spitzen *et al.* (1988) studied the permeation behaviour of polyacrylonitrile (PAN) membranes for the separation of ethanol and water using membrane thickness and morphology as variables. Flux increased with decreasing membrane thickness but the change was not inversely proportional for either permeant, and selectivity began to decrease at a thickness of approximately 50μm and dropped drastically below 20μm. Changing the membrane morphology by decreasing the solvent evaporation rate during membrane preparation improved selectivity but a decrease in separation factor with decreasing thickness was still evident. These workers concluded that membrane morphology, sorption resistance and concentration polarisation may all have been contributing factors to this behaviour.

Nijhuis, Mulder and Smolders (1991) did not find a linear relationship between the organic component flux and the reciprocal membrane thickness when using PDMS

and EPDM membranes for the removal of low levels of toluene from water. However, in this case, a concentration polarisation boundary layer in the feed was recognised as hindering mass transport. As the membrane decreased in thickness, the resistance to mass transport from the boundary layer increased in significance and became the limiting mass transfer step.

Further, Koops (1992) tested polyvinyl chloride (PVC), PAN and PSf membranes of different thicknesses for the dehydration of acetic acid (80wt% solution) and in all cases found that selectivity was constant above a certain limiting thickness but below this thickness (20μm) it decreased dramatically for PAN and PSf membranes, dropping at a smaller rate for the PVC membranes. The total flux obeyed Fick's law but Koops compared component fluxes and found that whilst the water flux obeyed Fick's law, the acetic acid flux increased exponentially with reciprocal membrane thickness. Neither differences in polymer morphology, sorption resistance or flow coupling could account for this behaviour.

From these results it can be concluded that the influence of active layer thickness is not always straightforward. In summary, factors which may cause deviation from the performance-thickness relationship specified by Fick's law are so-called sorption resistance, which can now be ascribed to concentration polarisation, and membrane morphology. Artifacts and temperature effects may also cause deviations (Spitzen, 1988): the former would lead to non-reproducible results whilst the latter results in a flux lower than expected. This occurs because of either temperature polarisation or the occurrence of a temperature profile across the membrane due to a phase transition of the permeant, although experimental evidence of either is not documented in the literature for binary mixtures.

4.1.2 RESISTANCES-IN-SERIES MODEL

Figure 4.1 shows a schematic diagram of the activity profile during permeation. Assuming that the porous support layer provides no resistance to mass transport, a two-part resistance model can be developed. An overall mass balance results in a flux equation which includes the overall driving force and the total resistance to mass transport (R_{TOTAL}):

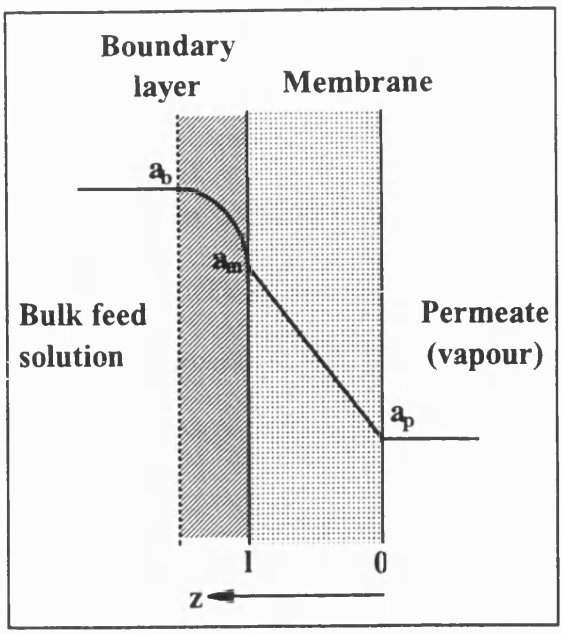

Figure 4.1 Activity profile of a component permeating through a composite membrane

$$J = M(a_b - a_p)/R_{TOTAL} \tag{4.3}$$

M is a factor to convert mass fractions to activities.

Similarly, flux equations can be written for each stage of the permeation process:

$$J = Mk_{BL}(a_b - a_m)F \tag{4.4}$$

where k_{BL} is the boundary layer mass transfer coefficient and F is a correction factor to account for the deviation from a simple, linear relationship between flux and activity. A derivation of this relationship is given in Chapter 5. Its result is:

$$F = [1 + w_b(1 + \frac{2}{3}w_b)] \tag{4.5}$$

where w_b is the weight fraction of water in the feed liquid.

Also:

$$J = MS\frac{D_0}{l}(a_m - a_p) \tag{4.6}$$

where D_0 is the concentration-independent activity-based diffusion coefficient for permeation through the active layer and S is the solubility coefficient. M is a conversion factor for the liquid phase.

The product D_0S is identical to the permeability, P_0. These equations can be combined to give:

$$R_{TOTAL} = \frac{1}{Fk_{BL}} + \frac{l}{P_0} \tag{4.7}$$

From this equation, the resistances to mass transport through the membrane can be calculated and their relative importance ascertained.

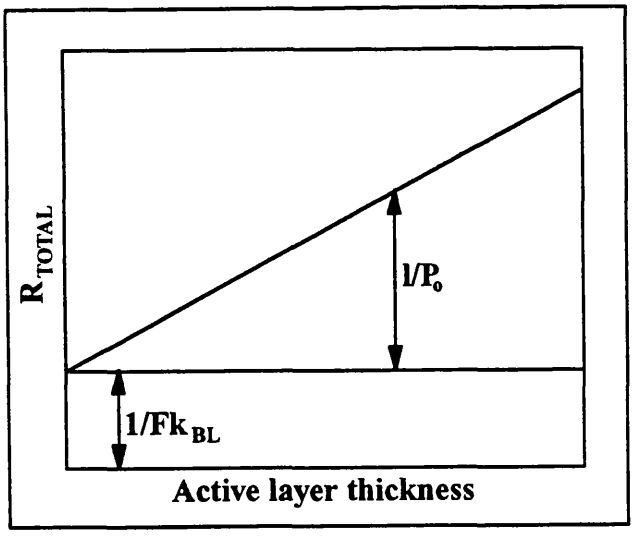

Figure 4.2 Determination of mass transfer resistances by variation of membrane thickness

If k_{BL} is kept constant and P_0 is independent of concentration, plotting total resistance as a function of active layer thickness should result in a straight line where the intercept is equal to the boundary layer resistance and the gradient is equal to the reciprocal permeability (Figure 4.2). This method has been applied, using concentration rather than activity driving

forces and without the use of correction factor, F, by Nijhuis, Mulder and Smolders (1991) and Field and Burslem (1992). M effectively cancels out in the equations and calculations can be performed using mass fraction, rather than activity-based driving forces.

4.1.3 MEASUREMENT OF ACTIVE LAYER THICKNESS

Of course, in order to investigate the influence of thickness upon membrane performance, the thickness must be measured. Scanning electron microscopy (SEM) is frequently used, but attention must be paid to sample preparation. Knowledge of the swelling of a membrane and the resultant steady state concentration profile within it is also useful as it facilitates the calculation of the plasticisation parameter, k_i (Néel, 1993). The stack technique has been used by several workers (e.g. Kim and Kammermeyer, 1970) but the pervaporation research group at Nancy, France, have attempted to observe directly the steady penetrant concentration profile as it was actually established in a working barrier (Néel, 1993). A pervaporation microcell was designed, placing a parallelepiped of homogeneous membrane material between two microscope slides (Figure 4.3). The polymer was viewed by directing a light microscope to the appropriate area. The microcell was sealed and one half evacuated, while the other was exposed to a very small quantity of penetrant. The progressive swelling of the polymer slice was observed and finally, the steady pervaporation regime. Néel observed little grains or defects in the polymer and found that by noting relative distances between them, the extent of local swelling could be ascertained. In the case of a single penetrant, the results of those measurements were analysed in a statistical way and translated into a penetrant concentration profile.

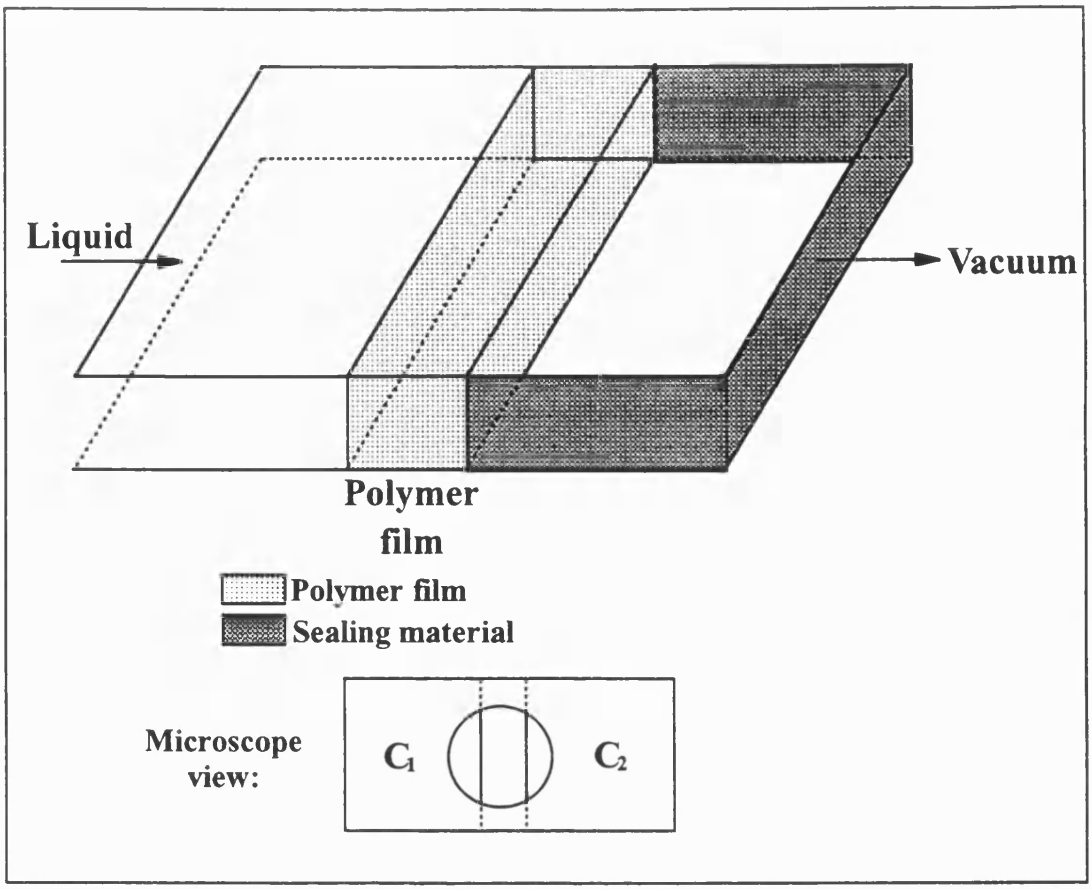

Figure 4.3 Pervaporation microcell designed for the observation of the steady pervaporation profile of a single penetrant (Néel, 1993)

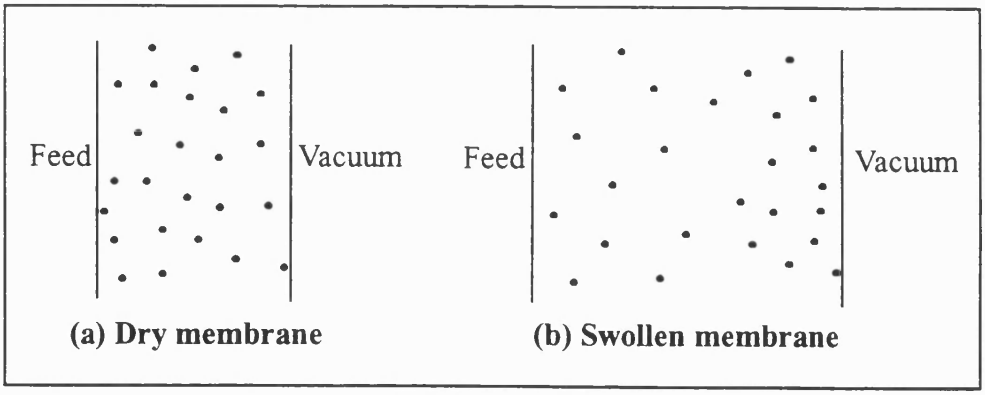

Figure 4.4 The steady pervaporation profile of a penetrant as viewed by a light microscope (Néel, 1993)

4.1.4 EXPERIMENTAL WORK

Results are presented within this chapter which indicate the effect on system performance of varying the active layer thickness, which was varied by changing the weight of polymer solution cast. Using the resistances-in-series model, resistances to mass transport were decoupled to reveal the controlling resistances for the system. Efforts to measure the active and support layer thicknesses are also detailed, along with an attempt to observe the swelling behaviour of the polymer.

The molecular weight of the polymer used also affects the casting properties of the polymer solution and allows a wider range of active layer thicknesses to be constructed. This has been investigated within this chapter.

4.2 EXPERIMENTAL

4.2.1 MEASUREMENT OF THICKNESS

The measurement of thickness was attempted using scanning electron microscopy (SEM). Firstly, the thicknesses of polysulfone (PSf) and Bekipor support materials were found, for comparison with SEM results, using a micrometer. Five readings of thickness were taken for each material and an average value determined.

Pervaporation membranes were prepared, as described in Method 1 of Section 2.2.2, casting onto PSf or Bekipor supports. In this instance, Bekipor support material was sprayed with Frekote 1711, a hydrophobic mould release agent, before being coated. The purpose of this was to partially prevent the polymer solution penetrating the larger pores of the microporous support.

Initially, samples were prepared for SEM work by simply cutting out small squares (4mm $\times$ 4mm approx.) from a substrate or dry membrane using a razor blade. At a later point, samples were first frozen in liquid nitrogen before being cut.

Each sample was stuck onto a stub using carbon conductive paste and sputtered with a thin layer of gold to prevent charging up occurring when performing SEM measurements.

In the first instance, a Jeol T330 Scanning Electron Microscope was used in the normal mode. Micrographs of top and bottom surfaces and cross-sections of support materials were taken along with cross-sectional profiles of composite membranes.

Subsequently, SEM analysis was carried out at the University of Plymouth using a Jeol JSM6100 microscope. Membrane samples were frozen in liquid nitrogen slush, then placed in the cryo-unit, where they were held at -160°C. Samples were either cut by a guillotine action or fractured, both processes occurring within the unit, to produce an edge for cross-section analysis. At this point water contained in the sample was sublimed off, if required. Samples were given a 90 second gold coat, then micrographs were taken. This method was particularly useful to gain an indication of the swelling of the polyacrylate layer. A membrane sample was soaked, prior to initial freezing, in a solution of 10wt% water, 90wt% IPA at room temperature for 45 minutes.

4.2.2 ACTIVE LAYER THICKNESS EFFECTS

Membranes were prepared by casting known weights of polymer solution, CsPA, MW 250K, pH 8.5 onto PSf support. The weights used were 5, 10, 20 and 40g of a CsPA solution of concentration 0.5wt%. Drying took place at 35°C. The performance of all prepared membranes was tested by batch dewatering of an IPA solution with a feed temperature of 70°C and stirrer speed of 1000rpm. The vacuum was less than 4.5mbar, measured next to the vacuum pump.

4.2.3 MOLECULAR WEIGHT AND THICKNESS

Membranes were prepared and tested under identical conditions to those stated in Section 4.2.2, except that the polymer solution used was 0.1wt% CsPA, MW 4M, pH 8.5. Weights cast were 10, 20 and 40g of solution.

4.3.1 MEASUREMENT OF THICKNESS

Micrographs of the surfaces of support materials are given in Chapter 6, where the structures and influence of these materials are also discussed.

Correct sample preparation was essential for the successful analysis of cross-sectional samples. Initially, samples were cut at room temperature with a razor blade. However, when viewed under a light microscope, it was noted that the cutting action stretched a layer of polyacrylate across the width of the support, obscuring the skin layer of the polysulfone. In the case of the Bekipor-supported membrane, in one instance the polyacrylate layer peeled away from the hydrophobic surface of its support (Figure 4.5). Viewing the toplayer of a composite membrane also revealed cracks on the surface (Figure 4.6). These were artifacts caused by the preparation method used.

Immersing the membranes in liquid nitrogen for several minutes before cutting resulted in the creation of a better surface and cracks were no longer viewed on the surface. Direct freeze-fracture was attempted but was unsuccessful, particularly with the Bekipor support, which being made of stainless steel, was not easy to fracture, even at low temperature.

Despite the use of special stubs, positioning the sample within the stub in order that the microscope is able to view the cut surface at a perpendicular angle also presented some problems. For example, Figure 4.7 shows a sample of Bekipor

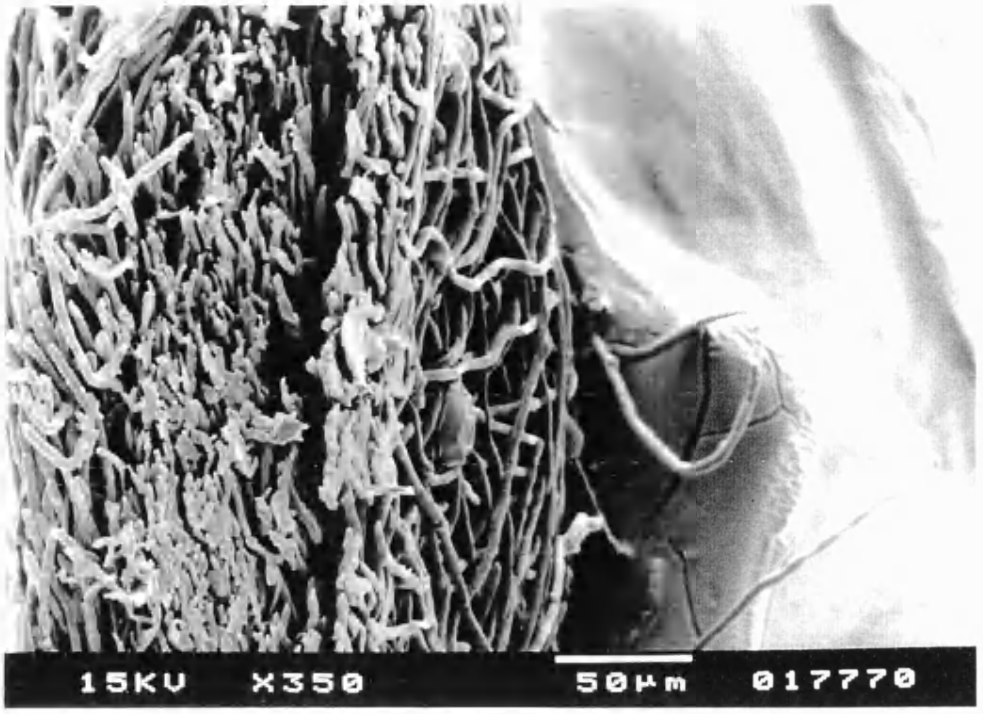

Figure 4.5 Scanning Electron Micrograph (SEM) of a cross-section of a Bekipor-supported CsPA membrane

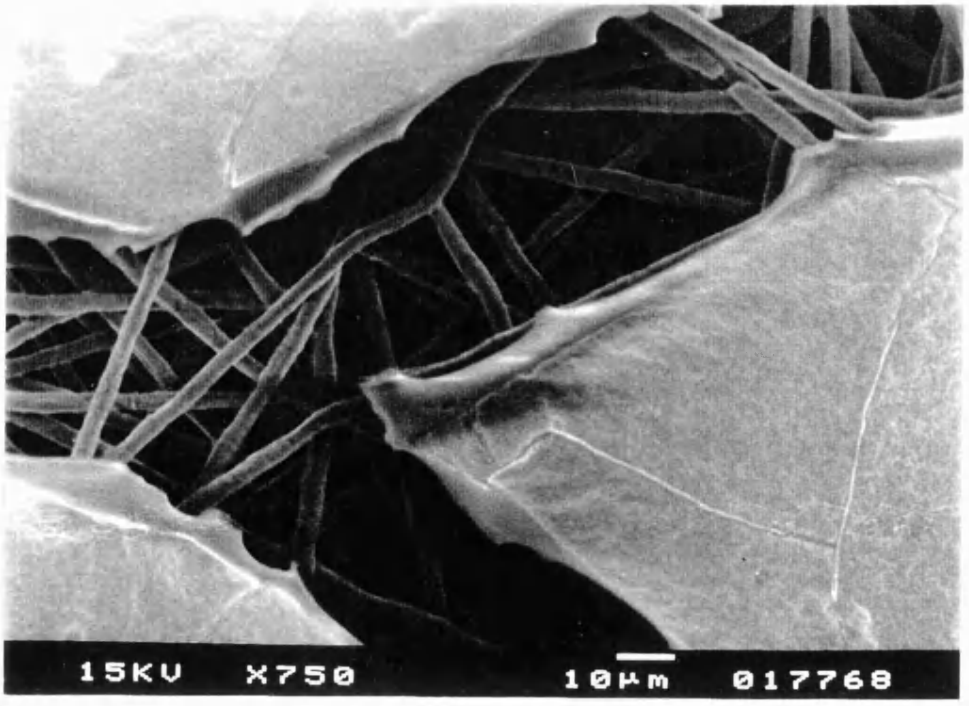

Figure 4.6 SEM of the top surface of a Bekipor-supported CsPA composite membrane

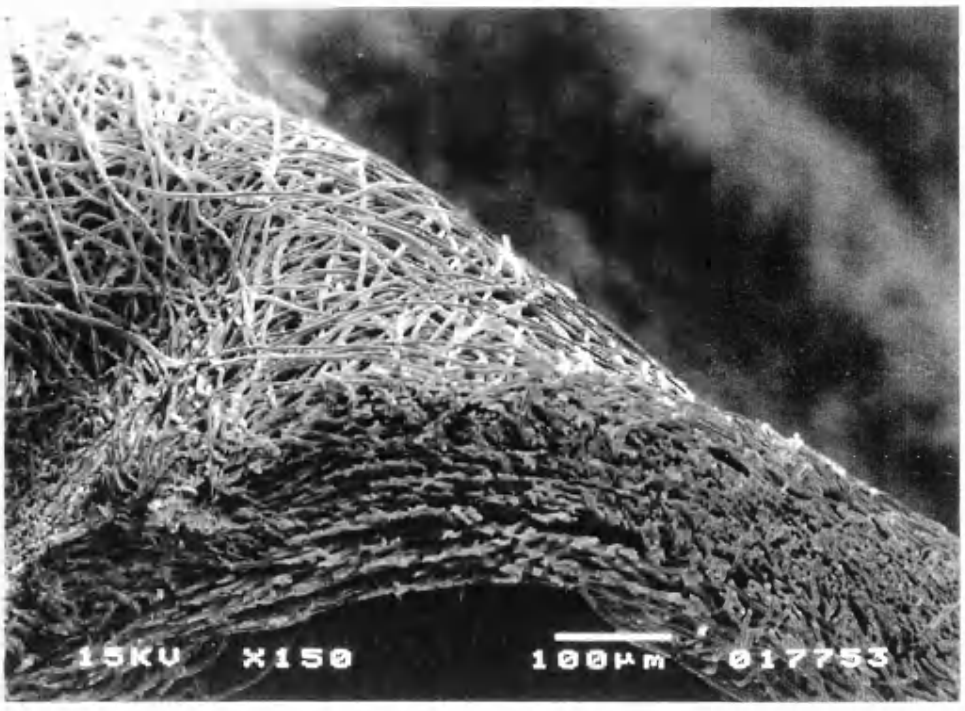

Figure 4.7 SEM of the cross-section of Bekipor stainless steel microfiltration membrane

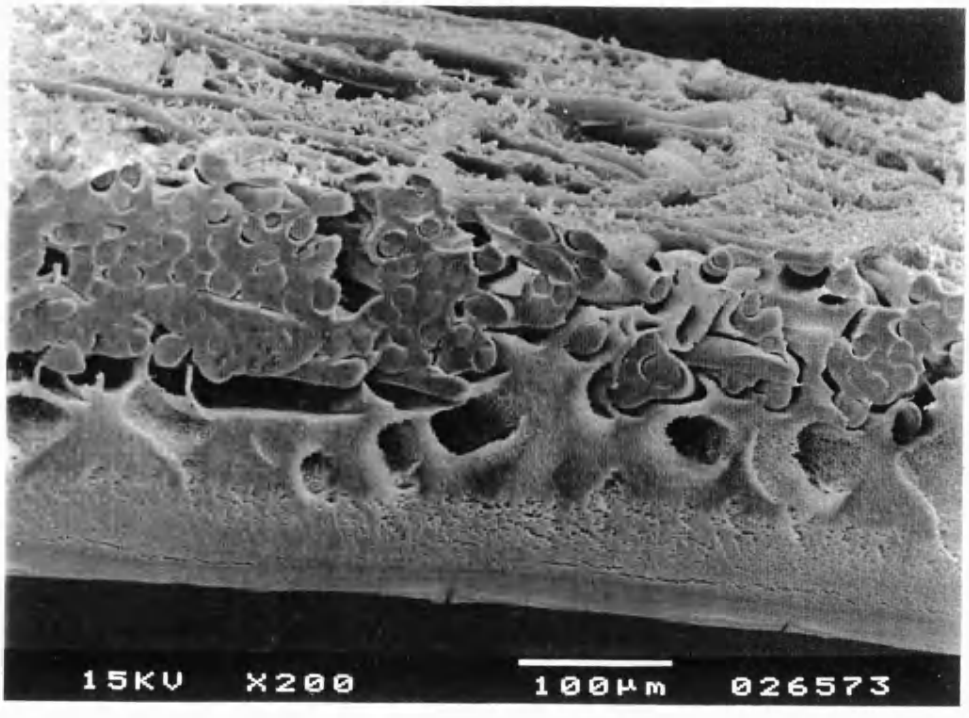

Figure 4.8 SEM of the cross-section of polysulfone ultrafiltration membrane

curling to one side whilst Figure 4.8 shows a sample of PSf correctly positioned to measure its thickness.

Four micrographs were taken to find an average value of support material thickness. Results of thickness measurement by SEM and by micrometer are given in Table 4.1. The two methods gave fairly consistent results although the thicknesses measured by SEM are slightly smaller. This may be due to material compression during sample preparation.

Material	Thickness (μm)	
	Micrometer	SEM
Polysulfone	300±0	275±25
Bekipor	244±5	190±17

Table 4.1 Measured thicknesses of support materials

Figure 4.9(a) shows the cross-section of a PSf-CsPA composite membrane, prepared by cutting the frozen sample within the cryo-unit of the Jeol JSM6100 microscope. Water within the sample has been sublimed off. The boundary between the PSf and polyacrylate layers cannot be distinguished. The polyacrylate layer seems to have stretched over the support edge whilst being cut. Fracturing produced a much better surface, as can be seen in Figure 4.9(b). In this, the boundary and the structure of the PSf can be seen much more clearly. However, the toplayer thickness seems to vary, although this may be due to the angle at which the photograph was taken. On average, the value for the thickness of a membrane prepared using 20g of polymer solution was found to be 36±5μm.

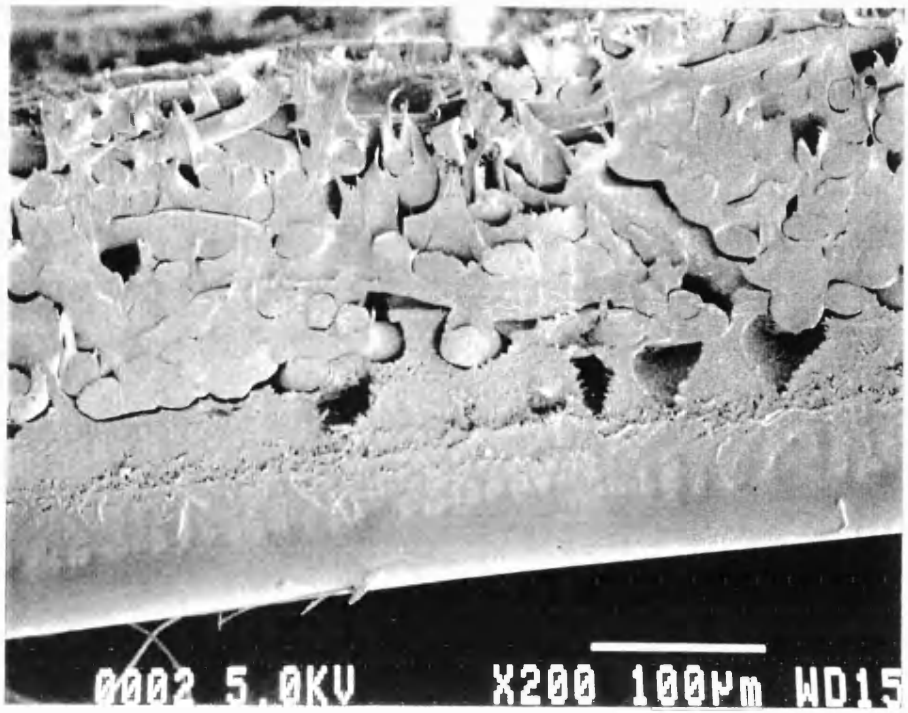

(a)

(b)

Figure 4.9 SEM of the cross-section of a 20g CsPA toplayer cast onto PSf. Edge (a) cut (b) fractured

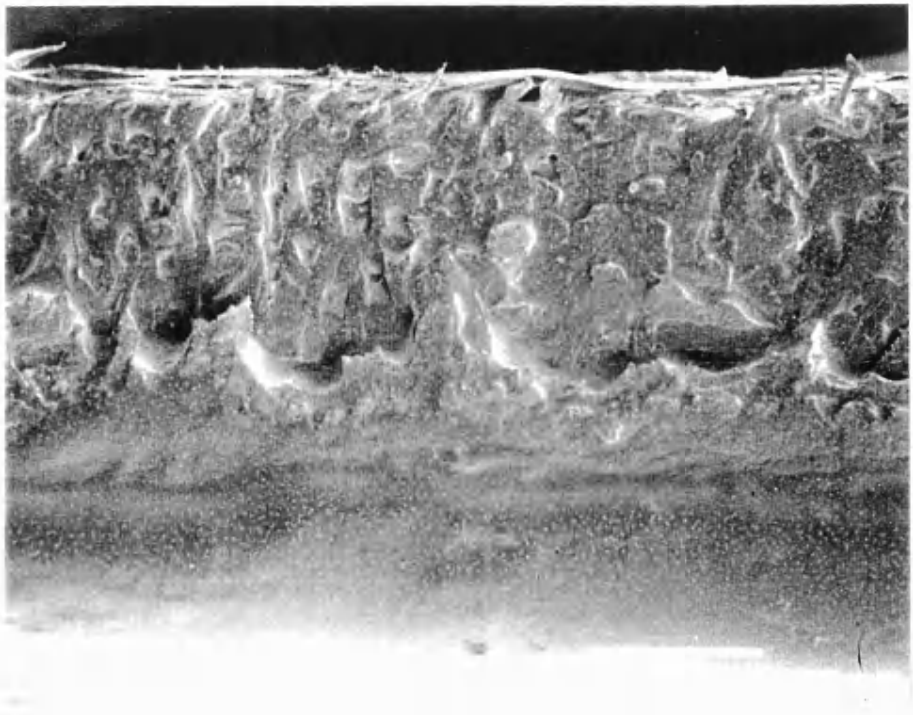

(a)

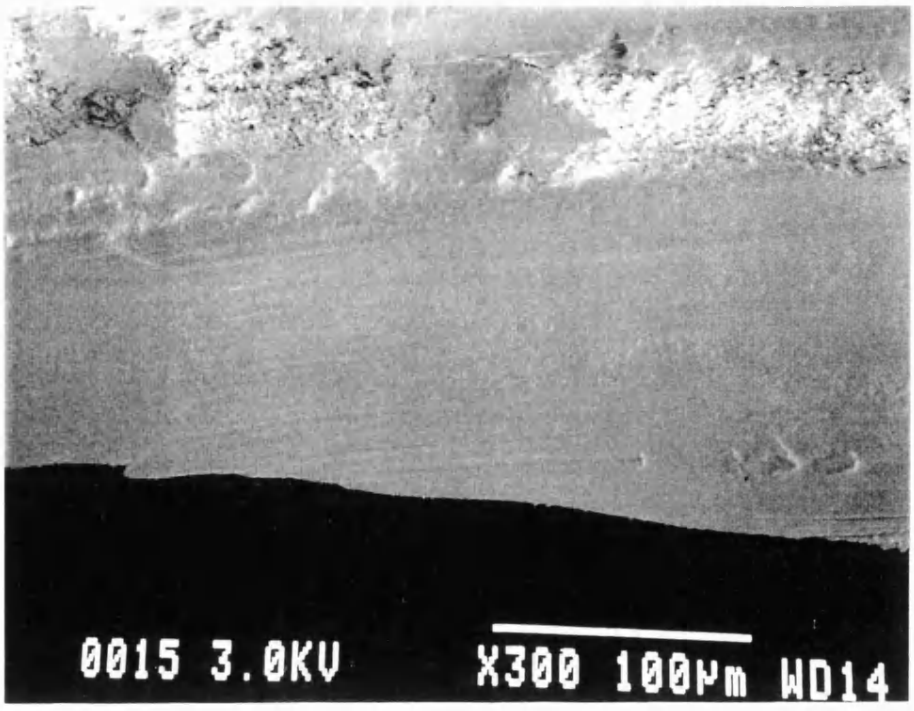

(b)

Figure 4.10 SEM of the cross-section of a 20g CsPA toplayer cast onto PSf. Soaked in IPA (90wt%)-water (10wt%) solution for 45 minutes prior to freezing. Edge (a) cut (b) fractured

SEMs taken from swollen membrane samples are shown in Figure 4.10(a) (cut sample) and 4.10(b) (fractured sample). Obviously, the membrane swells considerably, possibly to more than three times its original thickness, but even for the fractured sample, a distinct boundary between the active and support layers cannot be seen. Water has not been removed from these samples and experience suggests that this obscures the boundary between the two layers, as pores in the PSf would be filled with H_2O/IPA mixture. However, removing this fluid by sublimation would result in the collapse of the toplayer structure.

Another method has been used within the Chemical Engineering Dept. at Bath, but not by the author, to find the thickness of the CsPA top layer (Wu, 1994). The principle of the method was to find the density of dry CsPA using a volume-calibrated pycnometer filled with IPA, measuring its mass and volume before and after immersion of a membrane sample. Knowing the area and mass of the sample used, its thickness was then calculated. The thickness of a membrane prepared from 10g of polymer solution was calculated to be $14.05 \pm 0.11 \mu m$. The pycnometric method was simple and the results were highly reproducible. Therefore, a decision was made to use this result for the membrane thickness value. It was assumed that the membrane morphology was unaffected by the weight of polymer solution cast and therefore that the dry thickness was directly proportional to the cast solution weights (Table 4.2). This predicts a thickness of $28 \mu m$ for a 20g membrane, which compares favourably with the thickness found from the SEM technique ($36 \pm 5 \mu m$).

Wt of 0.5wt% CsPA solution, pH 8.5, MW 250000, used (g)	5	10	20	40
Active layer thickness (μm)	7	14	28	56

Table 4.2 Calculated active layer thicknesses

4.3.2 ACTIVE LAYER THICKNESS EFFECTS

The batch dehydration water flux curves are shown in Figure 4.11. As expected, water flux decreases with increasing membrane thickness. Similarly, IPA flux, whilst being considerably smaller than the water flux, also decreases with increasing membrane thickness (Figure 4.12) but the change does not seem as regular. It is also interesting to note that IPA flux increases with increasing feed water activity, i.e. decreasing feed IPA activity, and decreasing driving force. This may be due to coupling effects.

The water flux experimental results were fitted to the model described in Section 2.8 and the values of the parameters A and B are given in Table 4.3.

Membrane thickness (μm)	7	14	28	56
A ($kgm^{-2}h^{-1}$)	3.61	1.96	0.909	0.465
B	2.30	2.65	3.04	3.18

Table 4.3 Model parameters for effect of thickness experiments

Parameter A roughly doubles as the thickness of the membrane halves, as expected. Parameter B (taken to be a form of plasticization coefficient) increases with increasing thickness indicating that a larger proportion of the membrane is swollen and therefore the plasticisation coefficient, which is not constant across the

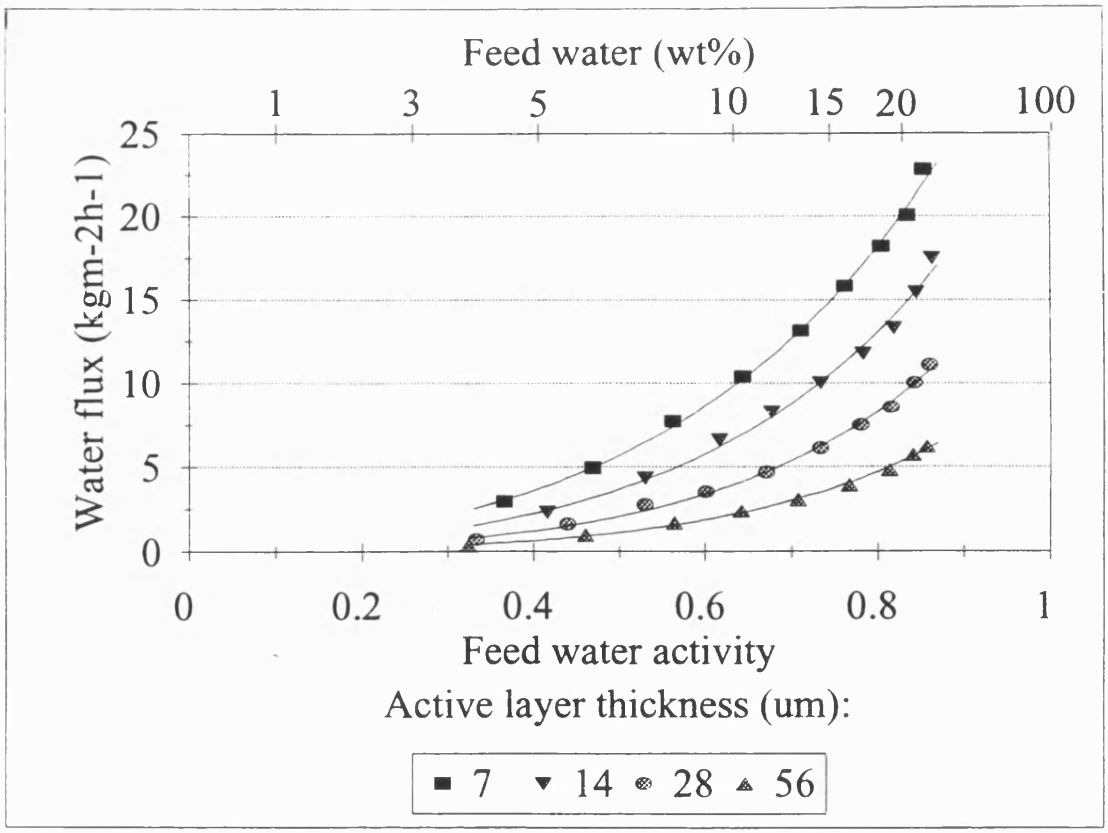

Figure 4.11 Effect of varying active layer thickness upon water permeation

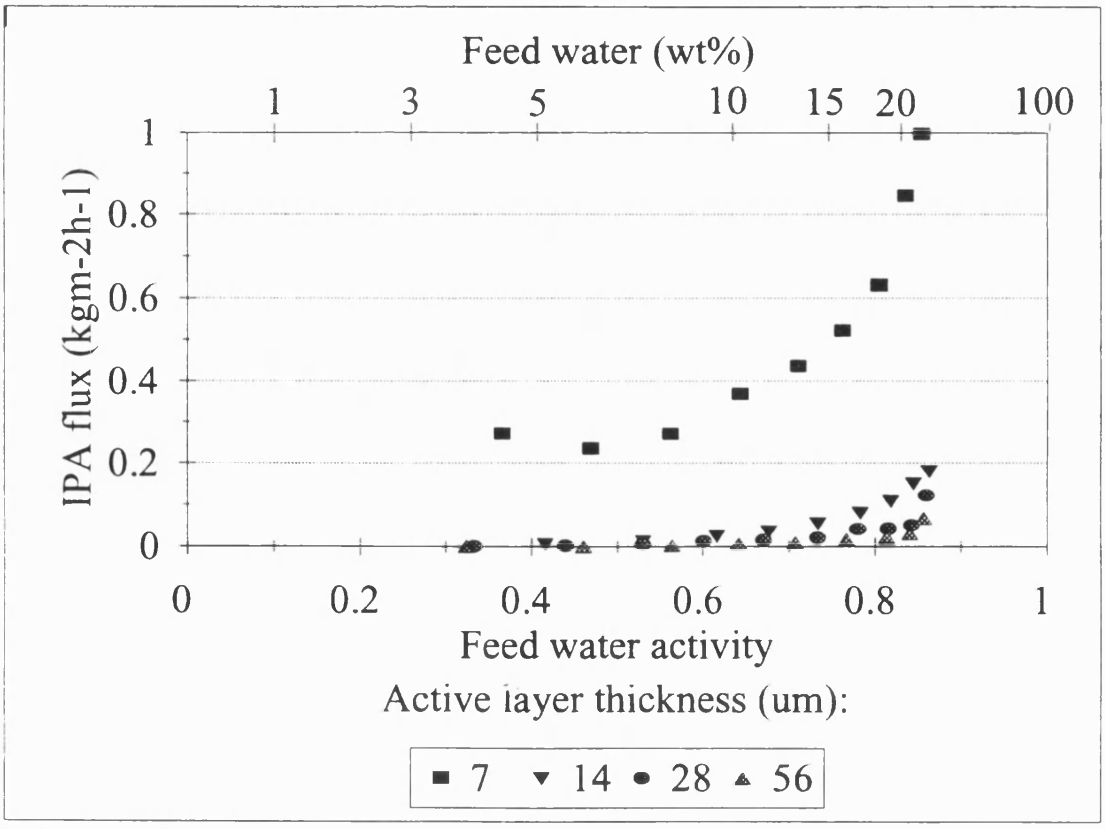

Figure 4.12 Effect of varying active layer thickness upon IPA permeation

membrane due to the anisotropic swelling, has a higher overall value. The rate of change of B with thickness is initially 0.049units/μm but this decreases to 0.005 units/μm for the final interval.

Interpolating the curves of Figures 4.11 and 4.12 and plotting flux against reciprocal thickness for an example feed concentration (10wt% water : Figure 4.13) indicates overall behaviour which deviates from Fick's law. The IPA flux-reciprocal thickness relationship can in fact be fitted to an exponential model. For water, the shape of the curve indicates that concentration polarisation may provide a significant resistance to mass transport. This is investigated below.

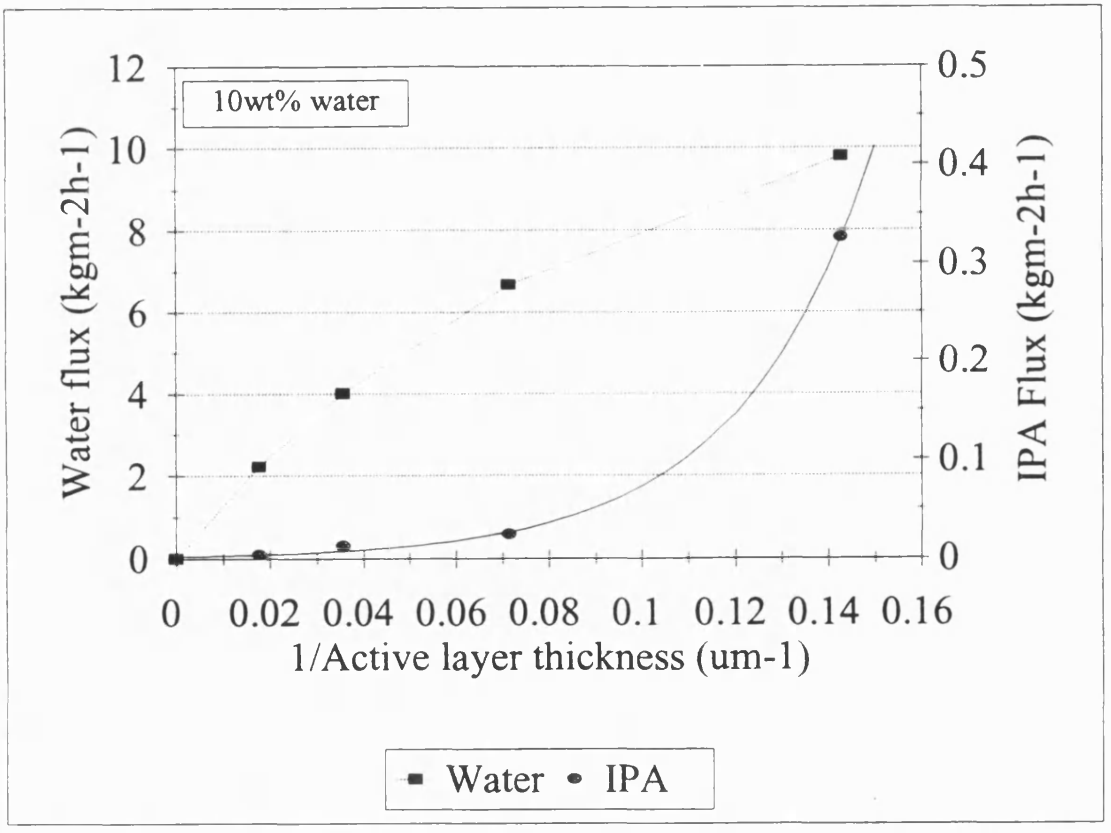

Figure 4.13 Variation of component fluxes with reciprocal membrane thickness

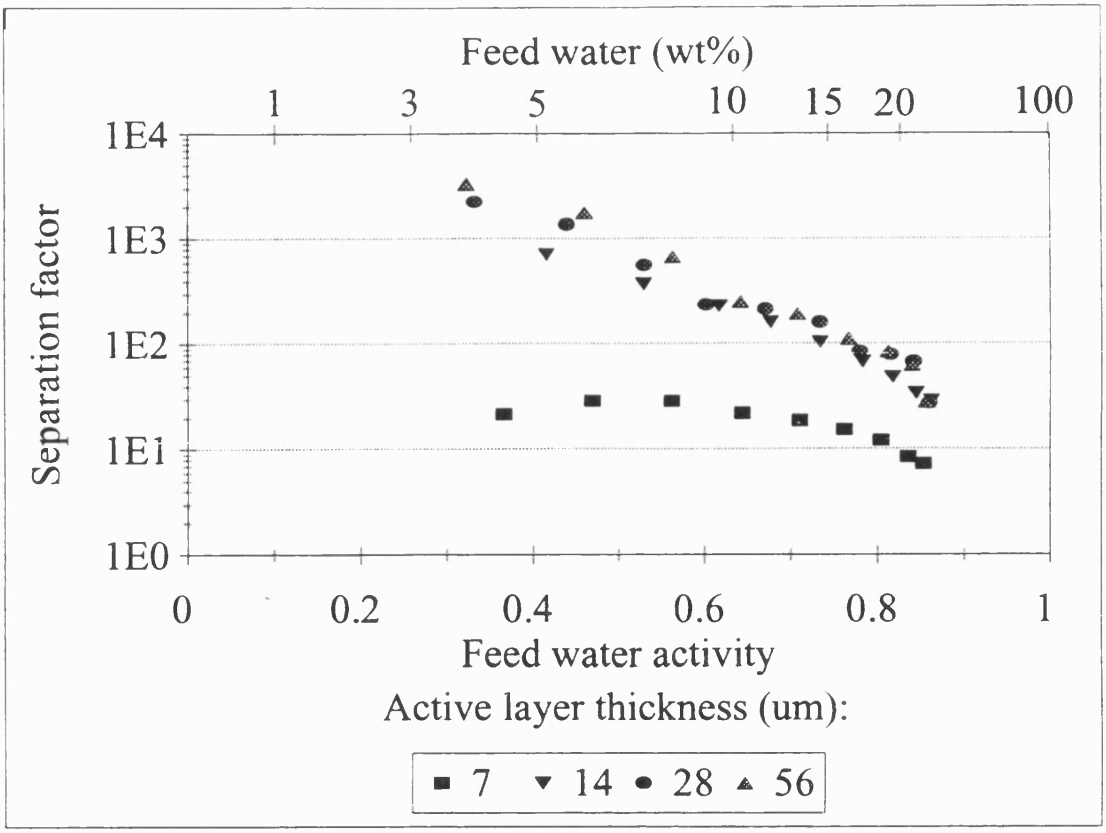

Figure 4.14 Effect of varying active layer thickness upon the separation factor

Figure 4.14 illustrates the significant loss of selectivity for the thinnest membrane used due to the increase in IPA flux. There is little difference in selectivity for the three other thicknesses tested which suggests that a critical membrane thickness may exist between 7μm and 14μm for a CsPA membrane made from Polyacrylic acid with a molecular weight of 250,000.

The resistances-in-series model was used, as described in the introduction to this chapter, to assess the significance of the boundary layer and that of the membrane itself. Total resistances to mass transport, for four example feed concentrations, were calculated from flux and activity data, assuming the activity of the permeate to be negligible. Straight lines were obtained using linear regression (Figure 4.15) and the correlation was excellent ($R^2 \geq 0.99$). Resistances to mass transfer, boundary layer

mass transfer coefficients and permeability values, shown in Tables 4.4 and 4.6, were calculated from equations 4.3 to 4.7.

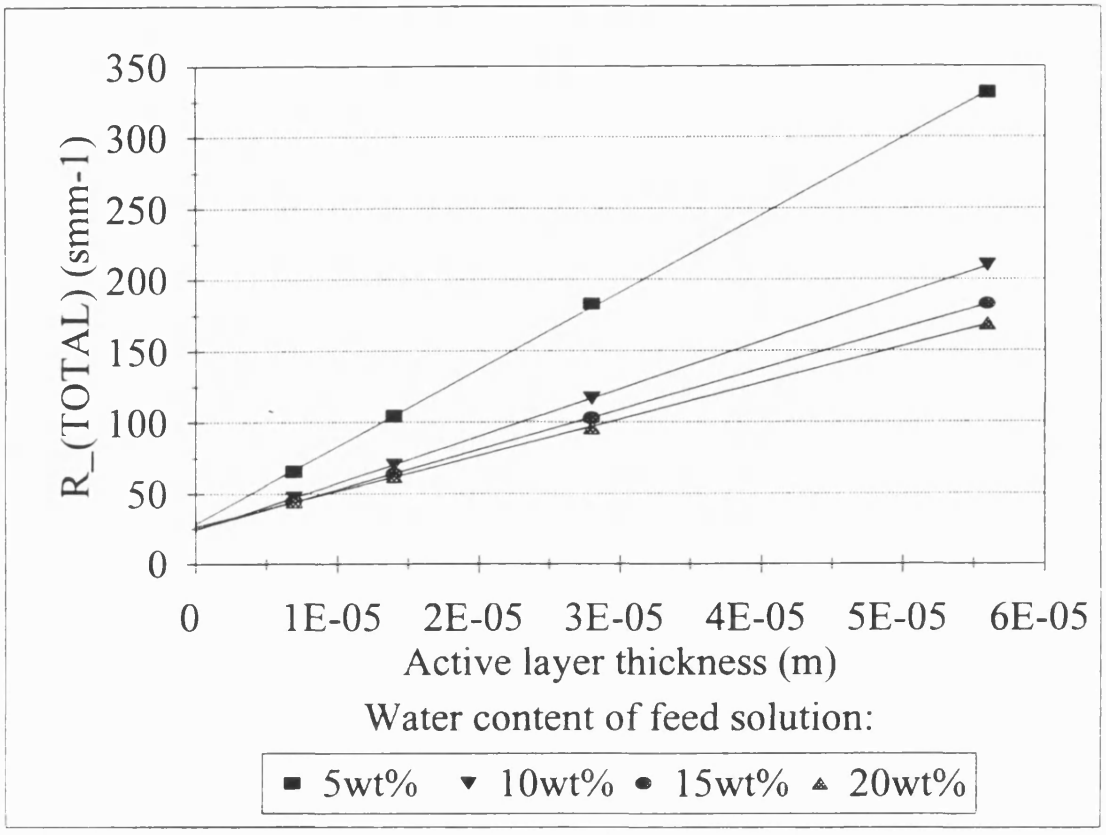

Figure 4.15 Determination of mass transfer resistances by variation of active layer thickness

Active layer thickness (μm)		7	14	28	56
Feed water (wt%)	R_{BL} smm-1	R_m smm-1	R_m smm-1	R_m smm-1	R_m smm-1
5	28.7	38.0	76.0	152	304
10	24.1	23.2	46.4	92.9	186
15	24.8	19.7	39.4	78.9	158
20	26.4	17.8	35.5	71.0	142

Table 4.4 Variation of boundary layer and membrane resistances with feed composition and membrane thickness

Although the resistance to mass transport provided by the liquid boundary layer is approximately constant ($26.01 \pm 2.04 \times 10^3 sm^{-1}$), its significance increases with increasing feed water content. For a membrane of 14μm thickness, at 5wt% feed water, the boundary layer resistance is 27.4% of the total, whilst at 20wt% it is 42.7%. This trend contradicts the assumptions of other workers e.g. Néel, (1993) who stated that "boundary layer effects are more perceptible as the faster permeant is less concentrated in the process liquid mixture." Boundary layer effects are further discussed in Chapter 5. Also, the boundary layer resistance increases in significance as the membrane thickness decreases, behaviour which was also found by Nijhuis *et al.* (1991), and is the limiting resistance for the 7μm thick membrane at most feed compositions. This fact is further emphasised when, using Equation 4.4, the actual composition of feed at the membrane surface is calculated. This is shown, in terms of wt%, in Table 4.5.

Active layer thickness (μm)	7	14	28	56
Bulk feed concentration (wt%)	c_m (wt%)	c_m (wt%)	c_m (wt%)	c_m (wt%)
5	2.79	3.61	4.02	4.56
10	4.86	6.49	7.88	8.82
15	6.55	9.02	11.3	12.9
20	7.86	11.2	14.3	16.7

Table 4.5 Variation of water concentration at the membrane surface with bulk feed concentration and membrane thickness

Feed H2O (wt%)	k_{BL} (μms^{-1})	P_0 (m^2s^{-1})
5	33.1	1.84×10^{-10}
10	37.44	3.01×10^{-10}
15	34.63	3.55×10^{-10}
20	30.87	3.94×10^{-10}

Table 4.6 Variation of mass transfer parameters with feed composition

The boundary layer mass transfer coefficient should not vary with feed composition but the slight variation in calculated values is acceptable and may be further corrected by a more precise calculation of the correction factor, F.

By using a membrane resistance value, rather than the total resistance, an "ideal flux" can be calculated for the most permeable component. Plotting these

fluxes against reciprocal membrane thicknesses (Figure 4.16) shows that Fick's law does hold, at least for the preferentially permeable component, and also demonstrates the potential performance of the membrane material.

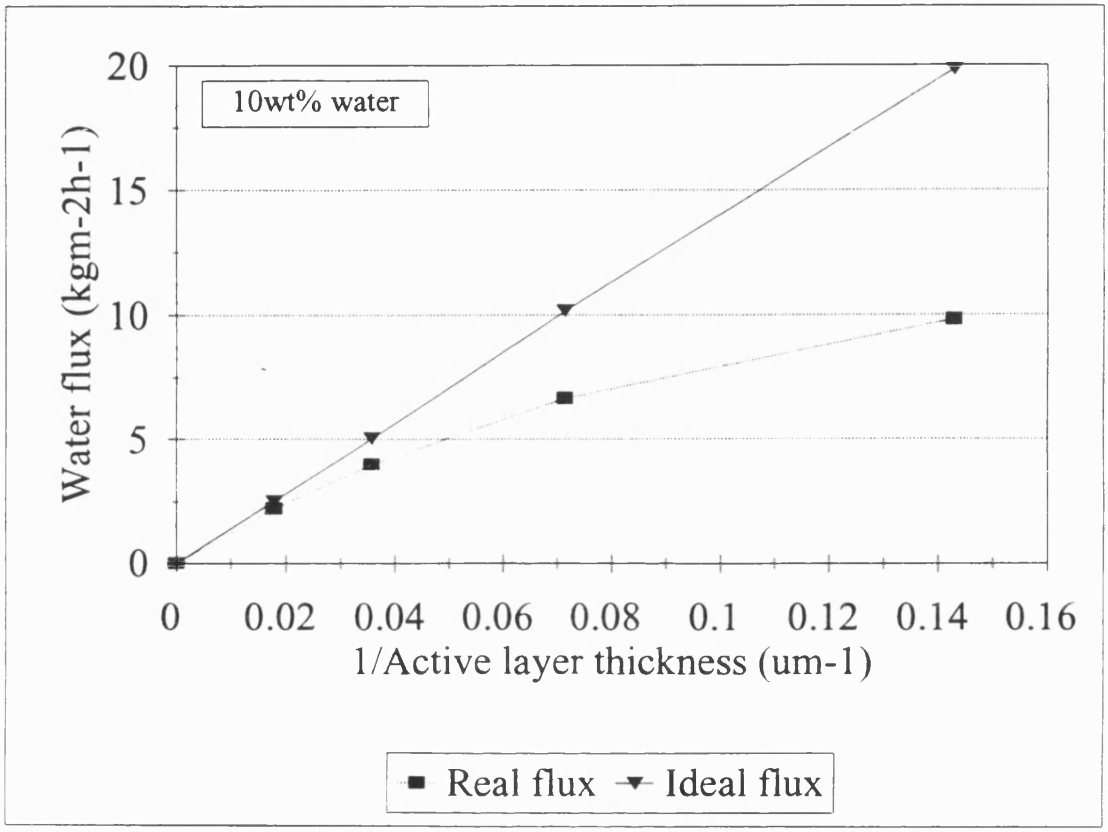

Figure 4.16 Comparison of "ideal" (no system mass transfer resistance) and real fluxes

Membrane permeability increases with increasing feed water content, particularly between 5wt% and 10wt% feed water (Figure 4.17 and Table 4.6). If P_0 was independent of concentration, all the points would fall on one line. The increase in P_0 cannot be accounted for by an increase in thickness due to swelling phenomena but may be due to increasing membrane plasticisation which corresponds to an increase in the empirical parameter, B. A variation in diffusivity (and hence permeability) could also be responsible for the changing *significance* of the boundary

layer mass transfer resistance with increasing water concentration.

If the assumption of one-component permeation is made, a relationship often used to symbolise the correlation between D and feed concentration for a rubbery polymer is (Nguyen, 1987):

$$D_i = D^0 \exp(k_i c_{im}) \tag{4.7}$$

where c_{im} is the local penetrant concentration.

For diffusion through a rubbery polymer, a homographic function is more applicable (Néel, 1993):

$$D_i = D^0 \frac{N c_{im}}{Q + c_{im}} \tag{4.8}$$

where N and Q are parameters which depend upon the difference between the operational temperature and the glass transition temperature, T_g, of the polymer. For polyacrylate, it is likely that the active layer works partly as a rubbery polymer (within the swollen region - T_g decreases sharply as concentration increases) and partly as a glassy polymer (in the vicinity of the downstream surface).

For this work, concentration profiles through the membrane and solubilities at the surface have not been measured or calculated so the relationship of diffusivity with concentration cannot be modelled. Only average permeabilities have been found. These appear to possess a linear relationship with both the bulk water activity (Figure 4.17) and the activity at the membrane surface (Figure 4.18). This is not fundamentally significant, but may prove a useful tool for future work. From Figure 4.18, it appears that for the same surface activity, the average permeability for water is higher than if the membrane is thinner. This may be due to the thinner membrane having a proportionately greater difference in swelling across its thickness.

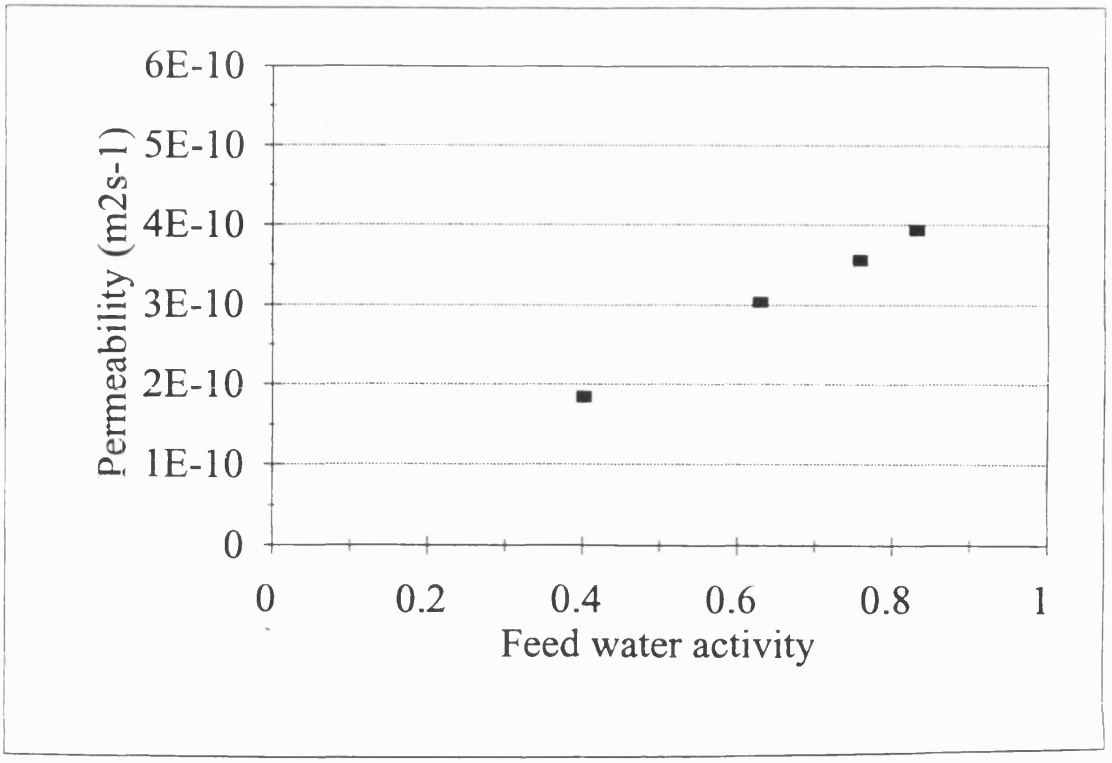

Figure 4.17 Variation in calculated average permeability with water activity in the bulk feed liquid

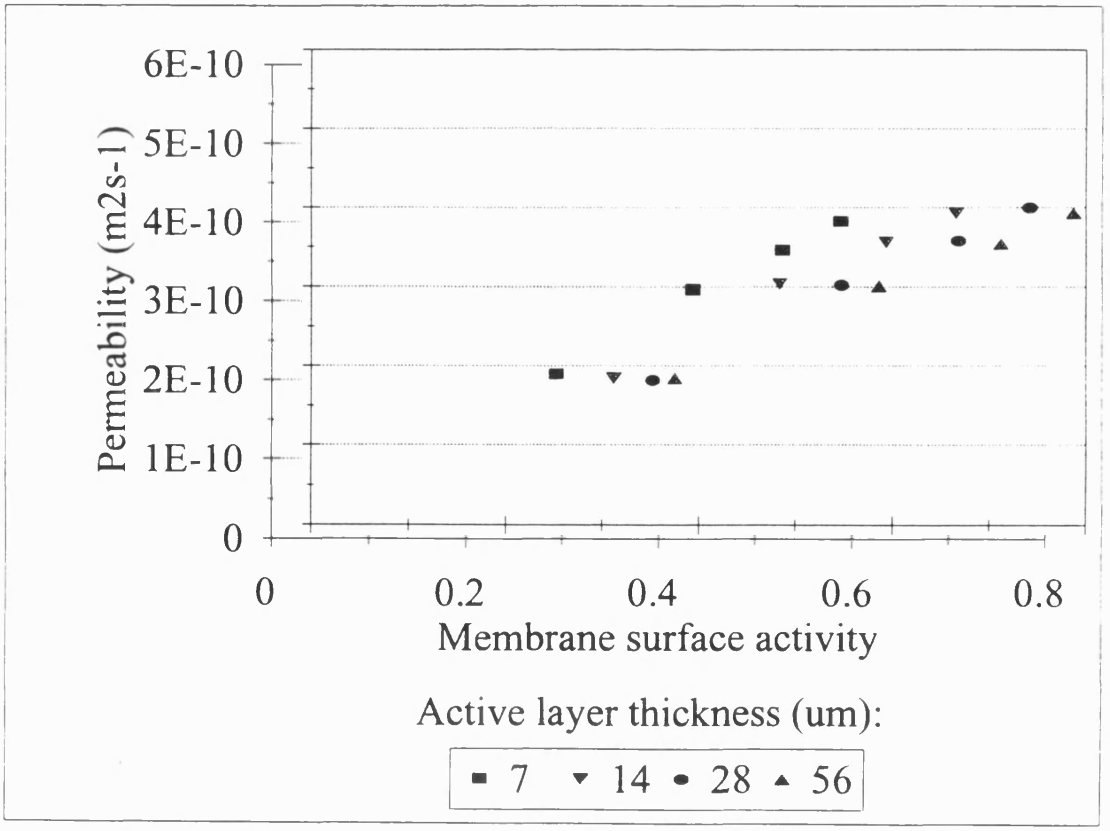

Figure 4.18 Variation in calculated permeability with water activity at the membrane surface

4.3.3 MOLECULAR WEIGHT AND THICKNESS

Assuming that molecular weight had no effect upon the density of the dry polymer, the dry thicknesses cast were 14, 5.6 and 2.8μm. Extremely thin membranes could be prepared using the higher molecular weight polymer. It has already been seen (Section 3.3.3) that molecular weight has no effect on permeation performance for a 14μm thick layer and the thin membranes prepared would be expected to give a higher water fluxes but be accompanied by loss of selectivity. The results pictured in Figures 4.19 and 4.20 do not comply with this prediction.

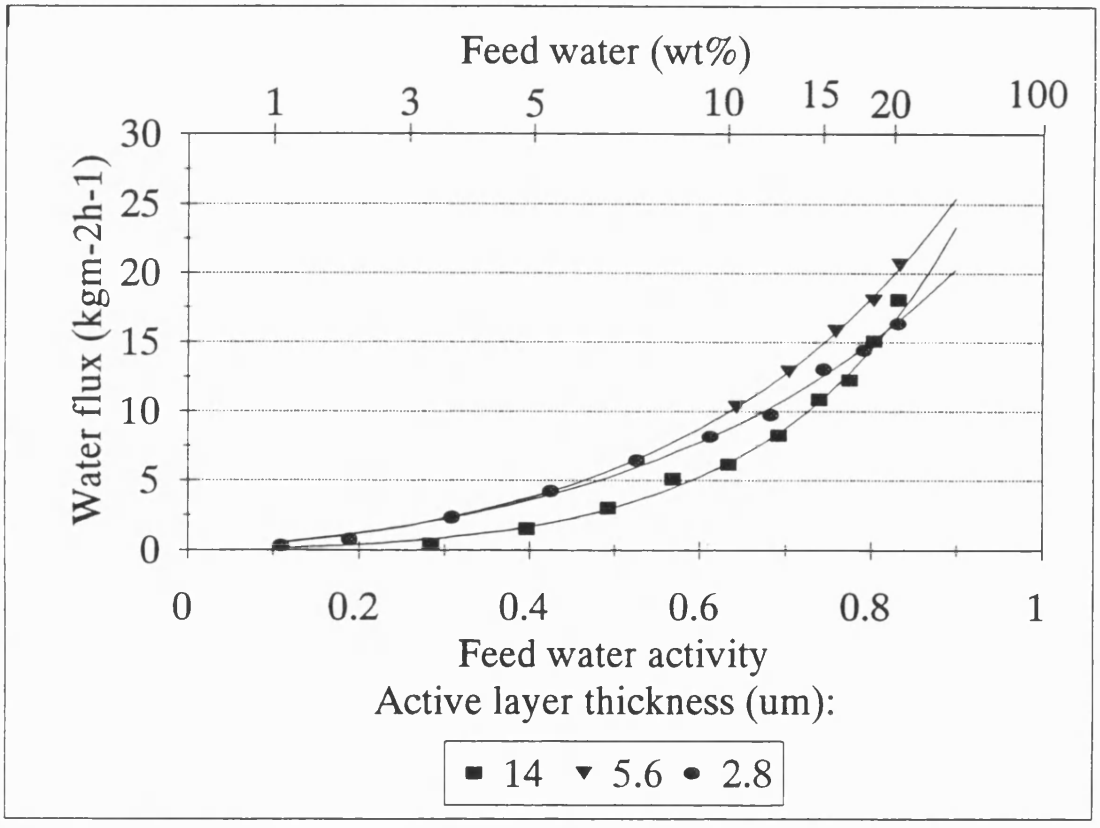

Figure 4.19 Effect of varying active layer thickness upon water flux. Polyacrylic acid molecular weight = 4 million

The small amount of data available for the 5.6μm thick membrane indicates a higher flux than, and similar selectivity to, the 14μm thick membrane, as might be

expected, but the performance of the 2.8μm thick membrane is more complex. At higher water concentrations (>18wt% water), its water flux is approximately the same as that of the 14μm membrane although below this level the flux is higher. This may be an example of boundary layer resistance being totally dominant. Also, the separation factor is lower than that attained with the thicker membranes at higher water content feeds, as expected, but below 5wt% feed water the separation factor is very high. No clear explanation for this is available but it probably relates to the longer chains of the polymer excluding IPA more effectively than the shorter chains, possibly by providing a defect-free surface even when thin and relatively dry.

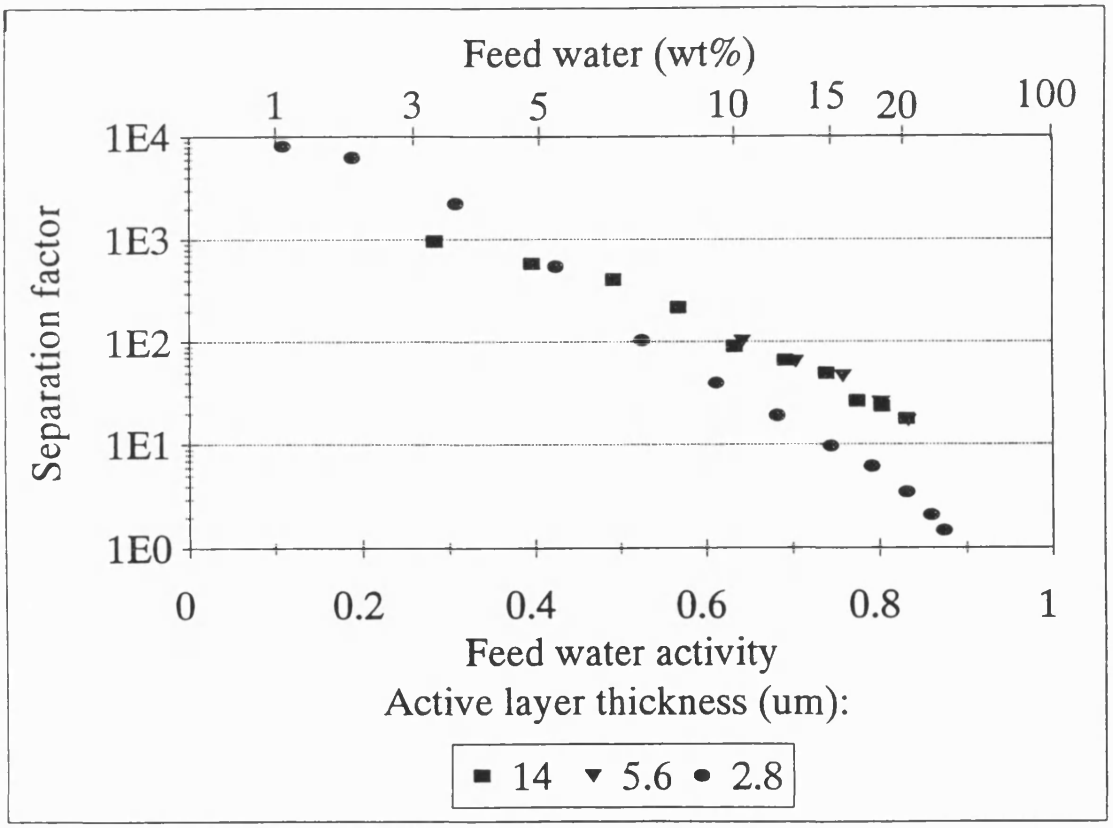

Figure 4.20 Effect of varying active layer thickness upon separation factor. Polyacrylic acid molecular weight = 4 million

Although more work is required to confirm this conclusion, use of a higher molecular weight polymer may be beneficial to produce very thin active layers

without loss of selectivity.

4.4 CONCLUSIONS

Sample preparation for the use of scanning electron microscopy has been discussed and a measurement of the thickness of the dry CsPA active layer has been achieved. The use of the pycnometric method for thickness measurement has also been described. The extent of membrane swelling when exposed to a mixture of water and IPA was also estimated using the SEM. Although this technique requires refinement and development, it may prove a useful tool for future studies.

Using 250K MW polymer, four membrane thicknesses were tested using an impeller speed of 1000rpm and a feed temperature of 70°C. Both water and IPA fluxes increased with decreasing membrane thickness but the thinnest membrane tested (7μm thick) suffered a significant loss of selectivity due to the increasing rate of IPA flux as a function of reciprocal thickness compared to the decreasing rate of water flux. The predictions of Fick's law (flux is proportional to reciprocal thickness) were not obeyed for the overall system.

The resistances-in-series model was used to determine the significance of boundary layer and membrane resistances to mass transport. The boundary layer increased in significance as the feed water concentration increased, although this may be due to an increase in the overall membrane permeability, and as the membrane decreased in thickness. The membrane resistance obviously increased in proportion to the thickness. "Ideal water fluxes" were predicted from the membrane resistances found and were found to possess a linear relationship with reciprocal thickness, proving that deviation from Fick's law for the water flux was due to concentration polarisation. The permeability of water in the membrane increased with increasing

feed water concentration, probably due to increased plasticisation of the polymer. Although this rendered the assumption of concentration-independent diffusivity invalid, this has no effect on the calculations made to decouple the resistances provided by the membrane and the boundary layer.

It has been shown that, from a small number of experiments and using only a few simple equations, a lot of useful information about the system performance can be found.

A higher molecular weight polymer was used to produce membranes of thickness as low as 2.8μm. The use of higher molecular weight polymer may allow such thin membranes to be used to enhance flux without loss of selectivity, although more experiments are required to confirm this theory.

CHAPTER 5

INFLUENCE OF LIQUID BOUNDARY LAYER

5.1 INTRODUCTION

5.1.1 BACKGROUND LITERATURE

The necessity of studying liquid boundary layers in membrane processes was probably first expressed by Smith *et al.* in 1961. They stated that "although the membrane evaluation literature is voluminous and historically quite old, much of it is of qualitative value only, since insufficient attention has been paid to the difference between the overall measured transport properties and those of the membrane itself."

Although studies of liquid hydrodynamics and its influence on system performance are now prevalent in other fields of membrane technology, indeed it could be said to be the dominant influence in most ultrafiltration processes, in the field of pervaporation, until recently, little interest has been paid to this area of study. Concentration polarisation leads to changes in flux and separation behaviour and is inherent to all membrane processes involving liquids. However, it was originally assumed to be negligible in pervaporation due to low transport rates through the membranes and because liquid mass transfer rates are much faster for the smaller molecules transported in pervaporation than for the macromolecules processed in UF and MF (Spitzen, 1988). In the pervaporation of a binary mixture, both molecules permeate but at different rates, leading to a depletion of the more permeable component at the membrane surface. A concentration gradient is set up involving the diffusion of the less permeable component back into the bulk fluid and the simultaneous diffusion of the more permeable component towards the membrane (Figure 5.1).

Three studies concerning concentration polarisation were published in 1988 (Côté and Lipski; Psaume *et al.*; Spitzen). Psaume and co-workers performed experiments to remove dilute (50-250μg/l) trichloroethylene (TCE) from water using a hollow fibre module containing Silastic medical grade tubings. The axial Reynolds number was varied between 10 and 60. TCE permeation was enhanced by higher channel velocities and mass transfer was strongly limited by concentration polarisation. A theoretical model based on liquid film theory and the Levèque correlation for laminar flow was developed based on the assumptions of very low concentration of solute in the inlet stream and of a highly selective membrane. It was inferred that a decrease in membrane thickness would not influence TCE permeation flux under the same experimental conditions.

The study of Côté and Lipski (1988) was again based on the removal of dilute organics (carbon tetrachloride (CCl_4), TCE and phenol) from water, in this instance using a PDMS hollow fibre module. Axial Reynolds numbers of between 200 and 670 were used, higher than for the previous study, and Psaume's simple film model was extended to a resistances-in-series model which included the contribution of the membrane to mass transfer inhibition. When the feed flow rate was increased from Re 200 to 670, the fluxes of CCl_4 and TCE increased by 400% whereas the flux of phenol remained relatively unchanged. Use of the resistances in series model indicated that for CCl_4 and TCE, the liquid film resistance essentially accounted for the observed total resistance whilst for the non-volatile phenol, the membrane resistance was the controlling factor and the flux of this component would only be increased by decreasing the thickness of the membrane. Further, for permeation of the two volatile components, separation factor was strongly affected by variation of

flow rate and membrane thickness because of the different controlling resistances for these solutes and for water. The authors suggested that module design be varied to take account of such factors.

Spitzen (1988) developed a theoretical concentration polarisation model based upon volume balances across an element. The parameters which affected concentration polarisation in his model were liquid densities, flux, feed concentration, separation factor and mass transfer coefficient and these were theoretically varied to estimate the extent of their influence. The results showed that concentration polarisation cannot be neglected "a priori" and that concentration polarisation leads to a decrease in flux and separation factor. Concentration polarisation effects were found to increase with decreasing liquid mass transfer coefficient and concentration of preferentially permeating component and increasing flux and intrinsic selectivity.

Colman *et al.* (1989b) studied the effect of feed flow rate on the performance of a tubular membrane module designed to dehydrate alcohols. The existence of a concentration polarisation boundary layer was evident even in the turbulent flow regime with a feed concentration of 10wt% water. It was modelled in terms of a "polarisation index," (PI), which was a function of the absolute membrane flux and the system hydrodynamics. When polarisation is minimised, PI→1.

The 1990s have seen an increase in the number of papers published which quantify the contribution of feed-side hydrodynamics to overall system performance (e.g. Field and Burslem, 1992; Gooding *et al.*, 1992; Hickey and Gooding, 1994; Karlsson and Trägårdh, 1992; Nijhuis, Mulder and Smolders, 1990; Raghunath and Hwang, 1992a and 1992b).

Nijhuis, Mulder and Smolders (1990) proposed that the starting point for the

commercialisation of any membrane process is the availability of high flux, highly selective membranes. Only once these have been developed should process conditions be looked at in greater detail. Yet, Gooding *et al.* (1992) propose that if the mass transfer coefficient in the boundary layer is less than that in the membrane, there is no incentive to produce highly permeable, thin membranes. Also, they state that the laboratory characterisation of membrane performance will be meaningless unless the influences which govern mass transport are quantified and the overall results adjusted accordingly. The fact that the performance of one membrane cannot be compared with that of another without knowing the contribution of the system to mass transfer limitation seems to be commonly accepted today.

Certainly, boundary layer effects are being found to be very significant. Nijhuis *et al.* (1990) found that the transport of toluene (250μg/g water) through a PDMS composite membrane (effective thickness 5.4μm) was almost wholly governed by transport through the boundary layer and that the resistance of the membrane itself could be ignored for $0 < Re < 80\ 000$ in a stirred cell system. He suggests that since the membrane mass transfer coefficient is so large for this case, future module design should focus upon increasing the boundary layer mass transfer coefficient at minimum cost.

Costs were also mentioned by Hickey and Gooding (1994) who state that increasing the operational flow rate would lead to an increase in boundary layer mass transport, but at extra expense. These authors used a modified Wilson plot to study the influence of the boundary layer. This is an extrapolative technique in which the feed flow rate is varied in a range over which the liquid film resistance is significant. The measured overall resistance is plotted against the inverse of the flow rate, raised

to a power, b. The exponent is determined from the best linear fit of data. By extrapolating the inverse flow rate back to zero, the membrane resistance (and "ideal" permeability) is found, and hence, the boundary layer resistance at different flow rates can be calculated. The same technique has been used by Karlsson and Trägårdh (1992) and in this work.

Raghunath and Hwang (1992a) have also recently analysed the importance of boundary layer effects in the permeation of trace organics, based on a two resistances model, ignoring the effects of coupling. They found that the concentration of organic in the feed (up to 1172ppm for the permeation of a solution of phenol through PDMS membranes) has no effect on the boundary layer resistance *as a proportion* of the overall mass transfer resistance. This is a contradiction to the commonly accepted, but false, view that concentration polarisation is more significant when the more permeable component is present at low concentration in the feed liquid. This view is evident from written statements such as "Concentration polarisation is probably much less important in pervaporation than in other membrane separation techniques. It may however induce some undesirable effects if the faster permeant is present as a trace in the feed mixture," (Néel, 1991), from the conclusions of the work of Spitzen (1988) and by the fact that almost all the work published on the influence of concentration polarisation has used the removal of trace organics from water as the model system. It will be shown later that concentration polarisation is a major influence under other conditions.

5.1.2 RESISTANCES-IN-SERIES MODEL

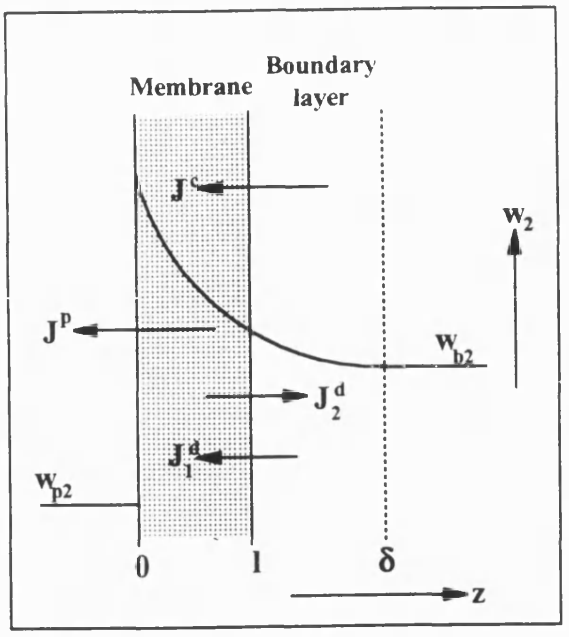

Figure 5.1 Concentration profile of the less permeable component (2) of a binary liquid mixture during the pervaporation process (adapted from Spitzen, 1988)

Figure 5.1 shows the concentration profile of the less permeable component (2) of a binary liquid mixture during the pervaporation process.

At steady state, the volume of an element within the liquid boundary layer must be constant. The total volume balance is:

$$J^c - J^d - J^p = 0 \qquad (5.1)$$

where J^c is the component flow due to convection, resulting from the removal of components from the feed due to permeation through the membrane,

J^d is the component flow due to diffusion, resulting from the concentration gradients of components in the boundary layer,

J^p is the component flow due to permeation, resulting from the concentration gradient within the membrane itself.

The component flows due to diffusion are described by Fick's law:

$$J_i^d = -Dd(\rho w_i)/dz \tag{5.2}$$

where w_i is the weight fraction (kg/kg) in the liquid mixture and the flux, J_i^d, is measured in $kgm^{-2}s^{-1}$. ρ is the liquid density (kgm^{-3}) and D is the diffusivity of component i within the mixture (m^2s^{-1}). Equation 5.2 can be applied to both components of the mixture but since at any point in the element the total concentration, $(w_1(z) + w_2(z))$, must equal 1:

$$J_1^d + J_2^d = J^d = 0 \tag{5.3}$$

Hence, the diffusional flow of component 1 towards the membrane is totally counterbalanced by the diffusional flow of component 2 away from the membrane.

The combination of equations 5.1 and 5.3 yields:

$$J^c = J^p \tag{5.4}$$

Considering component 2, a volume balance for this component is:

$$J_2^c - J_2^d - J_2^p = 0 \tag{5.5}$$

and the flows of component 2 are defined:

convection:

$$J_2^c = J^c \rho w_2(z) \tag{5.6}$$

permeation:

$$J_2^p = J^p \rho w_{p2} \tag{5.7}$$

diffusion:

$$J_2^d = -D_{BL}d(\rho w_2(z))/dz \tag{5.8}$$

Combining equations 5.5 to 5.8 and taking the permeation flux to be equal to the overall mass flux, J:

$$J\rho(w_2(z) - w_{p2}) = -D_{BL}d(\rho w_2(z))/dz \tag{5.9}$$

This is the most general form of the mass balance describing concentration polarisation.

Using the film model, the boundary conditions for the equation are:

$$z = 0 : w_2 = w_{m2}$$

$$z = \delta : w_2 = w_{b2}$$

where δ is the thickness of the laminar boundary layer.

In equation 5.9, J is only dependent on the wall concentration, w_{m2}, and is not a function of z. However, D can be a function of the concentration, w_2, in the boundary layer. Assuming D is concentration-independent is not a major assumption for the liquid boundary layer.

If the diffusion coefficient, D_{BL}, is assumed to be independent of concentration, equation 5.9 may be integrated:

$$\int_0^{\delta} J dz = -D_{BL}\int_{w_{m2}}^{w_{b2}}[\rho(w_2(z) - w_{p2})]^{-1}d(\rho w_2(z)) \tag{5.10}$$

$$\frac{J\delta}{D_{BL}} = -\ln\frac{\rho_b w_{b2} - \rho_p w_{p2}}{\rho_m w_{m2} - \rho_p w_{p2}} \tag{5.11}$$

According to film theory, the thickness of the boundary layer, δ, is related to the mass transfer coefficient, k_{BL}:

$$D_{BL}/\delta = k_{BL} \tag{5.12}$$

which, in equation 5.11, gives:

$$\frac{J}{\rho_b k_{BL}} = \ln[(\rho_m w_{m2} - \rho_p w_{p2})/(\rho_b w_{b2} - \rho_p w_{p2})] \tag{5.13}$$

Since the membrane under consideration is highly selective, the assumption $w_{p2} \rightarrow 0$ is made. Rearranging equation 5.13 to describe the transport of the more permeable component:

$$J/k_{BL}\rho_b = \ln[(\rho_m(1 - w_{m1}))/(\rho_b(1 - w_{b1}))] \tag{5.14}$$

From here on, all weight fractions will refer to the more permeable component. Assuming $\rho_m \approx \rho_b$ further simplifies the equation:

$$\begin{aligned} J/\rho_b k_{BL} &= \ln[(1 - w_m)/(1 - w_b)] \\ &= \ln(1 - w_m) - \ln(1 - w_b) \end{aligned} \tag{5.15}$$

For $-1 < w < 1$, the term $\ln(1+x)$ can be expressed as a convergent series:

$$\ln(1 + x) = x - x^2/2 + x^3/3 - x^4/4 + \ldots \tag{5.16}$$

Therefore,

$$\ln(1 - w_b) = -w_b - \frac{w_b^2}{2} - \frac{w_b^3}{3} - \ldots \tag{5.17}$$

Substitution into equation 5.15 gives:

$$J/k_{BL}\rho_b = w_b - w_m - \frac{1}{2}(w_m^2-w_b^2) - \frac{1}{3}(w_m^3-w_b^3)$$
$$= (w_b-w_m)+\frac{(w_b-w_m)(w_b+w_m)}{2}+\frac{(w_b^3-w_m^3)}{3}+\ldots \quad (5.18)$$
$$=(w_b-w_m)[1 + \frac{(w_b+w_m)}{2}] + \frac{(w_b^3-w_m^3)}{3} + \ldots$$

In pervaporation, it is often the case that $w_m < w_b < 0.05$, in which case, equation 5.18 may be simplified (Field and Burslem, 1992) to:

$$J = k_{BL}\rho_p(w_b - w_w) \quad (5.19)$$

However, for this work, $w_b > 0.05$ and further terms of the convergent series are required.

For the third term of the series, assume that $w_b \approx w_m$, then:

$$\frac{J}{k_{BL}\rho_p} \approx (w_b - w_m) + (w_b - w_m)(w_b + w_m)(\frac{1}{2} + \frac{w_b}{3}) \quad (5.20)$$
$$\approx (w_b - w_m)[1 + (w_b + w_m)(0.5 + w_b/3)]$$

Let $w_b \approx w_m$ for all but the first term of the equation:

$$\frac{J}{k_{BL}\rho_b} \approx (w_b - w_m)[1 + w_b(1 + \frac{2}{3}w_b)] \quad (5.21)$$

Define a correction factor, F, to account for the deviation from a simple linear relationship between flux and concentration:

$$F = [1 + w_b(1 + \frac{2}{3}w_b)] \quad (5.22)$$

Then, in equation 5.20:

$$J = k_{BL}\rho_b(w_b - w_m)F \tag{5.23}$$

Conversion from weight fractions to activities yields:

$$J = Mk_{BL}(a_b - a_m)F \tag{5.24}$$

where M is the factor to convert from weight fractions to activities. This is the flux equation for transport through the liquid boundary layer.

The flux equation for transport through the membrane can be written:

$$J = \frac{D_0 S}{l}(a_m - a_p)M \tag{5.25}$$

where the product of the membrane diffusion coefficient, D_0, and the sorption coefficient, S, is the permeability, P_0.

Finally, the flux equation which includes an overall driving force is:

$$J = M(a_b - a_p)/R_{TOTAL} \tag{5.26}$$

Combining the last three equations:

$$R_{TOTAL} = \frac{1}{Fk_{BL}} + \frac{l}{P_0} \tag{5.27}$$

and:

$$R_{TOTAL} = R_{BL} + R_m \tag{5.28}$$

In Chapter 4, the mass transfer resistance provided by the membrane was investigated. This chapter is concerned with mass transfer limitations provided by the liquid boundary layer. For a constant feed composition, the resistance provided by the membrane ($=l/P_0$) will be constant (if P_0 and l are assumed to be independent

of concentration) and variation of flow conditions across the membrane surface will result in a variation of the liquid boundary layer resistance.

Sherwood correlations provide a relationship between the liquid mass transfer coefficient and axial feed flow. They are generally represented as:

$$Sh = \frac{k_{BL} d_h}{D_{BL}} = pRe^q Sc^r \left(\frac{d_h}{L}\right)^s \qquad (5.29)$$

where Sh is the Sherwood number, Re the Reynolds number and Sc the Schmidt number. d_h is the hydraulic diameter and L, the length of the module of flow channel. The equation gives the boundary layer mass transfer coefficient as a function of the dimensions of the module, flow conditions and properties of the feed liquid. p, q, r and s are empirical coefficients, the values of which vary, depending upon operating conditions.

For a stirred cell (Smith *et al.*, 1961):

$$Re = \frac{\omega b^2}{\nu} \qquad (5.30)$$

where ω is the radial velocity ($rads^{-1}$), b is the cell radius (m) and ν is the kinematic viscosity (m^2s^{-1}).

Therefore, if liquid properties (viscosity, diffusivity) across the boundary layer and module dimensions are constant:

$$\frac{1}{k_{BL}} \propto \frac{1}{\omega^q} \qquad (5.31)$$

If a value of exponent q can be found such that a linear relationship between $(1/\omega^q)$ and the overall mass transfer resistance is evident, a second graphical method of decoupling transfer resistances resulting from the membrane and liquid boundary

layer is developed (Figure 5.2). The correction factor, F, has been included to take account of the fact that the weight fractions of water in the bulk feed and at the membrane surface are not equal.

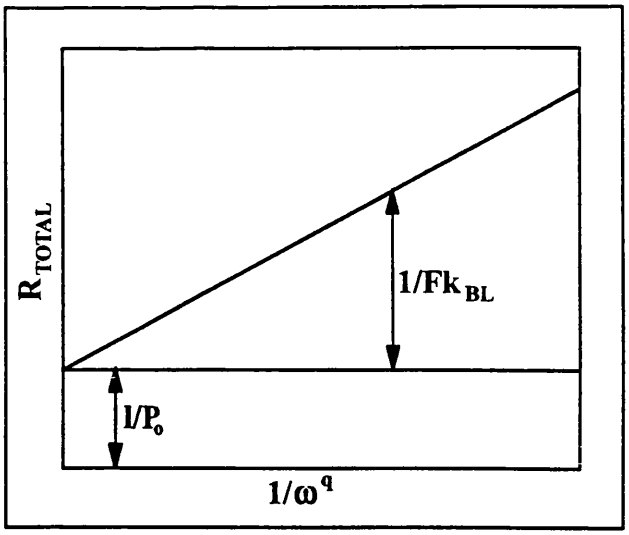

Figure 5.2 Determination of mass transfer resistances by variation of feed flow conditions (modified Wilson plot)

5.2 EXPERIMENTAL

5.2.1 POLYSULFONE-SUPPORTED MEMBRANES

Membranes were prepared by casting 10g of polymer solution, CsPA, MW 250K, pH 8.5 onto PSf support material, using Method 1 (Section 2.2.2). Each membrane was dried at 35°C. The performance of the membranes was tested by batch dewatering of an IPA solution using a feed temperature of 70°C and one stirrer speed from the following range: 0, 100, 250, 500, 750, 1000 and 1250rpm. A different membrane was used for each stirrer speed tested. The vacuum used was less than 1.5mbar, measured next to the vacuum pump.

Each stirrer speed used corresponded to a radial velocity, ω, and a Reynolds number, calculated from equation 5.30. These are shown in Table 5.1

Stirrer speed (rpm)	Radial velocity ($rads^{-1}$)	Re
0	0	0
100	10.47	6702
250	26.18	16755
500	52.40	33510
750	78.54	50265
1000	104.72	67021
1250	130.90	83776

Table 5.1 Calculated radial velocities and Reynolds numbers. $b=0.024m$ $\nu=0.9\times10^{-6}m^2s^{-1}$ (Colman and Naylor, 1991)

5.2.2 POLY(VINYLIDENE FLUORIDE)-SUPPORTED MEMBRANES

Identical membranes to those used in Section 5.2.1 were prepared except that the support material used was PVDF. The membranes were also tested in an identical manner to those prepared in Section 5.2.1, except that an experiment without stirring was not performed.

5.3 RESULTS AND DISCUSSION

5.3.1 POLYSULFONE-SUPPORTED MEMBRANES

The batch dehydration curves for IPA-dewatering using a CsPA membrane, 14μm thick, supported with a layer of PSf are given in Figure 5.3. Each curve represents a dewatering experiment carried out using the stirrer speed indicated. It can be seen that increasing the stirrer speed from 100 to 250 to 500rpm resulted in an increase of flux, but above this last speed, further increases caused only a minor

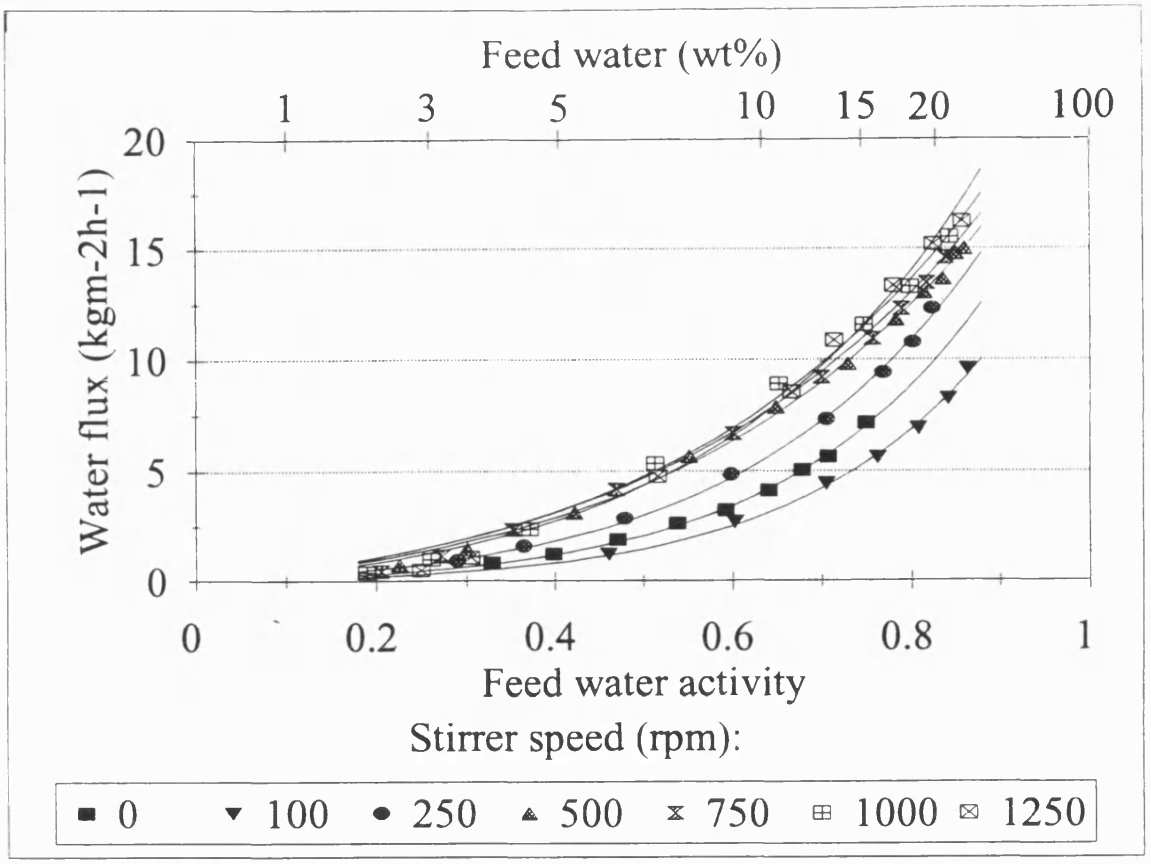

Figure 5.3 Effect of variation of stirring speed on water flux. PSf-supported membrane

variation. An interesting result is the dewatering curve gained from the system which utilised no stirring at all. A higher water flux is achieved than when the stirrer was revolving at 100rpm. A suggested explanation for this is that the membrane acts as a heat sink, due to the evaporation occurring. Temperature polarisation may occur such that there is a difference in temperature of a few degrees centigrade between the membrane and the bulk liquid and sides of the cell. When there is no stirring, natural convection currents are set up in the feed liquid which partially inhibit concentration polarisation. When the stirrer is switched on, these natural convection currents are destroyed and forced convection occurs. Since the design of the stirrer used promotes tangential flow, rather than flow normal to the surface, there is less disruption to the boundary layer. Hence, a lower flux results.

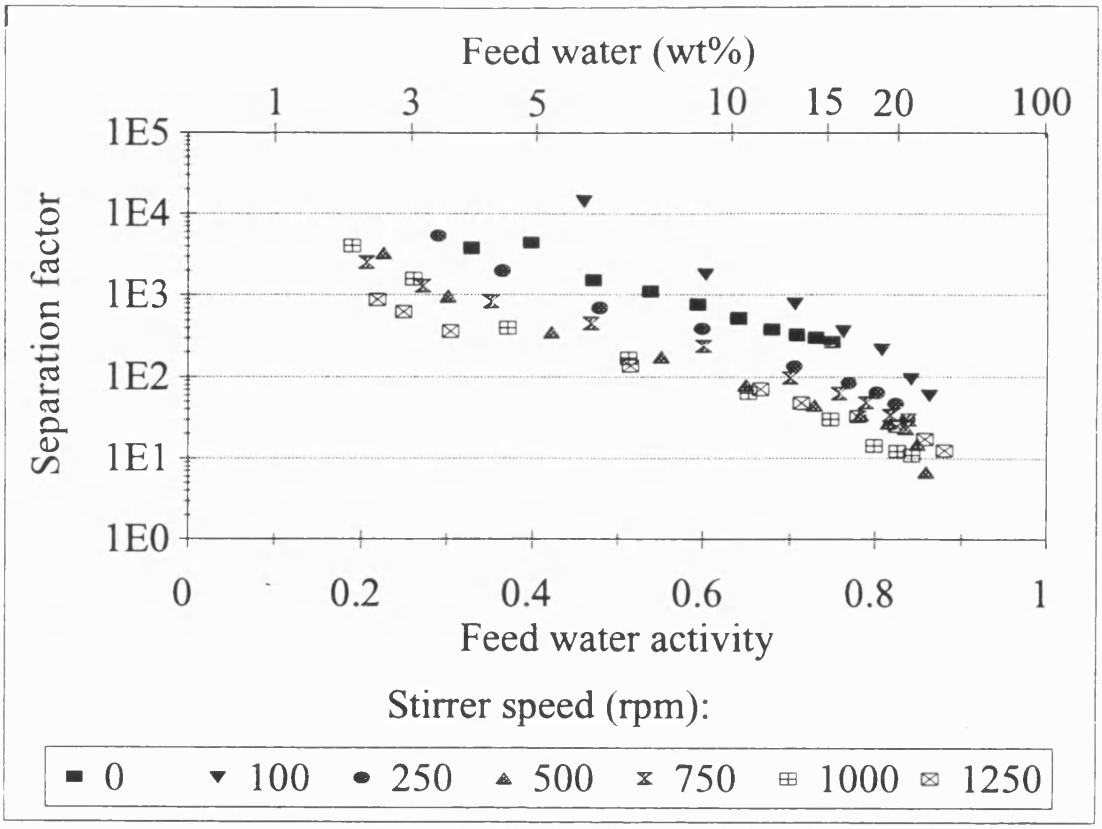

Figure 5.4 Effect of variation of stirring speed upon separation factor. PSf-supported membrane

The variation of separation factor with feed composition as a function of stirrer speed is shown in Figure 5.4. The highest membrane selectivities were found from dewatering experiments utilising laminar flow. As has been noted elsewhere (e.g. Huang and Yeom, 1990; 1991), flux increase is usually accompanied by selectivity decrease.

Despite the seemingly trivial difference in system performance within the turbulent flow regime, a Wilson-type plot was constructed, applying Equation 5.27 and correlation 5.31. The water fluxes at four compositions (5, 10, 15 and 20wt% water in the feed) were calculated for each stirring speed-membrane system used, using the activity-based model. From these, total system resistances were calculated

(Equation 5.26) and plotted against $1/\omega^q$. Theoretically, it should be possible to find a value of q which results in a linear correlation between R_{TOTAL} and $(1/\omega^q)$. It was impossible to find the "perfect" correlation, which is not surprising considering the number of data points available and the errors involved. Points arising from a stirrer speed of 1250rpm were ignored for regression purposes since it was felt that strange behaviour had occurred at this speed, i.e. the effect of composition upon performance is the opposite of that found at other stirrer speeds. The reason for this behaviour is probably the changed behaviour of the stirrer bar at high speeds- it was observed that a little rattle frequently occurred when a speed of 1250rpm was set. A value for q of 0.75 was chosen for use, as there was little variation in the coefficient of correlation by changing the value of q and experiments performed using a

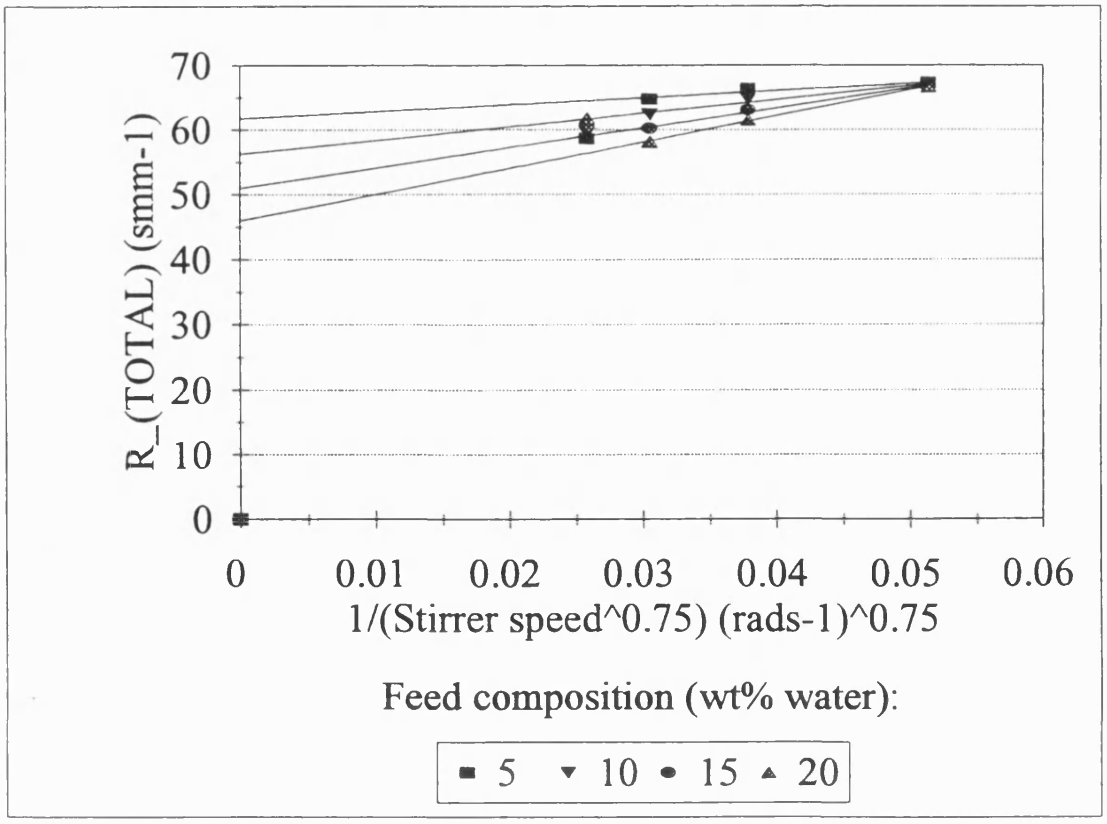

Figure 5.5 Modified Wilson plot illustrating the effect of radial velocity on system resistance. PSf-supported membrane

a similar stirred cell system by Smith *et al.* (1961) found q to be 0.75. It is appreciated that more data points are required to find q accurately. The plot of total resistance against ($1/\omega^{0.75}$) is shown in Figure 5.5. The coefficients of correlation varied between $R^2=0.86$ (5wt% feed water) and $R^2=1$ (20wt% feed water).

From Figure 5.5, assuming that the flow is turbulent and the intercept is the membrane resistance, it seems that it is this resistance, rather than the boundary layer, which is the major factor limiting mass transfer under turbulent flow conditions. All the component resistances calculated are shown in Tables 5.2 and 5.3.

Stirrer speed (rpm)	**0**	**100**	**250**	**500**	**750**	**1000**	**1250**
Feed water (wt%)	**R_{BL} (smm^{-1})**						
5	112	111	34.5	5.42	4.65	2.99	0
10	67.7	93.4	31.9	10.7	8.49	6.17	3.29
15	44.7	80.7	30.2	15.8	12.1	9.23	9.65
20	31.5	71.2	29.1	20.7	15.6	12.2	15.9

Table 5.2 Boundary layer resistance values, PSf-supported membrane, calculated from the subtraction of R_m from R_{TOTAL}

Feed water (wt%)	5	10	15	20
R_m (smm^{-1})	61.8	56.3	51.0	46.0

Table 5.3 Membrane resistance values, PSf-supported membrane, calculated from Figure 5.5

The calculated membrane mass transfer resistances decrease as the feed water concentration increases, as expected. The boundary layer resistances decrease with increasing stirring speed. This effect is particularly significant in the laminar flow regime (stirrer speed < 500rpm) although increasing the degree of turbulence within the turbulent flow regime still appears to be beneficial, up to Re = 67,000 (1000rpm). For example, at a feed water content of 10wt%, the boundary layer resistance decreased from $93smm^{-1}$ at 100rpm (62% of the overall resistance) to $6.2smm^{-1}$ at 1000rpm (only 10% of the overall resistance).

Each individual value of R_{BL} is subject to a certain degree of inaccuracy, especially since smaller values of R_{BL} are calculated from the subtraction of two larger values, and there are not 28 good, individual estimates of R_{BL}. However, one can clearly infer from the standard correlations of mass transfer that when viscosity and density variations are very minor, then the mass transfer coefficient, k_{BL}, is constant for a fixed stirrer speed. Thus, for each stirrer speed one can find a reasonable average estimate of k_{BL}.

The boundary layer mass transfer coefficients are calculated from the modified Wilson plot, taking into account the factor, F. From Equations 5.27 and 5.28:

$$k_{BL} = \frac{1}{F(R_{TOTAL} - R_m)} \qquad (5.32)$$

The calculated and average values of k_{BL} are given in Table 5.4.

Stirrer speed (rpm)	**0**	**100**	**250**	**500**	**750**	**1000**	**1250**
Feed water (wt%)	**k_{BL} (μms^{-1})**						
5	8.49	8.58	27.5	475	204	318	-
10	13.3	9.67	28.3	84.4	106	147	274
15	19.2	10.6	28.4	54.3	70.7	93.0	89.0
20	25.9	11.5	28.0	39.4	52.4	66.9	51.3
Average	16.7	10.1	28.0	88.4	108	156	121

Table 5.4 Variation of calculated boundary layer mass transfer coefficients with feed composition and stirring speed. PSf-supported membranes

The boundary layer mass transfer coefficient generally increases with increasing turbulence in the feed.

Now, using the average values of k_{BL}, modified values of R_{BL} may be calculated ($R_{BL} = 1/(Fk_{BL})$) (Table 5.5).

Stirrer speed (rpm)	0	100	250	500	750	1000	1250
Feed water (wt%)	R_{BL} (smm^{-1})						
5	56.8	94.3	33.9	10.8	8.77	6.10	8.85
10	54.0	89.6	32.2	10.2	8.34	5.79	7.46
15	51.3	85.1	30.6	9.71	7.92	5.50	7.09
20	48.7	80.8	29.1	9.22	7.52	5.23	6.73

Table 5.5 Modified boundary layer resistances. PSf-supported membranes

Figure 5.6 clearly shows that the significance of the boundary layer as a resistance to mass transport decreased as the level of turbulence is increased. The *actual* boundary layer resistance always decreased with increasing feed water concentration, however, its significance sometimes increased. Figure 5.6 shows that, for most levels of turbulence, the significance of the boundary layer remains approximately constant with feed concentration. This is similar to the finding of Raghunath and Hwang (1992a). For conditions of no stirring and a stirrer speed of 100rpm, the significance of the boundary layer actually increases with increasing water concentration. For example, for a stirrer speed of 100rpm, at 5wt% feed water, the boundary layer resistance accounts for 55% of the total, whilst at 20% it is 69%. This contradicts the assumptions of other workers (e.g. Néel, 1991) that

boundary layer effects are more significant when the permeating component is at low concentrations in the feed.

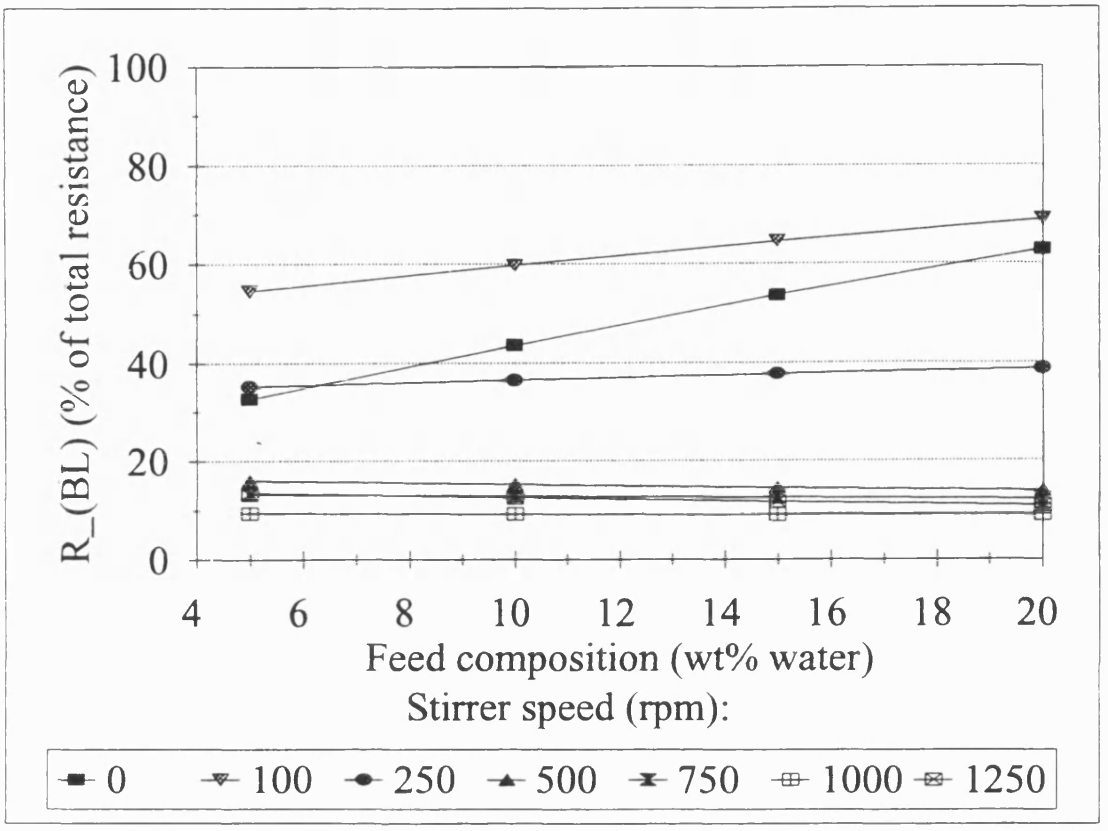

Figure 5.6 Variation of boundary layer resistance (as a % of overall resistance) with feed composition. PSf-supported membranes

From the modified values of R_{BL} and using values of R_{TOTAL} derived by experiment, a set of values of R_m may be found by subtraction (Equation 5.28). These modified membrane resistances are given in Table 5.6 and values for each feed composition have been averaged. They do not differ significantly from the values found from the intercepts of the Wilson plot.

Feed water (wt%)	5	10	15	20
Stirrer speed (rpm)	modified R_m (smm^{-1})			
0	117	70.0	44.4	28.7
100	78.3	60.1	46.6	36.3
250	62.4	56.0	50.6	46.1
500	56.4	56.8	57.1	57.4
750	57.7	56.4	55.2	54.1
1000	58.7	56.7	54.7	52.9
1250	50.7	52.1	53.6	55.1
Average R_m (smm^{-1})	68.7	58.3	51.7	47.2

Table 5.6 Modified membrane resistances, calculated from experimental R_{TOTAL} and calculated, modified R_{BL} values. PSf-supported membranes

Comparing the resistance values in Tables 5.2, 5.5 and 5.6 with those shown in Table 4.4, it seems that they are comparable. The boundary layer resistances calculated from variation of thickness experiments are slightly higher than the equivalent values calculated from the results of this chapter. For example, for a 10g (14μm thick) membrane, tested at a stirrer speed of 1000rpm with a feed composition of 10wt% water:

R_{BL} = 24.1smm^{-1} from variation of thickness experiments

R_{BL} = 5.79smm^{-1} from variation of stirring speed experiments

Also, membrane resistances calculated from variation of stirrer speed experiments are slightly higher than those calculated from the variation of thickness experiments.

For the same conditions as above:

R_m = 46.4smm^{-1} from variation of thickness experiments

R_m = 56.3smm^{-1} from variation of stirring speed experiments (intercept of Wilson plot)

R_m = 56.7smm^{-1} from recalculated values (Table 5.6)

These discrepancies are consistent with the hypothesis that there is a third mass transfer resistance present in the system: the porous support layer. In the graphical methods utilised, this additional resistance would contribute to an increase in the calculated boundary layer resistance found from the variation of thickness experiments, whilst it would contribute to the membrane resistance calculated in the variation of stirring speed experiments. This is illustrated in Figures 6.4 and 6.5 and is further discussed in Section 5.3.2 and in Chapter 6.

5.3.2 PVDF-SUPPORTED MEMBRANES

The batch dehydration curves for IPA-dewatering using a CsPA membrane, 14μm thick, supported with a layer of PVDF, are given in Figure 5.7. Comparing Figures 5.3 and 5.7, it is noticeable that the fluxes are higher and that the degree of turbulence appears to have a greater effect on the results for the PVDF-supported membrane. Whilst for the PSf-supported membrane, increasing the stirrer speed from 500rpm to 1000rpm had only a marginal effect, for the PVDF-supported membrane, the increase in turbulence has a significant effect on the flux.

The variation of separation factor with feed composition and stirrer speed is

shown in Figure 5.8. The separation factors found were very similar to those found using the PSf-supported membrane.

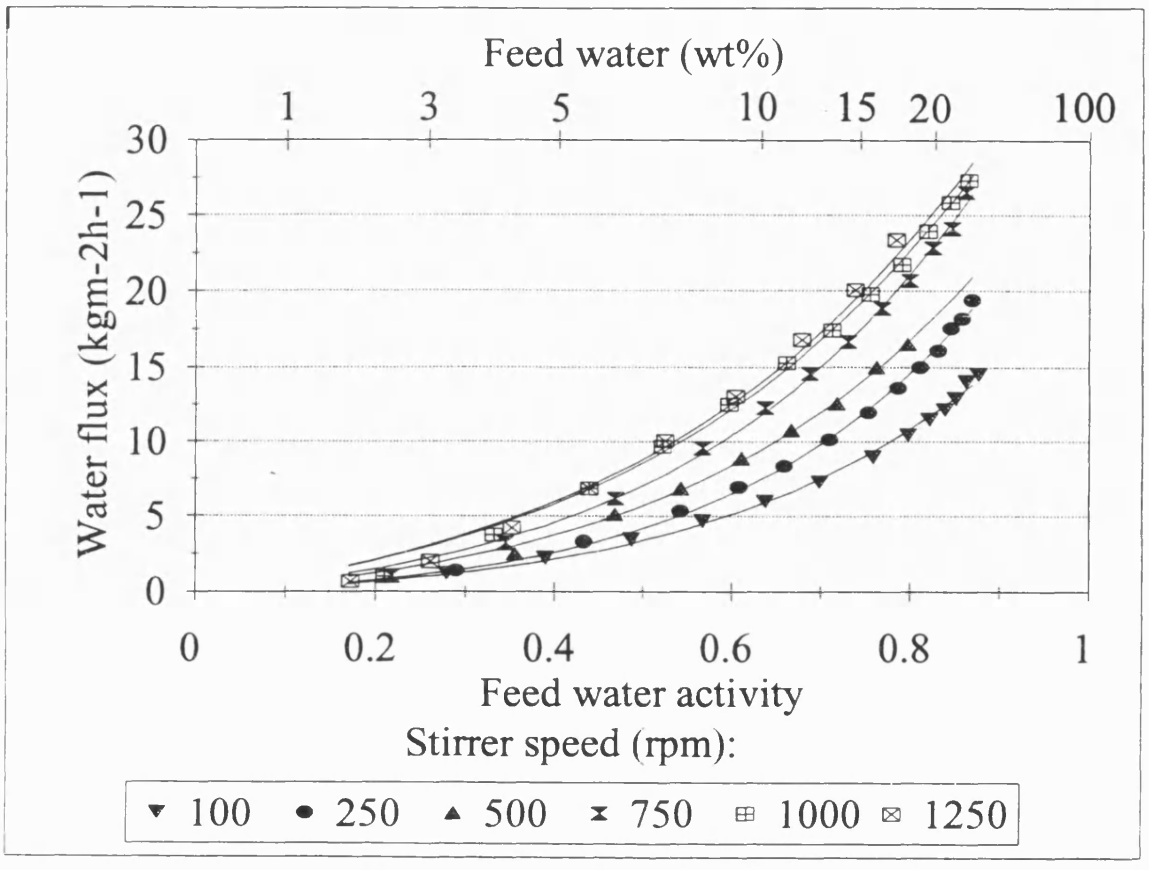

Figure 5.7 Effect of variation of stirrer speed upon flux for PVDF-supported polyacrylate membranes

Results were analysed in the same way as for Section 5.3.1, but using the results for stirrer speeds 500, 750, 1000 and 1250rpm to construct the modified Wilson plot (Figure 5.9). The coefficients of correlation varied between $R^2 = 0.94$ (5wt% feed water) and $R^2 = 0.99$ (20wt% feed water). Tables 5.5 and 5.6 show the component resistances calculated from this analysis.

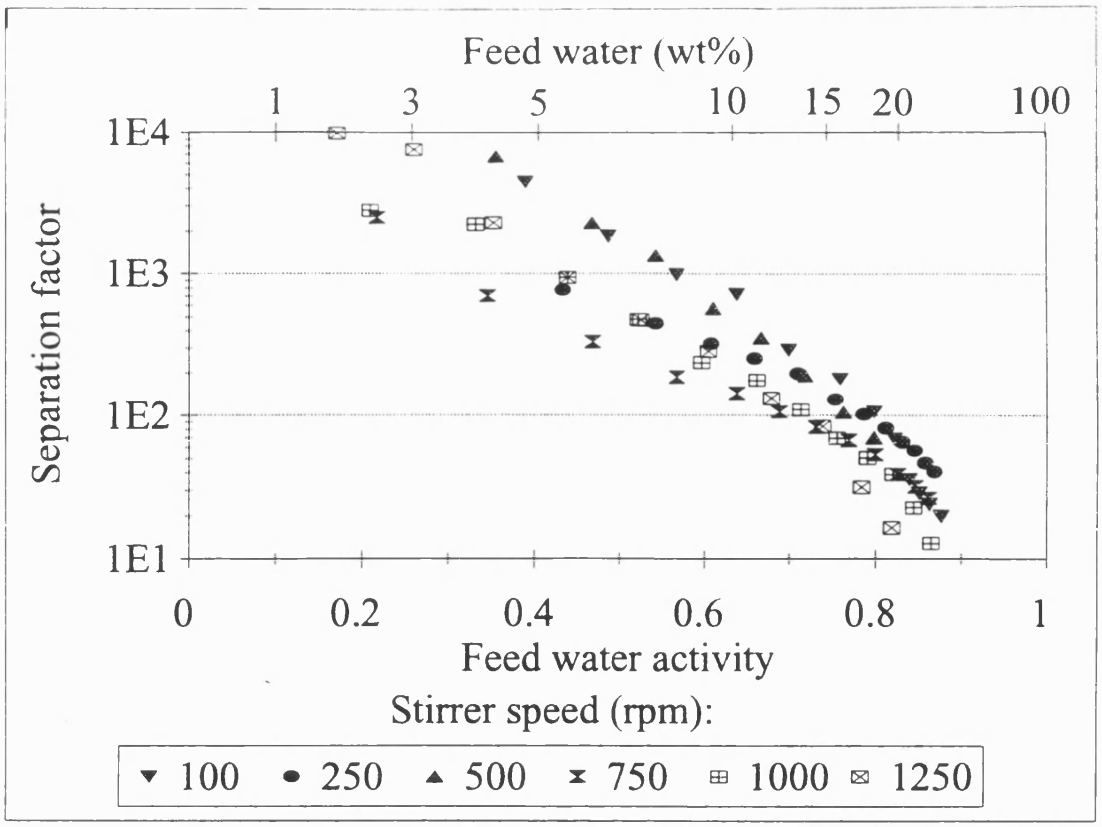

Figure 5.8 Effect of variation of stirrer speed upon separation factor for PVDF-supported polyacrylate membranes

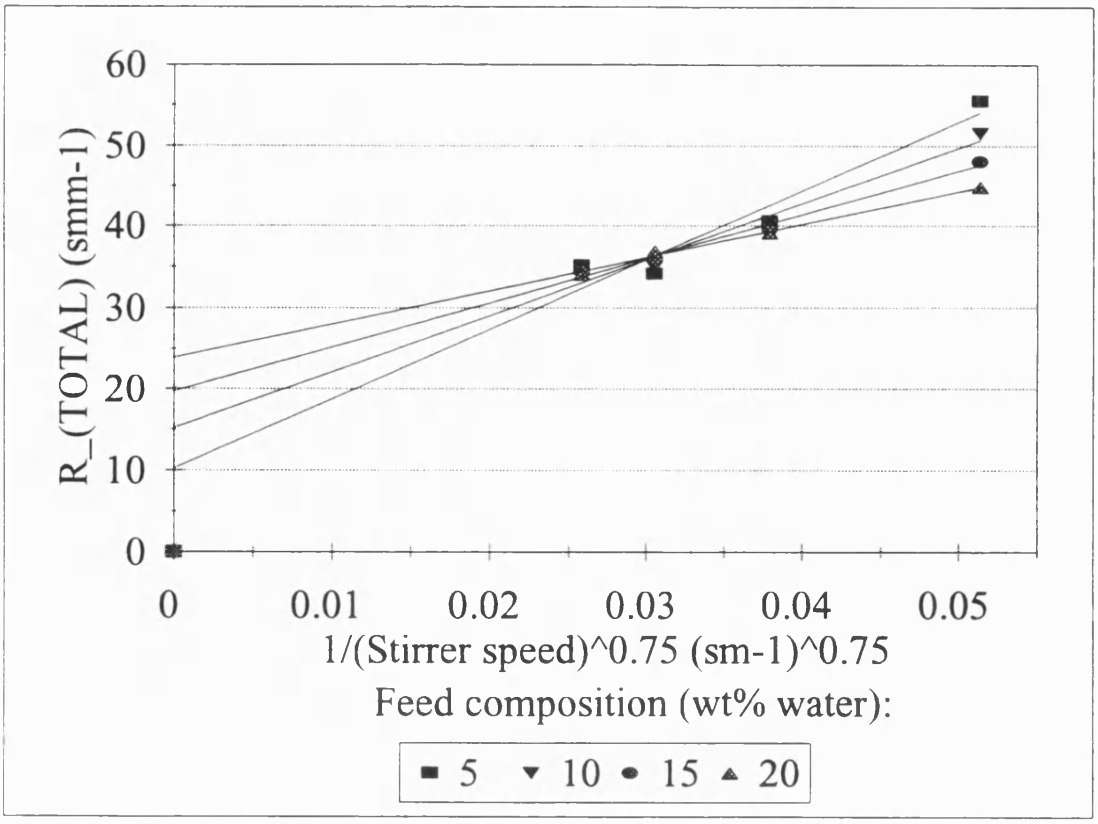

Figure 5.9 Modified Wilson plot for PVDF-supported membranes

Stirrer speed (rpm)	100	250	500	750	1000	1250
Feed water (wt%)	R_{BL} (smm^{-1})					
5	71.8	54.4	45.3	30.4	24.0	24.9
10	65.3	46.6	36.3	24.9	19.8	19.6
15	59.2	39.4	28.3	19.9	16.1	14.7
20	53.5	32.8	21.0	15.3	13.0	10.2

Table 5.7 Boundary layer resistance values, PVDF supported membrane, calculated from the modified Wilson plot

Feed water (wt%)	5	10	15	20
R_m (smm^{-1})	10.1	15.2	19.7	23.9

Table 5.8 Membrane resistance values, PVDF supported membrane, calculated from the modified Wilson plot

The membrane mass transfer resistance appears to increase with increasing feed water content, which is unexpected, and is thought to be due to errors in the experimental values being compounded in the analysis. For example, if the points for the lowest speed in Figure 5.9 had been ignored, then a series of lines with very

similar intercepts of around 20smm^{-1} would have fitted the data.

Further data analysis has been carried out, following the procedure used in Section 5.3.1, but it is appreciated that the individual values calculated are subject to significant error. Each calculated R_{BL} value was used to calculate a boundary layer mass transfer coefficient, values of which were then averaged for each stirrer speed (Table 5.9). These average k_{BL} values, along with the experimentally derived R_{TOTAL} values from the total resistances, generated new membrane resistance values, which have been averaged for each feed water concentration (Table 5.11).

Stirrer speed (rpm)	**100**	**250**	**500**	**750**	**1000**	**1250**
Feed water (wt%)			**k_{BL} (μms^{-1})**			
5	13.2	17.5	21.0	31.3	39.7	38.2
10	13.8	19.4	24.9	36.3	45.7	46.1
15	14.5	21.8	30.4	43.1	53.2	58.3
20	15.2	24.9	38.9	53.3	62.8	79.7
Average	14.2	20.9	28.8	41.0	50.3	47.5

Table 5.9 Variation of calculated boundary layer mass transfer coefficients with feed composition and stirrer speed. PVDF-supported membranes

Stirrer speed (rpm)	100	250	500	750	1000	1250
Feed water (wt%)	modified R_{BL} (smm^{-1})					
5	66.9	45.6	33.1	23.2	18.9	20.0
10	63.6	43.3	31.4	22.0	17.9	19.0
15	60.4	41.1	29.8	20.9	17.1	18.1
20	57.4	39.1	28.3	19.9	16.2	17.2

Table 5.10 Modified boundary layer resistance values. PVDF-supported membranes

Feed water (wt%)	5	10	15	20
Modified, average R_m (smm^{-1})	17.4	17.7	18.1	18.5

Table 5.11 Modified membrane resistances, averaged for each feed composition. PVDF-supported membranes

The significance of the boundary layer resistance, as a proportion of the total mass transfer resistance, is plotted in Figure 5.10.

The membrane resistances calculated for the PVDF-supported membrane are much lower than those calculated for the PSf-supported layer, e.g. $17.7smm^{-1}$ compared to $58.3smm^{-1}$ for a feed of 10wt water. This indicates that the support

layer must have a greater effect than was at first thought. This will be the subject of Chapter 6. Comparing the trends in Tables 5.3 and 5.11, the results from the PSf-backed membrane indicate a decreasing R_m with an increasing proportion of water in the feed, as expected, whereas the membrane resistances for PVDF-backed membranes change little with the variation in feed composition.

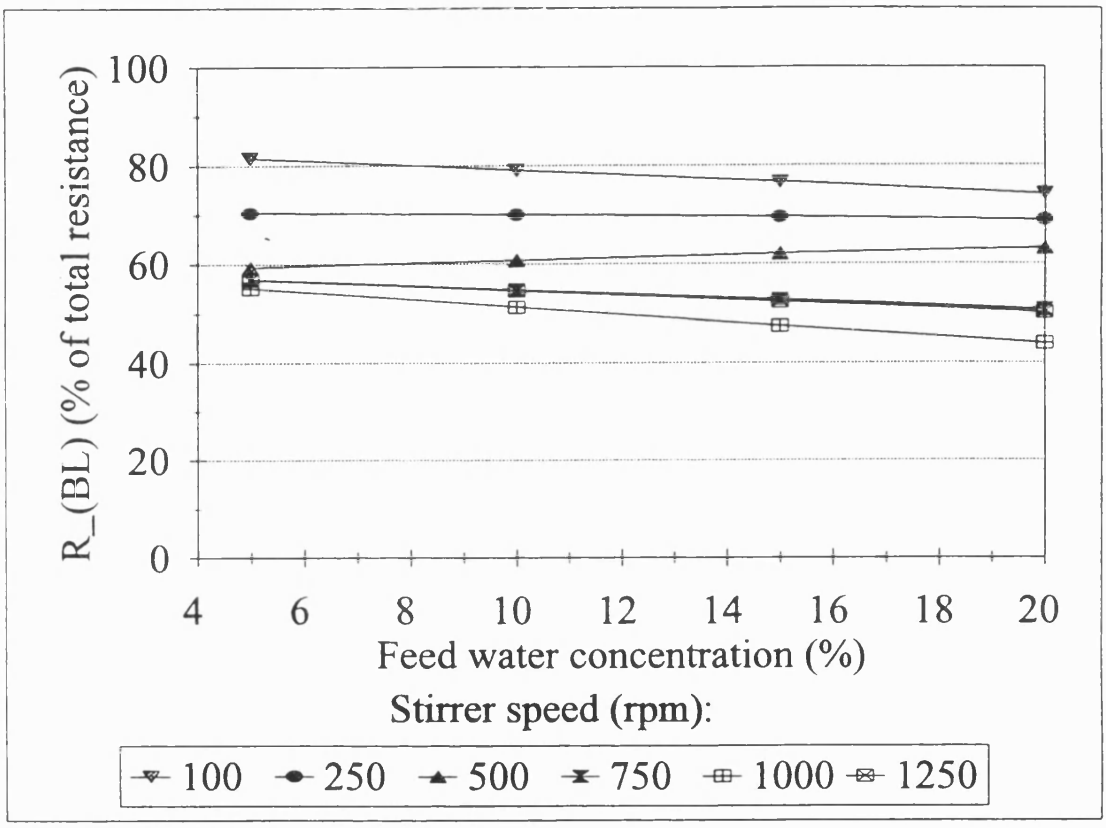

Figure 5.10 Variation of boundary layer resistance, as a proportion of the total resistance to mass transport. PVDF-supported membrane

Comparing the results of Tables 5.4 and 5.8, although in both cases the boundary layer mass transfer coefficient increases with stirring speed, the numerical values of this constant are very different. Mass transfer theory implies that, even if different membranes are used, the mass transfer coefficient on the feed side should not vary under the same conditions of stirring speed, feed composition and cell dimensions. There is no evidence to suggest why the two sets of values should be

so different, but the anomaly merits further investigation. The boundary layer resistances are consequently calculated as higher values for the PVDF-supported active layer. The significance of the boundary layer, as a proportion of the total resistance, is also higher for the PVDF-supported polyacrylate layer.

Nevertheless, in both cases the boundary layer resistance is highly significant, especially when feed flow conditions are laminar. For PVDF-supported membranes, whilst the significance of the boundary layer resistance with feed composition most often shows a slight decrease with increasing feed water concentration, this decrease is by no means large enough to account for the current widely held belief that feed-side resistance is only important when the permeating component is present in small quantities in the feed.

5.4 CONCLUSIONS

Experiments were performed to ascertain the significance of the liquid boundary layer within the pervaporation system. One set of experiments was conducted using polysulfone-backed polyacrylate membranes, the other used PVDF as the support layer material. In both cases, increasing the stirrer speed, and thereby the degree of turbulence in the feed, resulted in an increase of flux accompanied by a slight decrease in selectivity.

A modified Wilson plot was utilised to separate out the resistance derived from the boundary layer from that of the active layer. The active layer resistance varied slightly with the concentration of water in the feed and the type of support used was found to affect the numerical value of the "membrane" resistance. For PSf-supported membranes, the membrane resistance was higher than that found in Chapter 4 from variation of active layer thickness experiments. It is suggested that the value

calculated in Chapter 4 is the resistance of the active layer alone, whilst the value calculated from the intercept of the Wilson plot is the sum of resistances provided by the active and support layers. The fact that the membrane resistances for PSf-backed membranes were calculated, in this chapter, to be higher than those for the PVDF-supported membranes is assigned to the PSf layer and/or the interaction between the supporting UF membrane and the active layer resulting in a higher mass transfer resistance than the PVDF support layer. This is further discussed in Chapter 6.

For PSf-supported membranes, the boundary layer can account for between 5 and 70% of the total mass transfer resistance, depending upon water content in the feed and degree of turbulence, whilst for PVDF-supported membranes, the variation is 45-83%. This is principally due to the fact that the resistance not due to boundary layer effects is significantly smaller in the case of PVDF-supported membranes.

The boundary layer resistance becomes less important as the degree of turbulence is increased and its relative importance varies little with feed concentration, belying the frequently held belief that boundary layer resistance is only significant for systems where the permeating component is present in very low concentrations. It has been proved to be a major resistance to mass transport for this system.

Although not tested directly within this chapter, it is predicted that boundary layer effects would be more significant if thinner or higher flux membranes were used.

CHAPTER 6

PERMEATE-SIDE EFFECTS

6.1 INTRODUCTION

6.1.1 SUPPORT LAYER

Often, in the laboratory development of pervaporation membranes, research has been focused upon the development of highly selective, highly permeable, tailor-made polymers which have been characterised using free, non-supported films. However, in commercial pervaporation processes, it is usual for a thin pervaporation membrane to have to be mechanically supported by a thicker microporous layer. Further, the development of coating methods such as plasma deposition, where the active layer cannot exist alone, demand that the porous sublayer is an integral part of the system. Until recently, it was often assumed that such a layer acted only as mechanical support and did not influence membrane properties or system performance but recent studies, some outlined in Section 1.2.5 and some new experimental results which will be discussed in this section, have shown that the choice of support layer can be significant.

Heinzelmann (1991) states that "experience shows that the support and the interface between the support and the active membrane layer are strongly affecting the membrane properties." He goes on to recommend that the support material and composite membrane fabrication method be chosen carefully and provides a useful summary of the impact that the interface between the porous support and the active layer may have on performance (Figure 6.1).

Coating methods will affect the type of interface formed between the toplayer and support and should therefore be chosen carefully. Many coating and modification

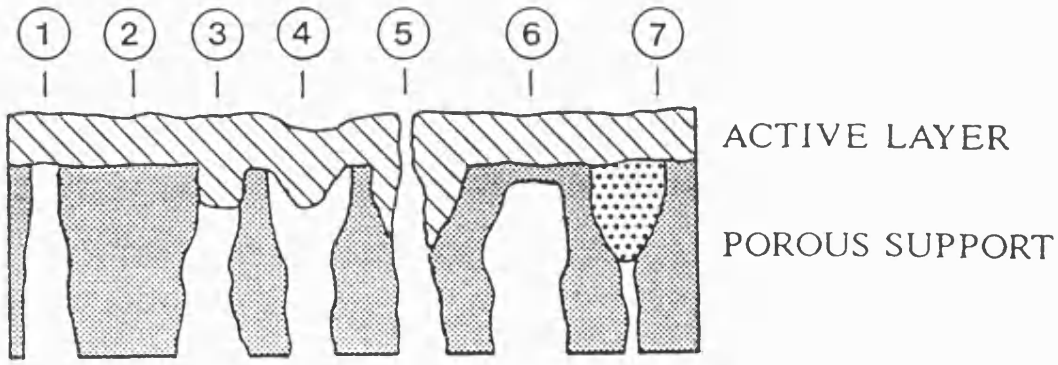

1 **Ideal situation**
No deformation of active layer
No open pores
High pore density in the support layer

2 **Low pore density**
Larger effective thickness of active layer
Reduced flux and possible effects to selectivity

3 **Penetration of coating into pores**
Larger effective thickness of active layer
Decreased flux; increased selectivity

4 **Support is not wetted by coating solution** or **deformation of active layer during transfer coating**
Increased active membrane area
Increased flux

5 **Insufficient matching of surface tension and viscosity** or **inappropriate coating method**
Formation of pin-holes
Low selectivity

6 **Support with dense skin layer**
Sorption-diffusion properties of support layer influential
Membrane performance is a superposition of two active layers

7 **Narrowed or closed pores**
Condensation of permeate
Support material is strongly influential
Decreased permeate flux

Figure 6.1 Possible interfaces between the active and porous support layers of a composite pervaporation membrane and their consequences (adapted from Heinzelmann, 1991)

Table 6.1 Coating and modification methods for the formation of composite pervaporation membranes (adapted from Heinzelmann, 1991)

COATING / MODIFICATION METHOD	POSITIVE POINTS	NEGATIVE POINTS
DIRECT COATING (e.g. dip, spray, roller, casting)	-Can vary the composition, viscosity and surface tension of coating solution -Can pre-treat the support layer -Can vary the drying conditions	-Coating solution may penetrate the pores of the support -Formation of pinholes should be avoided
TRANSFER COATING/LAMINATION (a flat, non-porous surface is direct coated, then the toplayer is transferred to the porous substrate)	-Can be adapted to achieve a defined penetration of the active layer into the pores -Can be used to circumvent difficulties in direct coating, e.g. insufficient wetting of support; incompatibility of solvents with support	-Process must be continuous for industrial scale-up
IN-SITU FORMATION (e.g. interfacial polymerisation or plasma deposition)	-Polymer films have excellent properties	-Can be difficult or time-consuming to produce layers of sufficient thickness
MODIFICATION OF POLYMERS (e.g. grafting reactions, formation of ionic functional groups or cross-linking reactions)	-Can be used to increase the resistance of the membrane to chemical or thermal attack without decreasing the polymer solubility (in the coating solution)	
AFTER-TREATMENTS (e.g.tempering, annealing, addition of other compounds, e.g. plasticisers)	-Membrane can be tailored to specific needs	

methods are available and these are summarised in Table 6.1.

The "ideal" pervaporation membrane would consist of a thin, dense homogeneous layer on a support of high porosity but the most extensively used supports are asymmetric ultrafiltration membranes. However, these do not necessarily have an negative impact. For example, a study by Nijhuis, Mulder and Smolders (1991) did include assessment of the resistance of the porous support layer. Polysulfone (PSf) ultrafiltration membrane supported a silicone rubber (PDMS) toplayer and the composite membrane was used for the removal of toluene from aqueous solution. The porous support layer had negligible resistance to the transport of the organic component *under the conditions used in this study,* although the authors state that no optimization was performed.

However, other researchers have found substrate effects. For example, Kaka, Fane and Ma (1992) prepared membranes by coating a range of commercially available microporous substrates (e.g. Millipore, Celgard and Separation Systems) with PVA. Although the toplayer was found to provide the controlling resistance, these workers found a significant substrate effect, especially for thin toplayers. Fluxes increased with increasing pore size (pore diameters of 0.02-0.2μm were used) and increasing porosity (28-70%). The authors suggest that the substrate affects the pervaporation flux by three factors:

(a) Pressure loss in the substrate - a minor effect

(b) Effect of substrate geometry - the "G" factor. Permeating molecules may have to travel for additional path length because of the spacing of pores. This effect is known to be important in composite RO and GS membranes and becomes more critical as the thickness of the toplayer

decreases (Figure 6.2).

(c) Penetration of the substrate by the selective layer. The authors provided evidence that this occurs with an SEM showing the penetration of a toplayer into PVDF substrate and they suggest that penetration reduces flux.

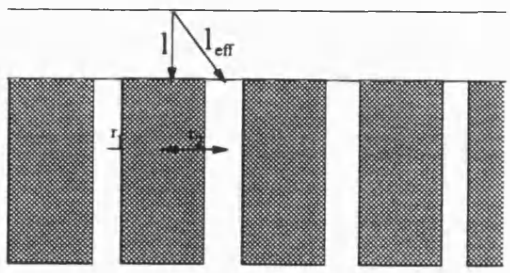

The average diffusion path, l_{eff}, through the selective layer, can be calculated as a function of the layer thickness, l, pore radius, r, and the surface porosity, ϵ ($=r_2/r_1$):

$$l_{eff} = \epsilon l + \frac{(1 - \epsilon)}{2}\left[\sqrt{r_1^2\left(\frac{1 - \epsilon}{\epsilon}\right) + l^2} + l\right]$$

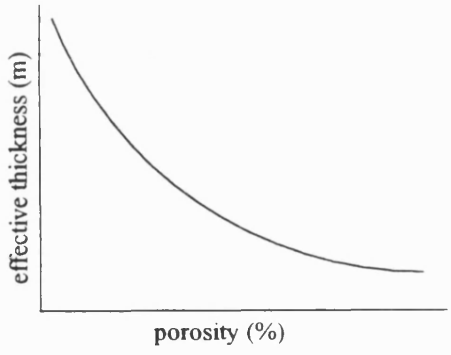

Figure 6.2 Effect of active layer thickness and porosity upon permeation path length (adapted from Peinemann, 1992)

A study investigating the effect of support layer on the water permeation properties of the BP polyacrylate membrane has also been undertaken (Burslem, Naylor and Field, 1992). It indicates that microporous metal support materials have

potential for use in place of the more commonly used polymeric supports. Substantially higher fluxes could be obtained using these materials, which possess greater open surface areas and porosities than polymeric substrates. However, their use is not without problems and these will be detailed within this chapter.

Gudernatsch and Kimmerle (1991) investigated the significance of support layer resistance during the pervaporation of an ethanol/water mixture across a PDMS capillary fibre module. They propose that for small pore diameters of 10-100nm in the support layer, Knudsen flow of the gaseous permeant occurs. Molecules of different molecular weights will have to overcome different resistances and lighter molecules will permeate preferentially. If pervaporation is selective to the heavier molecule, the support counteracts the permeability of the solution-diffusion layer. These workers also calculated that in the pervaporation of the said mixture through a fibre with a toplayer of 0.61μm thickness, the passage of molecules through the support consumed 50% of the driving force for mass transport.

As well as affecting flux, the support layer may also influence selectivity properties. It is often assumed that the dense layer governs the selectivity but Gudernatsch *et al.* (1991) suggest another functional arrangement: the microporous sublayer is cast as a dense, integral asymmetric membrane with a few imperfections and the function of the toplayer is simply to clog these pinholes. In this case, both materials contribute to the overall transport resistance. "Plugging" or "caulking," where an asymmetric "support" material is really the selective layer and the toplayer serves only to plug defects and discontinuities is already known in gas separation. As an example, these workers tested an asymmetric PES membrane (with an integral microporous sublayer) then coated it with a layer of PDMS and tested the resultant

composite. After coating, the flux decreased, but the selectivity increased. A model was developed which included five structural parameters, including the area of porosity penetrated by the toplayer, the thicknesses of the toplayer and the asymmetric skin and the resistance of the porous sublayer. The authors are confident that a membrane of a required selectivity can be developed by varying the morphology of the sublayer and using their model: "By properly adjusting the five discussed structural parameters of composite solution-diffusion membranes, one can obtain any intermediate characteristic between the intrinsic ones of the materials used. The range of those characteristics is particularly broad if the membrane consists of polymeric materials with inverse selectivities towards the given mixture" (Gudernatsch, Menzel and Strathmnn, 1991, p.29). They suggest that a useful application would be in expanding the detection range of sensors.

Flux and selectivity effects were also observed by Heintz and Reinhardt (1991), who used a resistances-in-series model for modelling PV transport through a composite membrane. Transport through the homogeneous toplayer was, as is common, modelled as a solution-diffusion process but transport through the sublayer was represented by a pore flow model. This support layer was assumed to consist of a bundle of ideal fibres, the fibres possessing a range of diameters. Transport through the pores is driven by a pressure gradient and the authors assume a composition change occurs in the gaseous permeant. Heintz and Reinhardt's quantitative model calls for many parameters but they claim that the parameters characterising the support layer only have to be adjusted once to a particular system. The model works well for their chosen system, the pervaporation of aqueous mixtures through a PVA-PAN membrane.

Two further studies by the same research group (Choi *et al.*, (1992); Ohya *et al.* (1994)) examined the effects of the characteristics of the sublayer on composite membrane performance. In the first study, a polyacrylic acid (PAA)-PSf composite membrane was used for the separation of water and ethanol. Separation characteristics were investigated in relation to the preparation conditions of the asymmetric PSf support. This layer was made by a phase inversion process, in which the concentration of the dope solution and the gelation time could be varied, and cast onto non-woven polyester support fabric. The PAA was then dip-coated onto the PSf support layer. The authors found that increasing the pore density (by increasing the concentration of PSf in the doping solution) lead to a decrease in flux whilst the selectivity to water went through a maximum. Decreasing the pore size (by increasing the gelation time) resulted in a substantial decrease in flux with little effect on selectivity.

Ohya's study is very similar, but using a PAA-PAN (polyacrylonitrile) composite membrane. Also, the experimental conclusions were similar, although pore size had a larger effect on selectivity than in the previous study, the separation factor going through a maximum at a MW cut-off of 100 000. The authors propose that it is the PAA layer which governs selectivity and preferentially permeates water, but when this layer is swollen, selectivity diminishes due to coupling effects. In the composite membrane, some PAA becomes embedded in the pores of the PAN layer and it is this which plays the main role in separation as its swelling tendency is restricted. If the pore size of the support layer is too small, the PAA layer cannot be embedded and confined mechanically and if the pore size is too big, the PAA can be embedded but swelling of this layer by water cannot be suppressed. They

conclude that an optimum pore size can be found. The study also concluded that increasing pore density results in a lower flux but a higher separation factor. Presumably, "pore density" must be interpreted as area per pore. Unfortunately, the authors neither commented on this matter not defined pore density clearly.

Analogies to gas separation indicate that as thinner and more permeable toplayers are produced, the influence of the support layer will become increasingly important. Peinemann's paper concerning the preparation and properties of composite membranes (1992) included examples from this field, where it cannot be assumed that the support layer has no effect. For example, Pinnau *et al.* (1988) studied the separation of carbon dioxide and nitrogen gases through a composite silicone rubber-PSf membrane. The asymmetric PSf layer, which had almost no selectivity for the gases, was coated with silicone rubber layers of different thicknesses. The intrinsic selectivity of this material was 11.5. Starting with very thin layers of rubber, the selectivity of the composite membrane increased as the thickness of the selective layer increased and selectivities close to the intrinsic selectivity of rubber were not achieved until a 2μm thick layer had been formed. Peinemann insists that "the development of suitable high flux support materials for thin film composite membranes is in many cases at least as important as the preparation of the selective layer itself."

To summarise, several papers have been published in the 1990s which indicate that the porous sublayer of a composite pervaporation membrane can have a larger effect on the system performance than was previously supposed. The coating method chosen will influence the type of interface formed between the top and support layers and this may influence the selectivity as well as the flux.

6.1.2 PERMEATE PRESSURE

The effects of varying permeate pressure are well-known and a precis is given in Section 1.2.7. There is often a region of very low permeate pressure where flux and selectivity remain constant, followed by a region of higher permeate pressure where flux decreases with increasing permeate pressure. Selectivity also decreases, provided the preferentially permeating component also has the lowest volatility.

For example, Nguyen and Clement (1991) used a PVA-PAN (GFT) membrane, permeating water-ethanol mixtures, to show that selectivity can be reversed by increasing the permeate-side pressure. This effect is easily explained. At low permeate pressure, the membrane is selective towards water. As the pressure increases, the water is nearer its saturation point and desorption is strongly limited. Concomitantly, the diffusion of ethanol is enhanced, since the membrane is more swollen and the ethanol is more volatile.

6.1.3 MEMBRANE FLAWS

In the same study, Nguyen and Clement (1991) tested an early generation of the GFT PVA-PAN dewatering membranes across the entire composition range of ethanol-water mixtures. They found that at low water concentrations, the selectivity of the composite membrane was similar to that of a thick PVA layer, but as the water content of the feed increased, the selectivity reversed and the composite's selectivity was more like that of the PAN layer alone, i.e. selective to ethanol. They initially proposed that this could be due to a large increase in the permeability of PVA to a value above that of the PAN support. However, applying a two resistances-in-series model, this would indicate that the change in permeate composition occurs progressively as the feed composition changes when in fact, there was a sharp

decrease in selectivity in the mid composition range. Therefore, they put forward a second proposal: cracks were occurring in the active layer resulting in direct contact between the feed and the PAN layer. These cracks could be caused by swelling stress, created by contact with the liquid mixture, having a deleterious effect on the layer of lowest mechanical resistance, i.e. the PVA. Successful visualisation of microcracks (approximately 0.5μm wide) using methylene blue dye, which stains PAN but not PVA, was achieved. They surmise that pervaporative use of the composite membrane in high water content samples, without pre-conditioning, lead to irreversible damage to the membrane and loss of selectivity, even at low water content feed solutions. Cracks form because the two layers do not expand at the same rate when swelling, leading to stress in the membrane which is further exacerbated under the external stress conditions of pervaporation. Nguyen and Clement add that more recent GFT membranes do not show the same behaviour and have better selectivity across the entire feed composition range. The support layer also has increased permeability.

Membrane flaws have also been found to be a problem with polyacrylate membranes. Trials undertaken at BP Research (Naylor, 1992) found that PSf-backed polyacrylate membranes consistently failed at a feed concentration of 0.5wt% water. Loss of selectivity was attributed to contraction and cracking of the selective film at low water contents. Furthermore, in the present work, membrane integrity of the non-crosslinked membrane was not maintained when the feed solution contained a high proportion of water. This is discussed later in Section 6.3.4.

6.1.4 RESISTANCES-IN-SERIES MODEL

In Chapters 4 and 5 there were assumed to be two major resistances within the system: the active layer and the liquid boundary layer. However, results contained within Chapter 5 indicated that the porous support also contributes to mass transfer resistance. This is illustrated in Figure 6.3. Another term may be included in Equation 4.7 (5.28) to account for this:

$$R_{TOTAL} = \frac{1}{FK_{BL}} + \frac{l}{D_0} + R_s \qquad (6.1)$$

where R_s is the mass transport resistance due to the support layer.

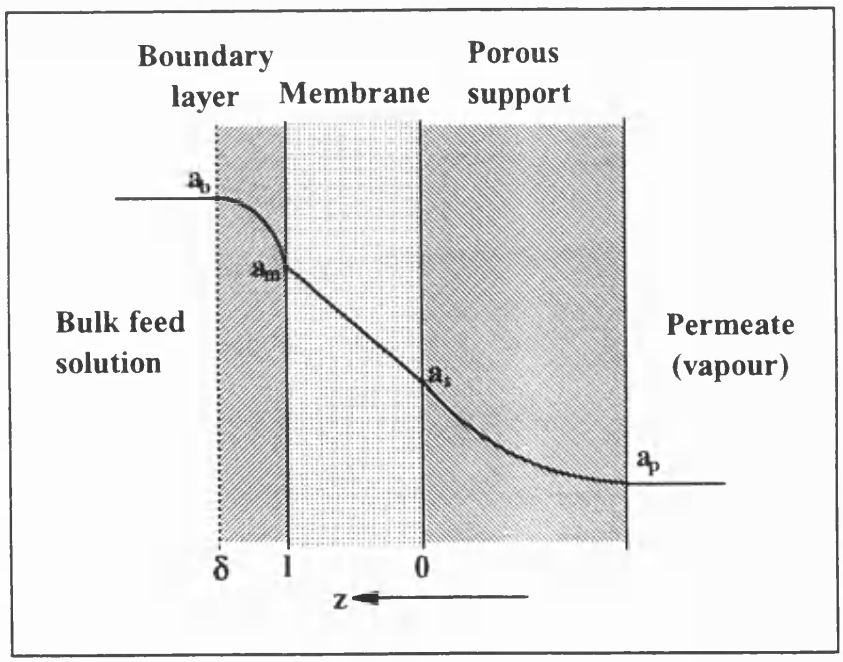

Figure 6.3 Activity profile through the composite pervaporation membrane

In the graphical analyses given in Chapters 4 and 5, the meaning of the intercepts now changes to include this extra term (Figures 6.4 and 6.5).

Using results from Chapters 4 and 5, approximate values of the support layer resistance, at different feed concentrations can be inferred for a 14μm thick

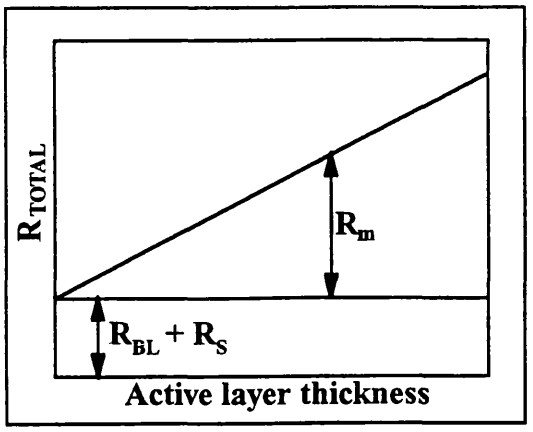

Figure 6.4 Calculation of component resistances from variation of active layer thickness experiments

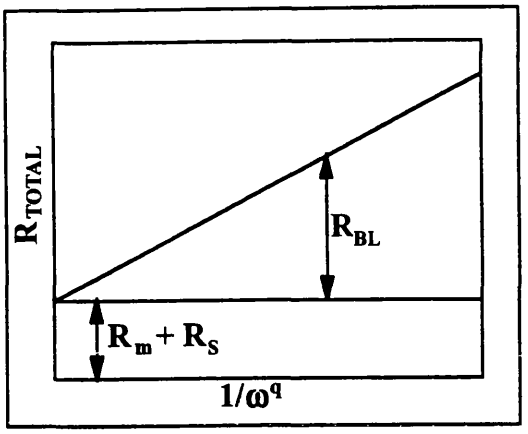

Figure 6.5 Calculation of component resistances from variation of turbulence experiments

polyacrylate layer, supported by PSf. These are shown in Table 6.2 for feed-side conditions of 70°C and 1000rpm.

	Section 4.3.2		Section 5.3.1		
Feed water (wt%)	**R_m (smm^{-1})**	**$R_{BL}+R_m$ (smm^{-1})**	**R_{BL} (smm^{-1})**	**R_m+R_s (smm^{-1})**	**R_s (smm^{-1})**
5	76.0	28.7	6.10	68.7	0-23
10	46.4	24.1	5.79	58.3	12-18
15	39.4	24.8	5.50	51.7	12-19
20	35.5	26.4	5.23	47.2	12-21

Table 6.2 Approximate calculation of the resistance of the polysulfone support layer

Because of the error in the numerical values calculated, it is difficult to tell

whether the support layer resistance is concentration dependent, however, it seems likely for conditions of high turbulence and the system used that the mass transfer resistance derived from the PSf support layer has more significance than that derived from the liquid boundary layer.

A quantitative model for transport through the support layer is not attempted within this work as there are insufficient experimental results, but the results of an experimental study of the effect of the support layer on flux and selectivity are reported.

6.1.5 EXPERIMENTAL WORK

The literature illustrates that support layer and permeate pressure cannot be ignored as influential variables. The former has already been recognised within this thesis as a significant resistance to mass transport for the system under investigation. Experimental work within this chapter includes a study of different support materials which can be used, a brief investigation of any permeate pressure and system design effects within the system and comments about the composition range within which the CsPA membrane can operate and the ways in which selectivity may be lost.

6.2 EXPERIMENTAL

6.2.1 SUPPORT MATERIALS

Five different support materials were used and their properties are shown in Table 6.3.

Polysulfone is often chosen as a support material for pervaporation membranes because it can be dried easily without curling, it has good compaction resistance and a high surface porosity in comparison with other asymmetric UF membranes (Peinemann, 1992). Comparison of Figures 6.6 and 6.7 illustrate that it is

Name	GR40PP	FS50	Gortex	Bekipor	Rigidmesh
Material	Polysulfone	Polyvinylidene-fluoride	Polytetrafluoro-ethene	Stainless steel	Stainless steel
Supplier	Der Danske Suker Fabriker	Der Danske Suker Fabricker	WL Gore Inc.	Bekaert Fibre Technologies	Pall International
Thickness (mm)	0.3	0.25	0.20	0.17*	0.12
Porosity (%)			70	77	31
Nominal pore diameter (um)			0.25-0.40	Average 5.3 (larger pores on surface = 25)	Surface = 1-5 Inside = up to 15
Molecular weight cut-off	100 000	30 000			
Absolute removal size (um)	0.006			5	15
Water flux (lm-2bar-1h-1)	150-300	300-600			>10
Air permeability at 200Pa (lm-2min-1)				34	0.97
Hydrophilicity	Hydrophilic	Hydrophilic	Hydrophobic	Hydrophilic	Hydrophilic

Table 6.3 Physical properties of porous support materials (information compiled from suppliers' data, tests performed at BP Research, Sunbury-on-Thames and Bath University)

*This value is different from the one quoted in Table 4.1, as a different generation of Bekipor was used.

asymmetric. It suffers the disadvantage of being attacked by many chemicals, including ketones, aromatic hydrocarbons and chlorinated solvents. This limits the number of solvents for coating solutions and feed mixtures with which it can be used.

PVDF is also an asymmetric UF membrane and the scanning electron micrograph shows it also has a high surface porosity (Figure 6.8). Figure 6.9 shows the structure of the underside of PVDF.

Gortex is a relatively recent addition to the membrane market and the only hydrophobic material tested. It is symmetric across its thickness and has excellent chemical and thermal resistance, however, visual inspection suggests its compaction resistance may be low. One could envisage that under pressure, its pores may become compressed. Viewed under the electron microscope, its surface morphology is seen to vary across an area (Figure 6.10).

Bekipor is formed from three separate layers of stainless steel fibres of different diameters which are laid down and sintered together under pressure. A range of these membranes are available since the porosity can be varied by using different weights and diameters of fibres in the separate layers. Rigidmesh membranes are made from stainless steel powder which has been sintered onto a stainless steel woven backing. The differences in fabrication between these two supports can be seen by comparing micrographs of their surfaces (Figures 6.11 and 6.12). Being made of stainless steel, both Bekipor and Rigidmesh are strong, chemically and thermally resistant.

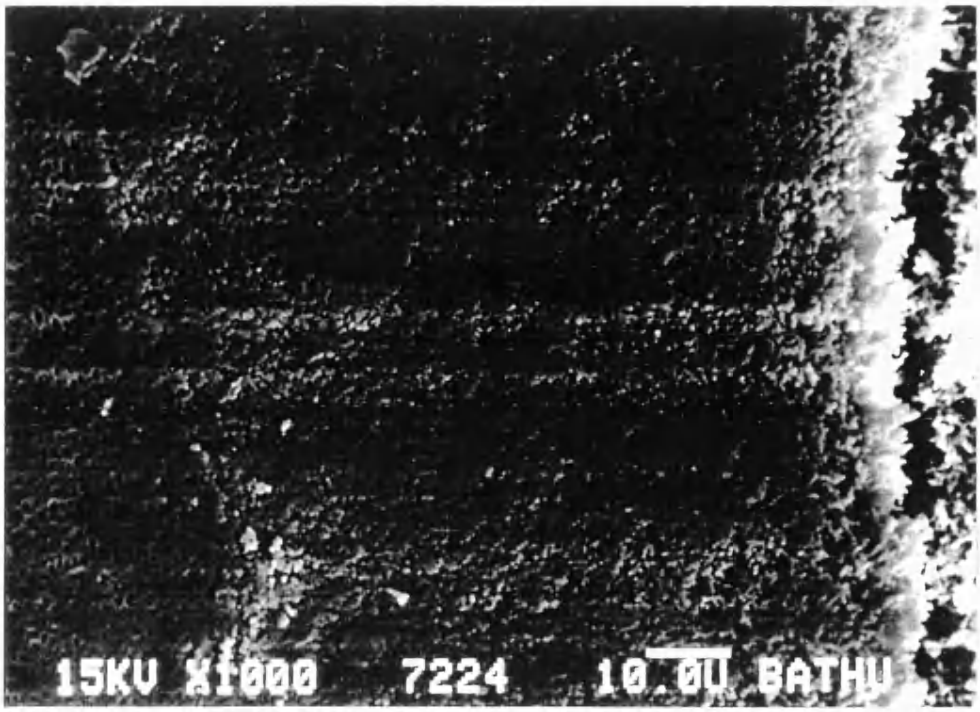

Figure 6.6 SEM of the upper surface (skin side) of polysulfone asymmetric UF membrane

Figure 6.7 SEM of the lower surface of polysulfone asymmetric UF membrane

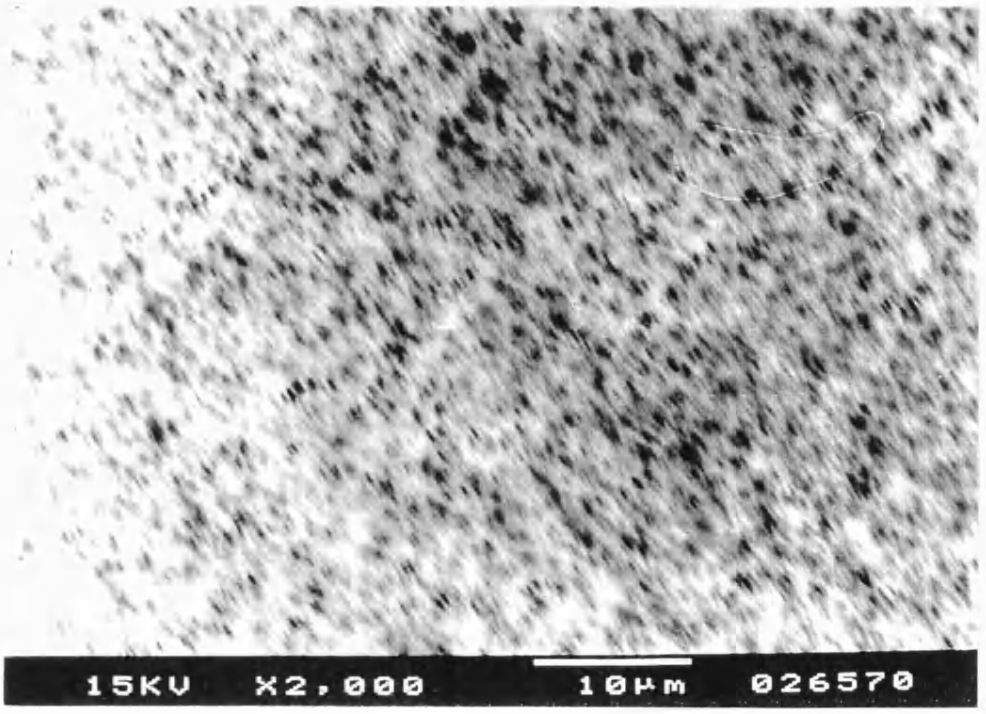

Figure 6.8 SEM of the upper surface (skin side) of polyvinylidenefluoride asymmetric UF membrane

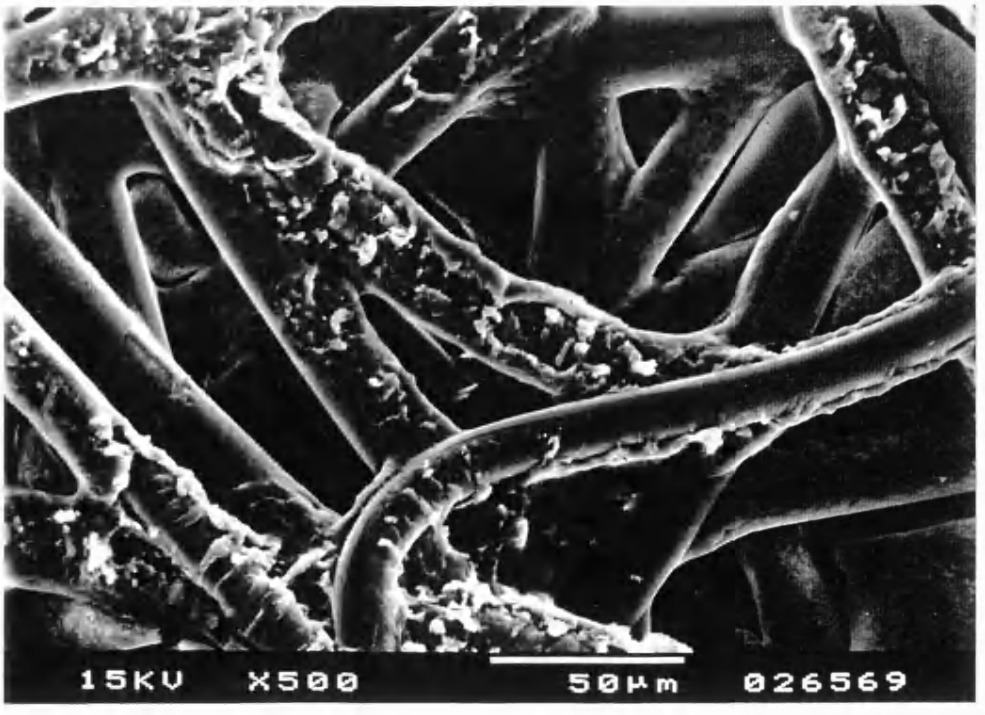

Figure 6.9 SEM of lower surface of polyvinylidenefluoride asymmetric UF membrane

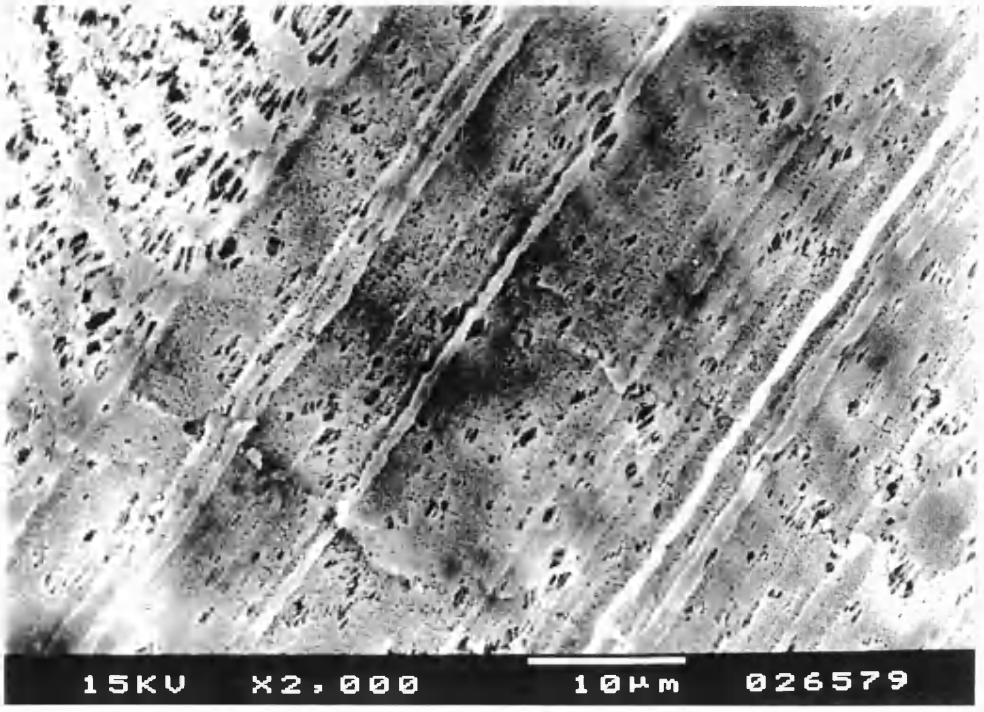

(a)

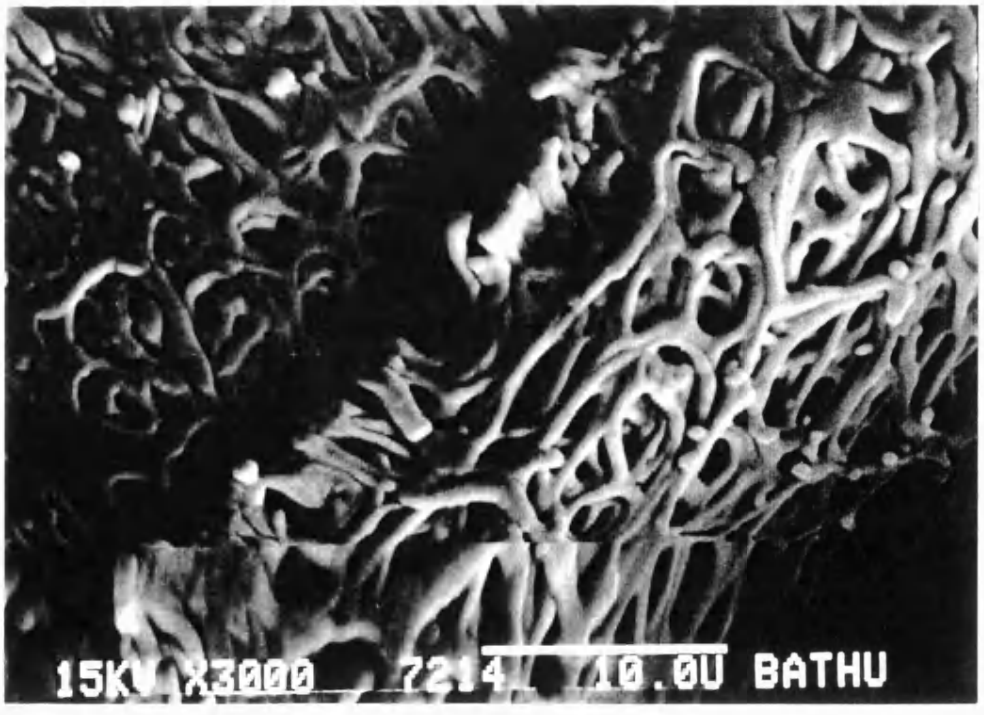

(b)

Figure 6.10 SEMs of the surface of a Gortex membrane (a) Magnification = 2000 (b) Magnification = 3000

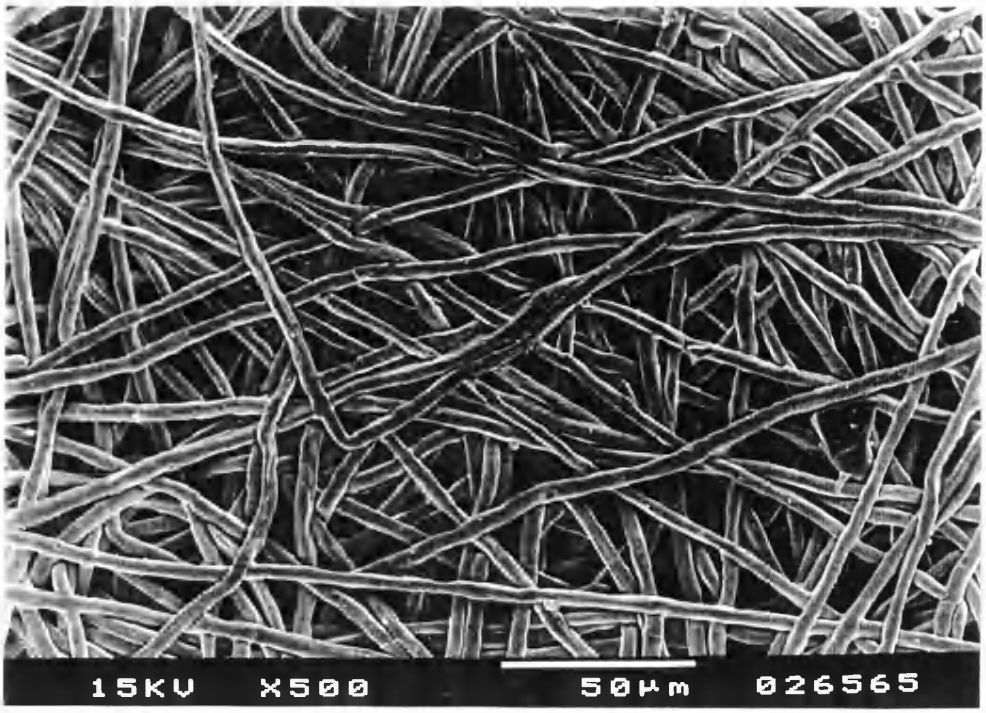

Figure 6.11 SEM of the surface of a Bekipor MF membrane

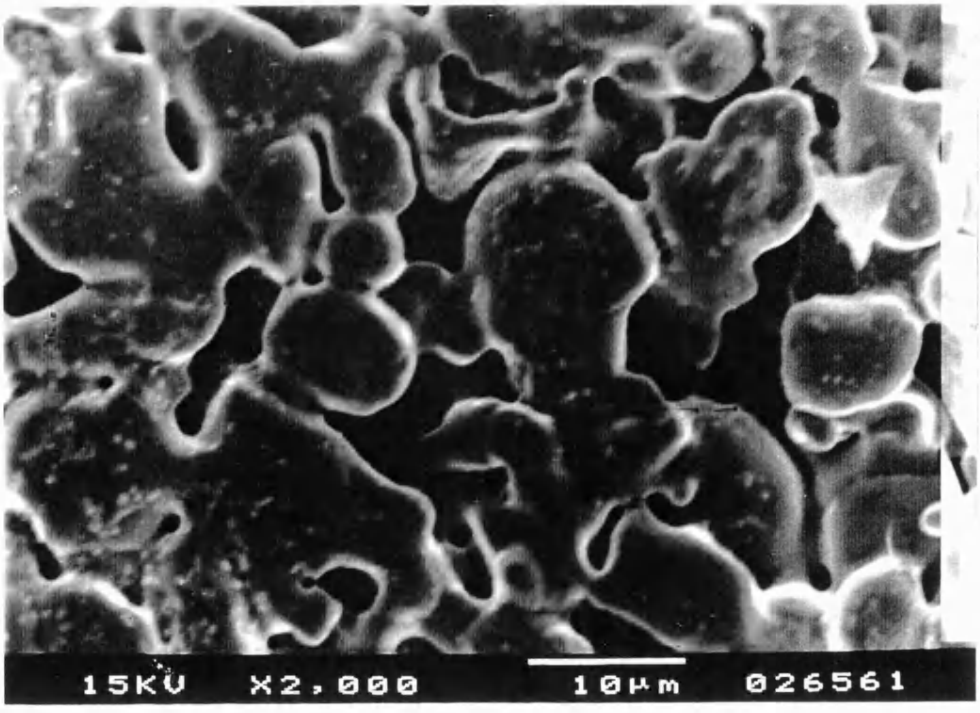

Figure 6.12 SEM of the surface of a Rigidmesh MF membrane

6.2.2 EFFECT OF SUPPORT MATERIAL

Selective layers used within this section were made from 20g 0.5wt% CsPA, MW 250 000, pH 8.5. Each membrane was dried at 35°C. Dewatering experiments were carried out at a temperature of 70°C and a stirrer speed of 1000rpm.

The PSf and PVDF supports were each first soaked in two changes of water for 2 hours, then dried before being coated directly using Method 1 (Section 2.2.2). No pre-treatment was required for the Gortex support which was coated using the same method as above.

Neither the Bekipor nor the Rigidmesh required any pre-treatment. These supports were coated using Method 2 (Section 2.2.2). The dry selective layer was first formed on Parafilm before being transferred to the porous support. The reason a thicker, 28μm layer was used in place of the standard 14μm thick film was because of the hydrophobic natures of the Gortex and the Parafilm. More polymer solution was required in order to wet and coat these surfaces entirely and form a defect-free layer.

The performance of each composite membrane was tested by batch dewatering using the conditions stated at the start of this section. The vacuum used was better than 1.5mbar, measured next to the vacuum pump.

6.2.3 EFFECT OF PERMEATE PRESSURE

Glass capillary tubes were made and inserted, one at a time, into the rig between the feed cell and the condenser to provide a constant "leak" into the system. Permeate pressure was measured next to the vacuum pump. Three permeate pressures were achieved using different capillaries: 0.4, 3.4 and 9.1mbar. Unfortunately, the highest pressure which could be achieved was only 10mbar as this

was the limit of measurement for the pressure gauge used. The effect of permeate pressure was assessed using the results of batch dewatering of an IPA solution using a 14μm thick CsPA membrane, pH 8.5, supported on PVDF. The conditions used were a feed temperature of 70°C and a stirrer speed of 1000rpm.

6.2.4 EFFECT OF METAL SUPPORT DISC

A porous metal support disc (porosity unknown) supports the composite membrane within the test cell (Figure 2.1). A different design of disc (Figure 6.13) was tested to see whether this has any effect, and a third disc which had been identical to the first (porous) but the surface of which had been damaged was also tested. It was suspected that some of the pores of this disc had been blocked. Assessment of the effect of changing the support disc was facilitated by using each system to batch dewater an IPA solution. The selective membrane used was a 14μm thick CsPA layer, supported with PSf. The conditions used were a feed temperature of 70°C and a stirrer speed of 1000rpm.

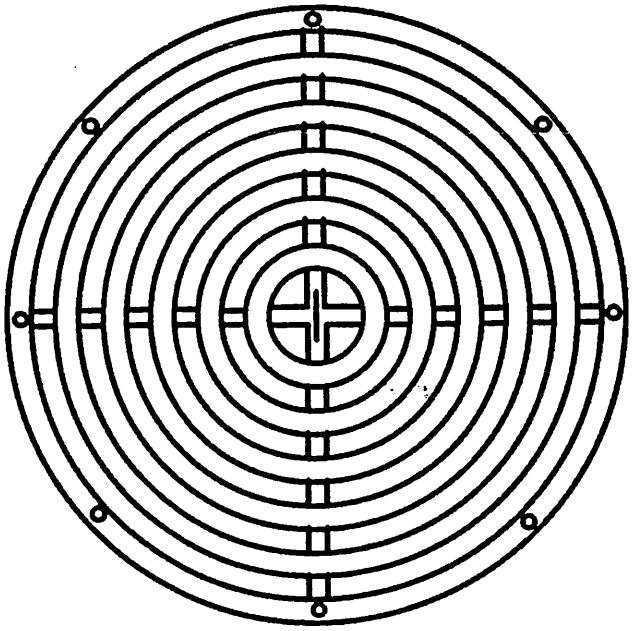

Figure 5.13 "Concentric rings" metal support disc

6.2.5 MEMBRANE FAILURE

Whilst most of the experiments carried out for this work feature feed mixtures containing 5-20wt% water, a brief investigation of the concentrations under which the

membrane looses its selectivity and usefulness was undertaken. This involved testing a 14μm thick CsPA layer, supported on PSf with feed solutions containing less than 1wt% and greater than 25wt% water at a feed temperature of 70°C and a stirrer speed of 1000rpm.

Further, included in this section are the results of an experiment where membrane selectivity decreased over a period of time.

6.3 RESULTS AND DISCUSSION

6.3.1 EFFECT OF SUPPORT MATERIAL

Coating PSf and PVDF support materials (skin-side up) with polymer solution was very straightforward as both materials are hydrophilic and the surface pores are very small. Gortex was coated by the same casting method but because of its hydrophobicity, a larger volume of casting solution was required to coat the surface and so form a defect-free membrane. If thinner selective layers are required, it is possible to soak the Gortex in a solution of surfactant, then dry it and cast on top. The surface of the Gortex is then hydrophilic, facilitating the use of less polymer solution. This method has been used successfully for previous reported work (Burslem *et al.*, 1992).

Similarly, coating Bekipor and Rigidmesh for this work, the selective layer was first cast onto hydrophobic Parafilm, dried, then transferred to the porous material. Although this is considered to be a useful method for forming a polyacrylate layer onto any material, regardless of porosity, it is a tricky process and practice was required for a high success rate of defect-free membrane production to be achieved. Also, it would be a difficult process to scale-up. The disadvantage of direct casting is that the polymer solution may seep into the pores of the support.

One way of making this less likely is to spray the surface of the metal support with a hydrophobic release agent. Frekote 1711 (Frekote Inc.), a mould release agent of silicone oil dissolved in kerosine, has been used successfully. However, neither this or casting onto Parafilm facilitates the fabrication of very thin membranes using such supports.

The effects of the support material upon flux and separation factor are shown in Figures 6.14 and 6.15.

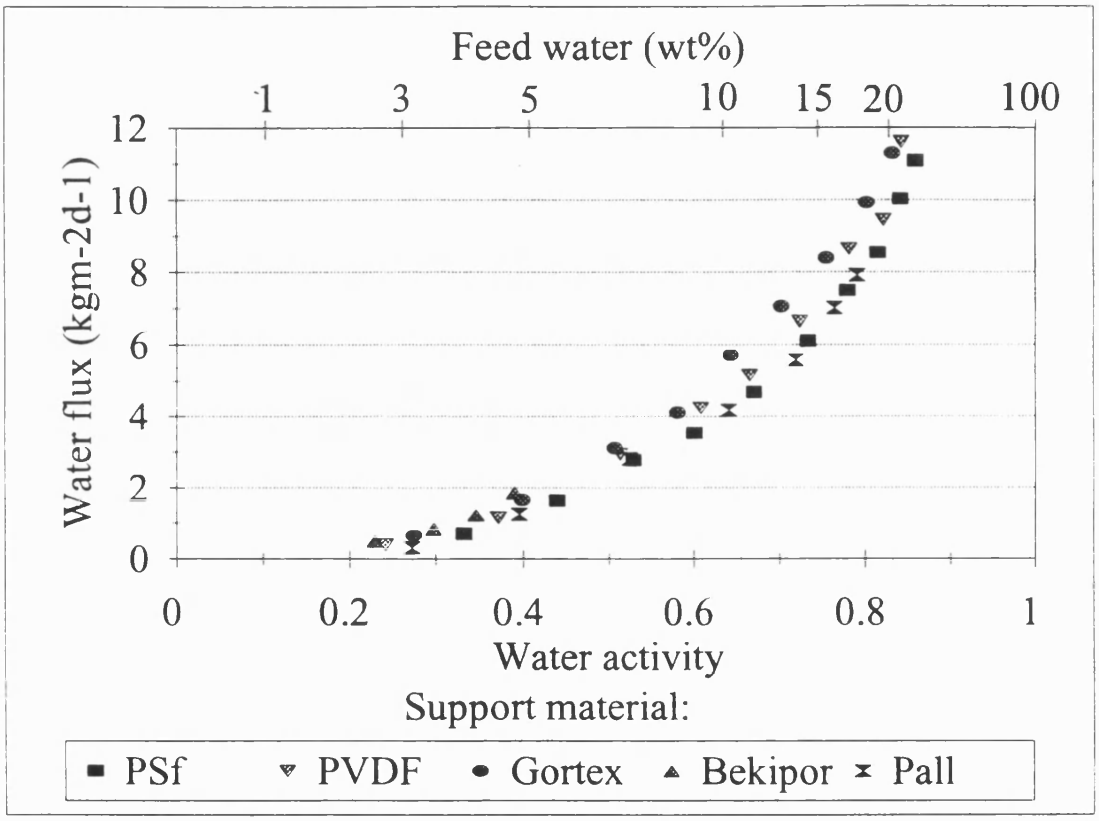

Figure 6.14 Effect of porous support material upon water flux. Pall = Rigidmesh

Gortex, PSf and PVDF support materials could be used over the entire range of feed concentrations tested whereas it was only possible to use Bekipor-supported membranes at feed concentrations of up to 5wt% water and Rigidmesh up to 17wt%. At higher water concentrations than these, the swollen polyacrylate layer lost its

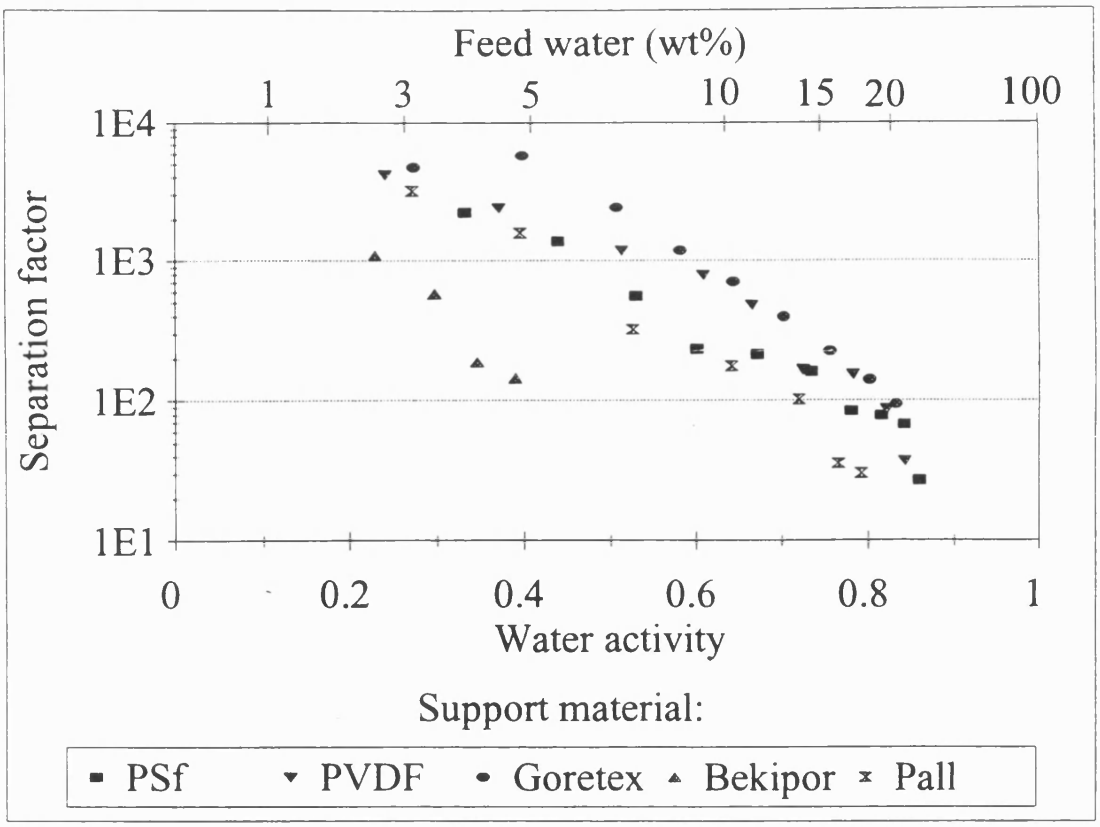

Figure 6.15 Effect of porous support material upon separation factor

selectivity, apparently because it looses its mechanical rigidity and penetrates the larger pores (see Section 6.3.4). Referring to Table 6.3, it seems obvious that it is the size of the pores on the surface which accounts for the differences between the support materials in this respect. Bekipor's larger pores are concentrated on the surface of the filter. Although the average pore size is 5.3μm, pores on the surface can be up to 25μm in diameter. When the polyacrylate layer swells, it loses its rigidity and may be drawn into these larger pores, creating flaws in the selective layer. In the Rigidmesh filter, the smaller pores are on the surface whilst the inner region contains the larger pores. At higher water concentrations, the swelling and loss of mechanical strength of the polyacrylate will cause this layer to also penetrate the pores of the Rigidmesh. This happens at a higher water content feed because the

pores are smaller. The nominal pore diameter of the Gortex is still large compared to those of the UF membranes, but it appears small enough to prevent any seepage of polyacrylate into the pores from affecting the selectivity, for the water concentrations used. It is, however, possible that some penetration may still occur. Thus, surface porosity, but not absolute removal size, appears to be a good initial indicator of the maximum feed water concentration which can be used with a porous support.

Comparing fluxes at low feed water content, Bekipor is the best support material to use, followed by Gortex, PVDF, then Rigidmesh and PSf which performed equally well. Bekipor's high porosity, air permeability, large pore diameter and thinness indicate that this should be so. Gortex also has a high porosity, along with a larger pore diameter than the UF membranes as well as a smaller thickness.

The higher flux of the PVDF-supported composite membrane compared to the PSf-supported one may be predicted from the higher water flux and smaller thickness, even though it can be assumed, from the MW cut-off data that PVDF has smaller pores. It would be useful to know the surface porosity of these materials. It is very surprising that fluxes gained from the Rigidmesh-supported membranes are similar to those from PSf-supported ones. Despite its low porosity (31% compared to 77% for Bekipor), Rigidmesh has a very high water flux ($>10^5 lm^{-2}bar^{-1}h^{-1}$) compared to PSf ($150\text{-}300 lm^{-2}bar^{-1}h^{-1}$). But, the air permeability of Rigidmesh ($0.97 lm^{-2}h^{-1}$) is much lower than that of Bekipor ($34 lm^{-2}h^{-1}$) so Rigidmesh would be expected to have a lower flux than Bekipor, as is found. A suggested explanation is that the surface porosity of the Rigidmesh is very low (a few larger pores) compared to that of the

PSf (many small pores). Also, water molecules cannot permeate through stainless steel (as they may do through PSf) and more widely spaced pores would lead to a much larger effective membrane thickness (Figure 6.2).

An overall comparison of the performances of each composite membrane is given in Table 6.4.

	Flux in comparison to that of the PSf-supported composite membrane				
Feed water (wt%)	**PSf**	**PVDF**	**Gortex**	**Bekipor**	**Rigidmesh**
5	1	1.20	1.50	1.62	1.08
10	1	1.15	1.32	-	1.02
15	1	1.12	1.23	-	0.98
20	1	1.11	1.18	-	-

Table 6.4 Comparison of the performances of composite membranes with different porous support layers

6.3.2 EFFECT OF PERMEATE PRESSURE

Three different permeate pressures were used, 0.4, 3.4 and 9.1mbar, and the results of dewatering experiments are shown in Figures 6.16 and 6.17. Within this region, permeate pressure had no effect on the flux but, interestingly, the separation factor at the highest permeate pressure was lower than for the other two. This is accounted for by the very small increase in IPA passing through the membrane because of the slight opening up of the polymer structure in the selective layer due

to the higher permeate pressure. Although in Figure 6.17 it seems as if this effect is very significant, it in fact only corresponds to a decrease in the permeate water composition of from 99.9wt% to 98.8wt% at 4wt% water in the feed. The increase in permeate partial pressure is insufficient to have an effect on the water flux and the small increase in IPA flux makes no difference to the overall flux. It should be anticipated that if the permeate pressure was increased significantly, the water flux would decrease.

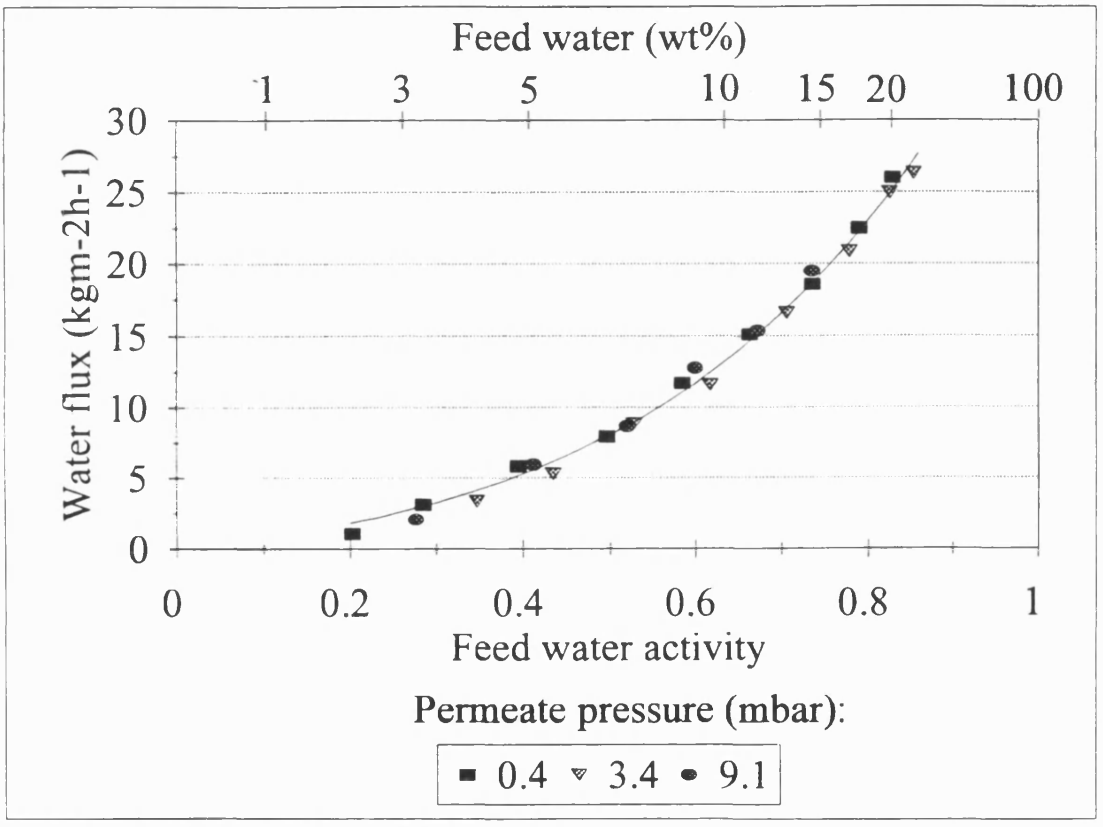

Figure 6.16 Effect of permeate pressure on water flux

These results are marginally different from those reported by Colman and Naylor (1991) for a similar membrane. They found that below a feed water content of 5wt%, variation of permeate pressure below 10mbar has no effect on flux, but at higher water concentrations, flux increases as permeate pressure decreases (although

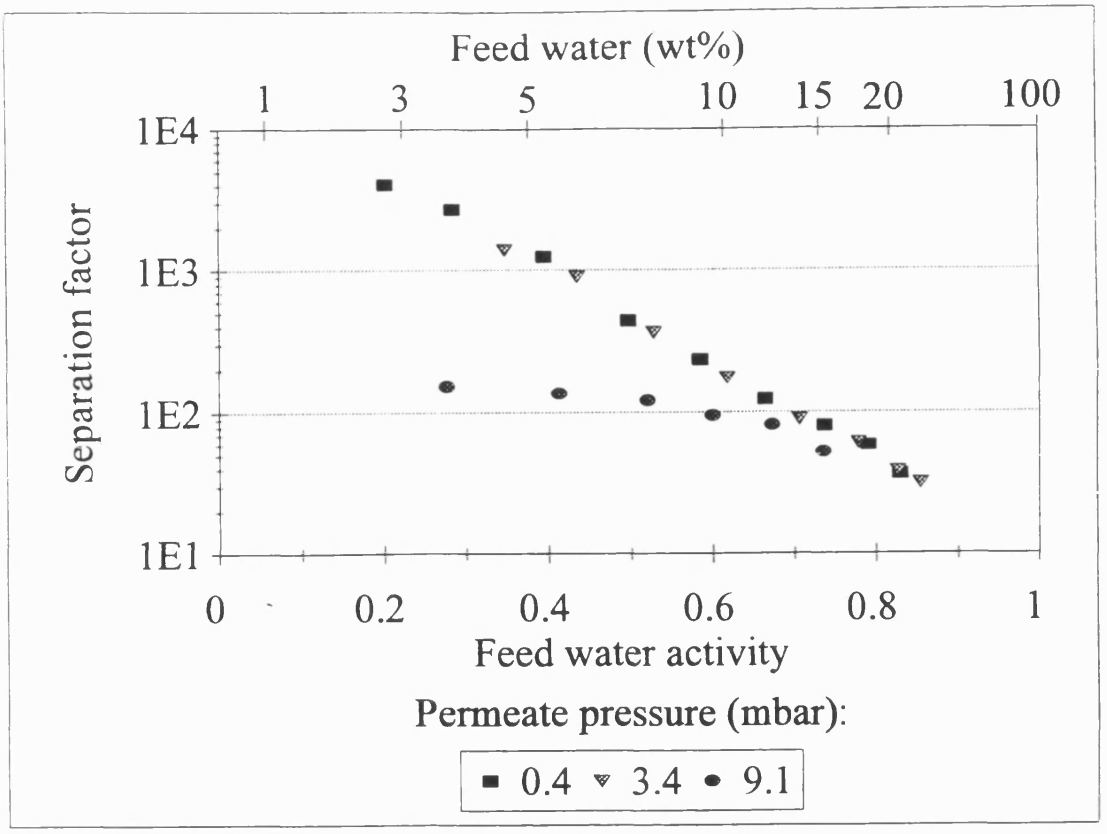

Figure 6.17 Effect of permeate pressure on separation factor

only one permeate pressure below 10mbar was tested). They ascribe this effect to changes in the membrane diffusivity at higher water concentrations. These authors also report no effects on selectivity with changing permeate pressure.

6.3.3 EFFECT OF METAL SUPPORT DISC

The effects on water flux and selectivity of changing the metal support disc are shown in Figures 6.18 and 6.19.

Comparing first the porous support disc with the support disc constructed from concentric metal rings, there is no significant effect upon either flux or selectivity. However, the porous metal disc with lower surface porosity, due to blocked pores, caused a lower water flux to be attained at higher concentrations of water in the feed. At higher water concentrations, the flux through the selective layer is much higher

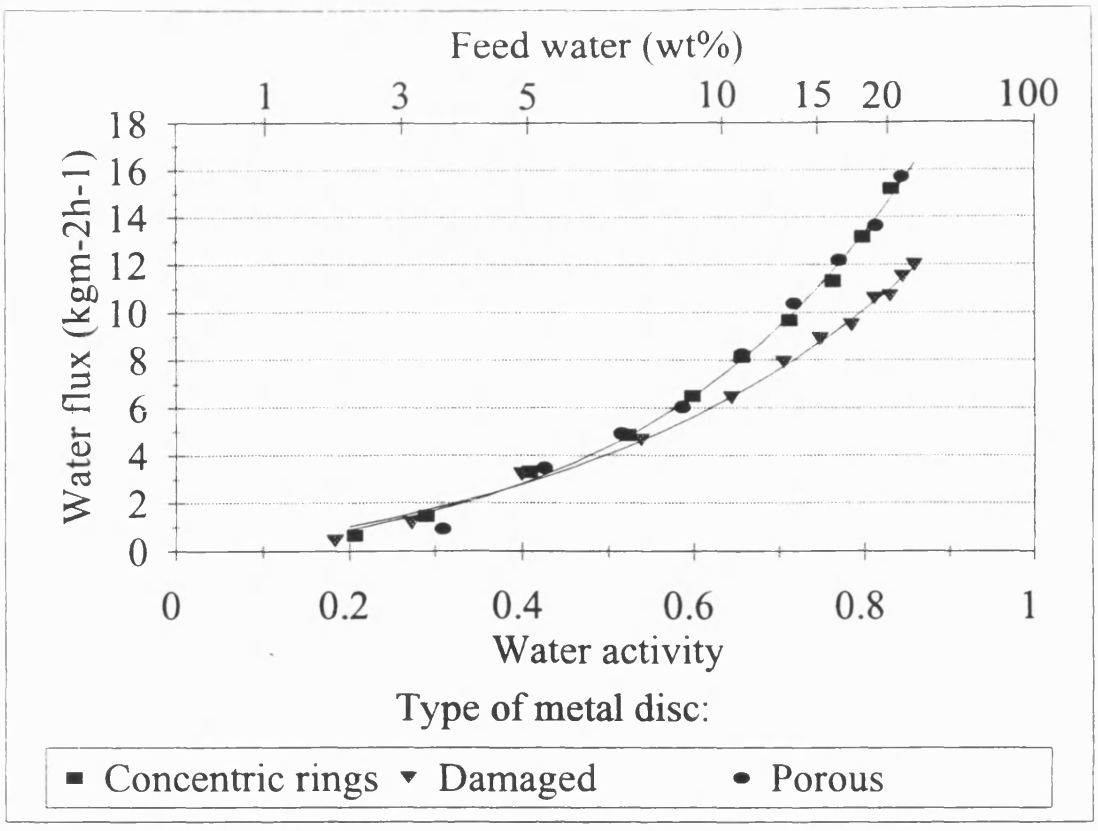

Figure 6.18 Effect of metal support disc used upon water flux

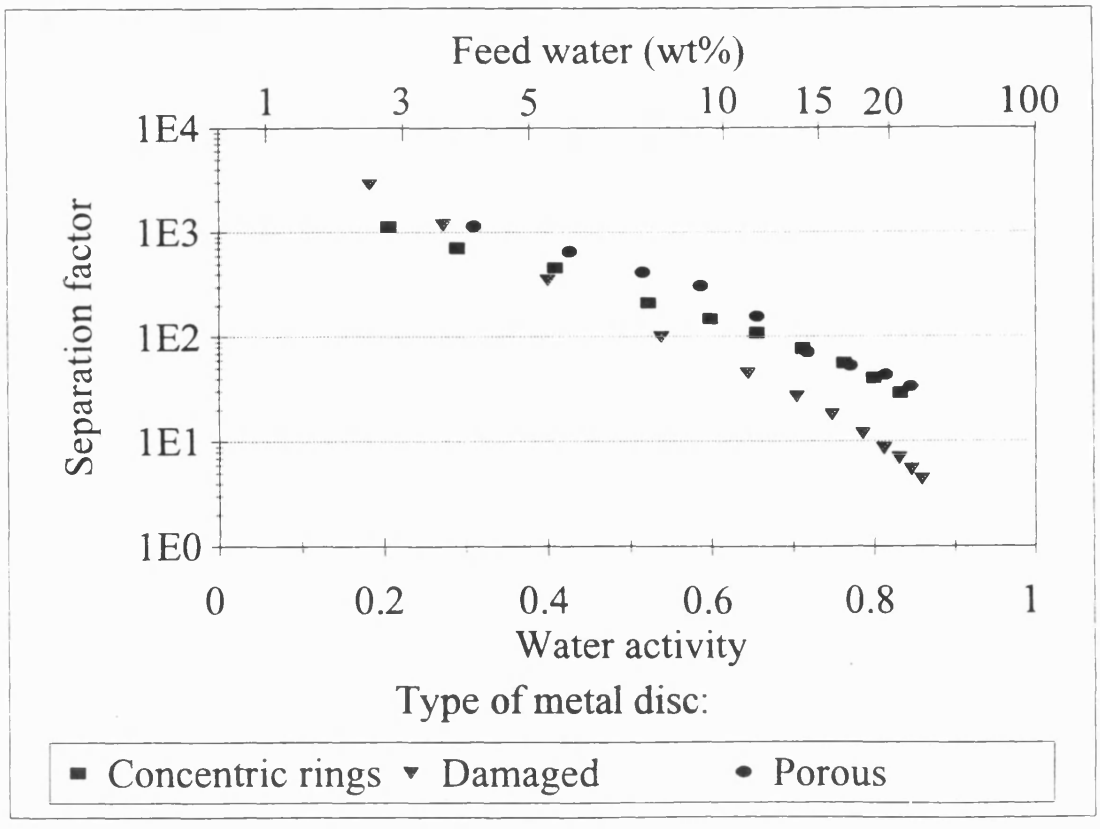

Figure 6.19 Effect of metal support disc used upon separation factor

and if the porosity of the metal disc is too small, it becomes a controlling resistance and flux decreases. This is similar to the effect that low porosity membrane support layers have upon flux. The effect on selectivity is marginal. The "blocked" support results in only a slightly lower selectivity at higher water concentrations in the feed.

6.3.4 MEMBRANE FAILURE

The ways in which a CsPA membrane irreversibly loses its selectivity have been found to be:

-Dissolution at very high concentrations of water in the feed solution

-Loss of selectivity at very low concentrations of water in the feed solution

-Defects in the membrane at start-up

-Gradual loss of selectivity during use

From experimental evidence, the CsPA active layer is not recommended for use at concentrations of above 40wt% or below 0.5wt% water when supported by PSf. This is because the selective layer starts to dissolve and selectivity is gradually lost. It has been shown in Section 6.3.3 that the suitable upper-level of water concentration varies with the support material, therefore, it is supposed that the lower-level also varies. Unfortunately, there was not time to test this hypothesis, but if true, it is further evidence for the suggestion that support materials, as well as selective layers, should be tailored to a particular application.

Occasionally, membranes were produced which were defective, e.g. contained pinholes. It is hard to see how this can be avoided.

Gradual loss of selectivity during use was noted a few times, in particular when testing the Bekipor membrane. In one instance, at a constant feed concentration

of 5wt% water, the quality of the permeate fell from 99.7wt% to 73.4wt% water over a period of 90 minutes. When the membrane was removed from the cell, some parts were seen to have the regular shiny appearance of the selective layer but there were some dull patches, where it looked as if the polyacrylate had penetrated into the pores of the Bekipor. It is interesting to note that the selectivity is not lost immediately, but is a time-dependent process.

A recommended way of preventing, or at least minimising all such membrane failures would be to cross-link the polymer. Cross-linking would result in a selective layer less prone to swelling, insoluble in feed solutions containing a high proportion of water and less likely to seep into large pores in the support material, although these advantages would be counterbalanced by a flux decrease. The cross-linking agent needs to be able to mix with the initial polymer solution without causing the polymer to precipitate. Tests would need to be carried out to find a suitable agent and appropriate level of use. One possibility is Baco 20, a solution of ammonium zirconium carbonate and tartaric acid.

6.4 CONCLUSIONS

The properties of several porous materials have been tested and their effectiveness as support layers in pervaporation considered. Bekipor was very successful at low water concentrations (<5wt%) but selectivity was lost at higher water levels as the polymer swelled and sunk into the large pores. Across a wider range of feed compositions, Gortex and PVDF supports provided the higher fluxes, with PSf and Rigidmesh-supported membranes achieving lower fluxes. Gortex also has the advantage of being thermally and chemically resistant because it is made from PTFE. Physical properties of the materials can be used as a guide to their success

as membrane supports. A high porosity, particularly surface porosity, and a large pore size are advantageous, but the pore size should not be so large that the active layer seeps into it. These effects become increasingly important as the active membrane layer is made thinner. A comparison of the PSf-PVDF ratioas in Table 6.4 with the results in Chapter 5 show that the effect of switching from PSf to PVDF is more significant when the active layer is thinner. The ratio changes from around 1.15 to about 1.78 as the active layer thickness is halved.

Permeate pressure was varied between 0.4 and 9.1mbar and was not found to affect water flux within this region, although a decrease in separation factor was found at the highest permeate pressure tested. The porous metal disc supporting the composite membrane can also affect the flux, lowering it at high fluxes, if the porosity is low.

The CsPA membrane will loose its selectivity at high ($>$40wt%) and low ($<$0.5wt%) water concentration in the feed when supported by polysulfone. It is suggested that cross-linking the polymer would improve the stability of the membrane.

CHAPTER 7

INFLUENCE OF FEED LIQUID TEMPERATURE

7.1 INTRODUCTION

7.1.1 BACKGROUND LITERATURE

Variation of the feed liquid temperature has a major influence upon the flux through a membrane and can also affect the selectivity (Section 1.2.10). The pervaporation flux can always be greatly accelerated by operating at the highest temperature compatible with the membrane. According to the free volume theory of permeation, thermal motion of polymer chains in the amorphous regions of the polymer randomly produces free volume for permeating species to move into. As the temperature is raised, the frequency and amplitude of chain jumping, or thermal agitation, increases, resulting in larger free volumes being produced. Since in pervaporation, molecules diffuse through the free volumes, when the temperature is high, the total permeation rate is high.

In terms of the separation factor, this has been found experimentally to both increase and decrease with temperature, although in most cases the separation factor decreases with increasing temperature (Néel, 1991). Utilising the free volume theory again, as the temperature is raised, larger free volumes are present and the diffusion of both permeating species is enhanced. If the non-selective molecule is larger than the other its permeation is particularly enhanced. Alternatively, if there is any tendency for the two feed molecules to mutually associate and thus permeate as interacting pairs, which are larger in size, diffusion of this species may be enhanced, thus lowering the selectivity. Sometimes there is little variation in α and in some cases α increases with temperature. In this case, the feed comprises a strongly self-

associating component and energy from the raised temperature can be utilised to overcome interactions between permeating molecules which hinder permeation.

Néel (1991) states that the permeability, P, of an amorphous, homogeneous, dense film to permanent gases increases with temperature, according to an Arrhenius relationship:

$$P = P_0 \exp(-E_P/RT) \tag{7.1}$$

where E_P is the activation energy of permeation and P_0 is the permeability at infinite temperature. Permeability is defined as the product of solubility, which is represented by the gas-polymer heat of solution (ΔH_s), and diffusivity. Diffusion may also be regarded as an energy activated process:

$$D = D_0 \exp(-E_D/RT) \tag{7.2}$$

where E_D is the activation energy for diffusion. E_P can then be viewed as the sum of the activation energy for diffusion and the heat of solution:

$$E_P = E_D + \Delta H_S \tag{7.3}$$

Néel continues by asserting the in pervaporation, the situation is more complex because the diffusion coefficients are rarely concentration-independent, there is a degree of inaccuracy in the evaluation of permeabilities if the thickness of the swollen membrane is unknown and anisotropic swelling means that the pressure gradient across the membrane is uneven. In the swollen section, the membrane behaves more as a viscous liquid with only a slight pressure gradient evident, whilst in the dry section, the membrane is more like a rigid slice of polymer with a high pressure gradient across its width. He also suggests that the phenomenon occurring at the feed/membrane interface is not dissolution but is more complex: a partitioning

between the feed liquid and the swollen membrane. The contribution of this process may be hard to quantify experimentally.

It seems remarkable that despite these difficulties, an Arrhenius relationship still holds for the temperature dependence of flux, or permeation rate. Many studies have found that this relationship is valid over a fairly large temperature range and a summary of a small selection of these is given in Table 7.1. Other than that of Blume *et al.*, all the studies utilise a mass flux, rather than permeability, and a concentration driving force to calculate the activation energy. This avoids the problem of evaluating the membrane thickness. A high activation energy value indicates that pervaporation flux is greatly accelerated by increasing the operating temperature of the process.

The effect of temperature upon selectivity can be calculated if the activation energies for both permeating components are known (Ping *et al.*, 1990):

$$c_{pi} = \frac{J_i^0 \exp[-\frac{E_i}{R}(1/T - 1/T_R)]}{J_i^0 \exp[-\frac{E_i}{R}(1/T - 1/T_R)] + J_j^0 \exp[-\frac{E_j}{R}(1/T - 1/T_R)]} \qquad (7.4)$$

where c_{pi} is the concentration of the preferentially permeating component in the permeate and T_R is the reference temperature, in Kelvin.

Provided a reasonably high reference temperature is defined, this equation can be simplified to:

$$c_{pi} = \frac{1}{1 + \frac{J_j^0}{J_i^0} \exp(-\frac{E_j - E_i}{RT})} \qquad (7.5)$$

Table 7.1 Summary of literature sources and findings for the influence of feed temperature upon pervaporation performance

REFERENCE	MEMBRANE	FEED MIXTURE	TEMPERATURE RANGE USED (C)	ACTIVATION ENERGY (kJmol-1)	EFFECT OF TEMPERATURE INCREASE ON SEPARATION FACTOR
Binning, Lee, Jennings and Martin (1961)	Not stated	n-heptane/iso-octane 50-50 wt%	70 to 100	36	Decrease
Blume, Bos, Schwering, Mulder and Smolders (1991)	PDMS EPDM	n-octane	-10 to +70	-7 to -28	-
Choi, Hino, Shibata, Negishi and Ohya (1992)	PAA-PSf composite	Water-ethanol		15	Small decrease
Huang and Jarvis (1970)	Cellophane PVA Cellophane	Pure water Pure water Pure n-propanol	30 to 50	18 37 29	-
Huang and Yeom (1990)	Cross-linked PVA	Water-ethanol	30 to 75	21 to 40	Decrease
Huang and Yeom (1991)	Cross-linked PVA	Water-acetic acid	30 to 75	24 to 34	Decrease
Ohya, Shibata, Negishi, Guo and Choi (1994)	PAA-PAN composite	Water-ethanol	25 to 70	11	-
Ping, Nguyen, Clement and Neel (1990)	Grafted PAA modified with alkali counter ions	Water-ethanol	25 to 70	0 to 59 for water 34 to 71 for ethanol	Decrease
Neel (1991) (Review article)	Various	Various	Various	21 to 92	Usually a decrease

The higher the difference in activation energies of the two components, the greater the change in permeate composition, and therefore selectivity, with temperature.

Binning, Lee, Jennings and Martin were probably the first to test the temperature dependence of permeation in 1961. They found that the permeation (on a log scale) of a 50-50 volume mixture of n-heptane and iso-octane through an unnamed membrane was proportional to the inverse feed temperature in Kelvins, i.e. an Arrhenius-type relationship. An activation energy of 8.5kcalmol^{-1} was calculated and was found to be unaffected by the thickness of the membrane. Selectivity decreased at higher temperatures.

Huang and Yeom (1991) suggest that the value of E_P is related to the strength of interactions between the permeants: strong interactions will result in a high value of E_P. They found that the pre-exponential factor varied with feed concentration for permeation of an acetic acid-water mixture through a cross-linked PVA membrane, and suggest that this parameter relates to the plasticising effect of permeant molecules upon the polymer. It is "the characteristic of permeation at infinite temperature where interaction effects are no longer important" (Huang and Yeom, 1991, p.44). In a similar study, Huang and Yeom (1990) found that both the activation energy and the pre-exponential factor varied with concentration for the pervaporation of a water-ethanol mixture through the same cross-linked PVA membrane. Huang and Jarvis (1970) surmise that increasing the concentration of a plasticising component in the feed (in their case, water and a PVA membrane) decreases the activation energy for diffusion by increasing the amount of swelling of the amorphous region of the polymer.

Ping, Nguyen, Clément and Néel (1990) looked for insight into the influence of the membrane's chemical properties on transport. They used a polyacrylic acid membrane grafted on top of a polyethylene layer. The acrylic acid membrane was modified with alkali counter ions. The membranes used differed from each other only in the nature of the cation associated with the carboxylate groups fixed onto the membrane. The membranes were tested with the permeation of an ethanol-water mixture. The authors found that the activation energy for the pervaporation of the alcohol was always higher than that for water. They also found that the activation energies for permeation varied with both the feed composition and the counter ion in the membrane. An increase in water concentration (up to 30wt%) resulted in a decrease in the activation energies for both permeating components. This behaviour was attributed to an increase in the swelling of the membrane at increased feed water content, resulting in a lowering of the energetic barrier for diffusion owing to plasticization of the polymer. Similarly, the highest activation energy was detected for the lithium counter ion , followed by sodium then potassium. The difference may be explained on a similar basis: the lithium type swells the least and therefore possesses the highest energy barrier to transport. Ping *et al.* found that if the sorption contribution to permeation energy was low, differences in the pervaporation activation energy result from the diffusion process, i.e. the difference in the energy barrier for diffusion.

Blume *et al.* (1991) tested the temperature dependence of liquid permeation through PDMS and EPDM membranes for a number of solvents. Interestingly, they found that, although the flux always increased with increasing temperature, the permeability actually decreased because the rate of increase of the pressure driving

force was faster than the rate of increase of flux. They submit that whilst the diffusivity is endothermic, the heat of solution (solubility), found from experiments, is strongly exothermic and dominates for the systems tested, consequently, a negative activation energy was calculated.

7.1.2 RESISTANCES-IN-SERIES MODEL

For pervaporation through the polyacrylate membrane:

$$J = k_{ov}M(a_b - a_p) \tag{7.6}$$

where k_{ov} is the overall mass transfer coefficient and has been taken to be the rate constant for the process. It has been used in preference to permeability in order to avoid placing a numerical value on the membrane thickness. M is a factor to convert mass fractions to activities.

For pervaporation systems, an Arrhenius type relationship of permeation with temperature is generally found over a reasonably large temperature range:

$$k_{ov} = k^*_{ov}\exp(\frac{-E_A}{RT}) \tag{7.7}$$

In this analysis, E_A is an apparent activation energy, i.e., that for the whole system, including any liquid boundary layer effects. If the mass transfer resistance of the boundary layer is significant, the activation energy should be recalculated after this resistance has been subtracted from the total. The new activation energy calculated is the intrinsic activation energy.

The Sherwood correlation for transport through the boundary layer, in a stirred cell system with turbulent flow is (Smith *et al.*, 1968):

$$Sh = \frac{k_{BL}b}{D_{BL}} = 0.044Re^{0.75}Sc^{0.33} \tag{7.8}$$

$$k_{BL} = 0.044\left(\frac{D_{BL}}{b}\right)\left(\frac{\omega b^2}{\nu}\right)^{0.75}\left(\frac{\nu}{D_{BL}}\right)^{0.33} \tag{7.9}$$

In the boundary layer, the kinematic viscosity, ν, and the mass diffusivity, D_{BL}, vary with temperature. Hence:

$$k_{BL} \propto \frac{D_{BL}^{0.66}}{\nu^{0.42}} \tag{7.10}$$

If the temperature and concentration dependencies of these parameters and the boundary layer mass transfer coefficient at a reference feed temperature are known, the values of k_{BL} at other temperatures may be calculated. From this, the liquid concentration at the membrane surface can be calculated (Equation 4.4) and hence the permeation rate through the composite membrane only can be calculated. A second Arrhenius plot will reveal a new activation energy: the ***intrinsic*** activation energy: that of the composite membrane only.

7.2 EXPERIMENTAL

Five batch dewatering experiments were performed at different temperatures. The membranes used were standard 10g CsPA, MW 250K, pH 8.5, cast onto PVDF support and dried at 35°C. Dewatering of IPA/water solution was carried out at a stirrer speed of 1000rpm and a permeate pressure of less than 4mbar, measured next to the vacuum pump. Temperatures used were 23, 42, 59, 70 and 79°C.

7.3 RESULTS AND DISCUSSION

Plots of the effect of feed temperature upon performance can be seen in Figures 7.1 and 7.2. When calculating the water activity values, the variations in activity coefficient and density with temperature were accounted for. Flux increases with feed temperature, as expected, at the higher feed water concentrations, as anticipated, but at high feed temperatures (T>59°C), the effect of increasing feed temperature diminishes as the feed water concentration increases. This will be commented upon further when activation energies are calculated. It is interesting to note the parameters A and B, used to model the flux-activity relationship (Equation 2.11). These are shown in Table 7.2. Ignoring the result for 79°C, which seems out of line with the others, the parameters A increases by around 0.1kgm^{-2}h^{-1}K^{-1}, although it is unclear what this signifies. The increase of parameter B with temperature indicates that the polymer becomes more plasticised as the temperature is raised. This is to be expected.

Temperature (°C)	23	42	59	70	79
A	1.39	3.50	6.29	7.45	5.53
B	1.08	1.19	1.56	1.67	2.28

Table 7.2 Empirical parameters used to model the water flux-activity relationship ($J = Ae^{Ba}a$)

Unexpectedly, the separation factor increases with the feed temperature. Although Néel (1991) asserted that this effect has been seen before, it is unusual. It could relate to water's strong tendency to self-associate through hydrogen bonding.

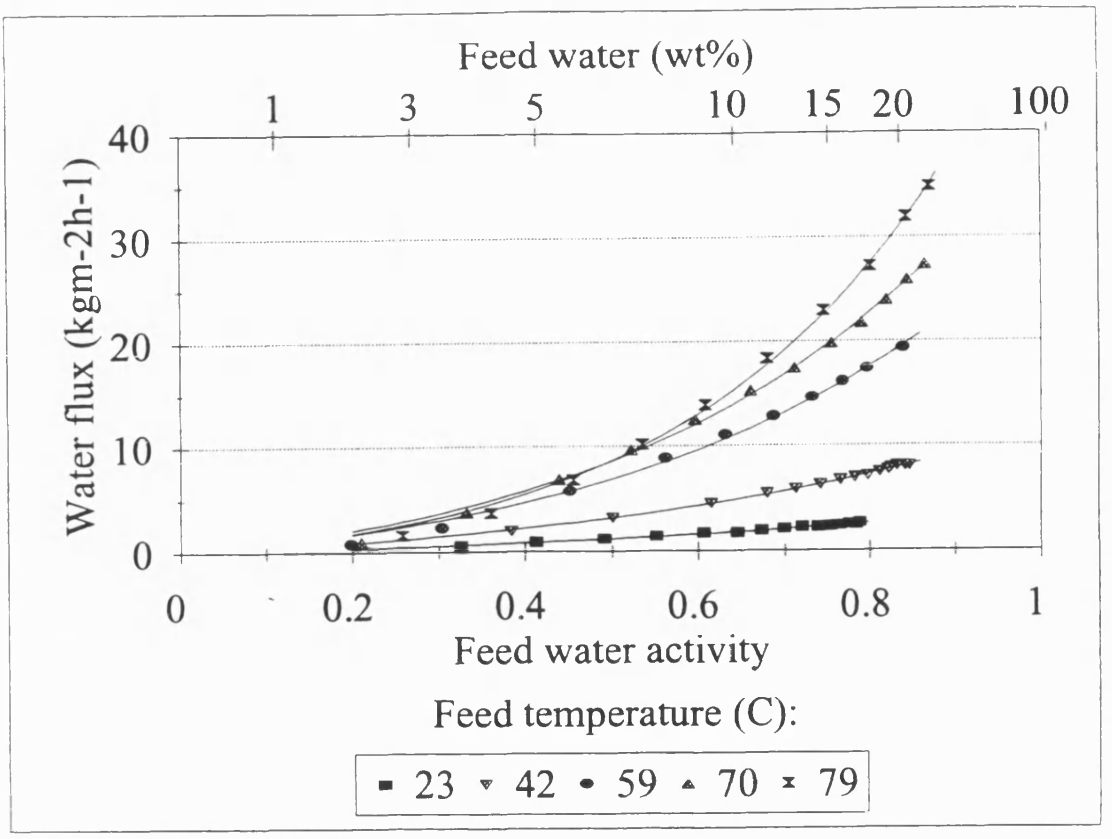

Figure 7.1 Effect of feed temperature upon water flux

Nguyen (1986) has before suggested that water may move in clusters through a membrane. A higher temperature provides more energy and this may be used to disrupt these clusters, leaving the smaller individual water molecules to diffuse through the membrane more easily. Additionally, a higher temperature may be used to disrupt the interactions which occur between caesium ions and water molecules within the membrane, again permitting easier diffusion of the water molecules. But, increasing the temperature should significantly promote IPA diffusion since it is the larger of the two molecules. As outlined in Section 7.1.1, a higher temperature boosts agitation of the polymer chains and larger free volumes are produced. Assuming it is diffusion which is the dominant effect over sorption, it must be assumed that a higher temperature promotes water diffusion to a greater extent than

IPA diffusion, although it should be remembered that although the separation factor at 78.9°C and 10% feed water is ten times that at 22.9°C, this equates to a difference in permeate water concentrations of only 2.3wt% (99.7wt% compared to 97.4wt%).

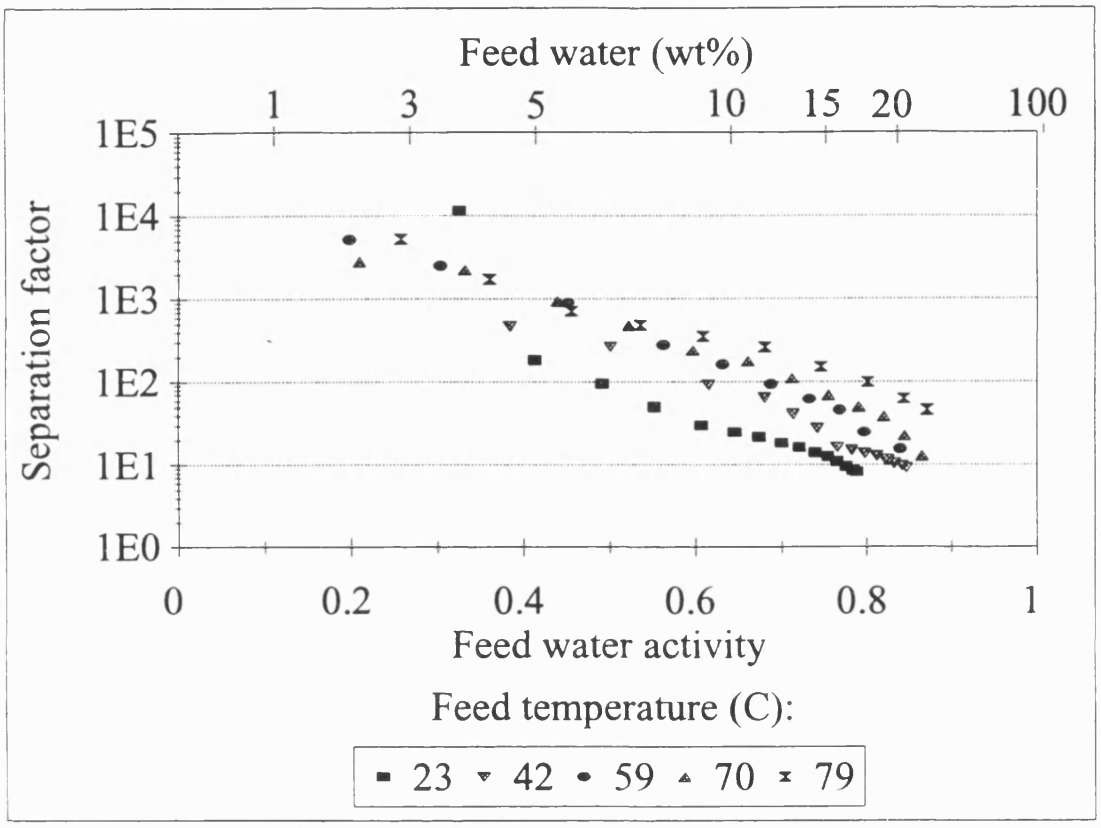

Figure 7.2 Effect of feed temperature upon separation factor

Using the model curves, flux results were found for four feed compositions (5, 10, 15 and 20wt% water) at each temperature. These were then divided by the activity driving force and M (Equation 7.6) to yield a set of overall mass transfer coefficients and an Arrhenius plot was constructed (Figure 7.3). The plot of ln k_{ov} against the reciprocal temperature were not linear above T = 59°C, therefore the pre-exponential factor and activation energy have been calculated from linear regression lines through only three points. The curvature in the Arrhenius plot will be discussed

later, after boundary layer effects have been accounted for. The parameters calculated are given in Table 7.3.

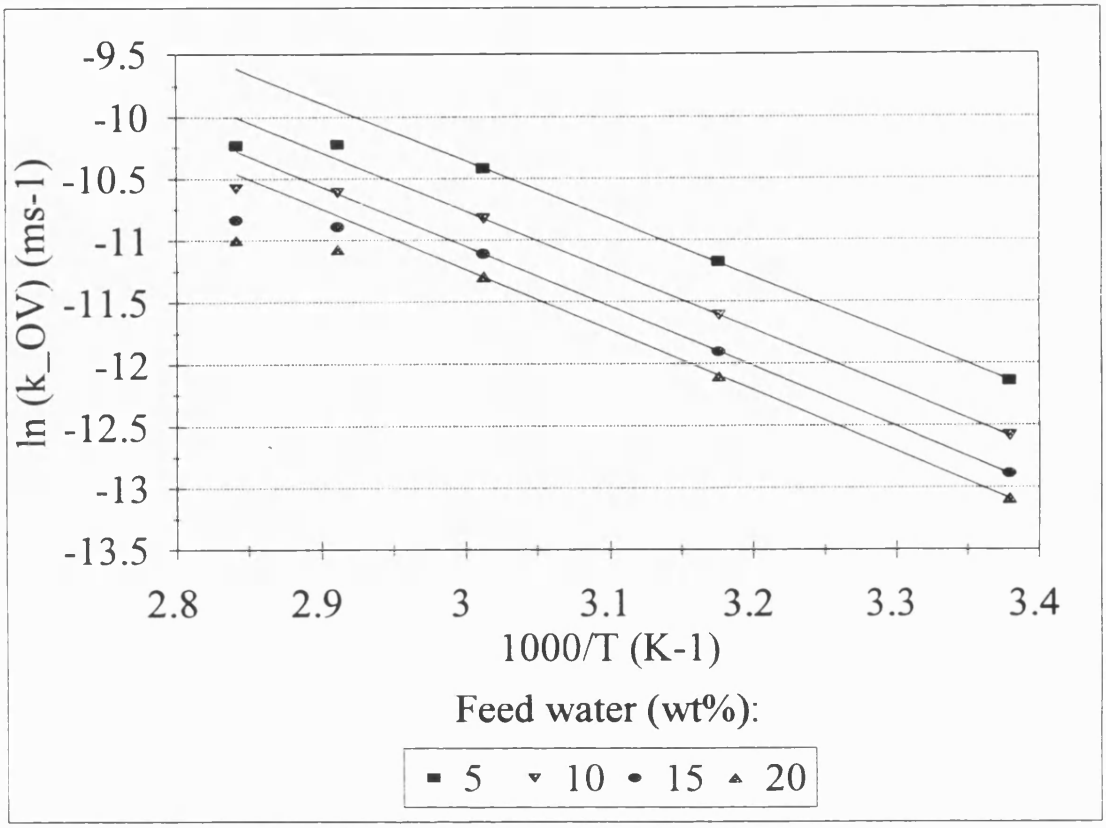

Figure 7.3 Arrhenius plot, from water permeation data for the complete system

Feed water (wt%)	5	10	15	20
E_A (kJmol^{-1})	39.1	40.0	40.4	40.7
k_{0v}^* (ms^{-1})	42.8	39.1	33.9	31.7

Table 7.3 Apparent activation energies and pre-exponential factors, calculated using the overall mass transfer coefficient

The activation energies found are within the range of those found by other workers (Table 7.1) and are in the mid-range of those found by Ping *et al.* (1990) for water permeation through a grafted polyacrylic acid membrane modified with counter ions. E_A seems to increase marginally with the concentration of water in the feed. This contrasts with the findings of Ping's study, where the activation energy for water permeation decreases with an increasing proportion of water in the feed until at 30% feed water the activation energy was negligible. Water interacts well with the polyacrylate membrane and the greater degree of swelling and plasticization occurring as the feed water content increased might be expected to lower the activation energy. This is obviously not the case, therefore it may be possible that the result of interaction effect between water molecules increases as the proportion of water increases. Although water molecules will hydrogen bond with ethanol molecules, hydrogen bond formation between water molecules is particularly favourable. The pre-exponential factor decreases with increasing water in the feed.

Next, the mass transfer through the boundary layer was examined. Equation 7.10 gives a correlation between the boundary layer mass transfer coefficient, k_{BL}, mass diffusivity, D_{BL}, and kinematic viscosity, ν. The temperature dependence of these last two parameters was taken into account. The temperature dependence of the kinematic viscosity has been found by experiment for a feed composition of 10wt% water and the concentration dependence of this parameter is assumed to be negligible. A value of D_{BL} at 70°C, given by Colman and Naylor (1991) has been used. The temperature and concentration dependence of D_{BL} has been calculated from the correlation (Perry and Green, 1984):

$$\frac{D_{BL}\mu}{T} = Constant \qquad (7.11)$$

Since $\mu = \nu\rho$, knowing the density, ρ, and the temperature dependence of both these parameters being known, the temperature and concentration dependence of the mass diffusivity was calculated. Using the values of the boundary layer mass transfer resistance at 70°C (Table 5.10), a set of R_{BL} values (R_{BL} being the inverse of the mass transfer coefficients multiplied by factor F) at other temperatures were calculated using:

$$(R_{BL})_T = (R_{BL})_{70} \left(\frac{\nu_T}{\nu_{70}}\right)^{0.42} \left(\frac{D_T}{D_{70}}\right)^{-0.66} \qquad (7.12)$$

where T is the temperature under investigation and 70°C is the reference temperature. The boundary layer resistances calculated are given in Table 7.4.

Feed water (wt%)	5	10	15	20
Feed temperature (°C)	**R_{BL} (smm^{-1})**			
23	73.7	69.9	66.2	62.7
42	40.8	38.7	36.7	34.8
59	25.6	24.3	23.1	21.9
70	18.9	17.9	17.1	16.2
79	15.8	15.0	14.3	13.6

Table 7.4 Calculated boundary layer resistance values for different feed temperatures

Obviously, the boundary layer resistance decreases as the temperature increases. However, the total resistance to mass transfer also decreases with temperature and it is interesting to note that the significance of the boundary layer resistance appears to vary greatly with this parameter (Figure 7.4). It should be remembered that R_{BL} is a calculated value, whilst R_{TOTAL} is derived directly from experimental measurements.

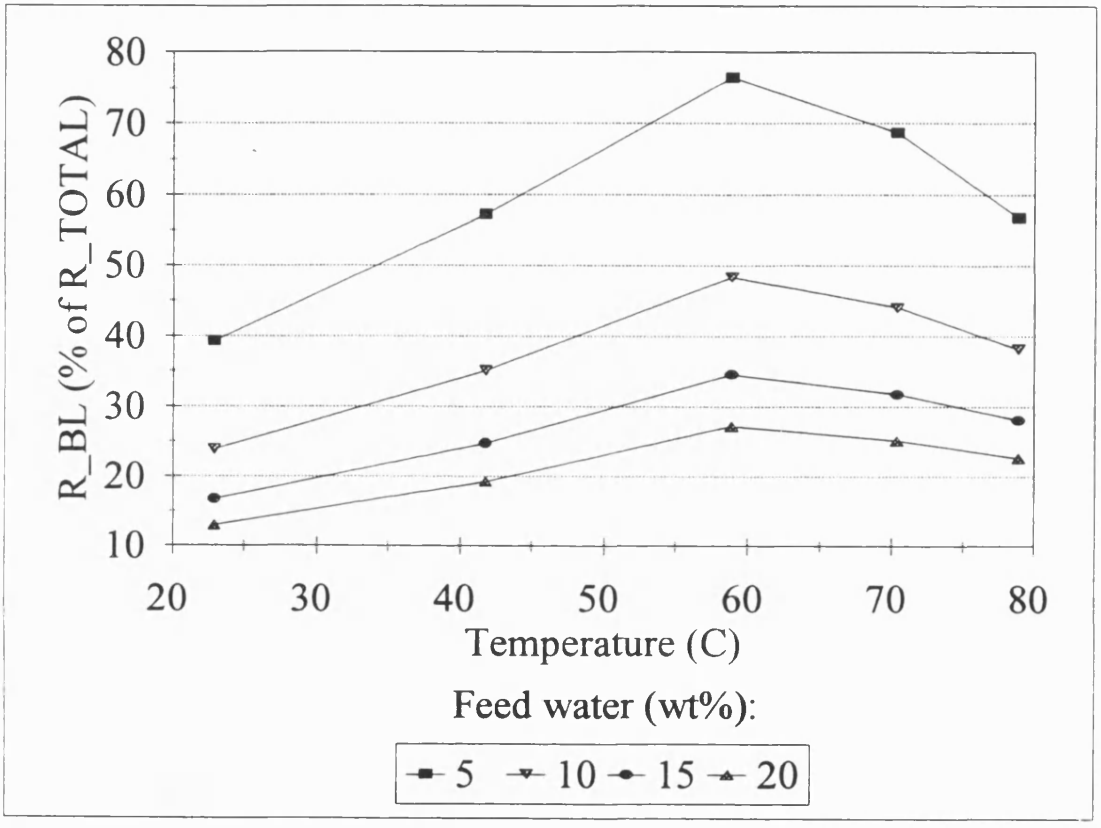

Figure 7.4 Significance of the boundary layer resistance as a percentage of the total mass transfer resistance

The contribution of the boundary layer to mass transfer resistance appears to increase greatly between 20°C and 60°C, where it reaches a maximum, then decreases at higher temperatures. The results indicate that transport through the boundary layer limits mass transfer when high temperatures are used, but as the feed

temperature is reduced, this resistance, although still a factor, becomes less significant and the membrane dominates the mass transfer process. It would be interesting to investigate the significance of the boundary layer at temperatures above 80°C. Changing the feed temperature has a similar effect on the significance of the boundary layer as changing the feed composition does.

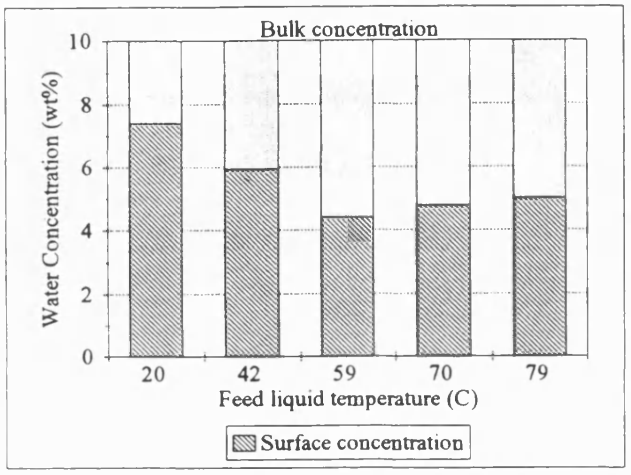

Figure 7.5 Water concentration at the membrane surface during pervaporation. Stirrer speed = 1000rpm Bulk concentration = 10wt% water

The influence of the liquid boundary layer is vividly illustrated by again calculating the water concentration at the membrane surface, as detailed in Chapter 4 (Table 4.6). Figure 7.5 illustrates the concentration at the membrane surface for a 10g CsPA membrane, supported by PVDF, during pervaporation at various temperatures. The driving force for mass transport across the membrane is, in all cases, significantly reduced.

Now, by subtracting out the boundary layer resistance from the total resistance, the *intrinsic* membrane resistance, i.e. that of the active layer plus support, can be found. A second Arrhenius plot (Figure 7.6) can be constructed using the new mass transfer coefficients calculated from the reduced driving forces, and a new activation energy calculated: E_I, the intrinsic activation energy:

$$J = k_m M(a_m - a_p) \qquad (7.13)$$

where k_m is the mass transfer coefficient for the composite membrane and a_m is the activity at the feed-side surface of the membrane. Also:

$$k_m = k_m^* \exp\left(\frac{-E_I}{RT}\right) \tag{7.14}$$

where E_I is the intrinsic activation energy.

Again, only the values for the lower three temperatures were used and the resulting values of E_I and k_m^* are shown in Table 7.4.

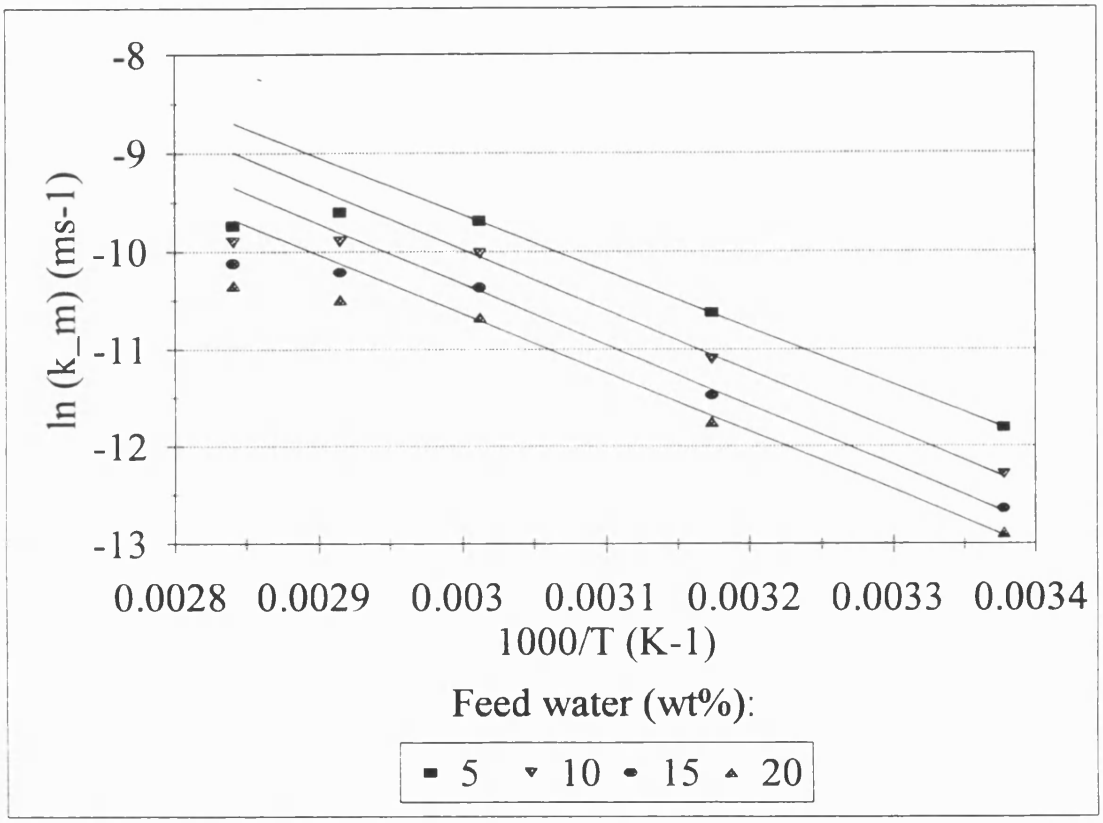

Figure 7.6 Arrhenius plot, for mass transfer across the composite membrane only

Feed water (wt%)	5	10	15	20
E_I (kJmol^{-1})	48.2	51.5	51.4	50.1
k_m^* (ms^{-1})	5.51	126	476	602

Table 7.5 Intrinsic activation energy and pre-exponential factor values

The calculated intrinsic activation energy values were higher than the previously calculated apparent activation energies, by approximately 25%. This indicates that the performance of the composite membrane is more dependent upon temperature than that of the system. Changes in viscosity, diffusivity and density of the feed mixture, and hence the significance of R_{BL}, retard the increase in flux achieved by increasing the temperature up to 59°C. Also, there is no trend of activation energy with feed water. A comparison of the apparent and intrinsic activation energies is illustrated in Figure 7.7.

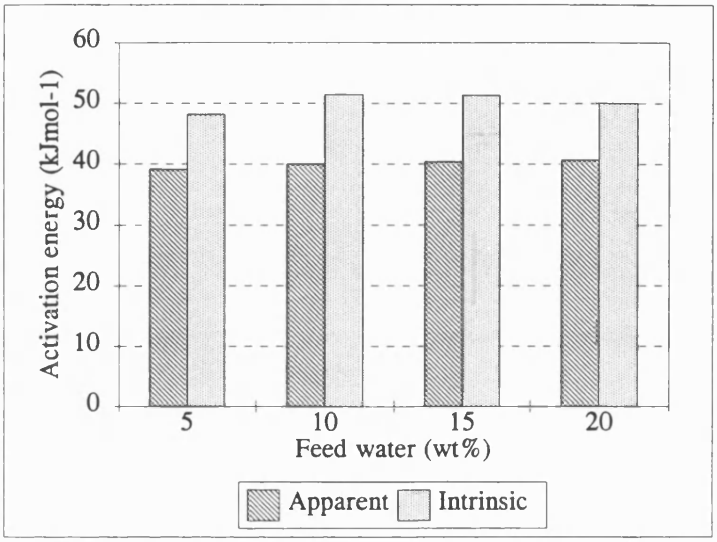

Figure 7.7 Comparison of apparent and intrinsic activation energies calculated

Once again, a curvature is observed in the Arrhenius plot. This is a puzzle but may be due to a change in either the heat of sorption or a change in the diffusivity of the active layer at higher temperatures. Furthermore, it is unclear why

the pre-exponential factors, k_{ov}^* and k_m^*, should hold such different numerical values and what this signifies.

7.4 CONCLUSIONS

Flux increased notably with feed temperature and selectivity also increased. An apparent activation energy can be calculated by constructing an Arrhenius plot. An average value of 40kJmol^{-1} was found for temperatures of 23 to 59°C. Above this value, non-linearity of the Arrhenius plot was observed.

Using a calculated boundary layer resistance value for a PVDF-supported membrane operated at 70°C and 1000rpm (from Chapter 5), the values of boundary layer resistance were calculated for the same membrane and stirring speed but at different temperatures. The percentage of the overall driving force that the boundary layer consumed was found to increase with increasing feed temperature up to a maximum at 60°C and then decreased slightly. Boundary layer effects were seen to be more important at higher temperatures.

Intrinsic activation energies were calculated utilising the flux and the calculated concentration driving force across the composite membrane only. These values were found to be higher than the apparent activation energies by around 25%, the average intrinsic activation energy being 50.3kJmol^{-1}.

Much of the reported analysis of feed temperature effects in pervaporation has used a classical approach, utilising flux or permeability with a concentration driving force. Boundary layer effects and the effect of temperature upon driving force are not usually considered. The analysis contained within this chapter has allowed for the former, although not the latter; an activity driving force has been used. A recent suggestion is that a vapour pressure driving force should be used in order to take

account of the effect of temperature upon the driving force and further work should include this alternative analysis.

A curvature was found in the Arrhenius plot (Figure 7.6) and no clear explanation for this is evident. To investigate this phenomenon, work with various pressure driving forces over a range of temperatures is suggested. Also, temperature polarisation has not been considered within this analysis and as it may influence the performance at high fluxes it is another factor worthy of investigation.

CHAPTER 8

CONCLUSIONS AND RECOMMENDATIONS FOR FURTHER WORK

8.1 CONCLUSIONS

BP Research developed a Caesium polyacrylate membrane for dewatering purposes and a number of its properties with regard to the removal of water from 2-propanol, as well as the effect of process parameters have been investigated. Several conclusions are evident from this work:

a) The water flux-bulk water concentration relationship can be modelled by an activity-based exponential expression:

$$J = Ae^{Ba}a \tag{8.1}$$

where a is the water activity in the feed liquid and A and B are semi-empirical parameters.

b) Active layer preparation conditions (drying temperature and atmosphere) have little effect on flux but may affect the separation factor. The most favourable conditions are those which allow the polymer solution to dry slowly, i.e. low temperature and/or a humid atmosphere.

c) There is little difference in the performance of membranes composed of polymer solutions of pH 8.5 or above. A solution pH of 8.5 is therefore recommended as casting solution viscosity, and therefore coating properties, decrease above this value. Below pH 8.5 the polymer is less neutralised and a lower flux is found, although little experimental evidence of this fact is contained within this work.

c) The molecular weight of polyacrylic acid used was 250 000 for most of the experiments performed. The use of a higher molecular weight polymer may be advantageous because flux attained is unaffected by polymer molecular weight, provided equivalent membrane thicknesses are used. A higher molecular weight membrane can withstand higher concentrations of water in the feed and very thin active layers may be produced without loss of selectivity. Lower molecular weight polyacrylic acid is not recommended for use as an uncrosslinked membrane because the shorter chains may migrate into solution.

d) Scanning electron microscopy and a pycnometric method can both be used to measure selective layer thickness. It is possible that the first technique may be used to investigate membrane swelling phenomena.

e) For Caesium polyacrylate membranes composed of 250 000 molecular weight polymer and a pH of 8.5, supported on polysulfone, a critical membrane thickness exists between 7 and 14μm. Below this thickness, there is a loss of selectivity, whilst above it a constant separation factor is observed.

f) A resistances-in-series model may be used to decouple resistances to mass transport. Variation of active layer thickness and stirring speed experiments can be used. Plots of overall mass transfer resistance against either membrane thickness or the inverse of radial velocity raised to the power 0.75 may be constructed to evaluate individual resistances.

g) The predictions of Fick's law (flux is proportional to reciprocal thickness) are not obeyed for the test system used. Concentration polarisation effects are significant and fully account for these deviations.

h) Membrane permeability increases with increasing feed water concentration and it is predicted that membrane diffusivity is not independent of concentration, due to the increased swelling and plasticization, represented by parameter B in Equation 8.1, of the polymer layer when in contact with water.

i) The liquid boundary layer is very significant within the system, contributing between 5% and 83% of the overall resistance, depending upon stirrer speed, feed concentration, active layer thickness, support layer and temperature used. Little variation in the significance of the boundary layer, as a contributor to total resistance, exists with feed concentration. This contradicts the common belief that this resistance is only significant for systems where the permeating component is present in very low concentration.

j) The support layer used influences the flux and selectivity achieved. Choice of support material should be tailored to a particular application. With the uncross-linked membrane, a microfiltration membrane support layer is unsuitable because the polymer seeps into the pores. Asymmetric ultrafiltration membranes reduce the flux attained if the pore size is very small and the surface porosity low. Of the support materials tested, Gortex is the best across the feed composition range tested.

k) Both flux and selectivity increase with increasing feed temperature. Neither the overall mass transfer coefficient nor the mass transfer coefficient of the composite membrane alone (boundary layer effects accounted for) conform to an Arrhenius relationship over the complete range of temperatures tested, although an excellent relationship was found at temperatures below 60°C. Apparent (overall system) and intrinsic (membrane alone) activation energies

can be found. The intrinsic activation energy is quantifiably higher than the apparent activation energy, indicating that boundary layer effects must be accounted for in the calculation of this parameter.

The resistances-in-series model has proved a simple and effective way of extracting a lot of useful information about a system from several experiments. Although there are some numerical inconsistencies in the data, the overall trends cannot be disputed.

8.2 RECOMMENDATIONS FOR FURTHER WORK

1. Investigation into cross-linking agents and the successful use of such is essential to the future use of the polyacrylate membrane. Whilst the current uncrosslinked membrane has an extremely high flux and very good selectivity properties, its industrial use is limited by its instability to solutions containing high concentrations of water. Although a decrease in flux will probably be a penalty, cross-linking the membrane will make it more stable and less prone to failure.
2. The use of scanning electron microscopy for measurement of swelling phenomena is a technique which could be developed and refined. Also, Néel's microcell for studying the steady state profile of a penetrant during pervaporation could be investigated.
3. Boundary layer effects within this system have generated substantial flux decreases. Future studies may investigate the use of baffles and pulsatile flow as methods of decreasing such effects without incurring a dramatic increase in feed pumping costs.
4. A systematic study of the effects of support material is necessary. The effects of pore size and surface porosity need to be modelled.

5. Further work on the analysis of temperature effects is required to explain the deviation from linearity of the Arrhenius plots constructed. The use of a pressure, rather than a concentration driving force, should be considered, and also the possibilities of temperature polarisation within the system.

REFERENCES

Aptel, P., Cuny, J., Jozefonvicz, J., Morel, G., Néel, J. (1974). Liquid transport through membranes prepared by grafting of polar monomers onto Poly(tetrafluoroethylene) films. II. Some factors determining pervaporation rate and selectivity. J. Appl. Polym. Sci., 18, 351-364.

Bartels, C., Kablaoui, M., Reale, J. and Shah, V. (1992). Industrial considerations in technology development. Proc. 6th Int. Conf. Pervaporation Processes Chem. Ind. Ed.: R. Bakish, Bakish Mater. Corp., 544-553.

Bengston, G., Böddeker, K.W. (1988). Pervaporation of low volatiles from water. Proc. 3rd Int. Conf. Pervap. Processes Chem. Ind., France, Ed. R. Bakish, Bakish Mater. Corp., 439-448.

Binning, R.C., Lee, R.J. (1960). US Patents, 2,953,502, 2,923,751, 2,923,749.

Binning, R.C., Lee, R.J., Jennings, J.F. Martin, E.C. (1961). Separation of liquid mixture by permeation. Ind. Eng. Chem., 53(1), 45-50.

Blume, I., Wijwams, J.G., Baker, R.W. (1990). The separation of dissolved organics from water by pervaporation. J. Membr. Sci., 49(3), 253-286.

Böddeker, K.W. (1990). Terminology in Pervaporation. J. Membr. Sci., 51(3), 259-272.

Bohlin Instruments CS User Manual (1990), U.K.

Brun, J.P., Bulvestre, G., Kegreis, A., Guillou, M. (1974). Hydrocarbons separation with polymer membranes. I. Butadiene-isobutene separation with nitrile rubber membranes. J. Appl. Polym. Sci., 18, 1663-1683.

Brüschke, H.E.A. (1988). State of art of pervaporation. Proc. 3rd Int. Conf. Pervap. Processes Chem. Ind., Ed. R. Bakish, Bakish Mater. Corp., 2-11.

Brüschke, H.E.A. (1991). State of art of pervaporation. Proc. 5th Int. Conf. Pervap. Processes Chem. Ind., Heidelberg, Germany, Ed. R. Bakish, Bakish Mater. Corp., 2-6.

Burslem, R.H. (1991). Membrane distillation and Osmotic distillation. A state of the art report. Report to a private company.

Burslem, R.H. (1993). Membrane distillation and pervaporation using a thermal gradient. In "Gas separation and pervaporation" Module of the Advanced Course on Membrane Technology, University of Bath.

Burslem, R.H., Naylor, T.deV., Field, R.W. (1992). The performance and stability of polyacrylate membranes. Proc. 6th Int. Conf. Pervap. Processes Chem. Ind., Ottawa, Ed. R. Bakish, Bakish Mater. Corp., 17-34.

Cabasso, I., Jagur-Grodzinski, J., Vofsi, D. (1974). A study of permeation of organic solvents through polymeric membranes based on polymeric alloys of polyphosphonates and acetyl cellulose. *II.* Separation of benzene, cyclohexene and cyclohexane. J. Appl. Polym. Sci., 18, 2137-2147.

Choi, H.S., Hino, T., Shibata, M., Negishi, Y., Ohya, H. (1992). The characteristics of a PAA-PSf composite membrane for the separation of water-ethanol mixtures through pervaporation. J. Membr. Sci., 72, 259-266.

Colman, D.A. and Mitchell, W.S. (1990). Enhanced mass transfer for membrane processes. IChemE Symp. Ser., 118, 119-134.

Colman, D.A. and Naylor, T.deV. (1991). The influence of operating variables on flux and module design in a high performance pervaporation system. Proc. 5th Int. Conf. Pervap. Processes Chem. Ind., Heidelberg, Germany, Ed. R.Bakish, Bakish Mater. Corp., 143-161.

Colman, D.A., Naylor, T.deV. and Pearce, G.K. (1989a). Alcohol dehydration by pervaporation. Food Sci. Tech. Today, 3(3), 186-189.

Colman, D.A., Naylor, T.deV. and Pearce, G.K. (1990). Alcohol dehydration by pervaporation. From "The membrane alternative, Energy implications for industry" Ed. J.A.Howell, Watt Committee on Energy, Report No. 21, Elsevier Applied Science, 99-104.

Colman, D.A., Naylor, T.deV., Pearce, G.K. and Whitby, R.D. (1989b). Applications of membrane pervaporation to the dehydrations of alcohols in chemicals and pharmaceutical processing. Proc. Membr. Sep. Processes Course, Brighton, U.K.

Côté, P. and Lipski, C. (1988). Mass transfer limitations in pervaporation for water and wastewater treatment. Proc. 3rd Int. Conf. Pervap. Processes Chem. Ind., France. Ed. R.Bakish, Bakish Mater. Corp., 449-462.

Drioli, E., Yonglie, W. and Calabro, V. (1987). Membrane distillation in the treatment of aqueous solutions. J. Membr. Sci., 33, 277-284.

Duggel, A., Thompson, E.V. (1986). Dependence of diffusive permeation rates on upstream and downstream pressures. *VI.* Experimental results for the water-ethanol system. J. Membr. Sci., 27, 13-30.

Field, R.W. and Burslem, R.H. (1992). The effect of concentration polarisation upon the performance of pervaporation membranes. Proc. 6th Int. Conf. Pervap. Processes Chem. Ind., Ottawa, Ed. R.Bakish, Bakish Mater. Corp. 275-289.

Gekas, V. and Hallström, B. (1987). Mass transfer in the membrane concentration polarization layer under turbulent cross-flow. J. Membr, Sci., 30, 153-170.

Gmehling, J., Onken, U. (1977). Vapour-liquid equilibrium data collection, Aqueous-organic systems. Chemistry Data Series, Vol. 1, Part 1. Dechema, Germany, 320-

327.

Gooding, C., Hickey, P., Dettenberg, P. and Cobb, J. (1992). Mass transfer and permeate pressure effects in the pervaporation of VOCs from water. Proc. 6th Int. Conf. Pervap. Processes Chem. Ind., Canada. Ed. R.Bakish, Bakish Mater. Corp., 80-89.

Greenlaw, F.W., Prince, W.D., Shelden, R.A., Thompson, E.V. (1977). Dependence of diffusive permeation rates on upstream and downstream pressures. *I.* Single component permeate. J. Membr. Sci., 2, 141-151.

Greenlaw, F.W., Shelden, R.A., Thompson, E.V. (1978). Dependence of diffusive permeation rates on upstream and downstream pressures. *II.* Two component permeant. J. Membr. Sci., 2, 233-348.

Hickey, P.J. and Gooding, C.H. (1994). Mass transfer in spiral wound pervaporation modules. J. Membr. Sci., 92(1), 59-74.

Huang, R.Y.M., Jarvis, N.R. (1970). Separation of liquid mixtures by using polymer membranes. *II.* Permeation of aqueous alcohol solutions through cellophane and poly(vinyl alcohol). J. Appl. Polym. Sci., 14, 2341-2356.

Johnson, R.A., Valks, R.H., Lefebvre, M.S. (1989). Osmotic distillation - a low temperature concentration technique. Australian J. Biotech., 3(3) (July), 206-217.

Kahlenburg. (1906). J. Phys. Chem., 10, 141.

Karlsson, Hans O.E. and Trägårdh, Gun. (1992). Feed flow effects on pervaporation of a multi-component aroma model. Proc. 6th Int. Conf. Pervap. Processes Chem. Ind., Ed.: R.Bakish, Bakish Mater. Corp., 35-45.

Kennedy, T.J., Merson, R.L., McCoy, B.J. (1974). Improving permeation flux by pulsed reverse osmosis. Chem. Eng. Sci., 29, 1927-1931.

Kim, S.N., Kammermeyer, K. (1970). Actual concentration profiles in membrane permeation. Sep. Sci., 5(6), 679-697.

Koops, G.H. (1992). Dehydration of acetic acid by pervaporation; material science aspects. Thesis, University of Twente.

Knight, F.K., Duggel, A., Shelden, R.A., Thompson, E.V. (1986). Dependence of diffusive permeation rates on upstream and downstream pressures. *V.* Experimental results for the hexane/heptane (ideal) and toluene/ethanol (non-ideal) systems. J. Membr. Sci., 26, 31-50.

Lefebvre, M.S., Johnson, R.A., Yip, V. (1987). Theoretical and practical aspects of osmotic distillation. Proc. Int. Congress Membr. Processes, Tokyo, 55-56.

Li, W., Xue, P. and Cabasso, I. (1988). Pervaporation of alcohol-water mixtures through sufonated polyethylene hollow fibre ion-exchange membranes. Proc. 3rd Int. Conf. Pervap. Proc. Chem. Ind., France. Ed. R. Bakish, Bakish Mater. Corp., 222-223.

Loeb. S., Sourirajan, S. (1962). Adv. Chem. Ser., 38, 117.

Lonsdale, H.K. (1982). The growth of membrane technology. J. Membr. Sci., 10, 81-

Lonsdale, H.K. (1987). The evolution of ultrathin synthetic membranes. J. Membr. Sci., 33, 121-136, 1987.

Lonsdale, H.K., Merten, U., Riley, R.L. (1965). Transport properties of cellulose acetate osmotic membranes. J. Appl. Polym. Sci., 9, 1341-1362.

Mackley, M. (1987). Using oscillatory flow to improve performance. The Chem. Eng., Feb., 18-20.

Mason, E.A. (1991). From pig bladders and cracked jars to polysulfones: an

historical perspective on membrane transport. J. Membr. Sci., 60, 125-145.

Mettler. (1987). Intruction manual for the Mettler Karl Fischer Titrator, DL18.

Mulder, Marcel. (1991). Basic principles of membrane technology. Kluwer Academic Publishers.

Naylor, T.deV. (1992). BP internal report.

Naylor, T.deV. (1993). Pervaporation : Fundamentals and applications. IChemE Symposia on Membrane Processes, Swansea, June.

Naylor, T.deV. (1994). Private communication.

Naylor, T.deV., Zelaya, F., Bratton, G.J. (1989). The BP-Kalsep pervaporation system - membrane performance and properties. Proc. 4th Int. Conf. Pervap. Processes Chem. Ind., USA, Ed. R. Bakish, Bakish Mater. Corp., 428-454.

Néel, J. (1991). Introduction to pervaporation, In "Pervaporation membrane separation processes," Ed. R.Y.M.Huang, Elsevier, Chapter 1,

Néel, J. (1993). Fundamental aspects of pervaporation. Regional Course in Membrane Processes, Torún, Poland.

Néel, J., Kujawski, W., Nguyen, Q.T. and Ping, Z. (1988). Mechanism for pervaporation selectivity of ion-exchange membranes for the separation of water-ethanol mixtures. Proc. 3rd Int. Conf. Pervap. Processes Chem. Ind., Ed. R. Bakish, Bakish Mater. Corp., 21-36.

Néel, J., Nguyen, Q.T., Clément, R., Lin, D.J. (1986). Influence of downstream pressure on the pervaporation of water-THF mixtures through a regenerated cellulose membrane (Cuprophan). J. Membr. Sci., 27, 217-232.

Nguyen, Q.T. (1986). The influence of operating parameters on the performance of the pervaporation process. AIChE Symp. Ser., 82 (248 Ind. Membr. Processes), 1-

11.

Nguyen, Q.T. (1987). Modelling the influence of downstream pressure for highly selective pervaporation. J. Membr. Sci., 34, 165-183.

Nijhuis, H.H., Mulder, M.H.V. and Smolders, C.A. (1990). Resistances in series : Boundary layer effects. From "Removal of trace organics in water by pervaporation." Thesis, H.Nijhuis, University of Twente.

Nijhuis, H.H., Mulder, M.H.V., Smolders, C.A. (1991). Removal of trace organics from aqueous solutions. Effect of membrane thickness. J. Membr. Sci., 61, 99-111.

Okada, Tomoyuki and Matsuura, Takeshi. (1991). A new transport model for pervaporation. J. Membr. Sci., 59, 133-150.

Okada, Tomoyuki and Matsuura, Takeshi. (1992). Theoretical and experimental study of pervaporation on the basis of pore flow mechanism. Proc. 6th Int. Conf. Pervaporation Processes Chem. Ind., Ed.: R.Bakish, Bakish Mater. Corp., 137-152.

Peinemann, K.-V., Ohlrogge, K. and Wind, J. (1994). Industrial applications of membranes to control VOC emissions. In "Characterisation and control of odours and volatile organic components in the process industries" Eds.: Vigneron, Hermia and Chaouli. Elsevier Science.

Perry, R.H. and Green, D. (Eds.) (1984). Perry's Chemical Engineers Handbook. Sixth Edition. McGraw-Hill. 3-258.

Ping, Z.H., Nguyen, Q.T., Clèment, R., Néel, J. (1990). Pervaporation of water-ethanol mixtures through a poly(acrylic acid) grafted polyethylene membrane. Influence of temperature and nature of counter-ions. J. Membr. Sci., 48, 297-308.

Poyen, S., Quemeneur, F., Bariou, B. (1987). Improvement of the permeate flux in ultrafiltration by turbulence promoters. Int. Chem. Eng., 27(3), 441-447.

Psaume, R., Aptel, Ph., Aurelle, Y., Mora, J.C. and Bersillon, J.L. (1988). Pervaporation: Importance of concentration polarisation in the extraction of trace organics from water. J. Membr. Sci., 36, 373-384.

Raghunath, B. and Hwang, S.T. (1992a). Effect of boundary layer mass transfer resistance in the pervaporation of dilute organics. J. Membr. Sci., 65, 147-161.

Raghunath, B. and Hwang, S.T. (1992b). General treatment of liquid-phase boundary layer in the pervaporation of dilute aqueous organics through tubular membranes. J. Membr. Sci., 75, 29-46.

Rautenbach, R., Albrecht, R. (1982). On the behaviour of asymmetric membranes in pervaporation. European Workshop on pervaporation, Nancy, Sept. 21-22.

Rautenbach, R., Albrecht, R. (1987). Pervaporation and gas permeation - fundamentals of process design. Int. Chem. Eng., 27(1), 10-24.

Rautenbach, R., Herion, C., Franke, M. (1988a). Dehydration of multi-component organic systems by a reverse osmosis-pervaporation hybrid process module - process design and economics. Desalination, 70, 445-453.

Rautenbach, R., Herion, C., Franke, M., Abdul-Fattah, A. Asfour, Bemquerer-costa, A., Bo, E. (1988b). Investigations of mass transport in asymmetric pervaporation membranes. J. Membr. Sci., 36, 445-462.

Rautenbach, R., Klatt, S. and Vier, J. (1992). State of the art of pervaporation. 10 years of industrial PV. Proc. 6th Int. Conf. Pervap. Processes Chem. Ind., Ed.: R. Bakish, Bakish Mater. Corp., 2-15.

Reid, R.C., Prausnitz, J.M. and Sherwood, T.K. (1977). The Properties of Gases and Liquids. 3rd Ed. McGraw Hill. Chapter 8, 288-316.

Sada, E. and Morisue, T. (1975). J. Chem. Eng. Jap., 8, 191.

Sander, U. and Janssen, H. (1991). Industrial application of vapour permeation. J. Membr. Sci., 61, 113-129.

Schwob, Y. (1949). On the semi-permeability of water through regenerated cellulose membranes. Thesis, Toulouse, France.

Shelden, R.A. and Thompson, E.V. (1978). Dependence of diffusive permeation rates on upstream and downstream pressures. *III.* Membrane selectivity and implications for separation processes. J. Membr. Sci., 4, 115-127.

Shelden, R.A. and Thompson, E.V. (1984). Dependence of diffusive permeation rates and selectivities on upstream and downstream pressures. *IV.* Computer simulation of non-ideal systems. J. Membr. Sci., 19, 39-49.

Smallwood, I. (1993). Solvent recovery handbook. Edward Arnold, G.B.

Smith, K.A., Colton, C.K., Merrill, E.W. and Evans, L.B. (1961). Convective transport in a batch dialyzer: determination of true membrane permeability from a single measurement. Chem. Eng. Prog. Symp. Ser., No. 84, Vol. 64, 45-58.

Smith, J.M. and van Ness, H.C. (1975). Introduction to chemical engineering thermodynamics, 3rd Ed., McGraw Hill, Chapters 7 and 8, 213-375.

Spitzen, J.W.F. (1988). Pervaporation membranes and modules for the dehydration of ethanol. Thesis, University of Twente.

Spitzen, J.W.F., Koops, G.H., Mulder, M.H.V., Smolders, C.A. (1988). The influence of membrane thickness on pervaporation performance. Proc. 3rd Int. Conf. Pervap. Processes Chem. Ind., France. Ed. R. Bakish. Bakish Mater. Corp., 252-256.

Strathmann, H. (1990a). Fundamentals of membrane separation processes. NATO Conference, The Azores.

Strathmann, H. (1990b). Pervaporation in Biotechnology. NATO Conference, The Azores.

Thompson Hughes, L.J. and Fordyce, D.B. (1956). Soprtion of water vapour by water-soluble polymers: Kinetic, equilibrium, and glass temperature data. J. Polym. Sci., XII, 509-526.

Wenzlaff, A., Böddeker, K.W., Hattenbach, K. (1985). Pervaporation of water-ethanol through ion exchange membrane. J. Membr. Sci., 22, 333-344.

Wijmans and Baker. (1993). A simple, predictive treatment of the permeation process in pervaporation. J. Membr. Sci., 79, 101-113.

Wu, P. (1994). Study of the pervaporation process of water-isopropanol in caesium polyacrylate membranes. Internal report, School of Chemical Engineering, University of Bath.

Yamada, S. and Nakagawa, T. (1991). Effect of metal ion on separation of alcohol-water mixture with dithiocarbamated poly(vinyl chloride) membrane. Proc. 4th Int. Conf. Pervap. Processes Chem. Ind., Ed. R. Bakish, Bakish Mater. Corp., 98-108.

APPENDIX A

MEASUREMENT OF POLYMER SOLUTION VISCOSITY

The success of the casting of pervaporation membranes was dependent upon the viscosity of the polyacrylate casting solution which in turn was dependent upon the molecular weight of the polymer used and the solution concentration. Since almost all membranes used were made from polymer of molecular weight 250 000, only this polymer is considered here. Considering the concentration, if the solution is too viscous, a greater quantity of it must be used to coat the support material which would result in a thicker membrane, unless the casting solution is spread manually, which could result in a membrane of uneven thickness. If the solution is not viscous enough, the substrate is unevenly wetted and on drying, the film breaks up. A concentration of 0.5wt% for the 250 000 molecular weight polymer was found to produce a solution of adequate viscosity but a viscosity change with pH was noted and investigated.

Principle of Rheological Measurement

If a sample of fluid is sheared between two rigid boundaries under an applied shear stress, σ, the shear rate, $\dot{\gamma}$, may be defined as the rate of change of velocity in the y-direction. The instantaneous viscosity of a fluid can then be calculated from:

$$\eta = \sigma / \dot{\gamma} \qquad (A.1)$$

If the fluid is Newtonian, the viscosity is independent of shear rate. The rheological properties of a liquid may be represented by curves of shear stress against shear rate and viscosity. An example is shown in Figure A.1, where the dashed lines represent the behaviour of a Newtonian liquid.

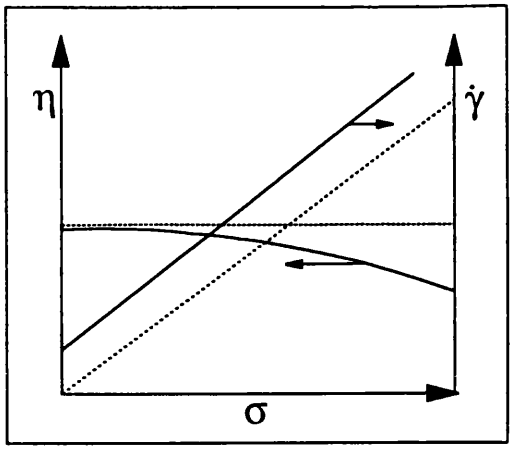

Figure A.1 Graph of shear stress against shear rate and viscosity for a pseudoplastic liquid with an apparent yield stress (Bohlin Instruments CS User Manual, 1990)

Experimental

A Bohlin controlled stress rheometer (Bohlin Instruments, UK) was used. The correct amount of polymer solution was located between two parallel stainless steel plates and the test system was kept at constant temperature. The rheometer imposed a known torque, T, on the measuring system shaft and detected the rate of change of angular deflection, $\dot{\theta}$. The torque and angular deflection are related to the shear stress and rate by measuring system constants.

The conditions used for the stress viscometry test were:

Temperature	25°C
Boost	25Pa, 10 seconds
Sweep	Up
Strain delay time	2 seconds
Gap	0.2mm
Integration time	15 seconds

Three samples of 0.5wt% polyacrylic acid (MW 250 000) solution were used. These were neutralised to different levels of pH, up to pH 13.2, to examine the effect of pH on viscosity. Each sample was tested at different shear stress levels, ranging from 1Pa to 85Pa.

Results and Discussion

A typical viscosity/shear rate against shear stress curve for caesium polyacrylate solution is given in Figure A.2. Caesium polyacrylate was found to be

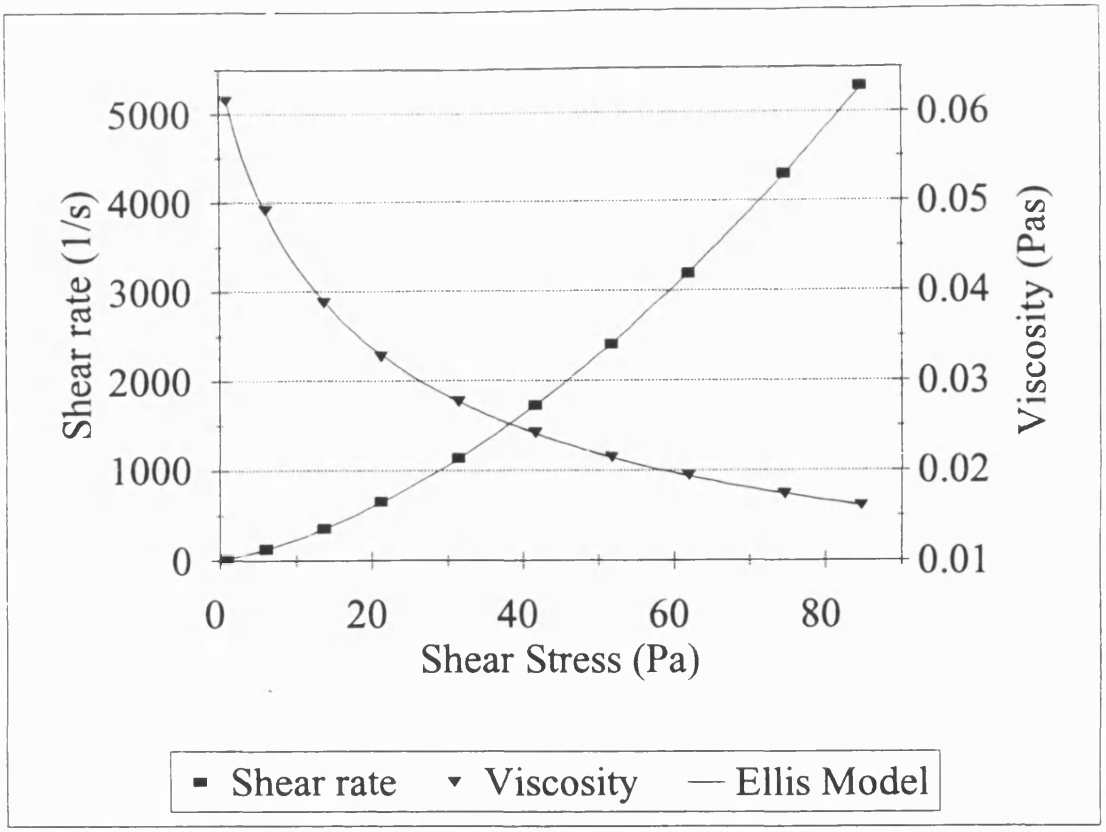

Figure A.2 Rheological properties of caesium polyacrylate, MW 250 000, 0.5wt%, pH 8.5, 25°C

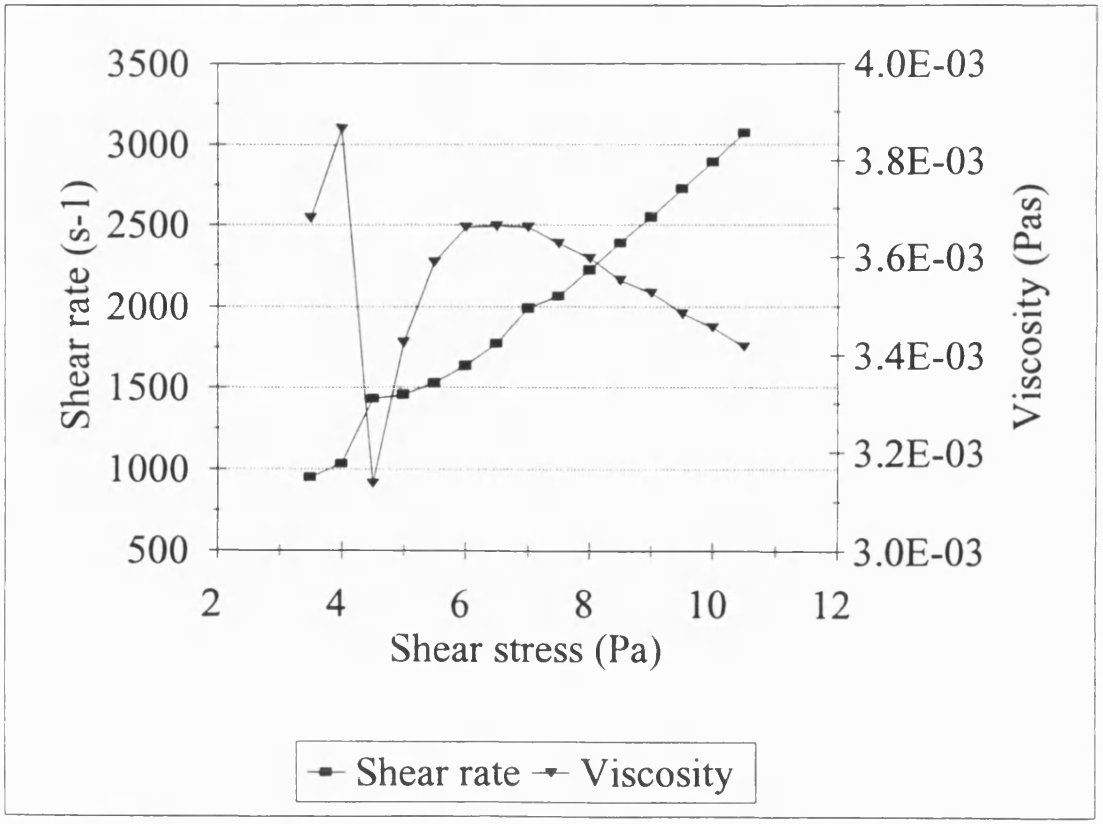

Figure A.3 Rheological properties of polyacrylic acid, MW 250 000, 0.5wt%, pH 2, 25°C

a shear thinning liquid with no yield stress. The experimental data fits the Ellis Model, an empirical model with three adjustable parameters, often used to describethe behaviour of polymers. For caesium polyacrylate:

$$\dot{\gamma} = 14.96\sigma + 1.275\sigma^{1.814} \qquad (A.2)$$

The behaviour of polyacrylic acid itself was apparently more complex (Figure A.3). Its viscosity was about three times that of water and it was much less viscous than any of the polyacrylate samples. Its low viscosity may imply that the polymer has a more linear than branched structure. The viscosity of polyacrylic acid solution appeared to vary widely with the applied shear stress between 3 and 6Pa. The only explanation offered for this peculiar and reproducible behaviour is that it is a function of the particular measuring system which is known to be inaccurate with low viscosity liquids. Above 6Pa, the acid exhibited shear thinning behaviour. Overall, the viscosity did not change significantly with the applied shear stress, falling within the range $3.55\times10^{-3}\pm0.15\times10^{-3}$Pas.

Figure A.4 demonstrates the variation of viscosity, at three different shear stress levels, with the degree of neutralisation of the polyacrylate solution. It can be seen that the viscosity went through a maxima at pH 8.7. The variation in viscosity for samples of different acid solution batches was $\pm6\%$. As the acid is neutralised, caesium atoms replace hydrogen in the polymer network. At low (acid) pH, the polymer chains are curled up due to intrachain hydrogen bonding and there is little interchain bonding. As the polymer acid groups are neutralised, up to pH 8.7, the chains extend and the amount of interchain hydrogen bonding increases, increasing the solution viscosity. Above pH 8.7, a shielding effect starts to occur and there are also fewer opportunities for hydrogen bonding as the number of carboxylic acid

groups decreases. Therefore, it is a combination of entanglement and interchain hydrogen bonding which is responsible for the viscosity maximum at pH 8.7.

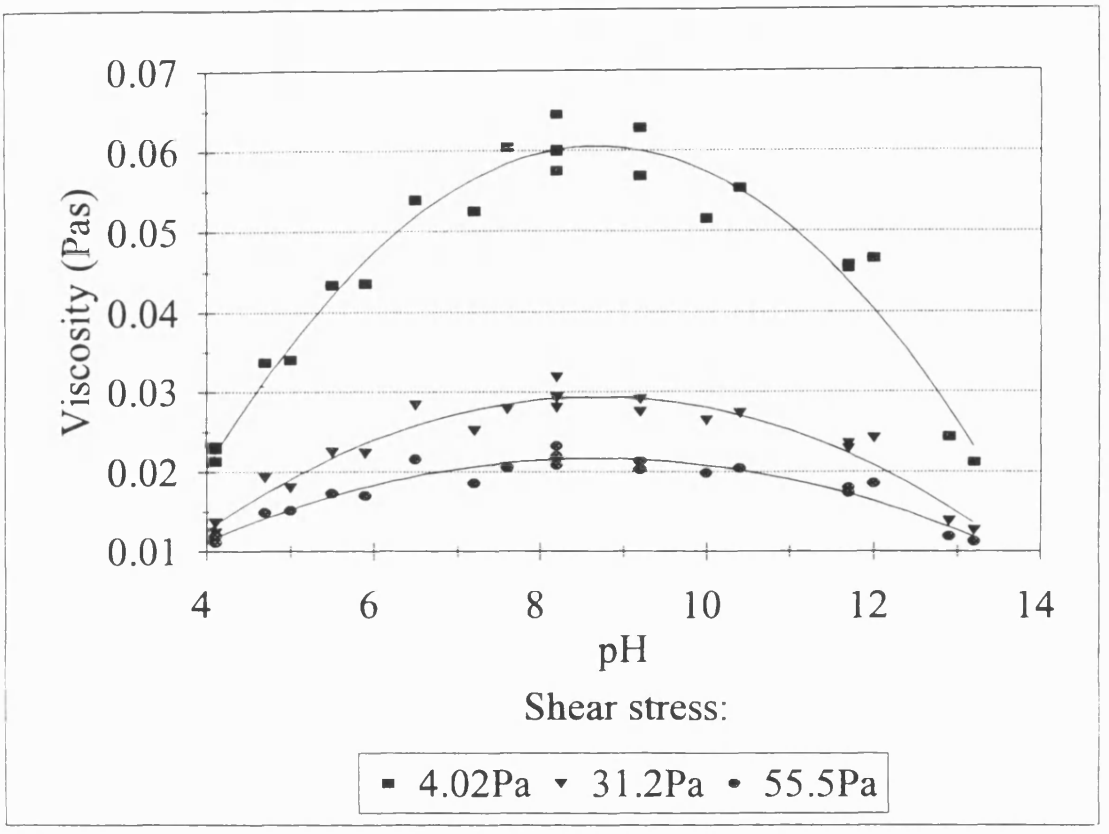

Figure A.4 Influence of degree of neutralisation on the viscosity of caesium polyacrylate solution, MW 250 000, 0.5wt%, 25°C

Conclusions

Caesium polyacrylate was found to be a shear thinning liquid whose viscosity varied with the degree of neutralisation, the maximum viscosity being at pH 8.7. This is advantageous for the production of CsPA membranes because the acidic polymer is 95% neutralised at pH 8.5 and, as revealed in Chapter 3, a high degree of neutralisation results in a high water flux.

APPENDIX B

METTLER KARL FISCHER TITRATOR FOR WATER DETERMINATION

Principle

The Karl Fischer titration is often used as the standard method of determining water content. Water is converted stoichiometrically in the presence of sulphur dioxide, methanol and a suitable base, by the addition of iodine.

$$H_2O + I_2 + SO_2 + CH_3OH + 3RN \rightarrow [RNH]SO_4CH_3 + 2[RNH]I$$

where RN = Base

Karl Fischer solvent will buffer weak acids and alkalis but stronger bases will require pre-treatment (Mettler, 1987).

Apparatus

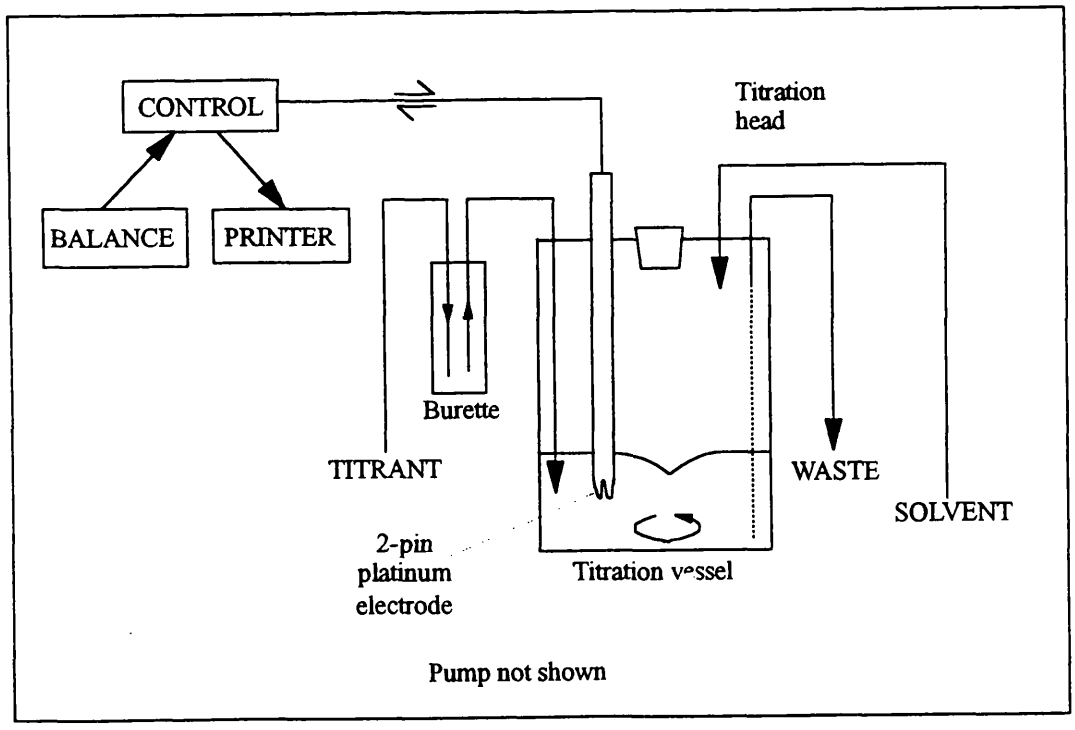

Figure B.1 Schematic diagram of Karl Fischer Apparatus

A Mettler Karl Fischer auto-titrator was used to determine the water content in weight per cent. It had a range of 10μg to 500mg water and a resolution of approximately 25μg water.

The glass titrant, waste and solvent bottles and the titration vessel were protected from atmospheric moisture by the attachment of drying cups containing molecular sieve particles. Plastic tubing between the titrant bottle and the titration vessel was double-walled. Standard plastic tubes were used for solvent dispensing and removal. The apparatus dispensed solvent and evacuated the hermetically sealed titration vessel automatically, when required, by means of a diaphragm pump. Titrant was dispensed via a 10ml interchangeable burette. The titration head contained a glass stopper which was removed for the introduction of the sample. Stirring was carried out by means of a built-in, variable speed magnetic stirrer.

Two-component pyridine-free Karl Fischer reagents (BDH) were used. The titrant was iodine in methanol, whilst the solvent was sulphur dioxide and base in methanol.

Titrant concentration was determined periodically using sodium tartrate dihydrate (BDH) (15.66% water) as a standard calibration sample. The background titrant consumption was also determined periodically to ensure that moisture leakage into the titration vessel was within the standard limit (25μg/min).

The connected balance (Mettler AE163) was used to automatically transfer the sample weight to the titrator. Results were automatically printed out by the connected printer (Mettler GA44).

Maintenance

The burette cylinder, piston, stopcock and tubes were cleaned every six

months with ethanol, at room temperature.

The diaphragm pump was subject to heavy stress by corrosive vapours. Molecular sieve material above each solvent bottle and above the titration vessel was changed frequently to minimise this problem and to minimise moisture absorption by the reagents. The molecular sieve was regenerated every 4 weeks by rinsing in distilled water, then drying in an oven at 180°C for longer than 24 hours.

Certain Karl Fischer reagents desensitise the electrode after prolonged use. To prevent this problem, the electrode was wiped with an acetone-soaked cloth at regular intervals.

Sample Preparation

Water in a 2-propanol/water mixture is freely available and therefore no sample preparation was necessary. The required sample weight was determined by aiming for a titrant consumption of 1-4ml. This corresponded to a sample size of 0.1-0.3g.

Method

A volume of Karl Fischer solvent, large enough to cover the pins of the electrode, was dispensed into the hermetically sealed beaker by pressing a button. A stirring speed was selected which stirred the solvent vigorously such that a well defined vortex was created. This stirrer speed was kept constant throughout subsequent titrations. A pre-titration, in which water present in the solvent is titrated out, was carried out.

The sample was weighed and then introduced to the titration vessel. Titrant was added to the titration vessel by the burette and detection was carried out by a two-pin platinum electrode. At the end of the titration the result was printed out by

the connected printer. The titration time was typically 1-2 minutes. Post-consumption was found to be negligible.

Several samples were analysed consecutively, until the solvent was consumed. The solvent capacity was 100mg water per 20ml solvent. If solvent capacity was over-stepped, a drifting titration endpoint was observed. The consumed solvent was evacuated from the sealed titration vessel at the press of a button. When the waste solvent bottle was full, waste was safely disposed of into a non-chlorinated solvents waste container.

Results

Results were given to 3 decimal places for a sample containing more than 10wt% water and to 4 decimal places for samples with less water than this. Analysis of a sample of 2-propanol containing 2% water yielded a standard deviation of 1.5% ($\pm$0.0358wt%) over 10 analyses. Analysis of a similar sample containing 17% water yielded a standard deviation of 0.7% ($\pm$0.1215wt%) over 10 analyses.

Safety

All Karl Fischer reagents are highly flammable solutions. Breathing in the fumes as well as ingesting such titrants is poisonous. Contact with skin should also be avoided.

APPENDIX C

GAS CHROMATOGRAPHY FOR PERMEATE ANALYSIS

The analysis of permeate samples was carried out using gas chromatography. The chromatograph used was an HP Series II, Model 5890 with auto injector (Model 7673) and integrator (Model 3396) installed.

Injection was on-column. A retention gap of about 3m in length was placed between the injector and the column. The column was a fused silica capillary-type with HP1 (cross-linked methyl cellulose gum) stationary phase. A flame ionisation detector was used and hence only IPA, not water, peaks were detected.

The conditions used were:

Injection temperature	103°C
Injection pressure	15.8psi at 100°C
Sample size	2μl
Carrier gas	Helium
Column temperature	100°C
Detector temperature	250°C
Run time	2.5mins

The external standard method was used. A series of standard solutions of known IPA concentration were analysed to produce a calibration graph and response factor, shown in Figure C.1.

During sample analysis, a known sample was analysed periodically to check for instrumental deficiencies. Ultra-high quality water was also passed through the column every 10 samples to check that the column was clean and there was no "bleed."

The standard deviation of the peak area was 1.0% over three injections.

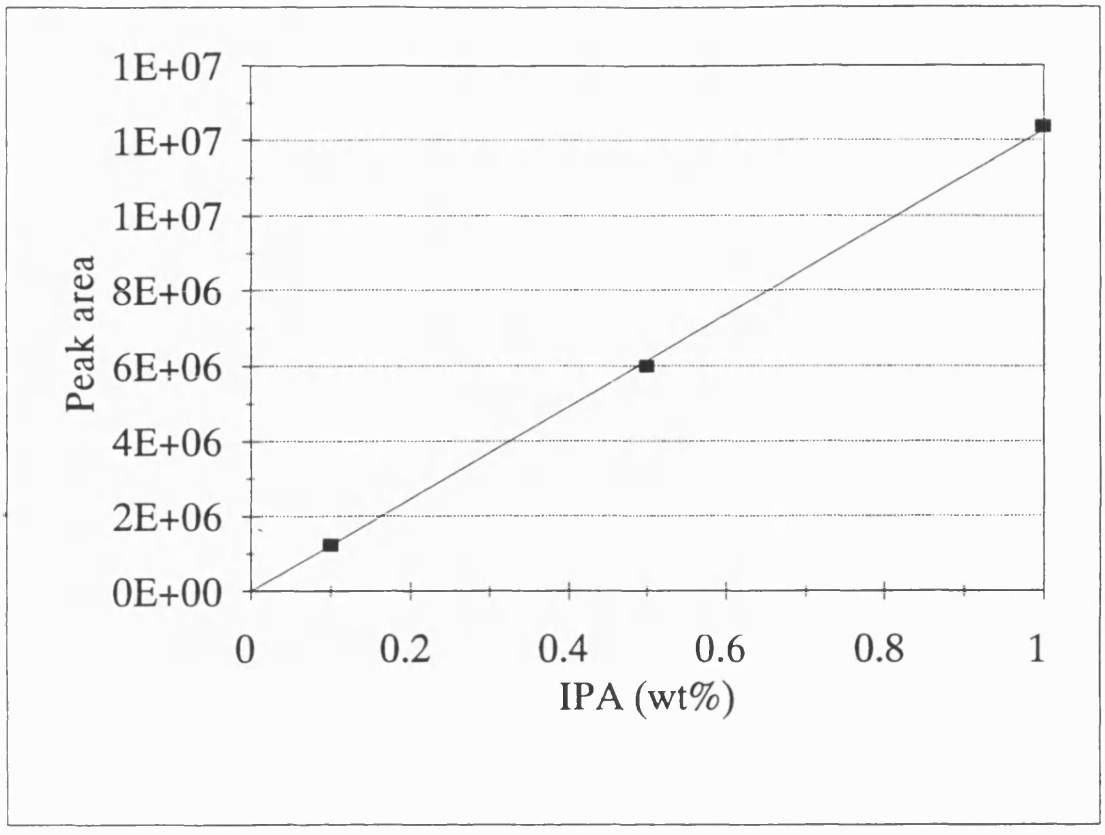

Figure C.1 Calibration graph for analysis of permeate samples Response factor = 1.228×10^7

APPENDIX D

ACTIVITY AND ACTIVITY COEFFICIENTS

The activity, a_i, of a liquid is a thermodynamic function used in place of concentration for non-ideal gases and liquids.

$$a_i = x_i \gamma_i \tag{D.1}$$

where γ_i is the activity coefficient and x_i is the mole fraction. A physical interpretation of the activity coefficient of a component in a solution is the ratio of its actual fugacity to the ideal-solution value (Smith and van Ness, 1975):

$$\gamma_i = \frac{a_i}{x_i} = \frac{f_i^L}{x f_i^0} \tag{D.2}$$

f_i^0 is the standard state fugacity which is the fugacity of component i at the temperature of the system and at some arbitrarily chosen pressure and composition. These values are chosen as a matter of convenience but are usually the system pressure and pure component. Activity and activity coefficient have no meaning unless f_i^0 is clearly stated. For a pure component, activity coefficients can be found from the determination of phase compositions at low to moderate pressures, where the equation

$$\gamma_i = \frac{y_i P}{x_i p_i^0} \tag{D.3}$$

is applicable. P is the total pressure. However, in a mixture, the activity coefficients of individual components are not independent of each other but are related by a differential equation.

Theoretically, for a binary mixture:

$$x_1\left(\frac{\delta \ln\gamma_1}{\delta x_1}\right)_{T,P} - x_2\left(\frac{\delta \ln\gamma_2}{\delta x_2}\right)_{T,P} \qquad (D.4)$$

This is the Gibbs-Duhem equation. It can be integrated to obtain thermodynamically consistent equations which relate γ_1 and γ_2 to x. There is no unique integrated form of the Gibbs-Duhem equation but each equation contains a few adjustable parameters which can be found from a limited amount of experimental data.

For practical work, the concept of excess Gibb's energy, G^E, can be utilised. That is the difference between the actual Gibb's energy and that which would be calculated for the same conditions of temperature and composition (excess Gibb's energy is only a weak function of pressure) by the equations for an ideal solution. All the activity coefficients for a system are related to this function:

$$\frac{G^E}{RT} - \Sigma(x_i \ln\gamma_i) \qquad (D.5)$$

For a binary solution:

$$g^E - RT(x_1 \ln\gamma_1 + x_2 \ln\gamma_2) \qquad (D.6)$$

Several expressions relating g^E (excess Gibb's energy per mole of mixture) to composition have been proposed and can be found in the literature (Reid *et al.*, 1977). These include Margules, van Laar, Wilson, NRTL and UNIQUAC. All models have a strong empirical influence and include adjustable parameters which, in theory, depend upon temperature. In practice, the number of adjustable parameters is typically either two or three. The larger the number of parameters, the better the representation of data but the larger the number of experimental values required. The value of each model is dependent upon the system it is applied to and the level of

accuracy required.

Simple mixtures where the components are similar in size and shape can be modelled adequately by the one component Margules model. For moderately non-ideal binary mixtures, such as 2-propanol/water, all equations for g^E containing two or more parameters give good results. Margules and van Laar are mathematically easier to handle than newer models such as NRTL and UNIQUAC. For strongly non-ideal mixtures, Wilson is the most useful model.

The van Laar equation was chosen to be the most appropriate for this work. It is based upon a power series in effective volume fraction. The van Laar equation is:

$$g^E = \frac{A_{12}x_1x_2}{x_1(A_{12}/A_{21}) + x_2} \qquad \text{(D.7)}$$

where A_{12} and A_{21} are adjustable parameters.

Applying the Gibbs-Duhem equation and differentiating:

$$\ln\gamma_1 = A_{12}\left(1 + \frac{A_{12}}{A_{21}}\frac{x_1}{x_2}\right)^{-2} \qquad \text{(D.8)}$$

$$\ln\gamma_2 = A_{21}\left(1 + \frac{A_{21}}{A_{12}}\frac{x_2}{x_1}\right)^{-2} \qquad \text{(D.9)}$$

The van Laar equations contain two adjustable parameters. If a set of experimental measurements provide a series of values for the g^E versus x_1 relation at constant temperature (or pressure), the best values of the two parameters can be found by numerical regression techniques based on a least mean square fit of the data. The goodness of the fit depends upon the suitability of the form of the equation. The parameters A_{12} and A_{21} are functions of temperature, but the dependence is not

specified. Values of A_{12} and A_{21} are available for various temperatures and pressures.

A number of sets of experimental equilibrium data were available for the 2-propanol/water system (Gmehling and Onken, 1977). The data was measured either at constant temperature or at constant pressure. For the system considered in this work, constant temperature data was preferable. The data gathered by Sada and Morisue (1975) was chosen for use as being the more consistent of the two sets available and covering the most appropriate temperature range. The van Laar parameters, A_{12} and A_{21}, were already calculated for the five temperatures used and this data was interpolated and extrapolated, as shown in Figure D.1, so that van Laar parameters could be found for the process temperatures of interest in this work. Rearranging equations D.8 and D.9, as given in Equations D.10 and D.11, then allowed the calculation of activity coefficients for both 2-propanol and water at various temperatures across the complete concentration range.

$$\gamma_1 = \exp\left(A_{12}\left(\frac{A_{21}x_2}{A_{12}x_1 + A_{21}x_2}\right)^2\right) \qquad \text{(D.10)}$$

$$\gamma_2 = \exp\left(A_{21}\left(\frac{A_{12}x_1}{A_{12}x_1 + A_{21}x_2}\right)^2\right) \qquad \text{(D.11)}$$

The variations with composition in both water and IPA activity coefficients and each component's activity in the mixture are given in Figures D.2 and D.3. It can be seen that for both components, activity is higher than concentration across the entire composition range. Also, as the proportion of water in the mixture decreases, its activity coefficient increases, partially compensating for the loss in pervaporative driving force from a decrease in concentration.

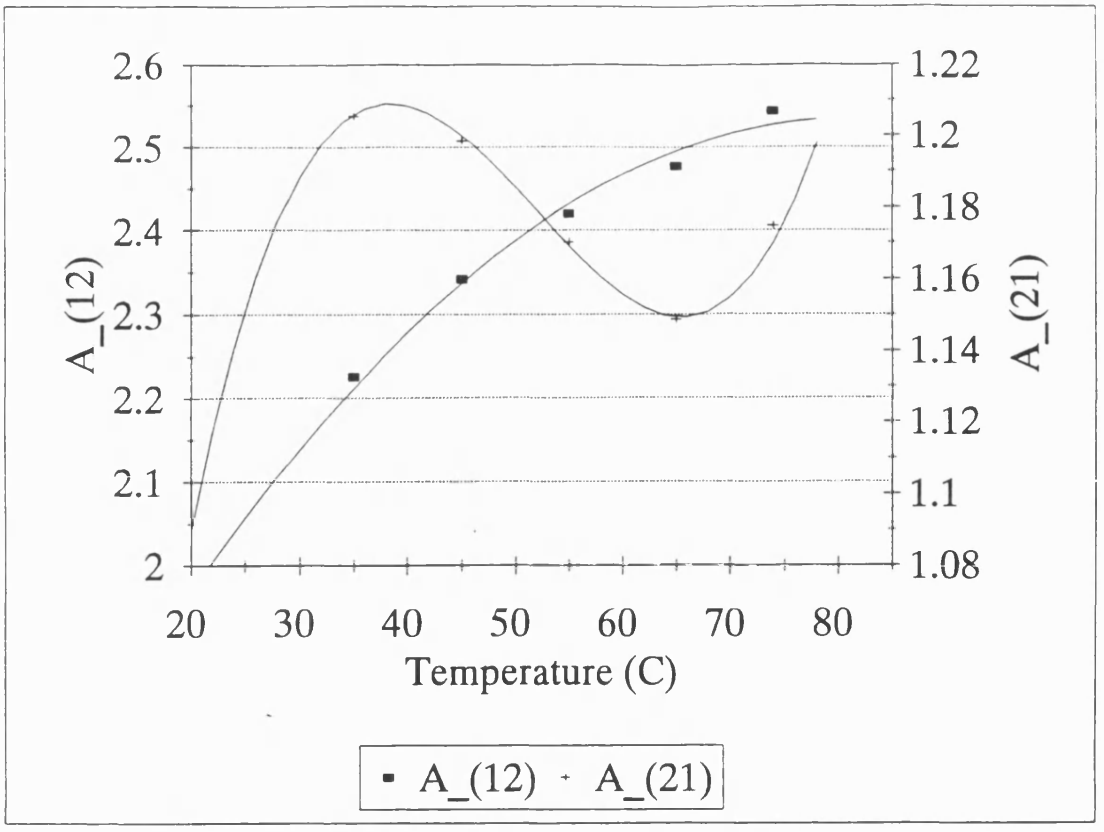

Figure D.1 Variation of van Laar coefficients with temperature for the 2-propanol (1)/water (2) system

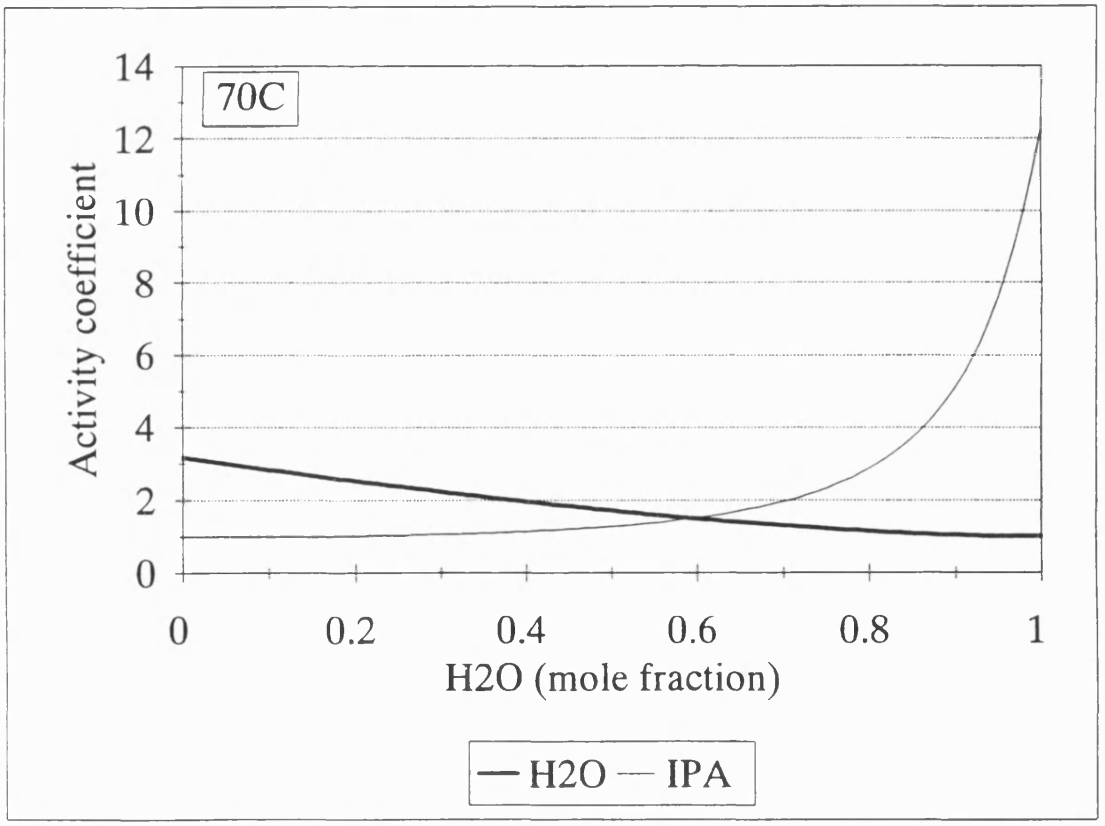

Figure D.2 Variation of activity coefficients with composition for a 2-propanol/water mixture

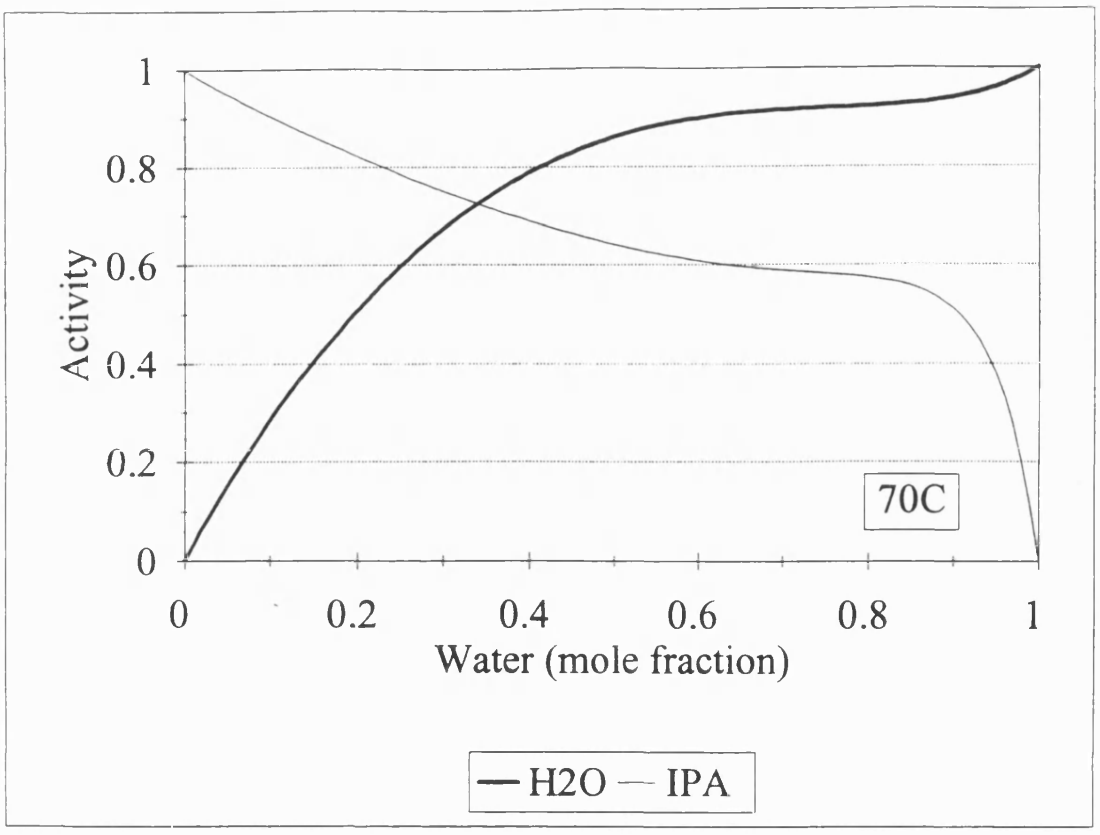

Figure D.3 Variation of activity with composition for a 2-propanol/water mixture

The influence of temperature upon activity is demonstrated in Figures D.4 and D.5. Variation of temperature causes little change in activity for either water or IPA over the composition range of interest in this work, except for a slight variation in water activity at the higher end of the range of water concentrations used.

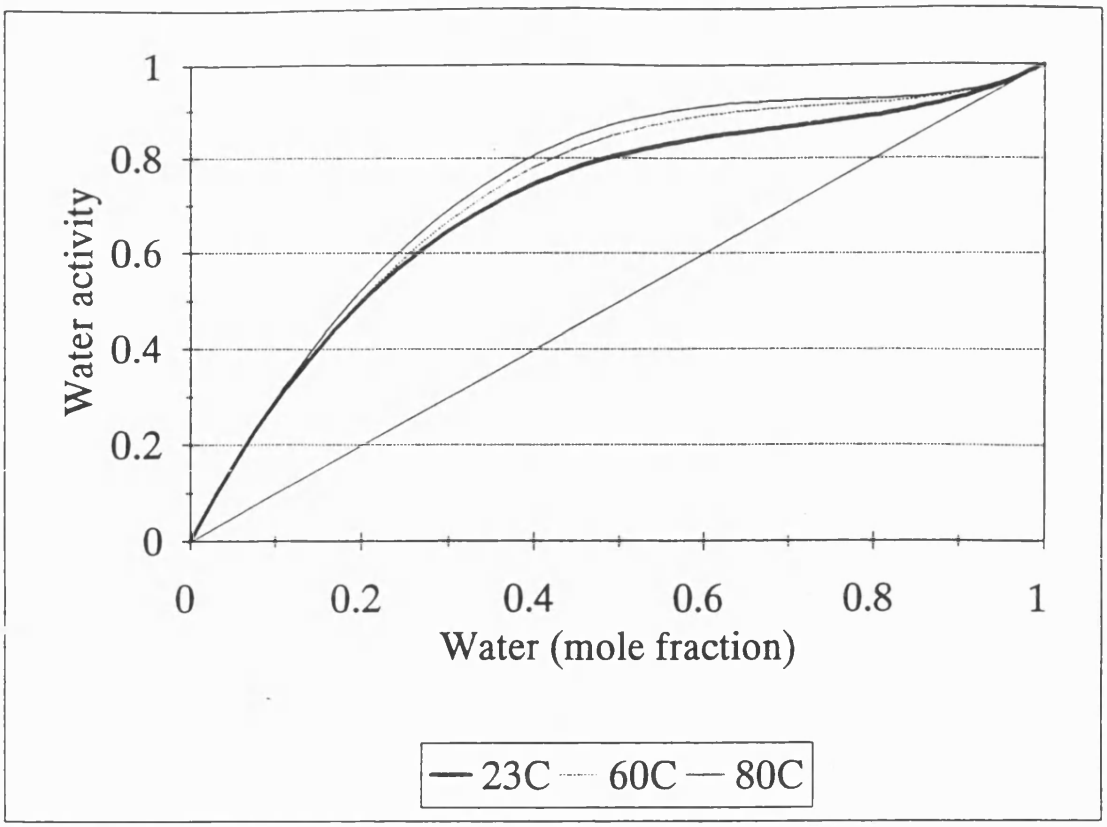

Figure D.4 Activity of water in a 2-propanol-water mixture as a function of composition and temperature

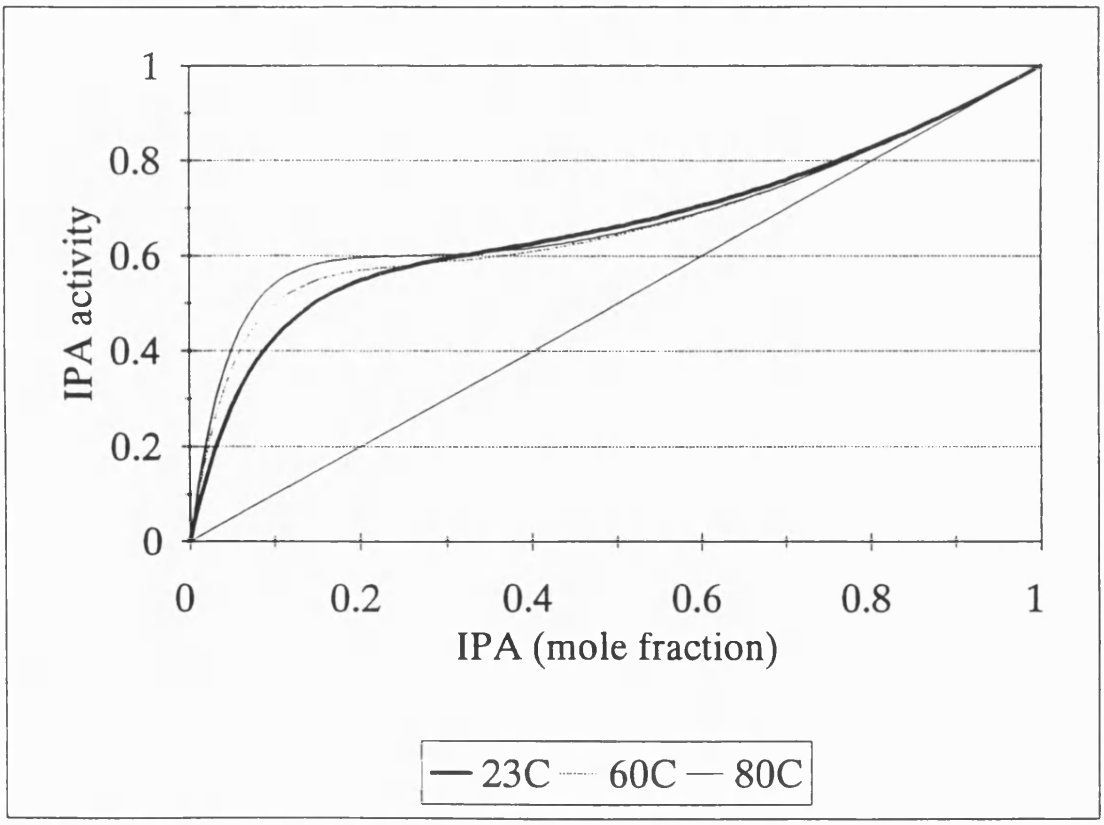

Figure D.5 Activity of 2-propanol in a 2-propanol-water mixture as a function of composition and temperature